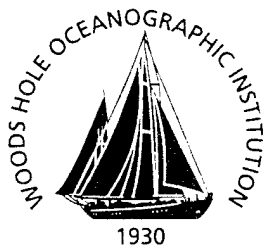


Woods Hole Oceanographic Institution



Fluid Mechanical Measurements within the Bottom Boundary Layer During Coastal Mixing and Optics

by

J.J. Fredericks
John H. Trowbridge

A.J. Williams III
George Voulgaris
William Shaw

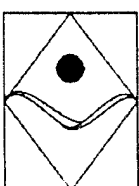
Woods Hole Oceanographic Institution
Woods Hole, Massachusetts 02543

August 2001

Technical Report

Funding was provided by the Office of Naval Research under contract number N00014-95-1-0373.

Approved for public release; distribution unlimited.



20020411 000

WHOI-2001-08

**Fluid Mechanical Measurements within the
Bottom Boundary Layer During Coastal Mixing and Optics**

by

J.J. Fredericks
John H. Trowbridge
A.J. Williams III
George Voulgaris
William Shaw

August 2001

Technical Report

Funding was provided by the Office of Naval Research under contract number
N00014-95-1-0373.

Reproduction in whole or in part is permitted for any purpose of the United States
Government. This report should be cited as Woods Hole Oceanog. Inst. Tech. Rept.,
WHOI-2001-08.

Approved for public release; distribution unlimited.

Approved for Distribution:



Timothy K. Stanton, Chair

Department of Applied Ocean Physics and Engineering

TABLE OF CONTENTS

LIST of TABLES.....	ii
LIST of FIGURES.....	iii
SECTION I. Introduction	1
SECTION II. Description of Instrumentation & Deployments.....	3
SECTION III. Data Processing	9
SECTION IV. Data Summaries	23
SECTION V. Data Comparisons	149
SECTION VI. Data File Descriptions.....	165
SECTION VII. Acknowledgments	169
SECTION VIII. References.....	171
APPENDIX A. Mfgrs. Calibration Sheets	173
APPENDIX B. Software to Read Archive Files.....	183

LIST OF TABLES

Table 1. BASS pre-cruise and post-cruise zeros with values used in processing	10
Table 2. Table of loss of data due to leg wake	11
Table 3. Calibration coefficients for YSI thermistors.....	18
Table 4. Calibration coefficients for conversion of AT counts to sound speed.....	21

LIST OF FIGURES

SECTION I

Figure 1. Site map of Coastal Mixing & Optics Program	iv
Figure 2. Locations of the SuperBASS deployments at the central mooring site	2

SECTION II

Figure 3. SuperBASS tripod schematic	4
Figure 4. Side-view of ADV relative to leg, channel and BASS tower	5
Figure 5. Top-view of ADVs relative to leg and BASS tower	5
Figure 6. Schematics relating the instrument frame to world coordinates	8

SECTION III

Figure 7. Truncated records (I/O problems) Deployments I & II	9
Figures 8-11. Schematic showing wake from tripod leg	12
Figures 12-13. Comparison of turbulence statistics of bottom-most BASS with the ADVs	17
Figure 14. Travel time (counts) vs 1/sound speed (s/m), Deployments I, II, III & IV	20

SECTION IV

Figures 15-19. Stickplots of low-pass filtered velocity	25
Figures 20-24. Eastward velocity time series	39
Figures 25-29. Northward velocity time series	53
Figures 30-34. Vertical velocity time series	67
Figures 35-39. Bottom-orbital velocity (Urms) time series	81
Figures 40-43. BASS Reynolds stress	95
Figures 44-47. BASS TKE dissipation	105
Figures 48-52. Salinity, temperature, sound speed, and ADV signal strength	115
Figures 53-56. Sound speed flux and gradient of density with sound speed	129
Figures 57-60. From sound speed, estimates of turbulent temperature variance dissipation ..	139

SECTION V

Figures 61-63. Comparison of burst averages of each ADV with the mean of other ADV sensors	150
Figure 64. Comparison of horizontal velocities with vertical velocities of ADV_a and ADV_b during Deployment III	153
Figure 65. Comparison of burst averages and Urms of bottom-most BASS with the mean of the burst averages and Urms of 'good' ADV sensors	154
Figures 66-69. Vertical profile of SuperBASS and VMCM (to 30 mab) burst averages and standard deviations of horizontal velocity	155
Figure 70-73. Empirical Orthogonal Function of SuperBASS and VMCM (to 30 mab) standard deviation of burst averaged velocity	159
Figure 74. Comparisons of BASS salinity with bottom-most VMCM salinity	163
Figure 75. Comparisons of BASS temperature with bottom-most VMCM temperature	164
Figure 76. Comparison of YSI temperature with SeaBird temperature	164

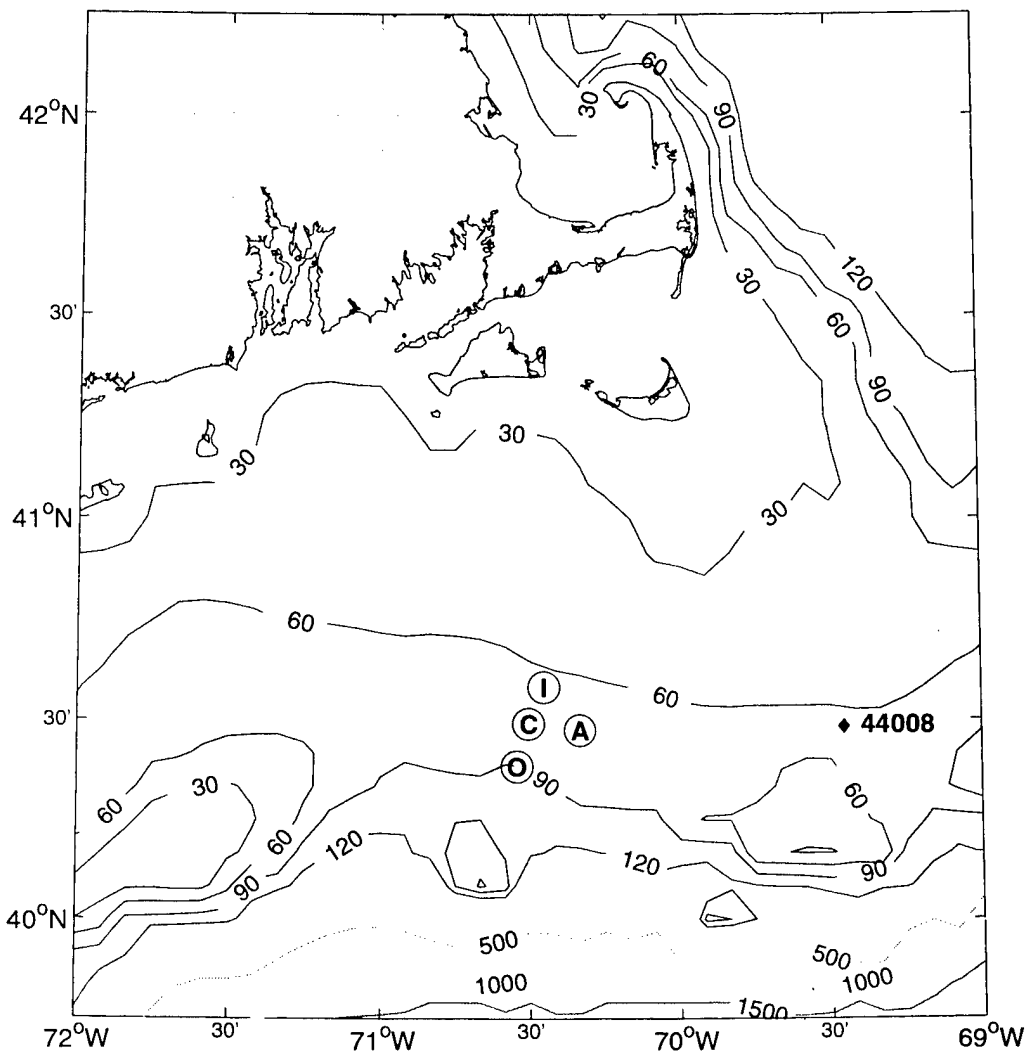


Figure 1. The deployment site was off the coast of New England along the 70 meter isobath near the central mooring site (**C**). Three other subsurface moorings were located near the site: inshore (**I**), offshore (**O**) and along-shore (**A**). A NGDB buoy (**◆**) was in close proximity.

SECTION I. INTRODUCTION

To quantify and understand the role of vertical mixing processes in determining mid-shelf vertical structure of hydrographic and optical properties and particulate matter, the Office of Naval Research (ONR) funded a program called Coastal Mixing and Optics (CMO), which was conducted at a mid-shelf location in the Mid-Atlantic Bight, south of Martha's Vineyard, Massachusetts. (See Figure 1.)

As part of the CMO program, a tall tripod, called 'SuperBASS', was equipped to collect a year-long, near-bottom time-series of velocity, temperature, salinity and pressure. The BASS sensors (Williams et al., 1987) were modified to measure absolute as well as differential acoustic travel time (Shaw et al., 1996, Voulgaris et al., 1997, and Trivett, 1991), to provide sound speed (a surrogate for temperature) and velocity in a single sample volume. Seven BASS velocity and travel time sensors were placed between 0.4 and 7 meters above bottom (mab). Three acoustic Doppler velocity (ADV) meters were mounted near the bottom-most BASS sensor at 0.3 meters above bottom. The ADV meters were separated horizontally to permit a technique for removing contamination by surface waves from estimates of turbulent Reynolds stress by differencing measurements from spatially separated sensors (Trowbridge, 1998, Voulgaris et al., 1997, Shaw and Trowbridge, submitted). The sensors were sampled rapidly (25 Hz for the ADVs and 1.2 Hz for the other sensors) and the measurements were recorded by synchronized in-situ loggers. The tripod was deployed at the central CMO site on the New England shelf (Figure 2), at a water depth of approximately 70 m, in August 1996. It was recovered and redeployed, for the purpose of offloading data and changing batteries, in October 1996, January 1997, April 1997, and June 1997. The final recovery was in August 1997.

The primary objectives of this component of the project were (1) to obtain high-quality time-series measurements of velocity and temperature throughout a large fraction of the bottom boundary layer on the New England shelf; (2) to use the measurements to determine the vertical structure of the Reynolds-averaged velocity and temperature fields, to obtain direct covariance estimates of turbulent Reynolds stress and turbulent heat flux, and to obtain indirect inertial range estimates of dissipation rate for turbulent kinetic energy and temperature variance; (3) to test simplified budgets for turbulent kinetic energy and temperature variance; and (4) to test empirical flux-profile relationships for momentum and heat. These data will also be used (5) to test vertically integrated budgets for momentum and heat; (6) to compare estimates of flow characteristics obtained from velocity and temperature measurements with corresponding estimates obtained from a near-bottom tracer-release experiment and shipboard microstructure measurements; and (7) to understand the interaction between the dynamics of the boundary layer and the resuspension and transport of fine sediments.

The purpose of this report is to describe the SuperBASS instrumentation and deployments, to provide summaries of the data collected, and to document the processing, preliminary analysis and archival of the data collected for this component of the program.

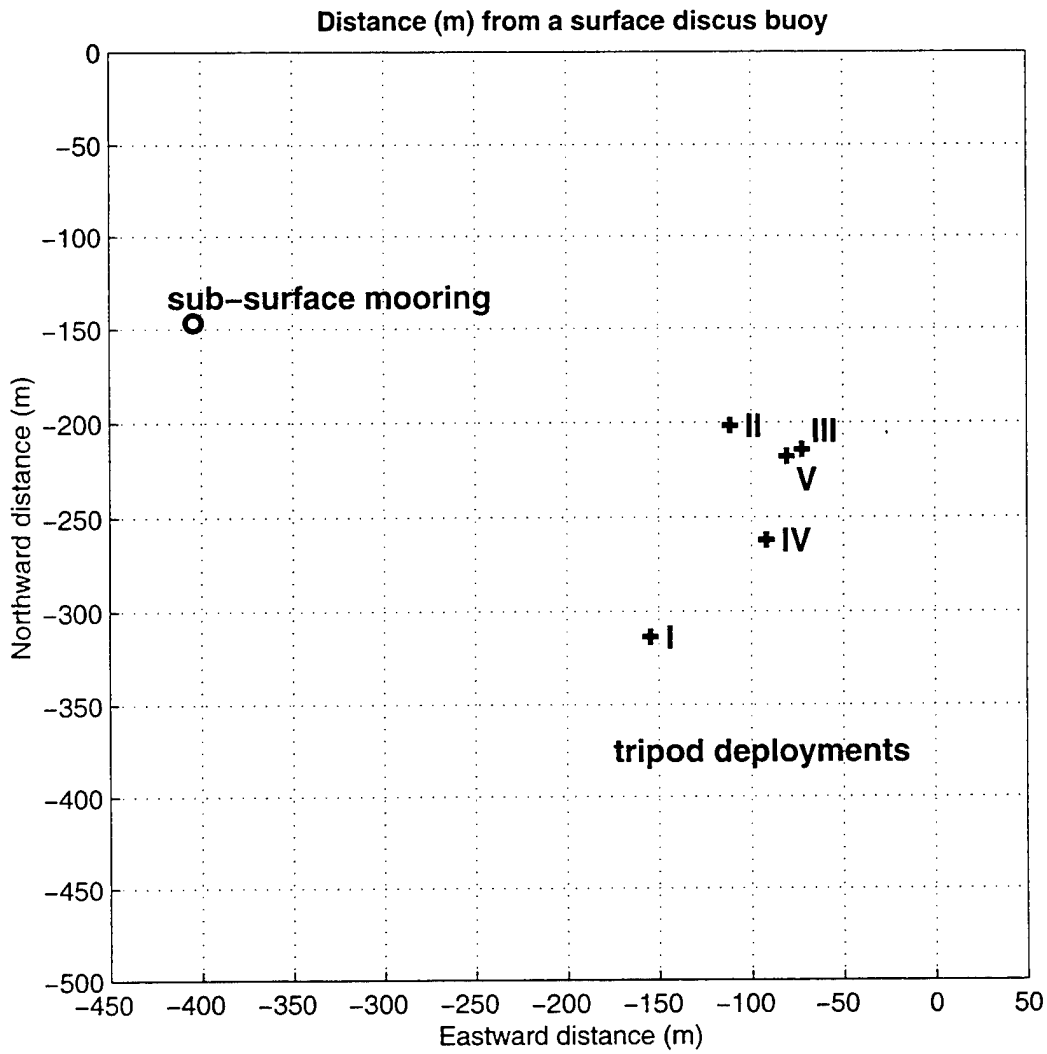


Figure 2. The superBASS tripod was deployed at the central mooring site near the sub-surface mooring deployed by the Upper Ocean Processes Group (WHOI).

SECTION II. INSTRUMENTATION & DEPLOYMENTS

This section describes the instrumentation of the SuperBASS tripod together with the sampling schemes and details of each deployment. Figure 2 shows the SuperBASS deployment sites relative to each other and the subsurface mooring at the central site, which is described in Galbraith et al. (1997). The structural design of the tripod and issues relating to the tripod structure are discussed in detail in Williams et al. (1997). Schematics of the instrumentation are in Figures 3-5.

Central to the SuperBASS tripod was a tower of BASS acoustic current meter (ACM) sensors. The BASS electronics measure differenced travel time to provide three-dimensional velocity (Williams et al., 1987). The electronics were modified to also provide absolute travel time in counts along each direction of the C path of each BASS sensor. The average of the absolute travel times is proportional to sound speed and can be used to estimate temperature fluctuations at the same frequency as velocity. A Tattletale® Model 6 logger, Onset Computers¹, recorded data from the ACM and acoustic travel time (AT) sensors at 1.2 Hz. The BASS logger also recorded data collected using a counter (Williams and Fraenkel, 1995) which sampled data from the Seabird² temperature and conductivity pairs strapped to the legs at the bottom-most and top-most ACM sensors (pods) and from a ParoScientific³ pressure sensor, which was mounted on the platform at 4.2 mab. BASS logger data were recorded for approximately 29 minutes, beginning at 0:01, 0:31, 1:01, 2:01, 2:31, 3:01, 4:01, 4:31, 5:01 etc., providing 36 bursts per day. A compass and tilt meter were placed in the BASS. The rubber-line was aligned with path D (Figure 5). To convert velocity data for Deployment I, for example, to real world coordinates, we subtracted the magnetic deviation, 15.5°, from the compass reading, 50°. Therefore, path D was +34.5° from North True. Figure 6 shows the tripod orientation for each deployment. Compass readings were updated hourly, but recorded with each record. Tilt was updated with each record at 1.2 Hz. Each BASS ACM path was adjusted for a zero offset (Morrison et al., 1993). Each pre- or post-cruise zero determination was conducted by wrapping the sensor in stiff plastic sheets to minimize flow through the sensing volume and deploying the tripod alongside the dock at the Woods Hole Oceanographic Institution (WHOI), where flow is minimal. For Deployments IV & V, the bottom most BASS ACM & travel time sensors were not logged and eight YSI⁴ thermistors were placed alongside the BASS tower at the heights of the remaining pods.

Three SonTek®⁵ acoustic Doppler velocity (ADV) meters were mounted on each of the 5 cm x 15 cm channels at the base of the SuperBASS tripod. (See Figures 3-6.) These side-looking 10 MHz field probes were mounted facing upward and oriented such that each +x was along the channel toward the center of the tripod; y was perpendicular in the horizontal plane; and +z was downward. The serial numbers of each probe are given in Figure 5. Data were collected at 25 Hz for 9.6 minutes beginning at the top of each hour, providing 24 bursts per day. The three ADV sensors were logged using three separate Tattletale® Model 6F loggers. A master/slave relationship was used to synchronize the observations: the master logger checked the clock and at each designated start time (on the hour), the logger began sampling and simultaneously sent a sync pulse to signal the slave loggers to begin sampling and logging.

¹Onset Computer Corporation, Pocasset, MA 02559

²Seabird Electronics, Inc., Bellevue, WA 98005

³ParoScientific, Inc., Redmond, WA 98052

⁴YSI Inc., Yellow Springs, OH 45387

⁵Sontek, Inc., San Diego, CA 92121

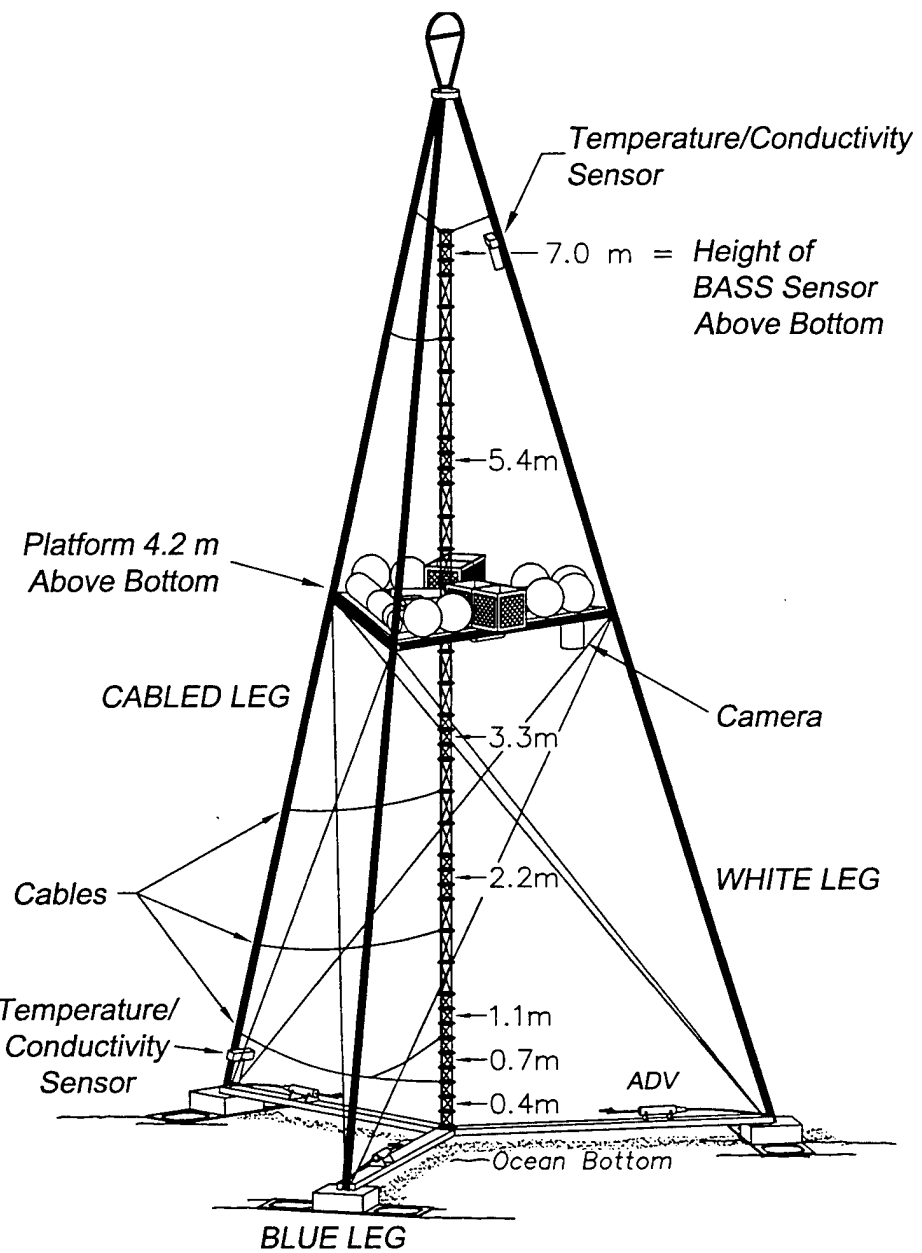


Figure 3. The configuration for Deployments I - III is shown here. ADV_A, ADV_B & ADV_C were mounted on the channel adjacent to the cabled leg, the white leg and the blue leg, respectively. For Deployment V, no ADV sensors were deployed. For Deployments IV & V, the bottom-most BASS sensor was not recorded and the corresponding temperature/conductivity sensors were moved up to the height of the second BASS sensor, and the top-most conductivity was rotated to lie along-side the channel, rather than perpendicular to the channel, as shown here.

Figure 4. The configuration of ADV_A is shown below. ADV_B and ADV_C were similarly placed, but did not have the cabling above the sensors or the temperature/conductivity pair on the leg near the sensors. For Deployments IV & V, the temperature/conductivity pair were moved up to 0.55 m above the channel.

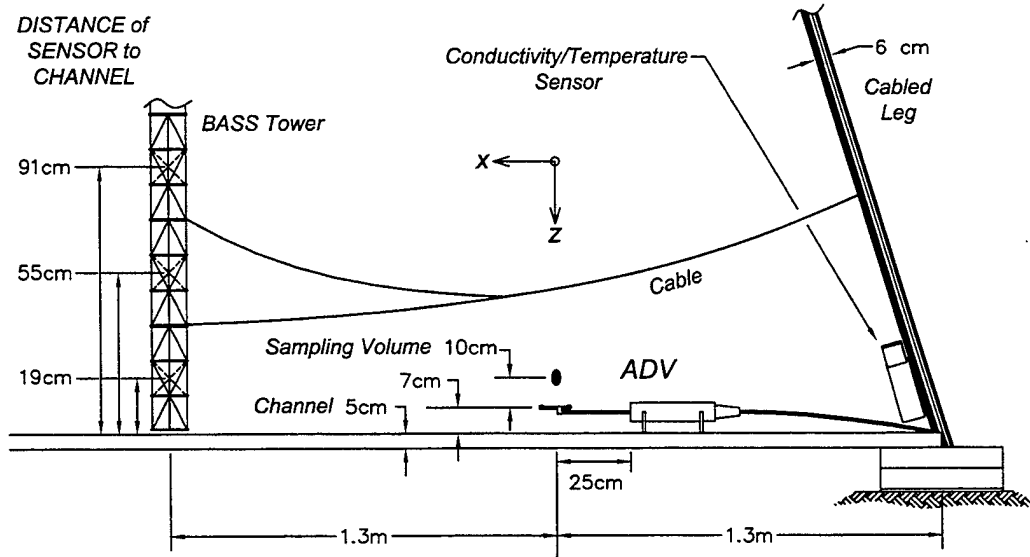
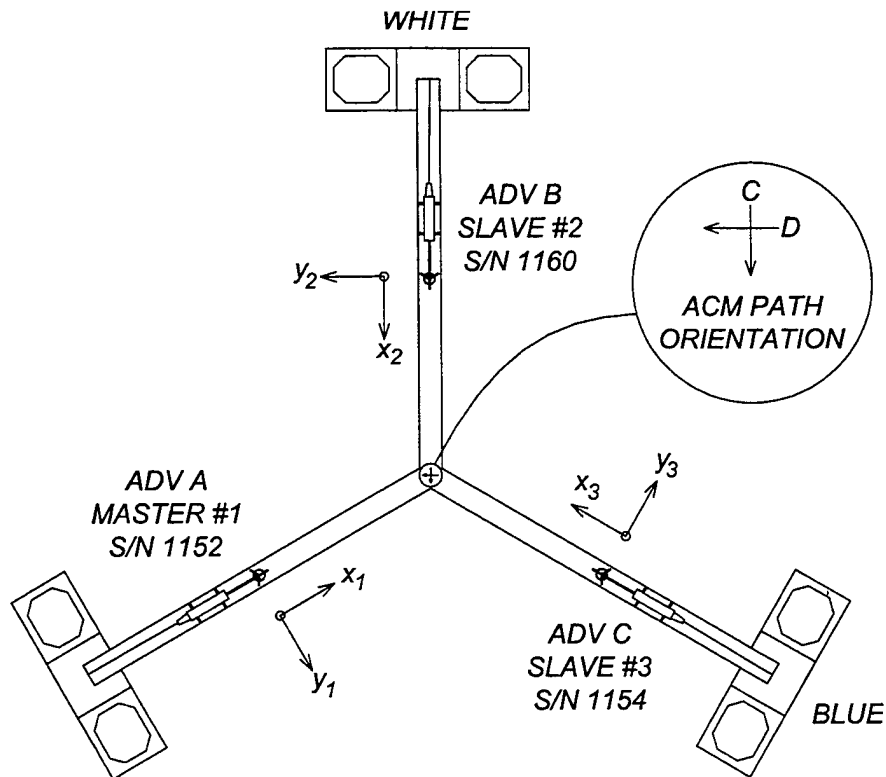


Figure 5. Top-view showing SuperBASS orientation with Serial Numbers of ADVs and ACM path orientation.



Deployment I: 8/18/96 - 9/27/96

Instrumentation:

Three ADV loggers sampled 9.6 minutes hourly at 25 Hz:

3 - ADV velocity sensors at 0.35 meters above bottom

The BASS logger recorded data at 840 msec intervals (1.2 Hz), sampling 3 half-hours every two hours:

7 - BASS (ACM) velocity sensors at (0.38, 0.72, 1.1, 2.2, 3.3, 5.4 & 7.0 mab)

7 - BASS travel-time sensors at the BASS ACM heights

2 - Seabird temperature, conductivity sensor pairs

7.0 mab: SN/041482, SN/032101

0.4 mab: SN/041425, SN/032100

1 - ParoScientific pressure sensor (SN/59118) at 4.2mab

1 - Compass, pitch & roll

Deployment Description: The tripod was deployed on August 18 at 14:31 GMT at approximately $40^{\circ} 29.359'$ N and $70^{\circ} 30.281'$ W. The tripod compass reading was 50° from magnetic north; pitch and roll was less than 1° with the standard deviation within each burst below 0.2° . Two hurricanes (Edouard and Hortense) passed over the deployment site during September. Due to a power supply failure, the ADV system failed on 9/1/96. Upon recovery, it was found that many guy wires had corroded and broken away from the BASS central tower. The structure was reassembled before redeployment.

Deployment II: 10/7/96 - 12/27/96

Instrumentation:

Same configuration as Deployment I, except the Seabird conductivity cell SN/041425 was replaced with SN/041481.

Deployment Description: The SuperBASS tripod was deployed at approximately the same site on October 7, 18:48 GMT, at $40^{\circ} 29.42'$ N, $70^{\circ} 30.25'$ W. The compass reading was 250° from magnetic north; pitch and roll was less than 1° with the standard deviation within each burst below 0.2° . Upon recovery of the tripod, it could be seen that the whole structure was covered with 1-2 cm of 'furry' growth. Both the ADV and BASS velocity and acoustic travel-time systems worked throughout the deployment, although after mid-November the data are noisy and the ADV correlation coefficients are primarily below the 70% threshold recommended by the manufacturer as the minimum for acceptable data. For reasons not fully understood, the counter failed on 10/16, after which there are no salinity, temperature or pressure data for Deployment II.

Deployment III: 1/6/97 - 4/9/97

Instrumentation:

(Same configuration as Deployment I).

Deployment Description: The tripod was deployed on 1/6/97, 8:16 GMT, at $40^{\circ} 29.413'$ N and $70^{\circ} 30.222'$ W. The BASS logger disk failed and data (including compass) were lost for this deployment. ADV records were oriented using comparisons with concurrently sampled moored data. The original conductivity cell (SN/041425) was replaced on the tripod at 0.4 mab.

Deployment IV: 4/17/97 - 6/10/97

Instrumentation:

The ADV sensors did not function during this deployment.

The BASS logger recorded data at 850 msec⁶ intervals (1.2 Hz), sampling 3 half-hours every two hours:

6 - BASS (ACM) velocity sensors at 0.7, 1.1, 2.2, 3.3, 5.4 & 7.0 mab

6 - BASS travel-time sensors at BASS ACM heights

2 - Seabird temp, salinity sensors at 0.7 & 7mab

7.0 mab: SN/041482, SN/032101.

0.7 mab: SN/041481, SN/032100.

1 - ParoScientific pressure sensor (SN/59118) at 4.2mab

8 - YSI thermistors between 0.7 & 7 mab

Deployment Description: The tripod was deployed on 4/16/97, 23:40 GMT, at 40° 29.387' N, 70° 30.236' W. The compass reading was 82° from magnetic north; pitch was less than 1° with the standard deviation within each burst below 0.2°; and, the roll was approximately -1.4°. After the beginning of May, the observed pitch would intermittently spike to about -1°, with standard deviations approaching 1°. It is believed that these observations reflect problems with digitization of the tilt sensor, rather than shifting of the SuperBASS tripod. The bottom-most BASS pod (0.4 m) was disconnected to accommodate eight (8) YSI thermistors, which were attached to the BASS tower at the same height as each of the remaining BASS pods. The yellow and white ACM connectors (for pods 4 & 5) were switched; therefore, the ACM data stream (1:6) represented data from pod 2, 3, 5, 4, 6 and 7, respectively. The thermistor stream (1:8) represented data from YSI thermistors (11,12,14,13,15 to 18) and were mounted at 0.7, 1.1, 2.18, 2.2, 3.3, 5.4, 5.4 and 7.0 mab. No ADV data were recorded during this deployment, due to a broken pin on the master data logger. The BASS clock had gained 5 seconds by the recovery date (6/10/97). The upper tower was bent, most likely during recovery.

Deployment V: 6/16/97 - 8/14/97

Instrumentation:

The ADV sensors were not deployed.

The BASS logger and instrumentation was the same as Deployment IV, with the following exception: the Seabird sensors at 0.7 mab were SN/041425, SN/032100.

Deployment Description: The tripod was deployed on 6/16/97, 10:15 GMT, at 40° 29.411' N, 70° 30.228' W. The compass reading was 97° from magnetic north; roll was about 1.4°; and pitch was less than 1° with the standard deviation within each burst below 0.2°. The digitization problem in the pitch, as described in Deployment IV, persisted during Deployment V. The BASS clock had gained 5 seconds by the recovery date (8/14/97). The bottom-most Seabird temperature sensor failed and the pressure and Seabird conductivity cells also appear to be corrupted. The YSI data stream (1:7) represents data from YSI thermistors (11:18) at 0.7, 1.1, 2.18, 2.2, 3.3, 5.4 and 7.0 mab, respectively. The eighth YSI thermistor, which was also at 7.0 mab, failed during Deployment V.

⁶The sampling interval was increased to accommodate the longer data stream.

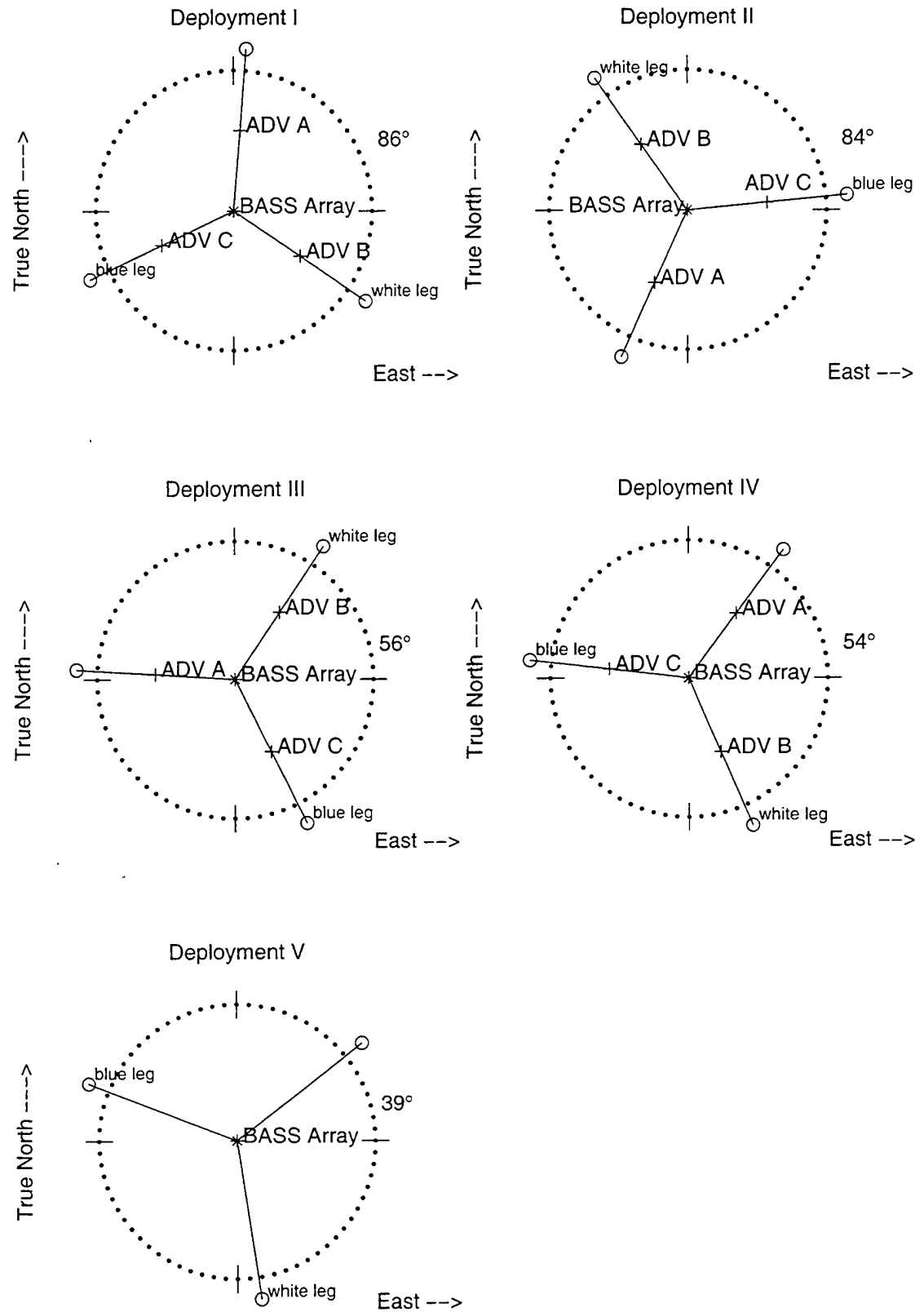


Figure 6. Schematics relating the instrument frame to world coordinates for each deployment.

SECTION III. DATA PROCESSING

This section describes the steps which were taken in processing the data from the SuperBASS tripod.

Due to BASS logger disk I/O problems, there are periods during Deployments I & II, when some of the bursts were truncated, causing loss of up to 1-2 minutes of the half-hour burst at the end of those records. (See Figure 7.) Therefore, the user must be aware of changing record lengths in the BASS logger data.

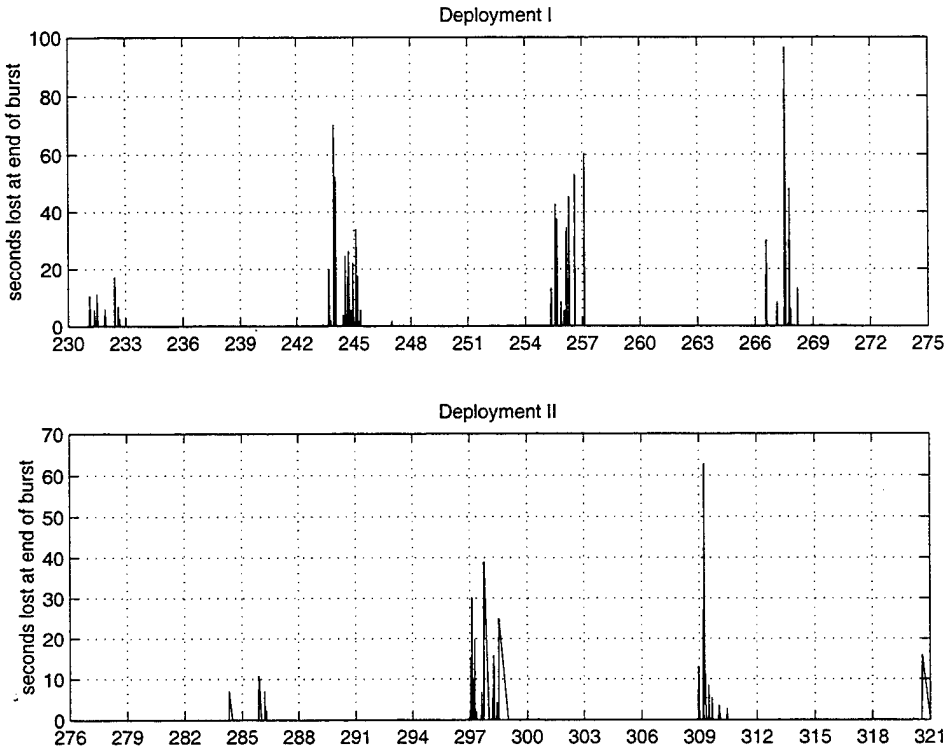


Figure 7. Data loss from faulty disk writes during Deployments I & II. The disk was replaced and the problem did not persist in Deployments IV & V.

BASS Velocity

BASS velocity data were converted to meters per second, using 2.4 m/s per 32768 counts, and zeros were subtracted from each path. Table 1 provides a summary of the pre- and post-cruise zeros taken from the WHOI dock, along with the actual zeros used for each deployment. At times, the pre- and post-cruise zeros differed. To determine the best zero adjustment, it was assumed that in situ vertical velocity from the D and B paths should be close to the vertical velocity from the C and A paths and both should be centered around zero. Some paths drifted throughout the experiment and were reconstructed when possible. The remaining uncertainties in the zero drift problem are documented in the plots of vertical velocity in Section IV. For Deployment V, the pre-cruise and post-cruise zeros were significantly different and for that deployment we assumed a circular tidal ellipse and that the mean vertical velocity was zero.

Table 1. BASS ACM zeros (m/s) from pre- and post-cruise tests along with values used in processing

	8/15	8/16	8/96	10/96	10/96	4/97	6/97	8/97	6/97
	pre- zeros	pre- zeros	zeros used	pre- zeros	zeros used	pre- & used	pre- zeros	post- zeros	zeros used
Pod 1									
1	0.009	0.007	-0.017	-0.018	-0.018				
2	-0.021	-0.024	-0.021	-0.016	-0.016				
3	0.003	0.002	0.003	0.001	0.001				
4	0.025	0.024	*	*	0.021				
Pod 2									
5	0.016	0.016	0.013	0.016	0.016	0.013	0.021	0.019	0.012
6	0.020	0.019	0.014	0.019	*	0.010	0.017	0.036	0.017
7	-0.005	0.002	0.0002	0.000	0.000	0.015	0.001	0.045	0.016
8	-0.005	-0.005	-0.005	-0.004	-0.043	-0.001	-0.001	0.031	0.015
Pod 3									
9	-0.005	-0.004	-0.002	-0.002	0.006	-0.003	-0.005	-0.014	-0.005
10	-0.003	-0.002	-0.004	-0.002	-0.006	*	0.001	-0.018	-0.003
11	-0.027	-0.045	-0.025	-0.046	-0.038	-0.018	-0.030	-0.051	-0.025
12	0.005	-0.014	*	-0.014	-0.014	0.002	0.004	0.012	0.014
Pod 4									
13	0.006	0.007	0.018	0.018	0.018	0.016	0.004	0.011	0.017
14	*	*	*	*	*	*	-0.001	-0.004	-0.007
15	0.002	0.003	-0.001	-0.002	-0.002	0.004	0.014	0.020	0.006
16	-0.011	-0.009	-0.010	-0.023	-0.023	0.002	*	-0.04	*
Pod 5									
17	0.009	0.008	0.0053	0.007	0.007	0.007	0.004	0.011	-0.001
18	0.000	-0.001	-0.0003	-0.001	-0.001	-0.001	-0.001	-0.004	-0.006
19	0.008	0.008	0.0053	0.008	*	0.000	0.005	0.006	0.016
20	0.007	0.007	0.007	*	0.007	*	*	0.014	*
Pod 6									
21	-0.003	-0.002	-0.002	-0.002	-0.002	-0.006	0.014	0.002	-0.015
22	0.031	0.030	*	0.031	0.015	0.012	-0.001	-0.008	-0.007
23	-0.001	-0.001	0.001	-0.001	-0.001	*	0.002	-0.006	*
24	-0.007	-0.007	-0.005	-0.008	-0.007	-0.003	-0.008	0.005	-0.009
Pod 7									
25	-0.001	-0.002	-0.002	-0.002	-0.002	-0.007	0.011	0.039	0.007
26	0.001	-0.000	-0.012	-0.011	-0.011	0.008	*	-0.038	*
27	0.001	0.000	0.002	0.007	0.007	-0.003	*	-0.008	-0.008
28	0.004	0.008	-0.007	-0.003	-0.003	0.000	-0.003	-0.017	-0.002

* indicates acoustic paths rejected during analysis because of low quality and then reconstructed from the remaining three paths

Velocities were converted from the instrument frame to real world coordinates (Figure 6) using the compass which was mounted in the logger. Points which were more than four times the burst standard deviation away from the burst average were replaced with NaN's, usually accounting for less than 1% of the data.

Bottom orbital velocities within each burst were computed as the square-root of the sum of the variance of each component of the horizontal velocity, which represents wave induced velocity.

Half-hour burst averaged estimates of stress were computed using a wave filtering technique (Shaw and Trowbridge, in press) developed to remove the waves from the spectral estimates by differencing pairs of sensors. For Deployments I and II, sensors 1 through 7 were paired with sensors 4, 5, 6, 1, 2, 3, 4, respectively. For Deployment IV, sensors 2 through 7 were paired with sensors 5, 6, 7, 2, 3, 4. For Deployment V, since sensor 7 failed at the beginning of the deployment, sensors 2 through 7 were paired with sensors 5, 6, 2, 2, 3, 4. The stress estimates were derived from the filtered estimates of covariance, $\text{cov}(\Delta\hat{U}, W)$.

Dissipation rates for turbulent kinetic energy and sound speed variance, ε and χ , were corrected for spatial filtering, temporal aliasing and noise floor (Shaw et al., 2001). The inertial sub-range model fits were limited at low frequencies by large surface wave peaks below 0.2 Hz. Dissipation from each of the four acoustic paths was computed; cleaned up by removing any points where there was an imaginary component (indicating a negative slope in the inertial sub-range) and any points greater than 5×10^{-5} (outliers); and, then, the four paths were averaged to provide one estimate per sensor.

Sound speed flux, $\langle c' w' \rangle$, was estimated directly using the eddy correlation technique. Because of problems with contamination from internal waves (Shaw et al., 2001), the flux estimates were also made using a technique involving time derivatives. The flux estimates from the time derivatives were empirically corrected to match the original estimates by fitting the two estimates during times when there were no internal waves. This quantity is denoted $\langle c_t' w_t' \rangle / \omega^2$.

Flow disturbance from the tripod legs was apparent when the angle of flow was plotted with the normalized variance in horizontal acceleration (Shaw et al., 2001). To detect the wake, a quantity was computed from each burst by taking the square root of the sum of the variances of each component of the horizontal acceleration at each sensor. This quantity was then normalized by dividing each estimate by the same quantity averaged over the bottom three sensors, which were assumed to be well away from the tripod legs. In Figures 8 - 11, black points identify data flagged bad by assuming a cutoff of 1.5 in the normalized variances. This affected a Gaussian shaped histogram between 0.5 and 1.5, producing the following percentages of data loss:

Table 2.

Sensor	% of data lost from wake						
	1	2	3	4	5	6	7
meters from leg:	2.3	2.2	2.0	1.8	1.4	0.8	0.3
Deployment_I:	0	0	0.3	2.4	7.3	25.7	40.9
Deployment_II:	5.2	5.3	2.4	8.1	24	18.9	38.8
Deployment_IV:	-	0.1	0.3	3.5	12.3	16.7	30.5
Deployment_V:	-	0	0	26.2	6	35	16.6

Figure 8. Deployment I: Measure of flow disturbance from legs

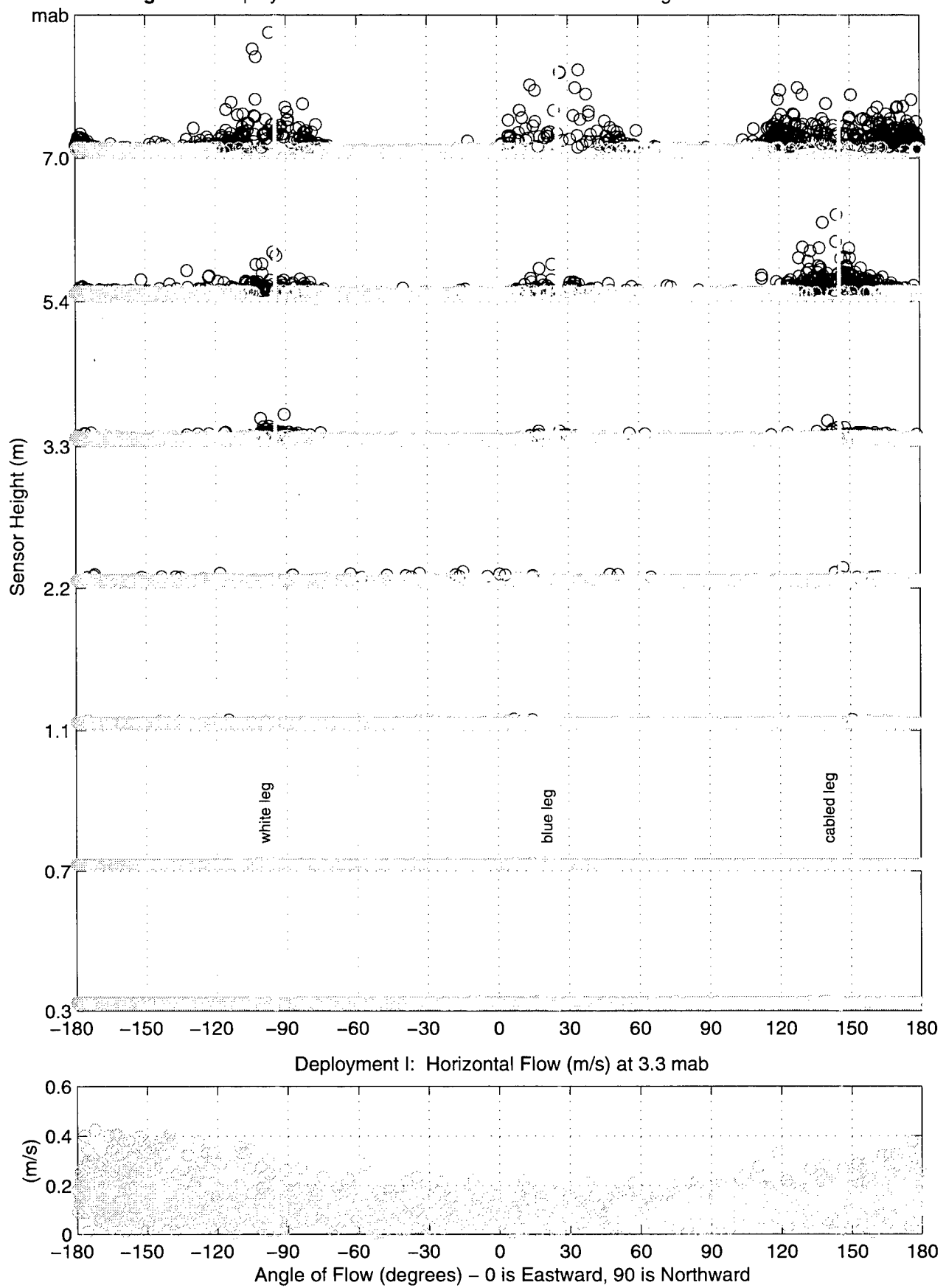


Figure 9. Deployment II: Measure of flow disturbance from legs

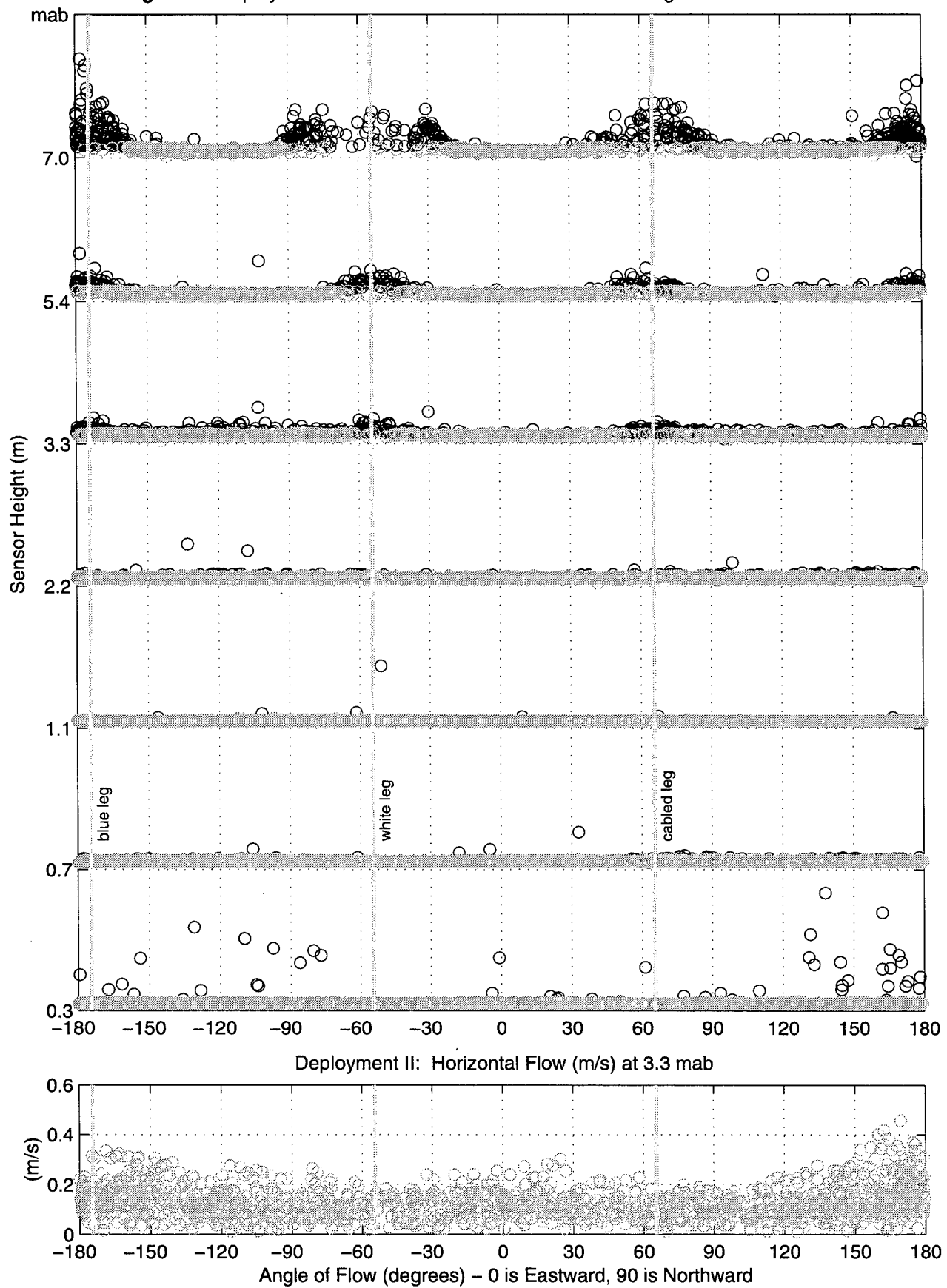


Figure 10. Deployment IV: Measure of flow disturbance from legs

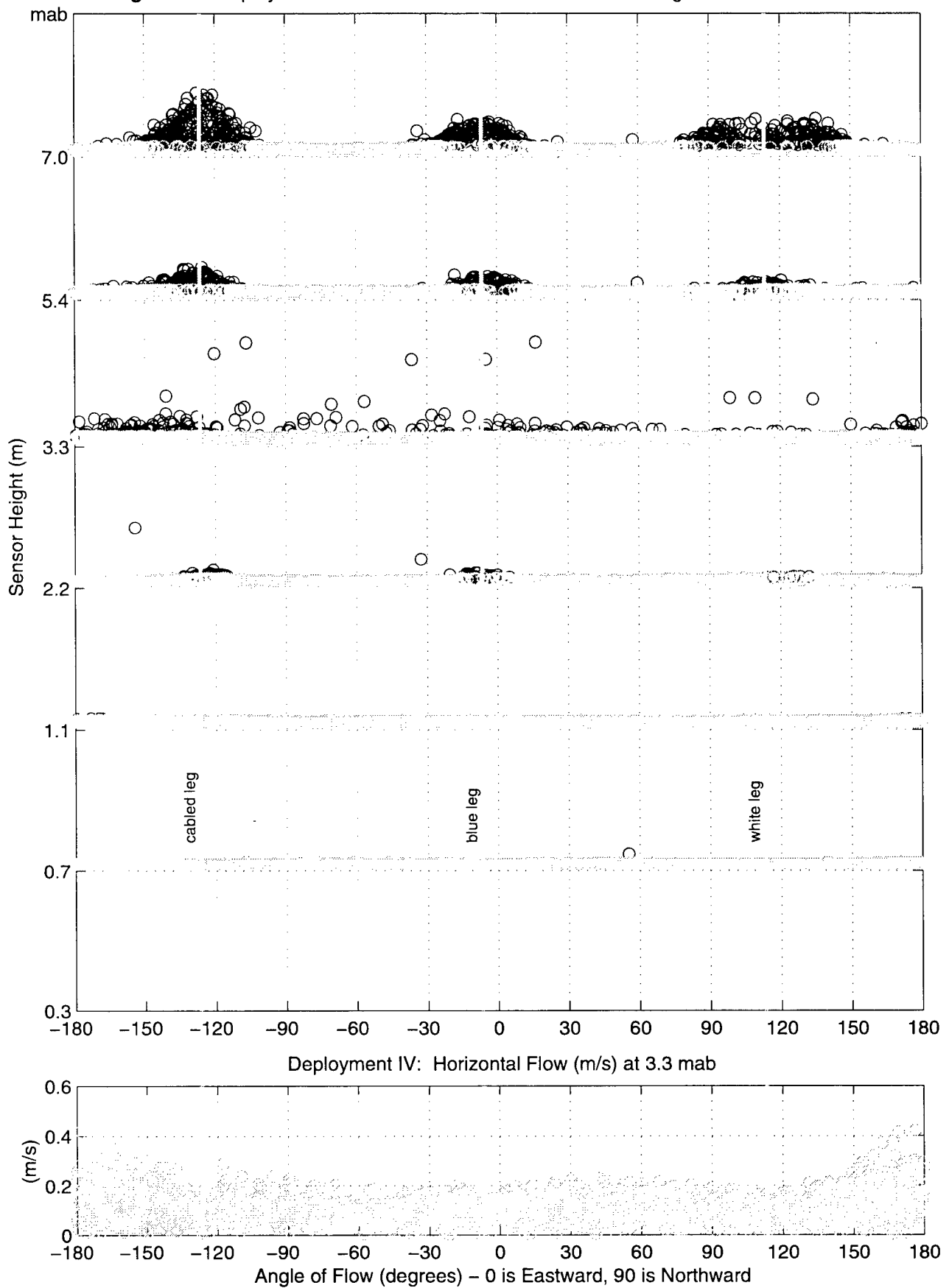
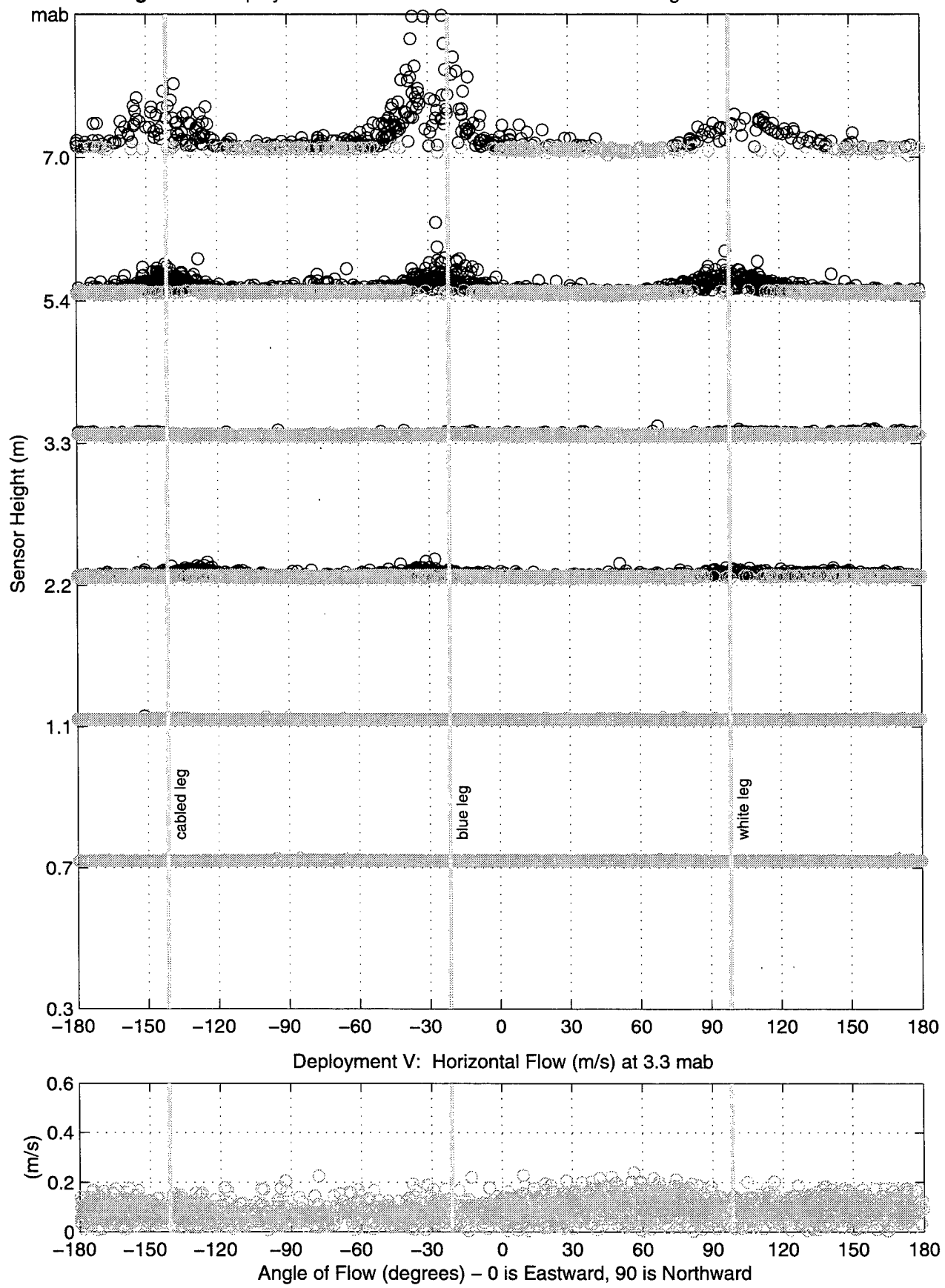


Figure 11. Deployment V: Measure of flow disturbance from legs



ADV Velocity

All ADV records were truncated to 14400 points. The velocity data were recorded as 0.1 mm/s in the x, y and z instrument coordinate system. These data were unpacked and converted to north, east and upward components. For Deployments I & II, rotations to world coordinates were based on the relationship of the ADVs with the instrument frame and the BASS compass. For Deployment III, there were no data from the BASS, so data were converted by comparing horizontal variances of these data to the data from the VMCM 10 meters above bottom at the central mooring site. For verification, the technique was applied to the data for Deployments I & II, when the tripod orientation was known. A summary follows:

During Deployment I, the orientation of the principal axes were:

ADV_a = 51.1°, ADV_b = 40.0°, ADV_c = 38.7° (Average ADV = 43.3°)
VMCM, at 10 mab = 47.4°

During Deployment II:

ADV_a = 66.6°, ADV_b = 63.7°, ADV_c = 58.6° (Average ADV = 63.0°)
VMCM at 10 mab = 60.8°

During Deployment III (after applying a 303.5° rotation for the ADVs):

ADV_a = 57.8°, ADV_b = 64.8°, ADV_c = 65.9° (Average ADV = 62.8°)
VMCM at 10 mab = 59.9°

A quality index (between 0 & 10) was defined as the average correlation coefficient from the three radial beams of the sensor divided by ten and then rounded to the nearest integer. Values greater than 7 denote good data. This parameter was not used in processing the data. Data which were four standard deviations away from the mean were replaced by linear interpolation of the surrounding points. More than 99% of the time fewer than 2% were removed. During the remaining 1% of the time, less than 10% of the data were removed as outliers.

As with the BASS velocity data, bottom orbital velocities within each burst were computed as the square-root of the sum of the square of each component of the horizontal velocity minus its burst average.

Estimates of stress and dissipation were computed from the ADV measurements, by using the differencing procedure described by Shaw and Trowbridge (in press) for stress and the procedure described by Shaw et al. (2001) for dissipation. As seen in Figures 12 - 13, flow distortion along the channel and over the processing units caused apparent over-estimates of these parameters and time series are not included in Section IV.

Figure 12. Deployment I

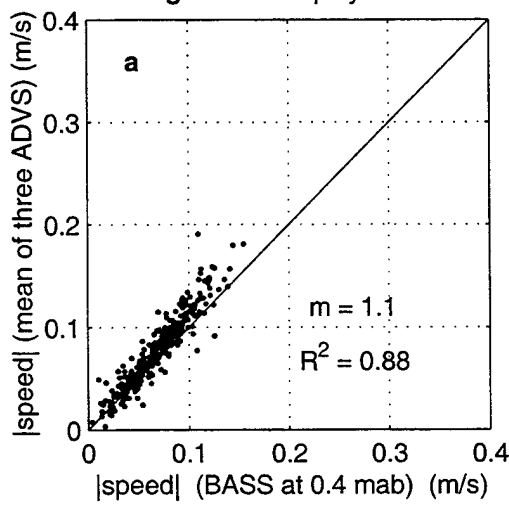
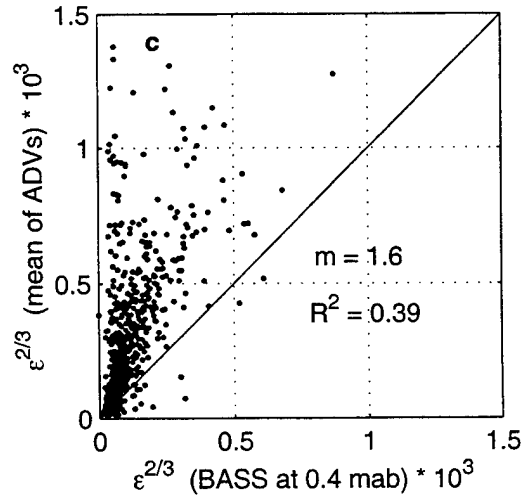
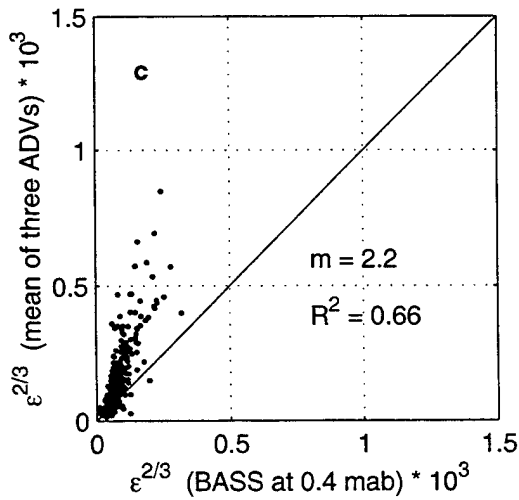
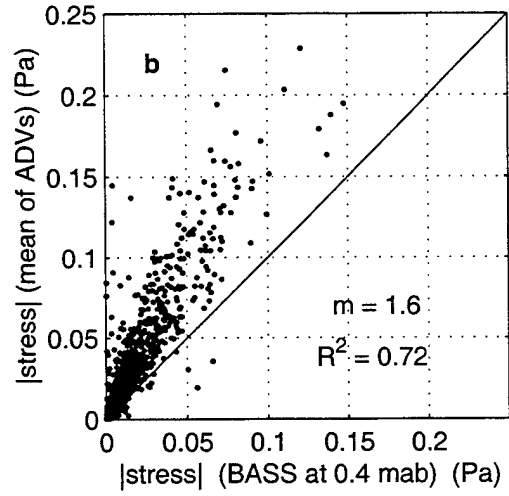
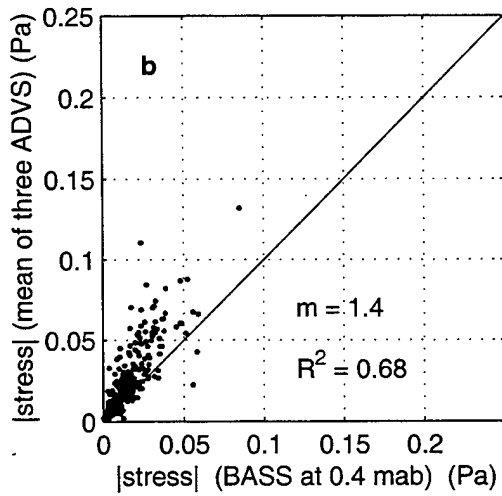
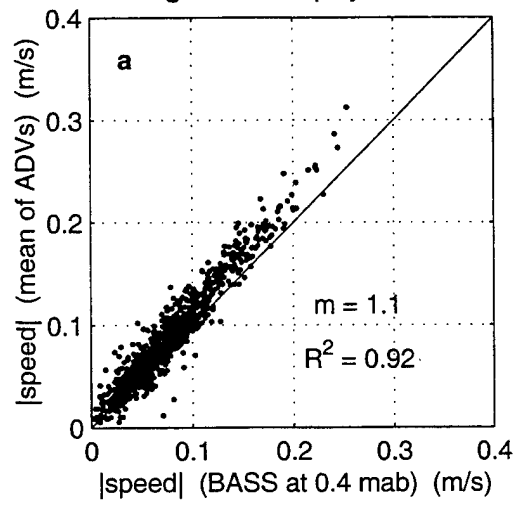


Figure 13. Deployment II



Pressure

Pressure counts were converted to psia using the calibration from ParoScientific (Appendix A) and then converted to meters. The sensor returned banded pressure values, which were up to 2 meters apart, making even burst averages meaningless. The pressure also seemed to be correlated to temperature in a non-physical way, affording another reason to suspect that the pressure measurements are inaccurate.

Seabird Temperature

Temperature data were converted from counts to degrees centigrade using lab calibrations provided by Seabird, Inc, and included in Appendix A.

YSI Temperature

Eight YSI thermistors provided temperature during Deployments IV & V. The thermistors were calibrated in the lab using SeaBird temperature sensors SN/032100, SN/032101 and SN/032103. A third order polynomial fit of approximately 12 hours of data, between 5 - 15°C, provided the following calibration coefficients provided in Table 3. These coefficients were used to compute temperature, as follows:

$$\text{temperature} = A0 * \text{counts}^3 + A1 * \text{counts}^2 + A2 * \text{counts} + A3$$

Table 3. Calibration Coefficients of YSI thermistors
(using temperature bath from 5 to 15 °C)

sensor	A0	A1	A2	A3
1	1.0e-13 x	1.0e-08 x	1.0e-03 x	1.0 x
2	0.3967	-0.3281	0.5686	0.3205
3	0.4380	-0.3475	0.5715	0.3324
4	0.2501	-0.2777	0.5630	0.3500
5	0.2485	-0.2728	0.5623	0.3648
6	0.3829	-0.3280	0.5687	0.3434
7	0.1874	-0.2525	0.5597	0.3714
8	0.3524	-0.3125	0.5664	0.3428
	0.3340	-0.3119	0.5672	0.3386

Seabird Salinity

Conversion of the counts to conductivity was made using calibration coefficients from Seabird, Inc., which are included in Appendix A. The conductivity was converted to salinity using the temperature from the Seabird thermistors. Depth was estimated from the pressure record, when appropriate, or hard coded, when no pressure record was available.

Table 4 (below) lists the slope and intercept for the calibration of sound speed counts (AT) with the computed sound speed from the salinity, temperature and pressure data. The 95% confidence interval (CI) of the slope and intercept is also included. N represents the number of samples used and min(c) and max(c) represent the range of the sound speed data used in fitting the data. (Also see Figures 14 a-d.).

Sensor	slope ± CI	intercept ± CI	N	R^2	min(c)	max(c)
	1e-09 x	1e-03 x				
8/96						
1	-0.7761 ± 0.0056	0.7235 ± 0.0004	134	0.9991	1478.7	1488.7
2	-0.7735 ± 0.0052	0.7234 ± 0.0003	134	0.9992	1478.7	1488.7
3	-0.7783 ± 0.0043	0.7278 ± 0.0003	134	0.9995	1478.7	1488.7
4	-0.7643 ± 0.0039	0.7263 ± 0.0003	134	0.9996	1478.7	1488.7
5	-0.7818 ± 0.0036	0.7264 ± 0.0002	134	0.9996	1478.7	1488.7
6	-0.7624 ± 0.0037	0.7253 ± 0.0002	134	0.9996	1478.7	1488.7
7	-0.7571 ± 0.0035	0.7279 ± 0.0002	99	NaN	1478.7	1488.7
10/96						
1	-0.7872 ± 0.0339	0.7239 ± 0.0022	44	0.9900	1486.1	1488.5
2	-0.7778 ± 0.0342	0.7232 ± 0.0022	44	0.9896	1486.1	1488.6
3	-0.7773 ± 0.0335	0.7244 ± 0.0022	44	0.9900	1486.1	1488.6
4	-0.7571 ± 0.0330	0.7258 ± 0.0023	44	0.9898	1486.1	1488.6
5	-0.7651 ± 0.0343	0.7251 ± 0.0024	44	0.9892	1486.1	1488.6
6	-0.7469 ± 0.0543	0.7241 ± 0.0038	44	0.9723	1486.1	1488.5
7	-0.7326 ± 0.0338	0.7260 ± 0.0025	44	0.9885	1486.1	1488.6
4/97						
2	-0.7713 ± 0.0031	0.7229 ± 0.0002	646	0.9986	1470.0	1475.4
3	-0.8017 ± 0.0021	0.7270 ± 0.0001	646	0.9994	1470.0	1475.4
4	-0.7760 ± 0.0030	0.7260 ± 0.0002	646	0.9988	1470.0	1475.4
5	-0.7589 ± 0.0029	0.7265 ± 0.0002	646	0.9988	1470.0	1475.4
6	-0.7763 ± 0.0019	0.7265 ± 0.0001	646	0.9995	1470.0	1475.4
7	-0.7643 ± 0.0015	0.7286 ± 0.0001	646	0.9997	1472.3	1475.4
6/97						
2	-0.7684 ± 0.0012	0.7228 ± 0.0001	671	0.9998	1483.8	1490.4
3	-0.7827 ± 0.0010	0.7261 ± 0.0001	671	0.9999	1483.8	1490.5
4	-0.7743 ± 0.0011	0.7259 ± 0.0001	671	0.9998	1483.8	1490.5
5	-0.7672 ± 0.0012	0.7289 ± 0.0001	671	0.9998	1483.8	1490.4
6	-0.7690 ± 0.0010	0.7261 ± 0.0001	671	0.9999	1483.8	1490.5
7	-0.7762 ± 0.0044	0.7269 ± 0.0003	100	0.9996	1483.8	1490.6

— THIS PAGE INTENTIONALLY LEFT BLANK —

SECTION IV: DATA SUMMARIES

This section provides time series of the data collected during the five deployments of the SuperBASS tripod. Year day is the day of the year with 0.5 representing January 1, at noon. These data are presented as follows:

stick plots of the low-pass filtered velocity (m/s)
(based on filter pl64t, half-power point 38 hours,
see, e.g., Limeburner, 1985),
eastward velocity (m/s), northward velocity (m/s), vertical velocity (m/s),
bottom-orbital (wave induced) velocity (m/s),
stress (Pa), covariance of the filtered horizontal velocities with the vertical velocity:

τ_{bx} - East-west component of stress

τ_{by} - North-south component of stress,

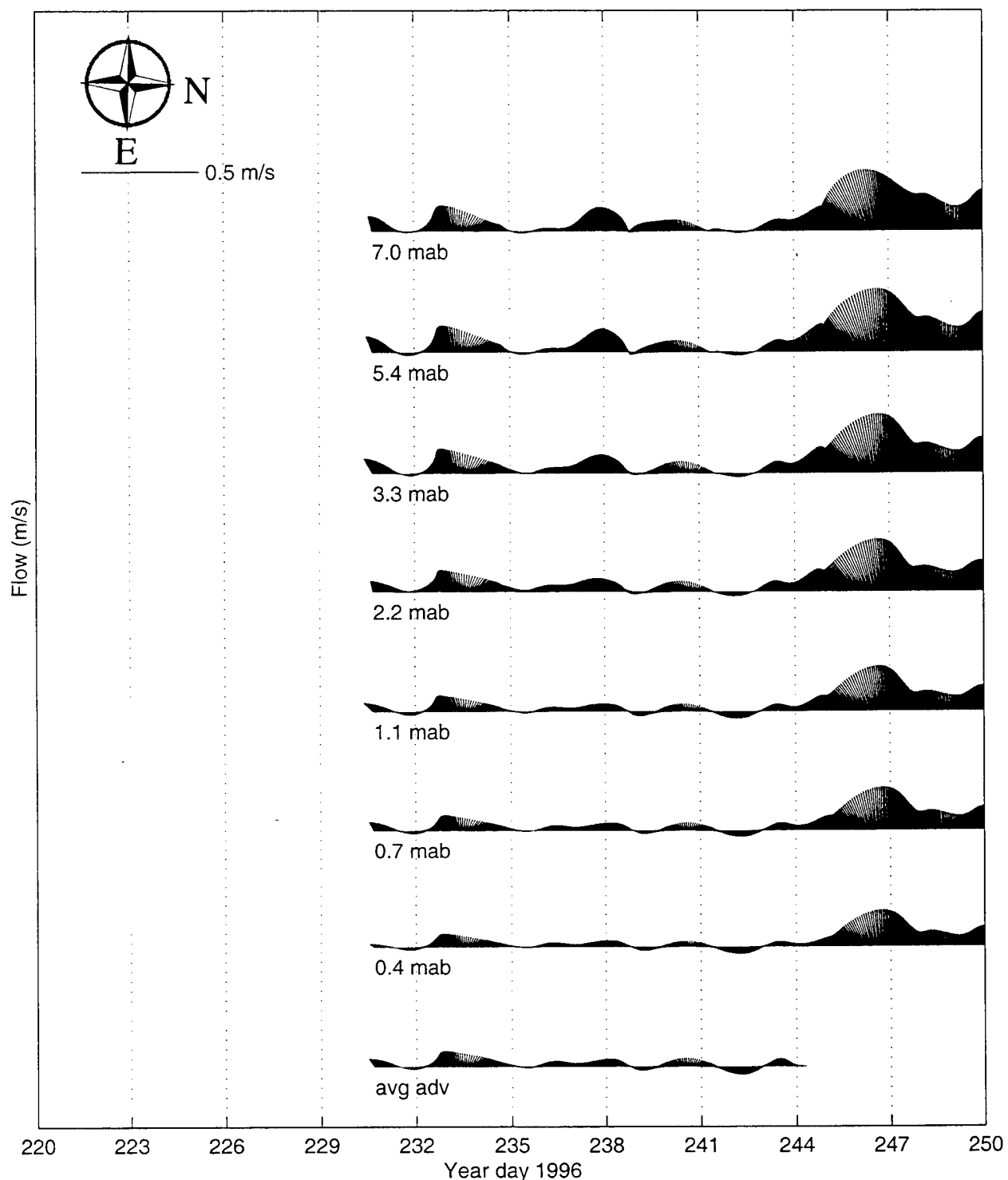
dissipation (W/kg),
temperature ($^{\circ}$ C) from SeaBirds and YSI thermistors, salinity (PSU) from SeaBirds,
sound speed from the acoustic travel time observations (m/s), and
amplitude of the ADV signal strength (dB), as an uncalibrated indicator of suspended sediment concentration,
sound speed flux (m^2/s^2) with the gradient of density (from central mooring data) with
sound speed, and
dissipation of the sound speed variance (m^2/s^3).

As described in Section II, during Deployment II, BASS data after year day 321 and ADV data after day 315 were degraded and are not presented here.

— THIS PAGE INTENTIONALLY LEFT BLANK —

Low-pass Filtered Velocity

Deployment I Low-pass filtered velocity (continued on next page)



Deployment I Low-pass filtered velocity

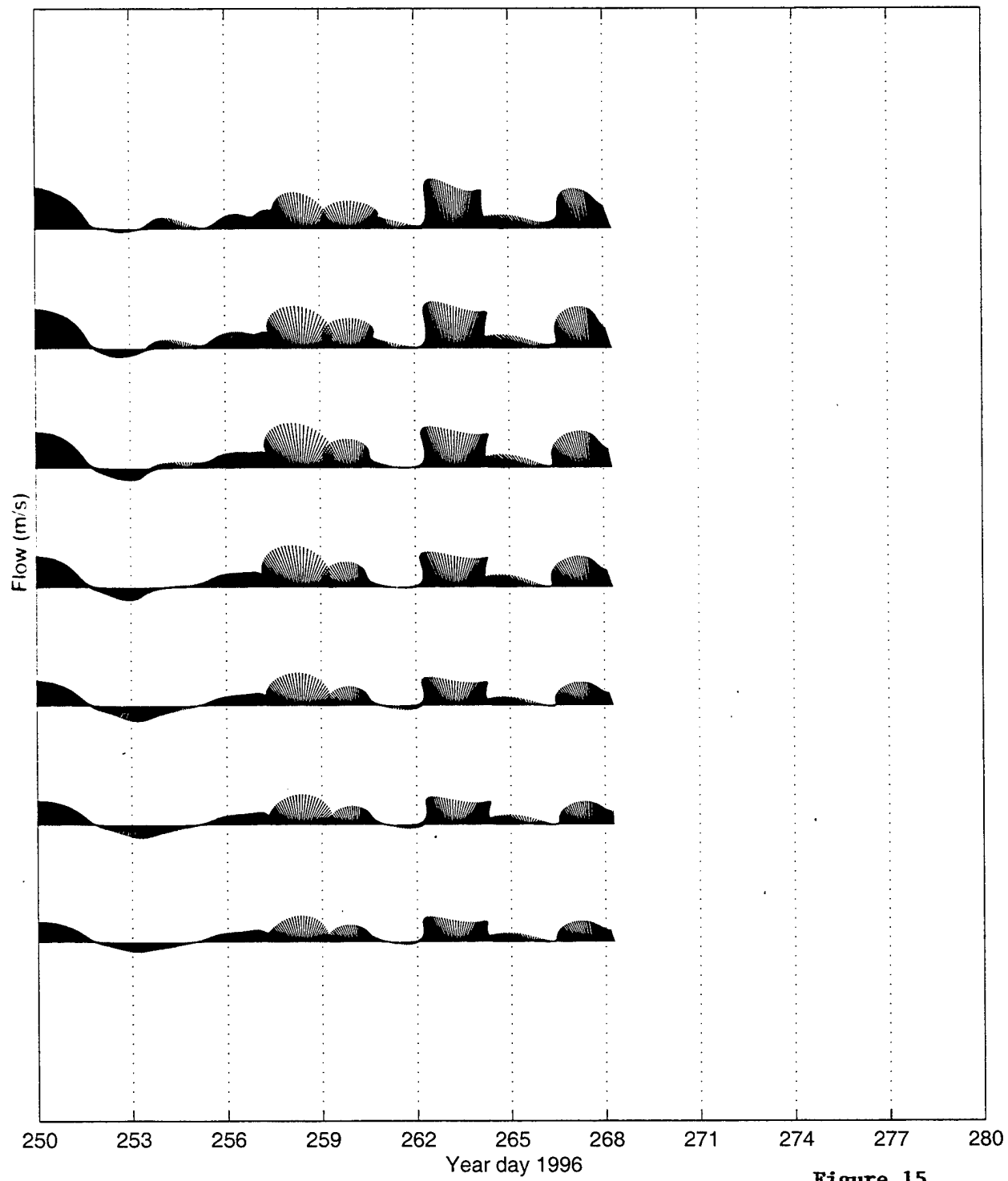
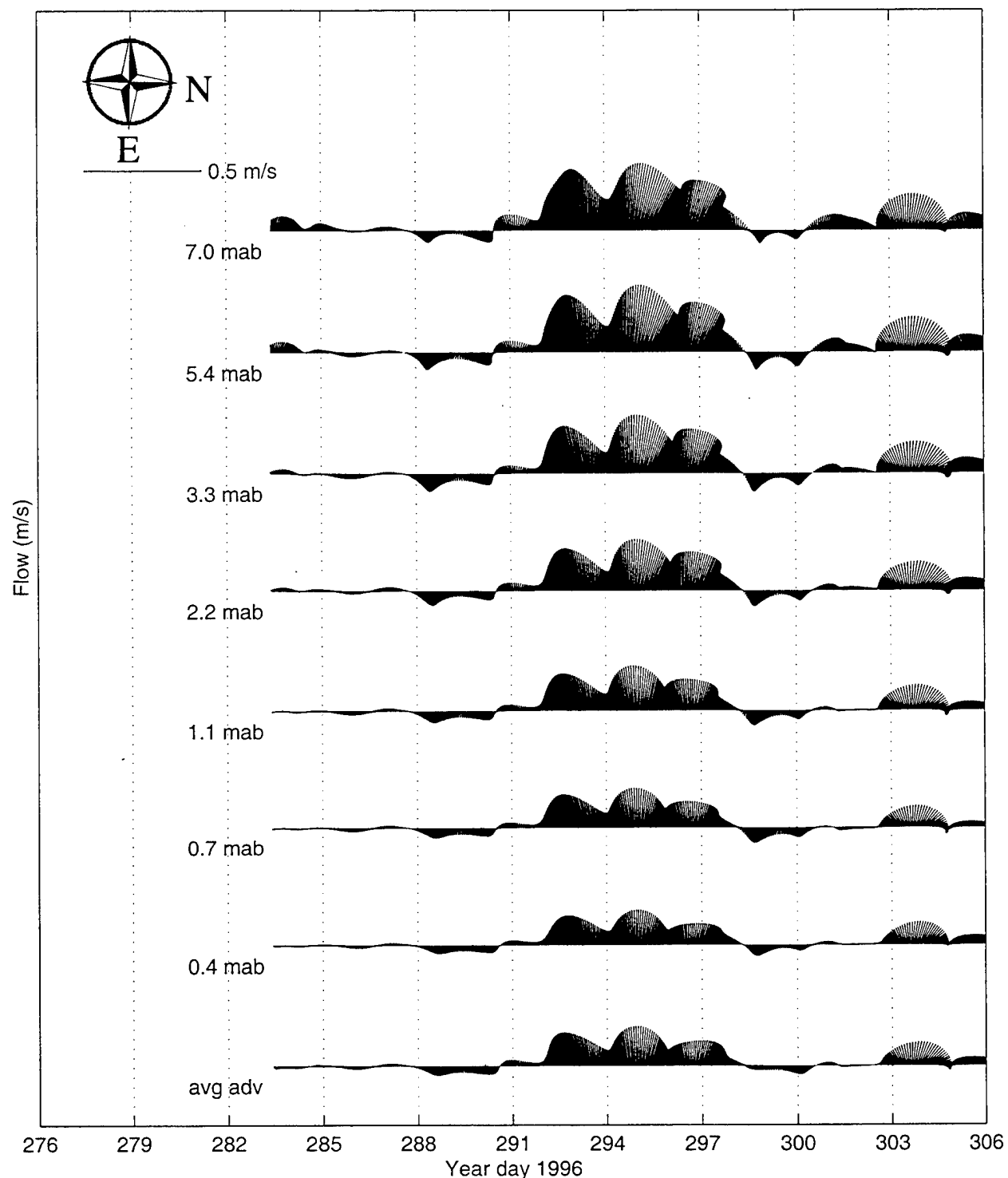


Figure 15

Deployment II Low-pass filtered velocity (continued on next page)



Deployment II Low-pass filtered velocity

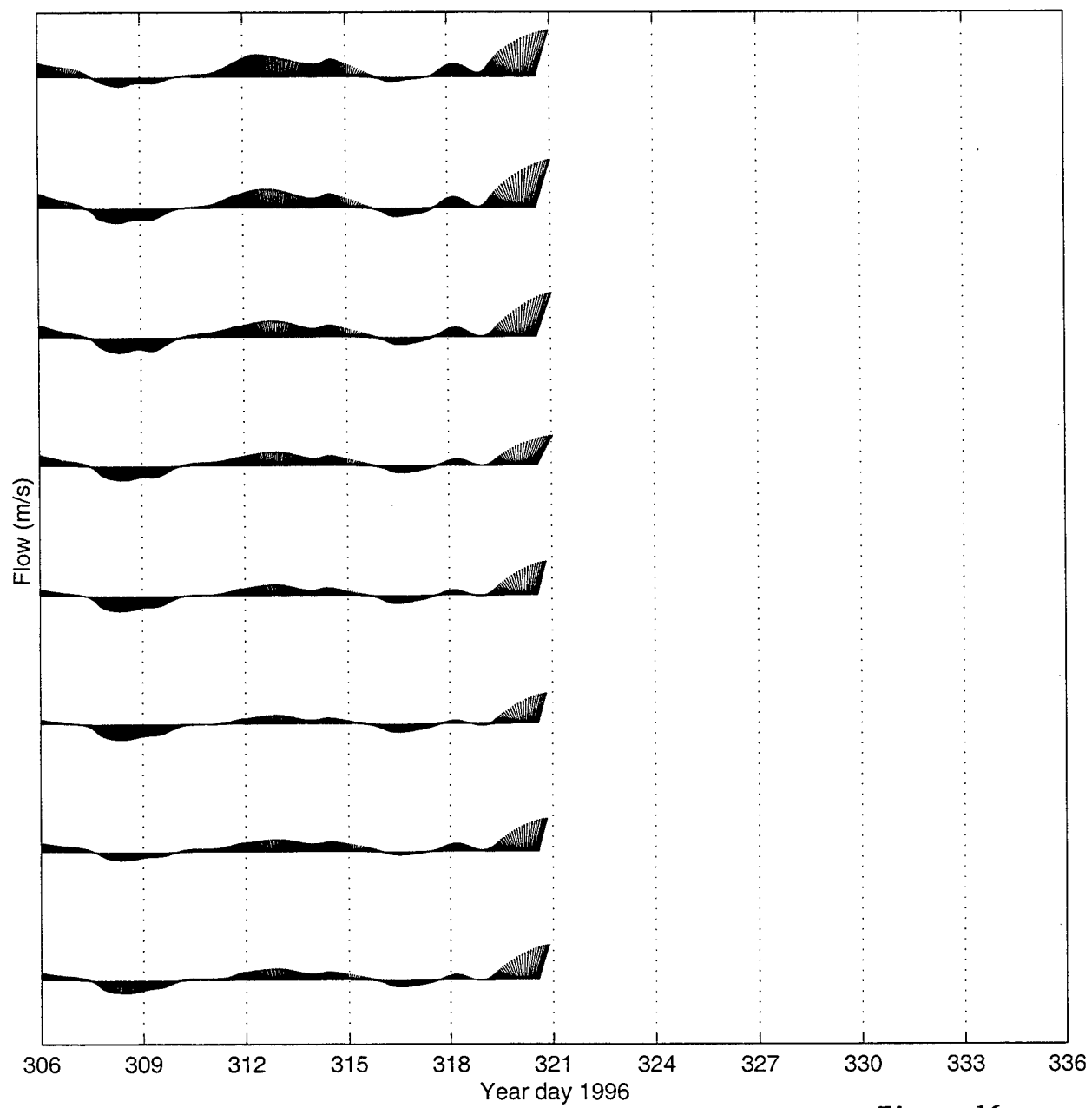
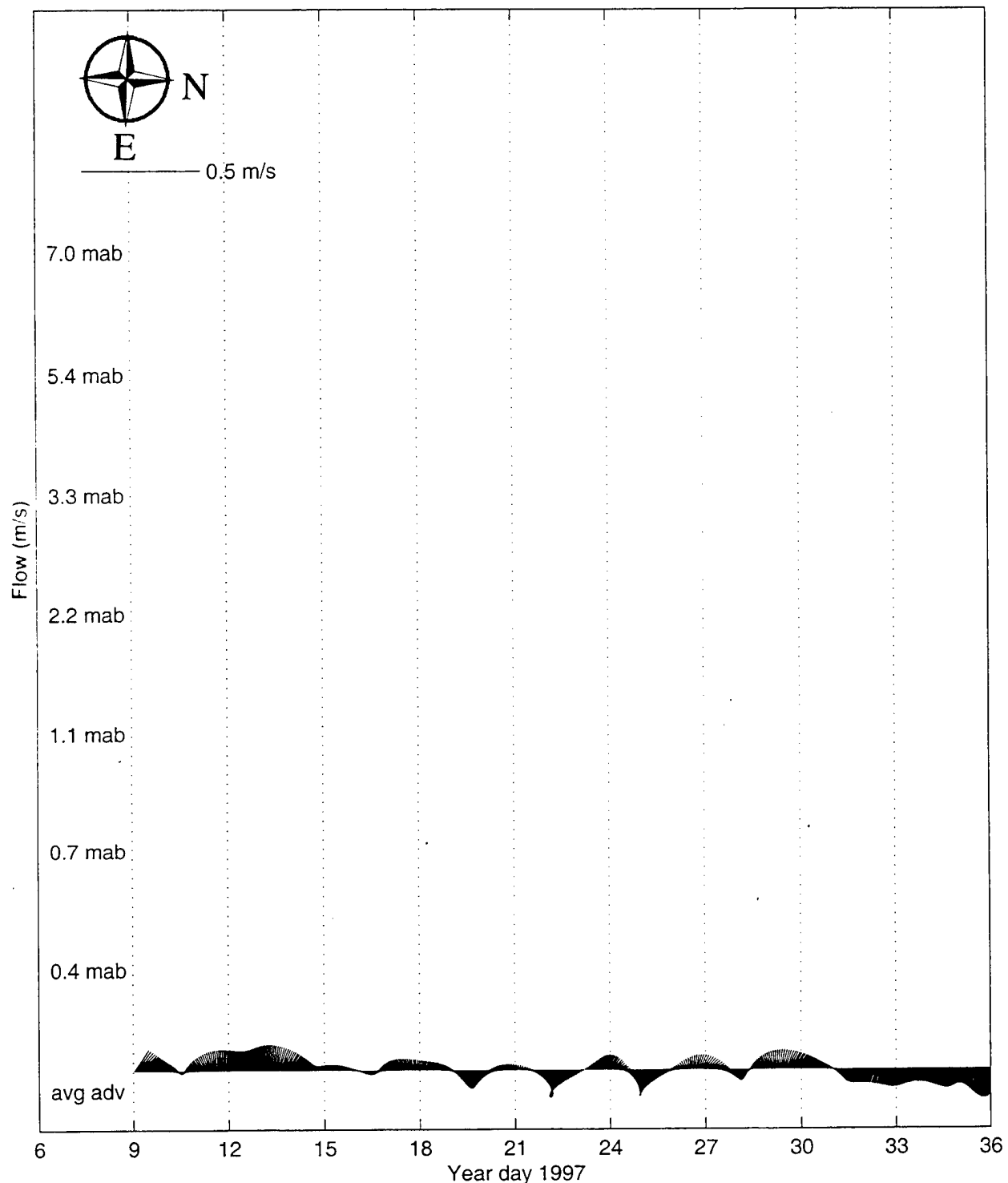


Figure 16

Deployment III Low-pass filtered velocity (continued on next page)



Deployment III Low-pass filtered velocity (continued on next page)

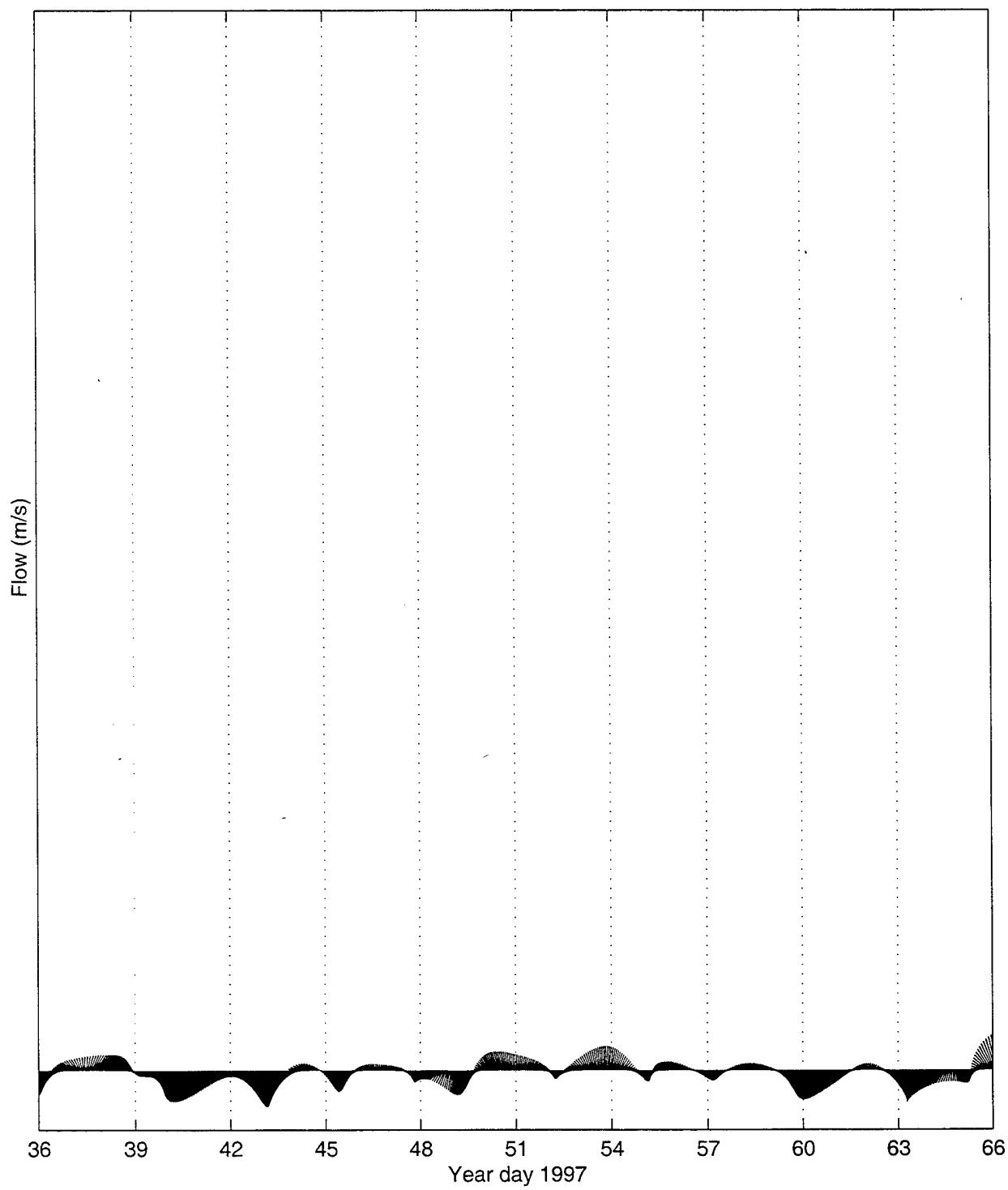


Figure 17

— THIS PAGE INTENTIONALLY LEFT BLANK —

Deployment III Low-pass filtered velocity

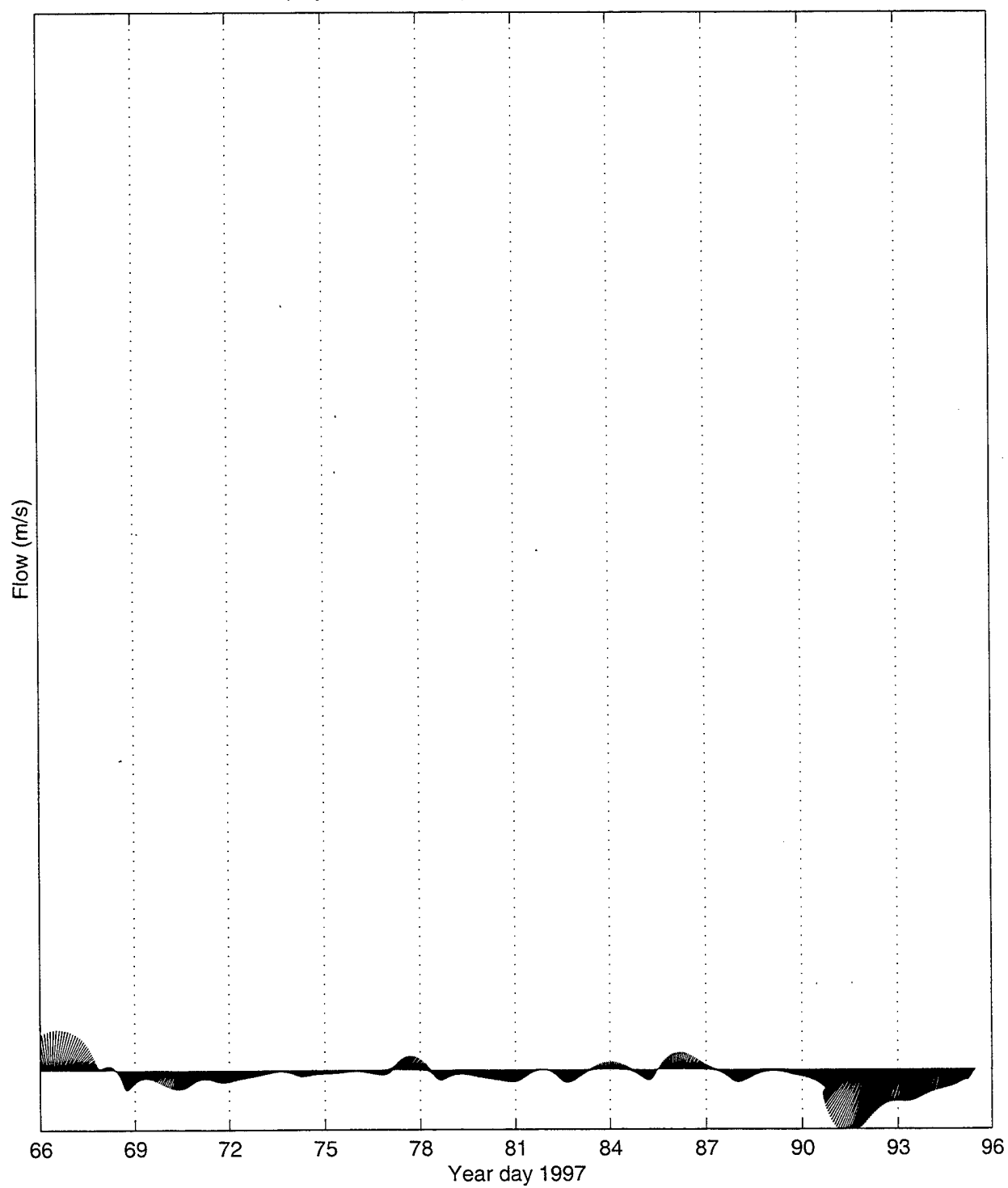
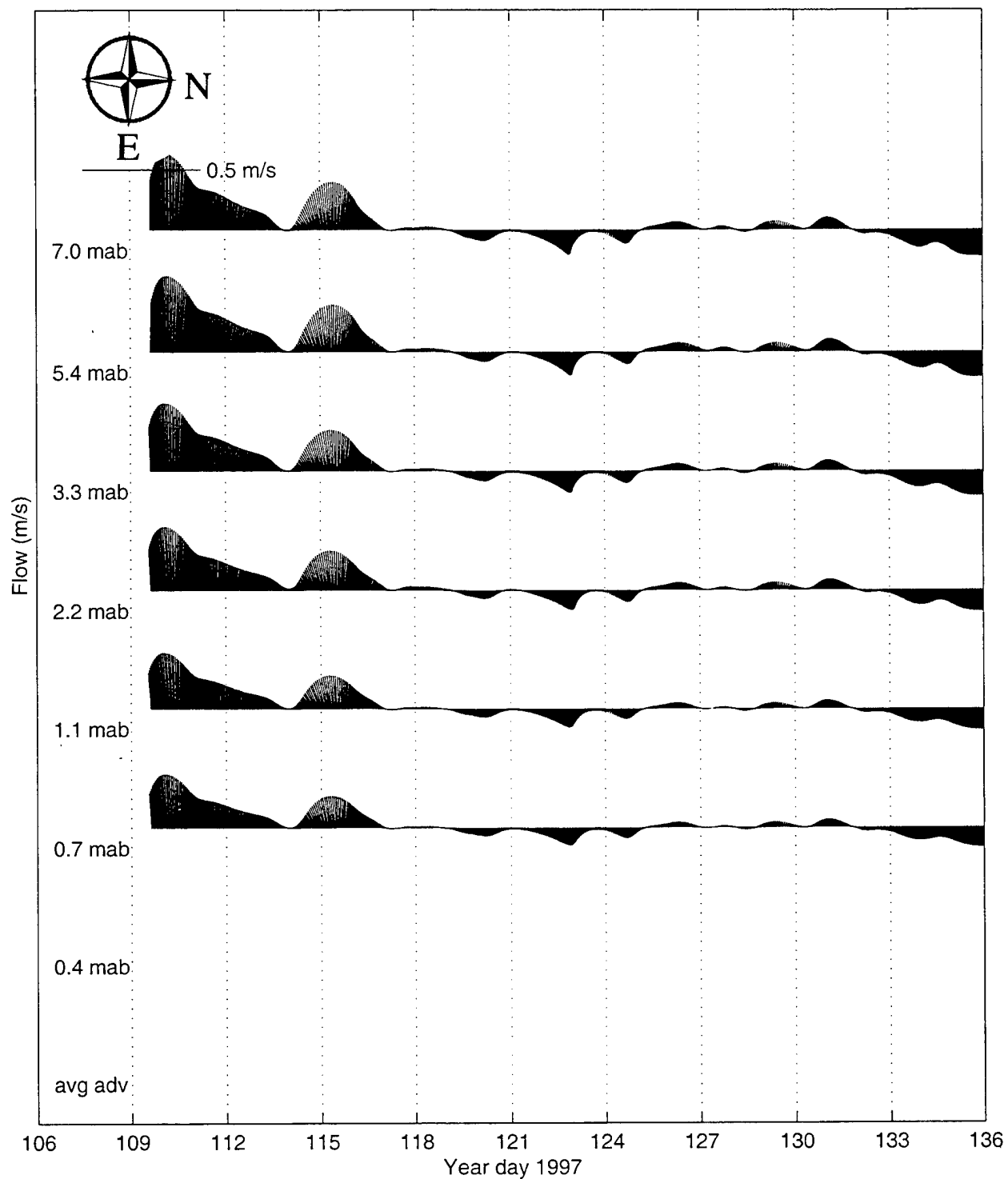


Figure 17 (continued)

Deployment IV Low-pass filtered velocity (continued on next page)



Deployment IV Low-pass filtered velocity

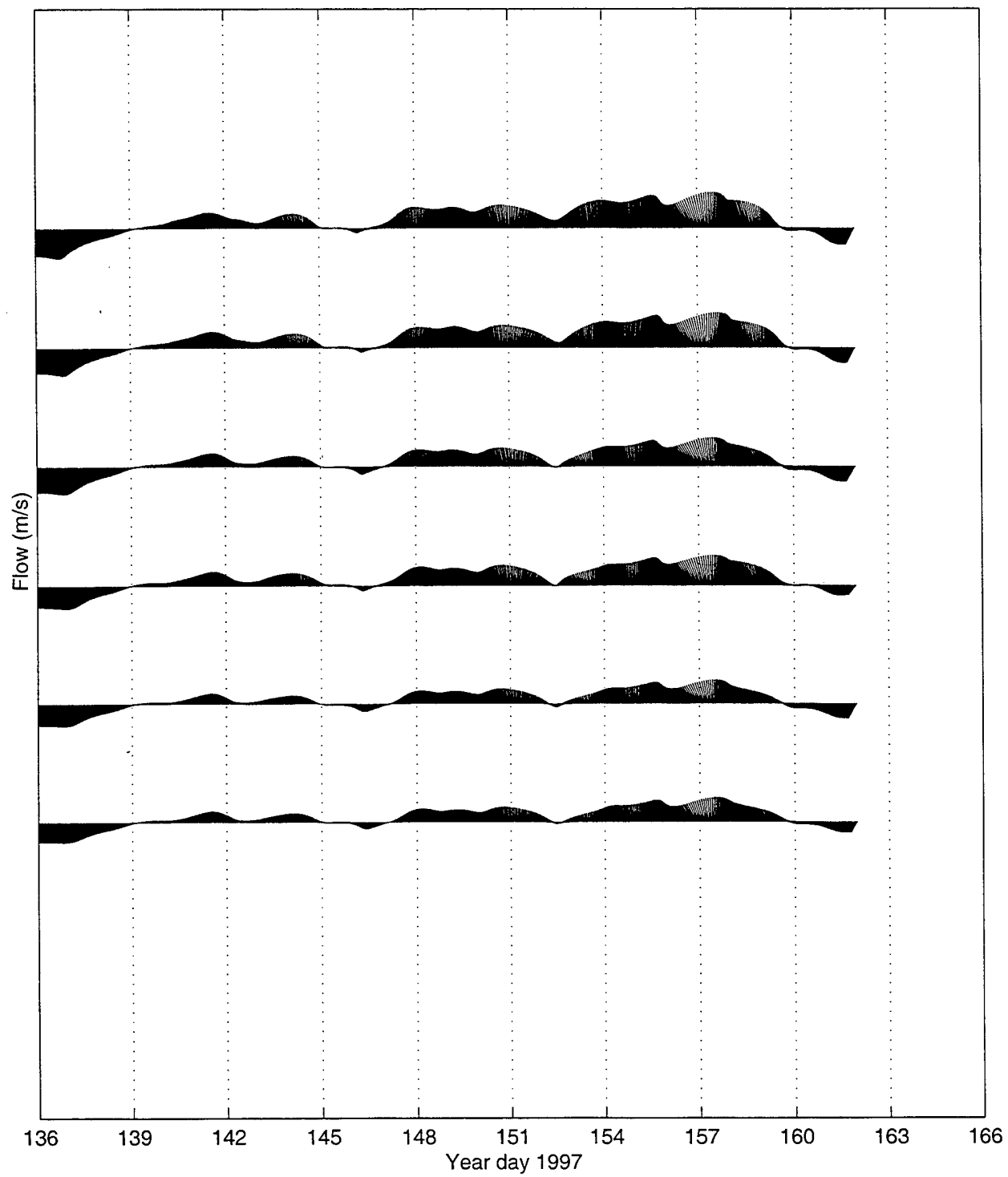
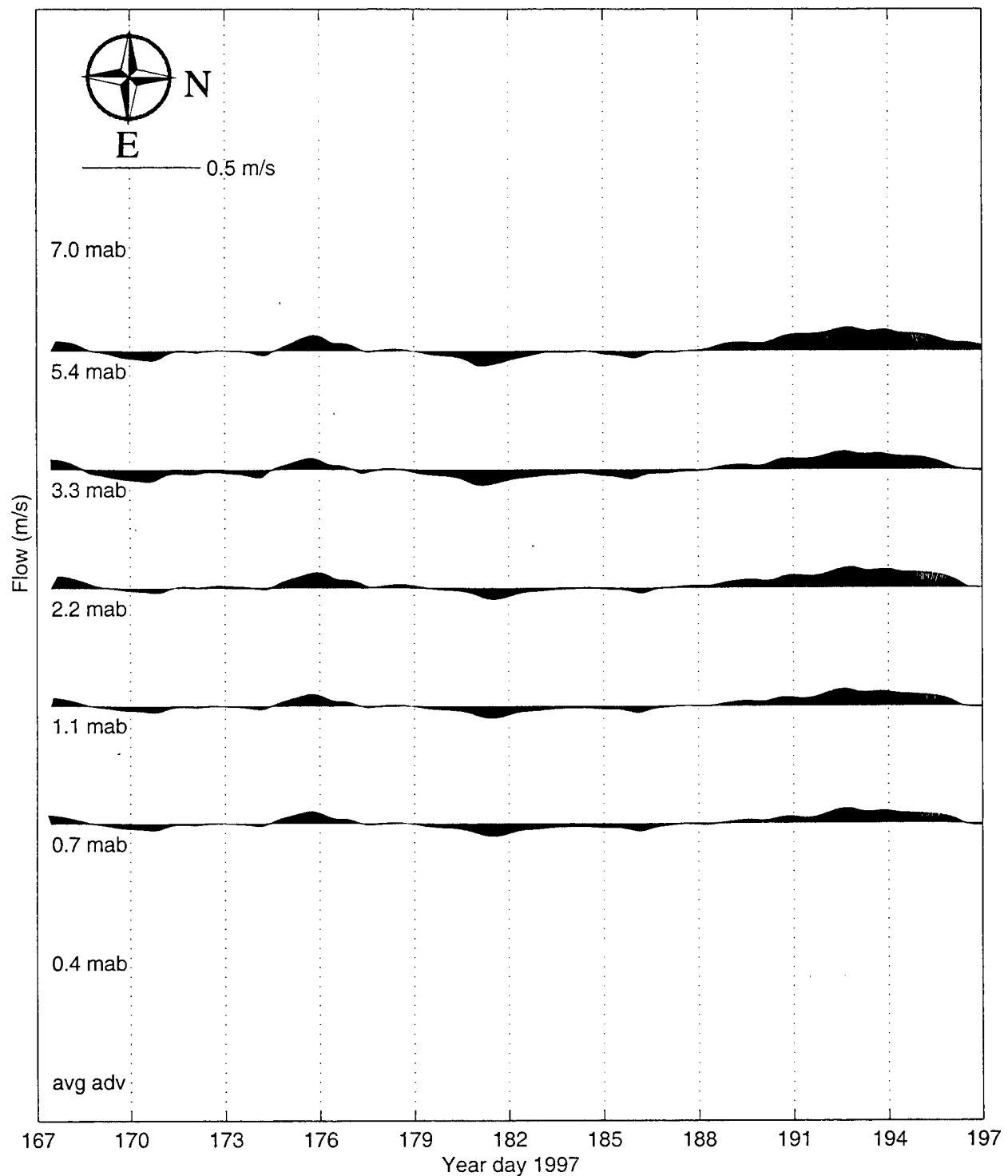


Figure 18

Deployment V Low-pass filtered velocity (continued on next page)



Deployment V Low-pass filtered velocity

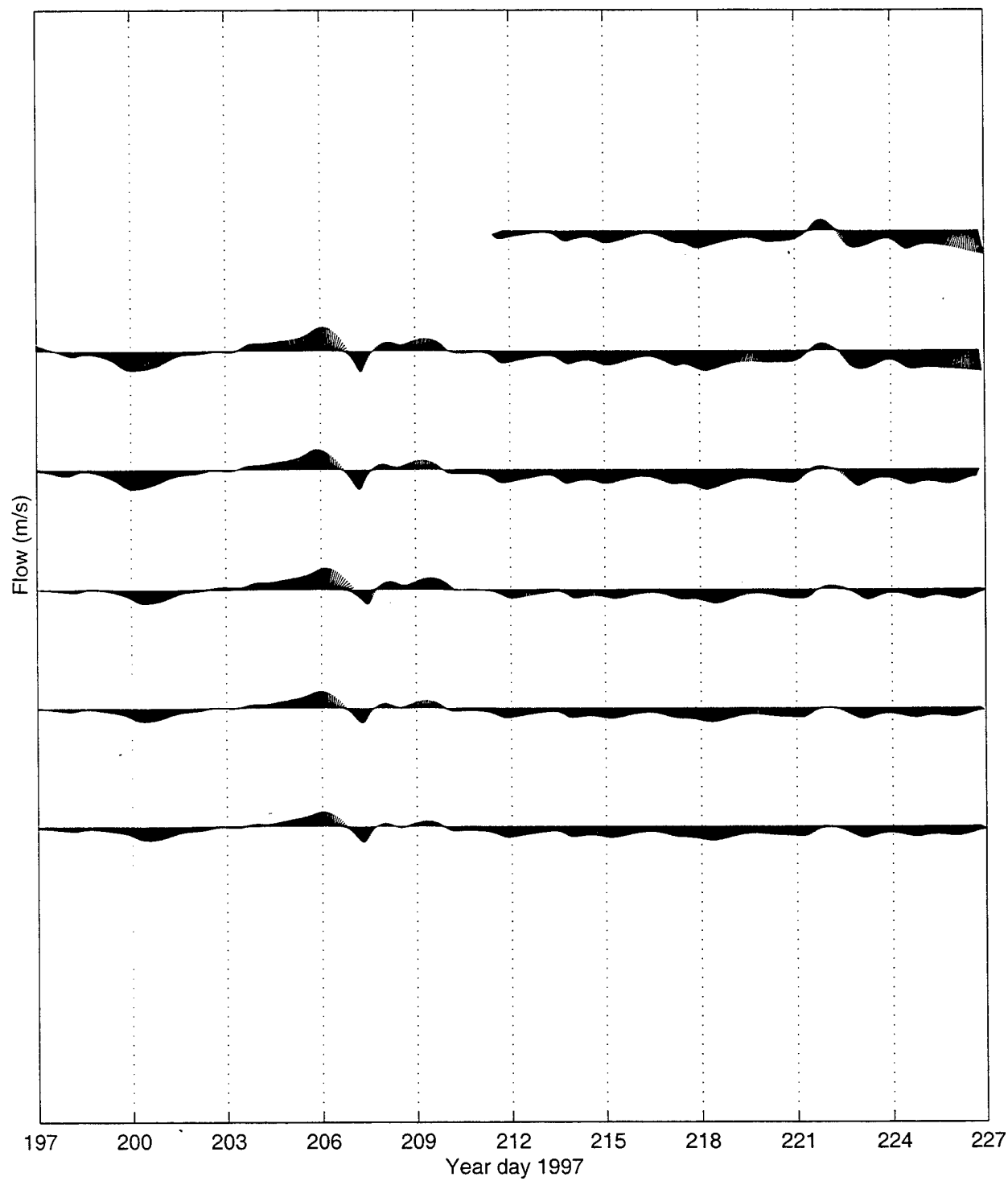
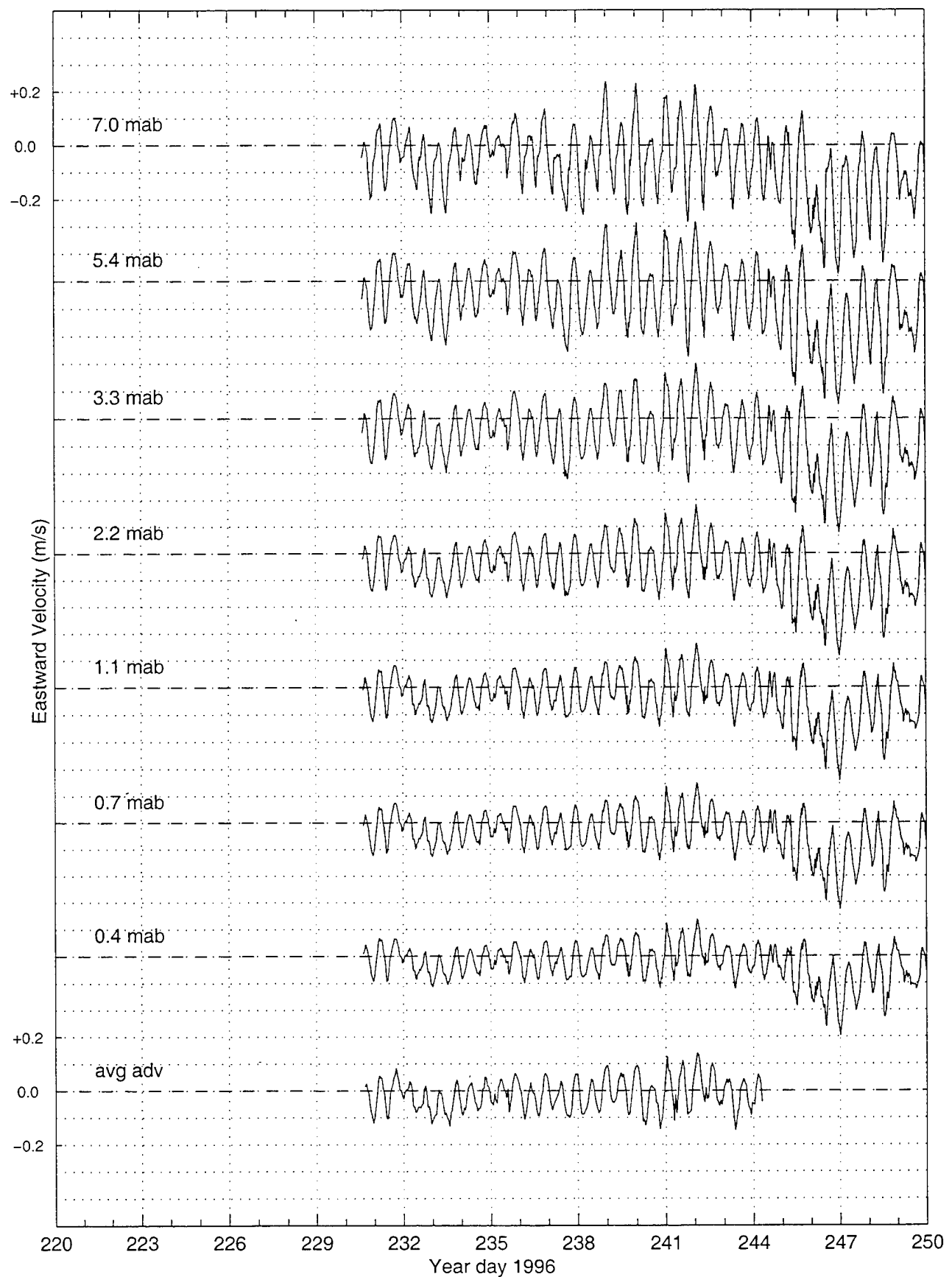


Figure 19

Eastward Velocity

Deployment I (continued on next page)



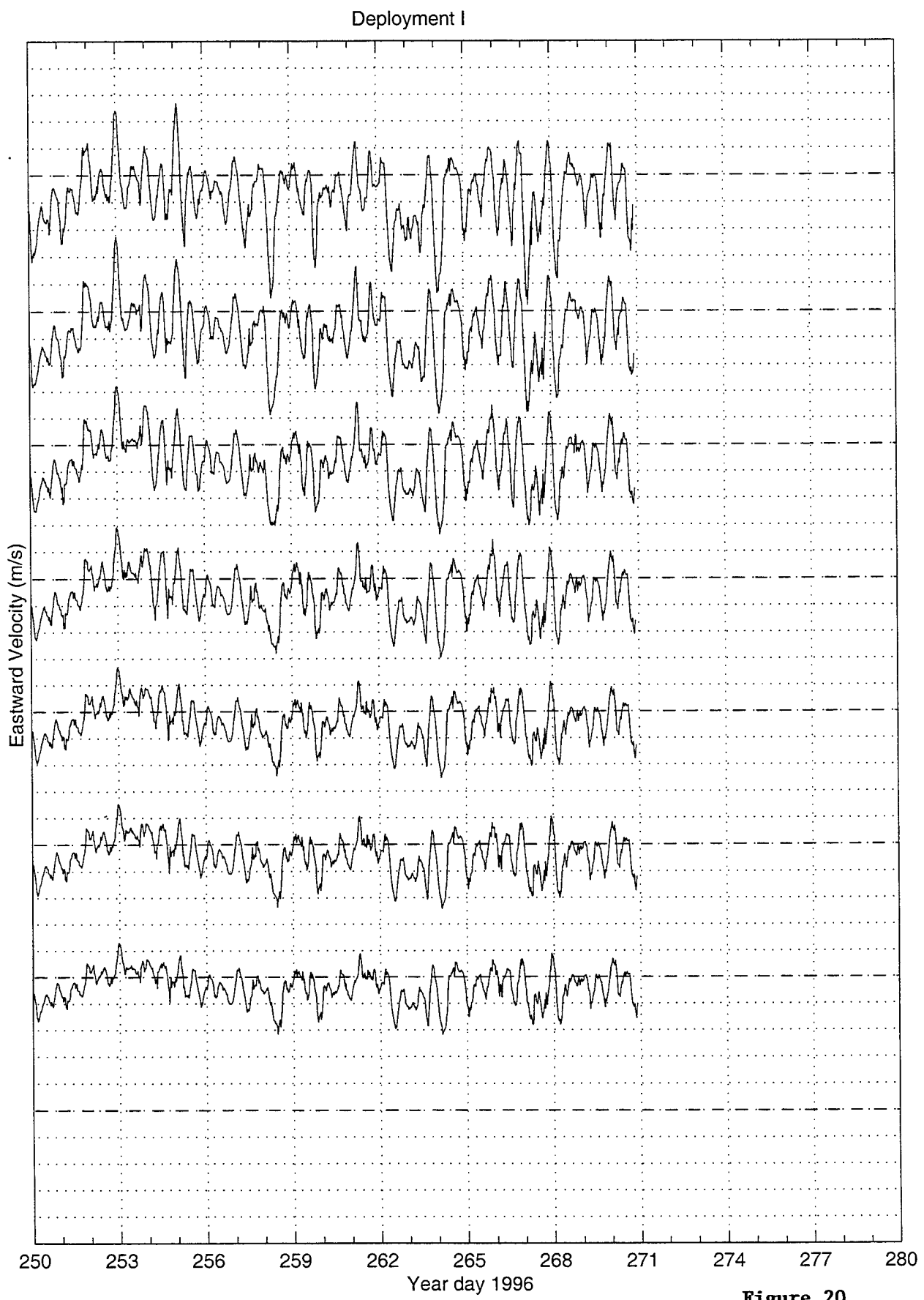
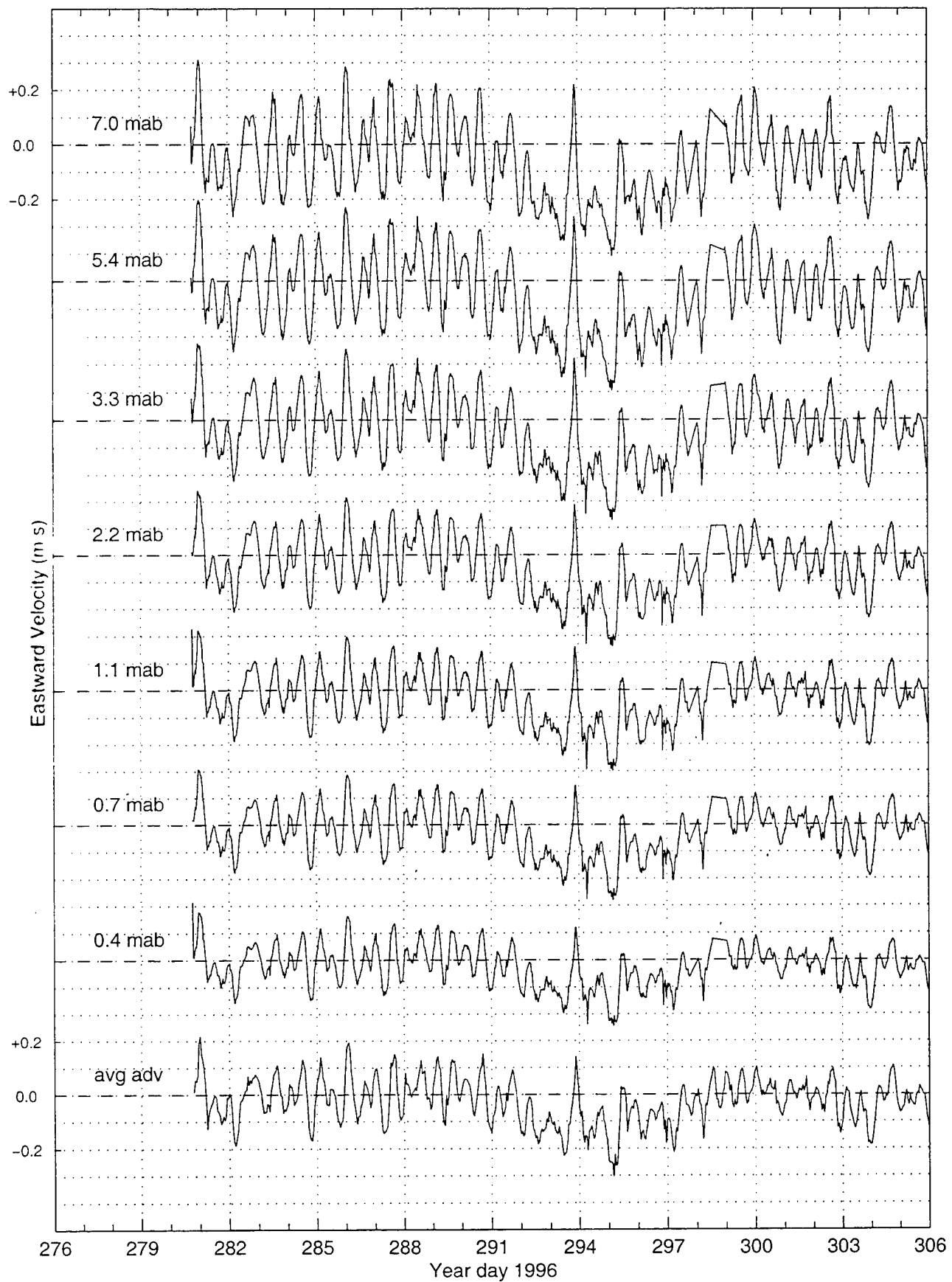


Figure 20

Deployment II (continued on next page)



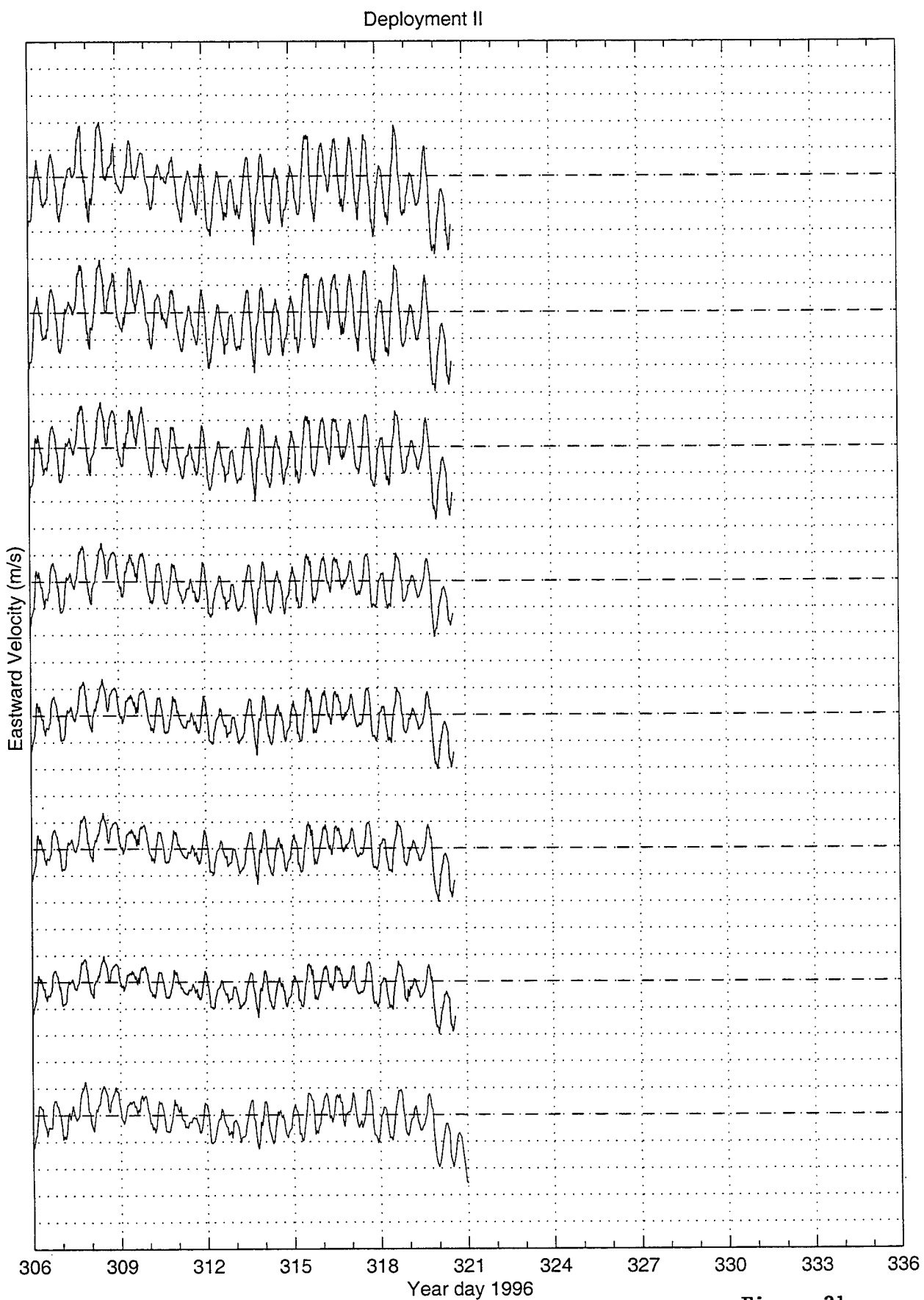
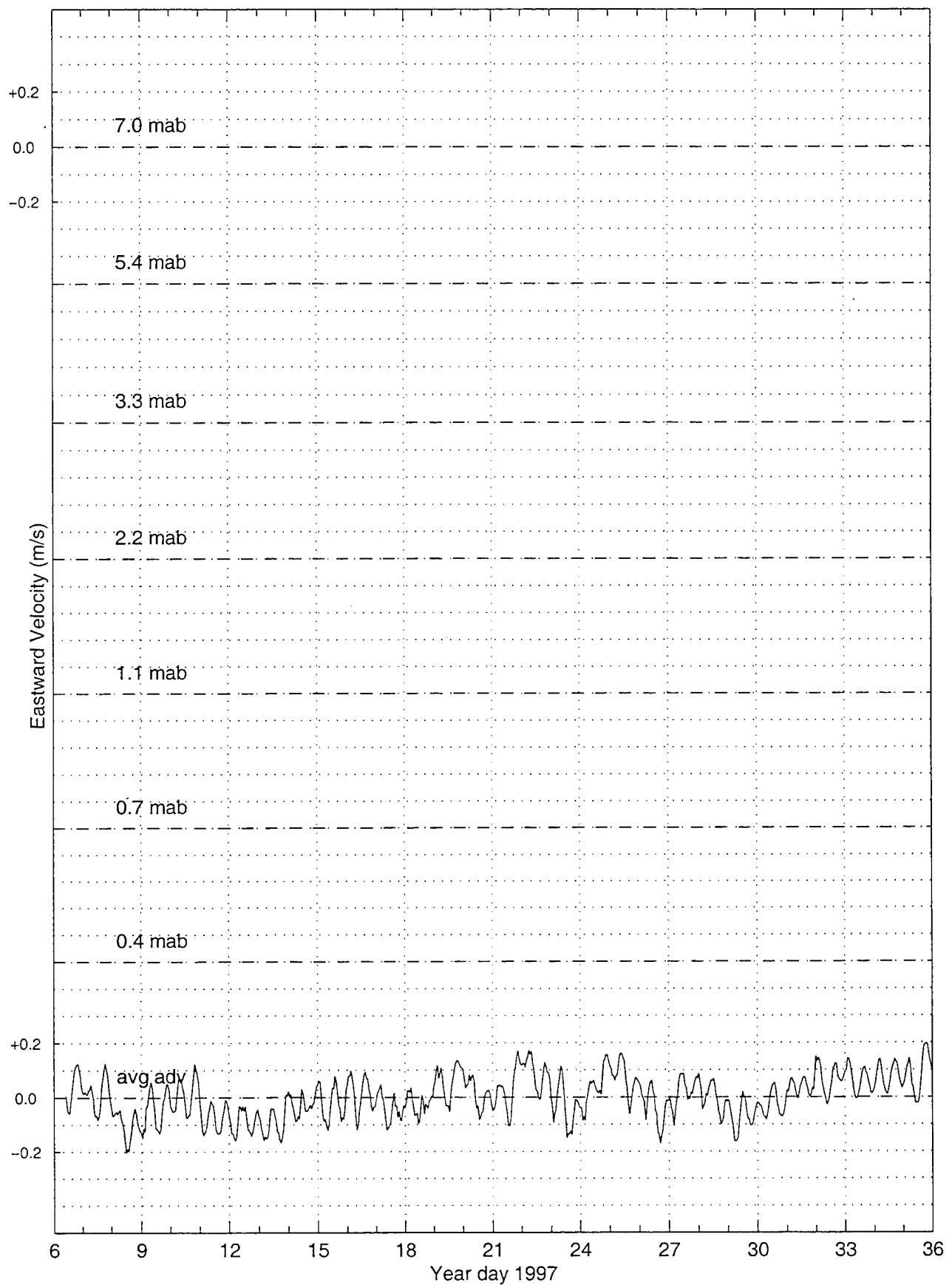


Figure 21

Deployment III (continued on next page)



Deployment III (continued on next page)

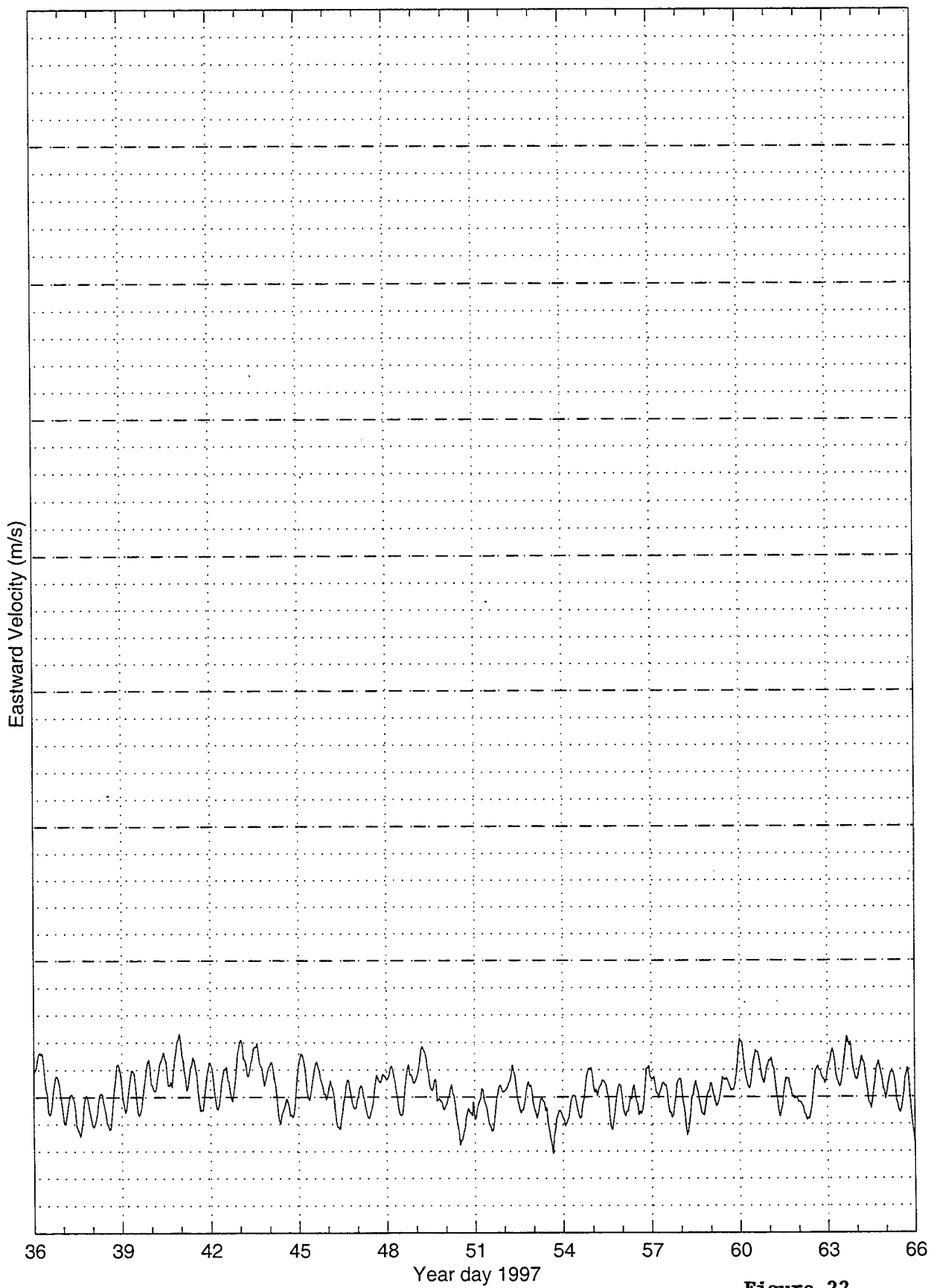


Figure 22

— THIS PAGE INTENTIONALLY LEFT BLANK —

Deployment III

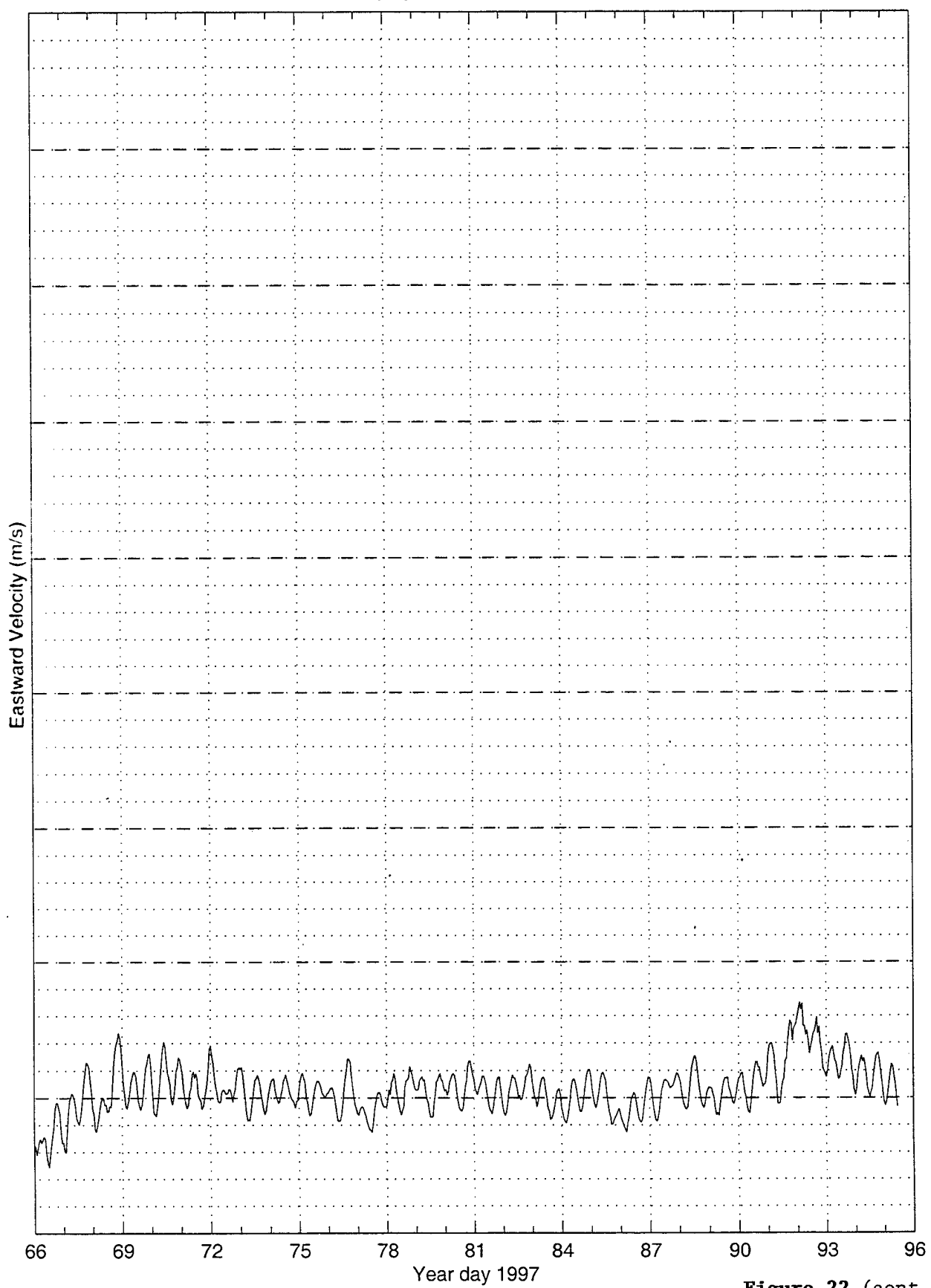
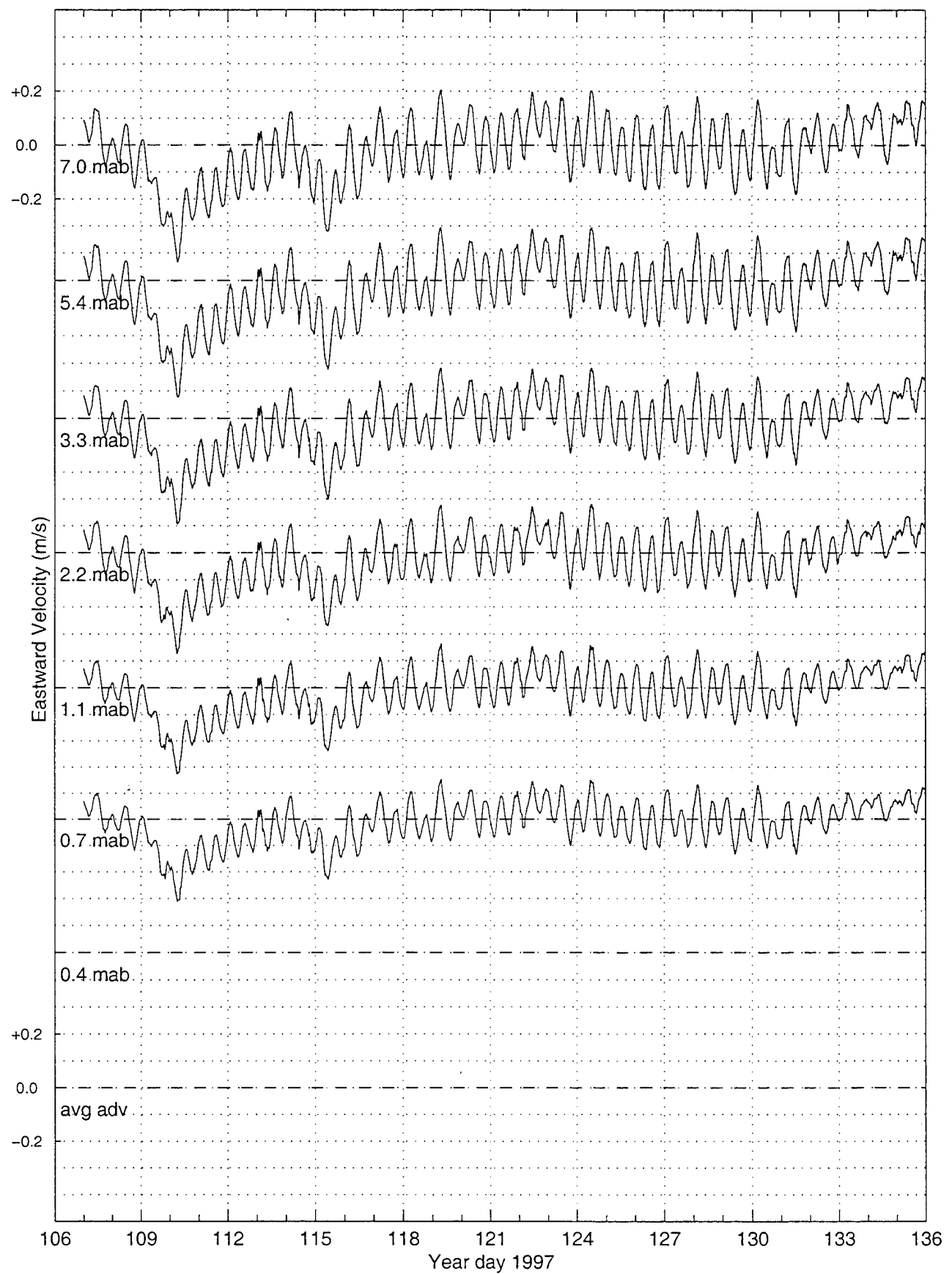


Figure 22 (cont.)

Deployment IV (continued on next page)



Deployment IV

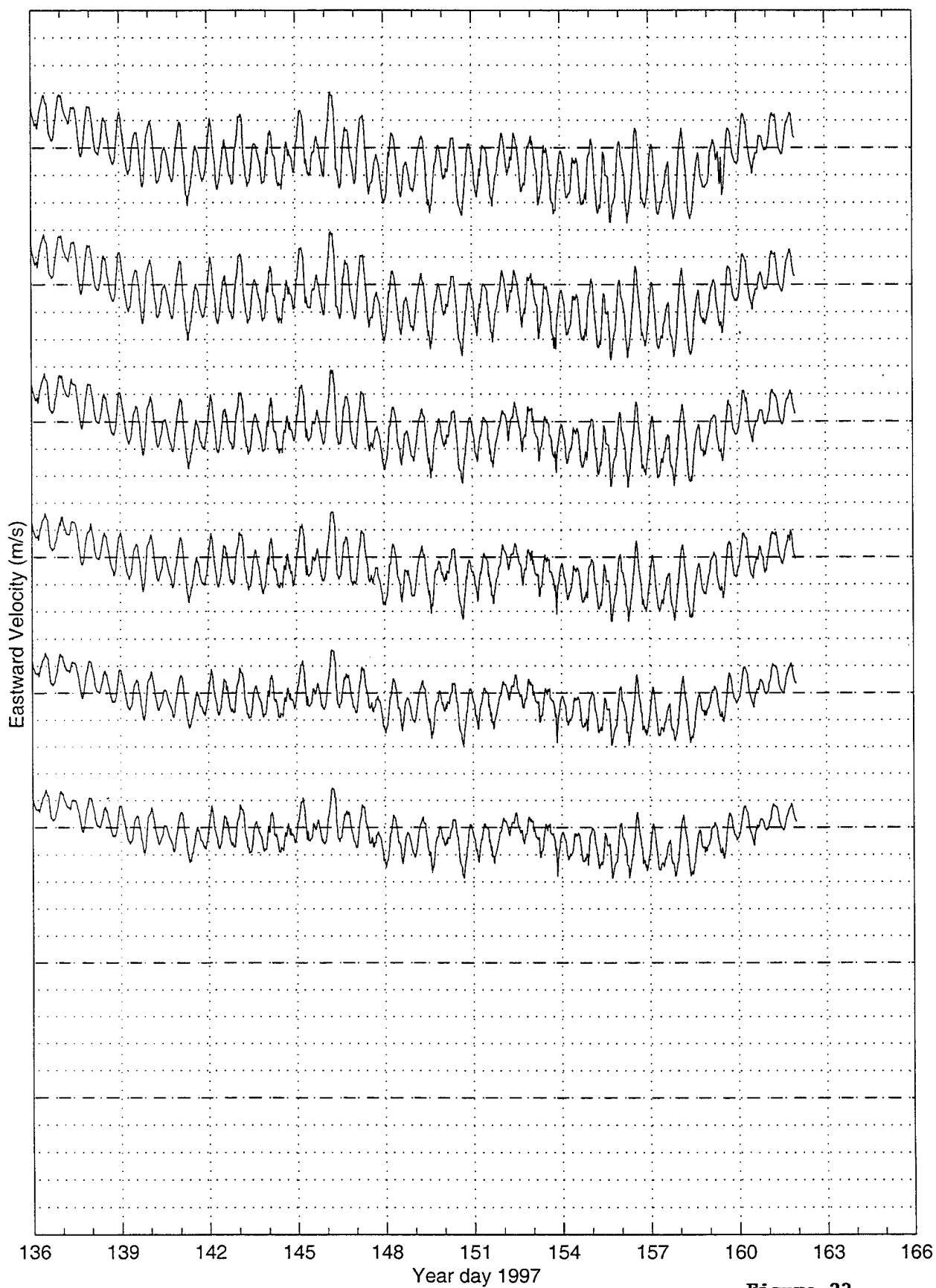
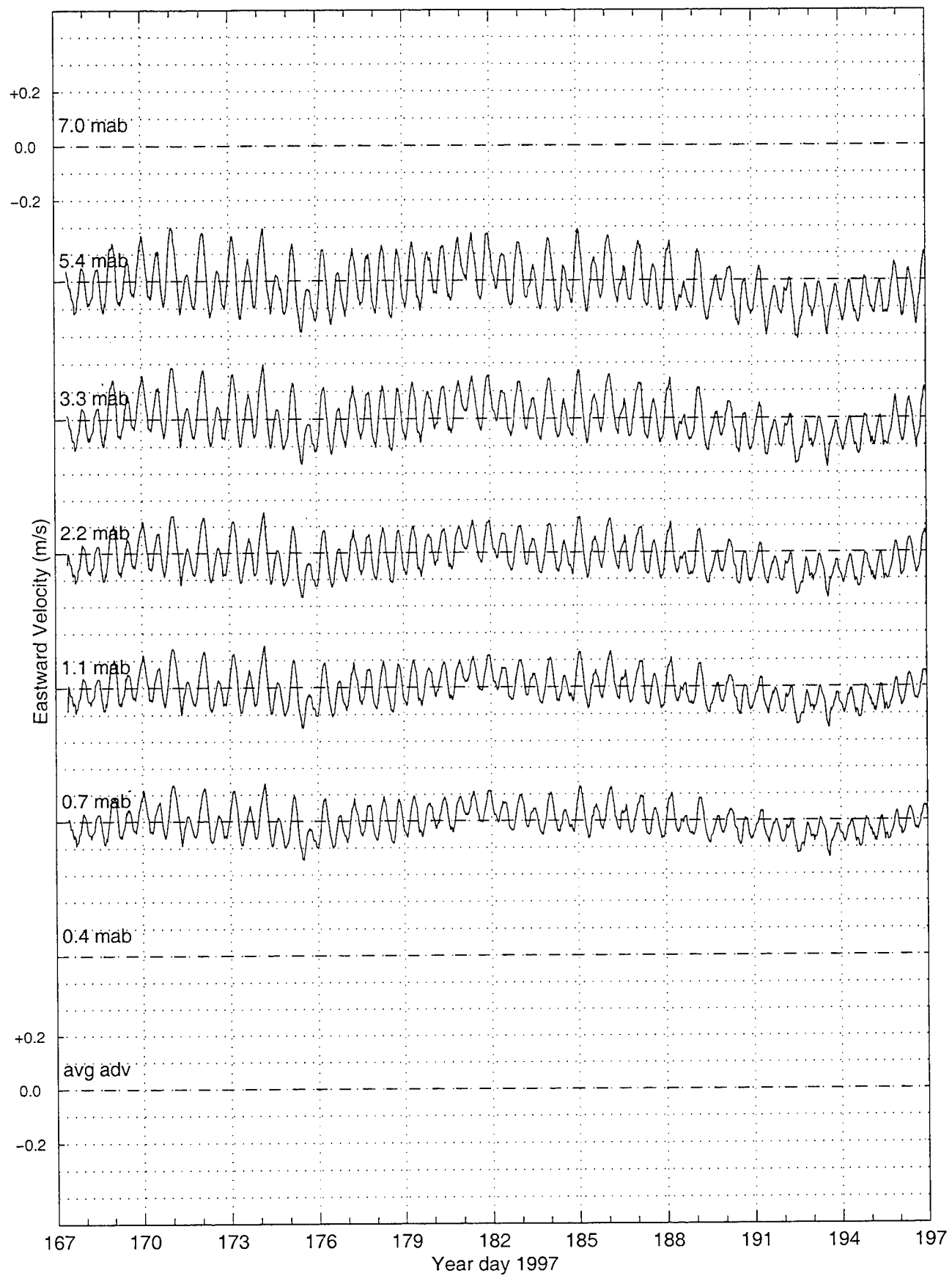


Figure 23

Deployment V (continued on next page)



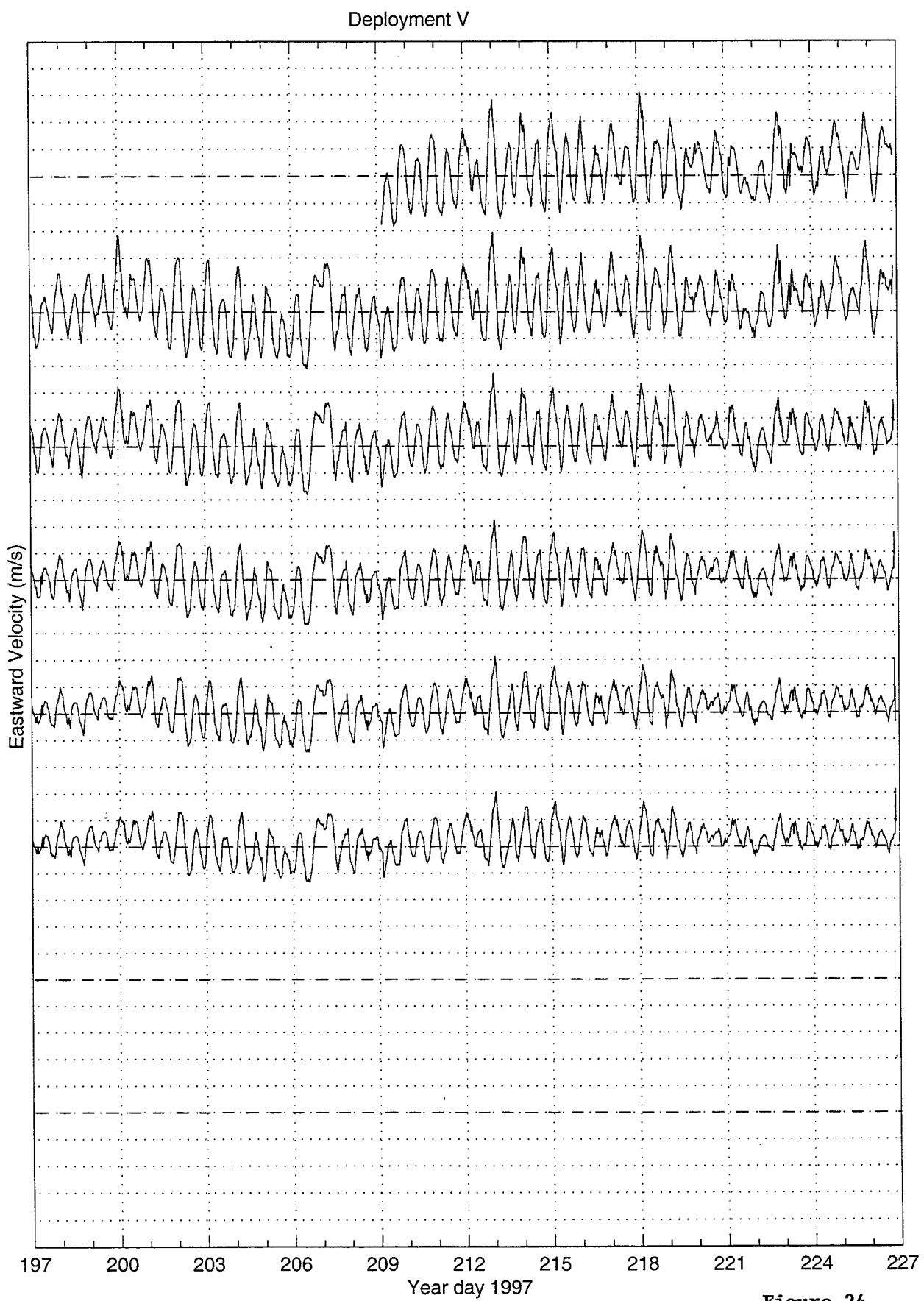
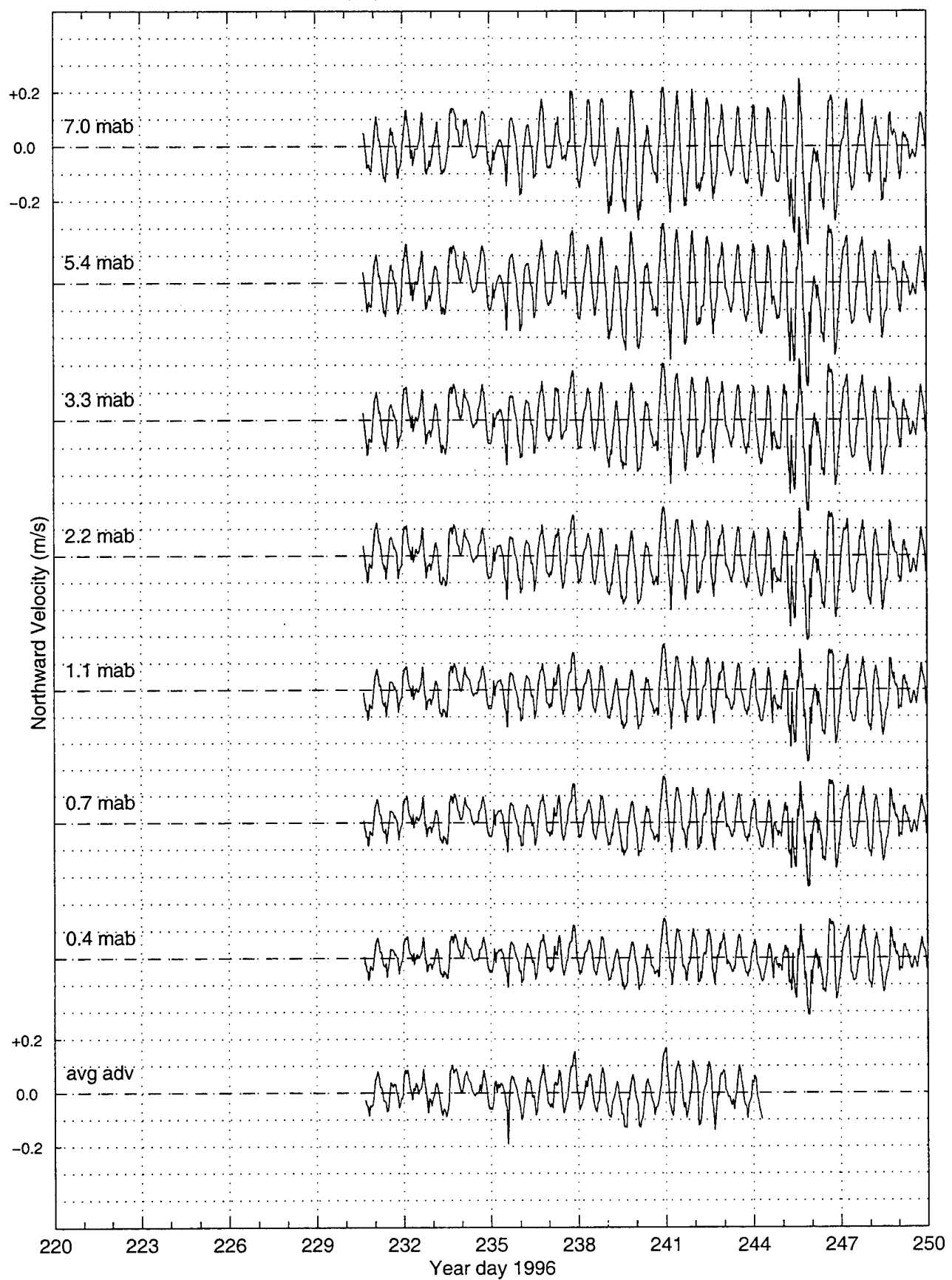


Figure 24

Northward Velocity

Deployment I (continued on next page)



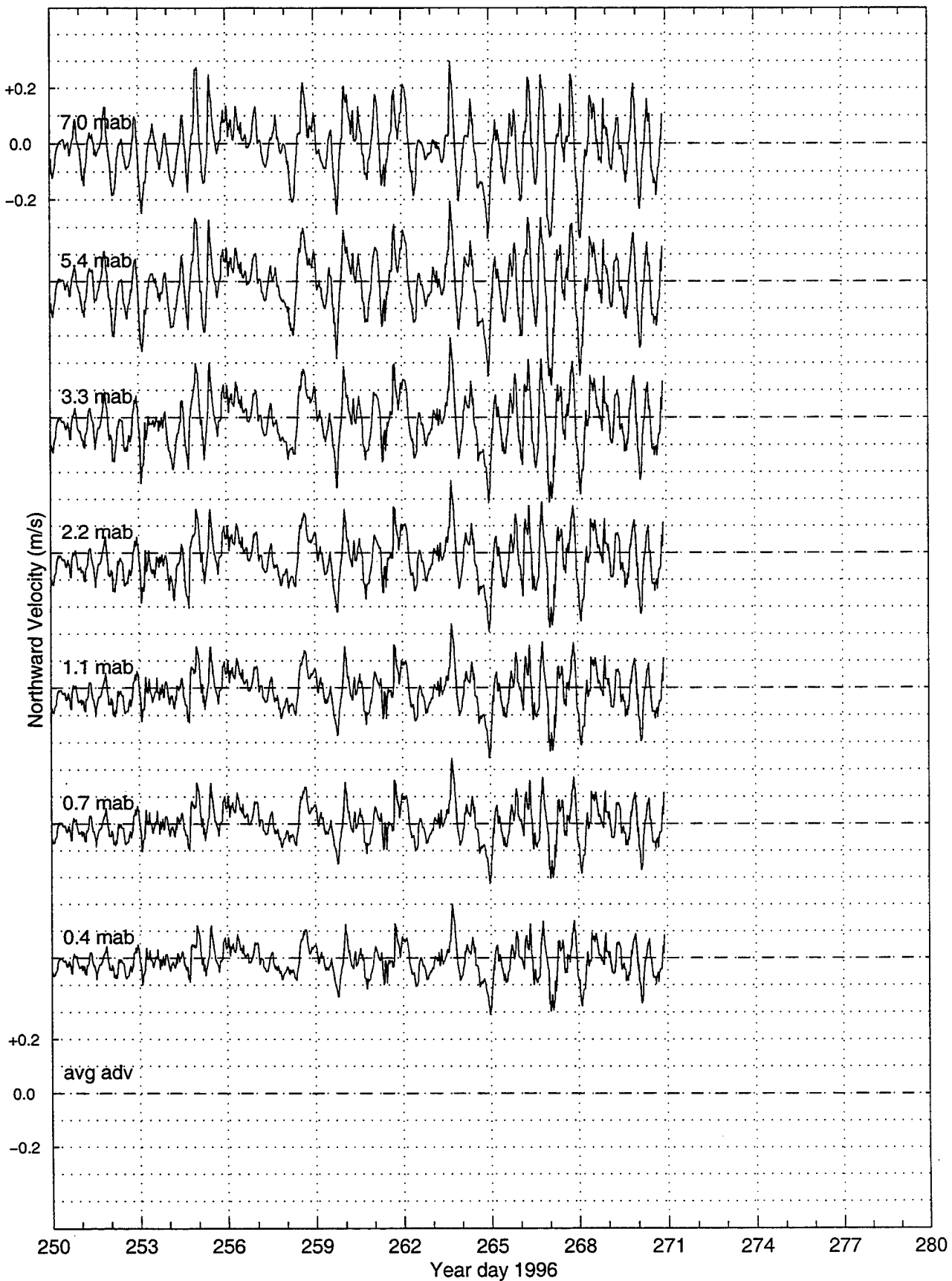
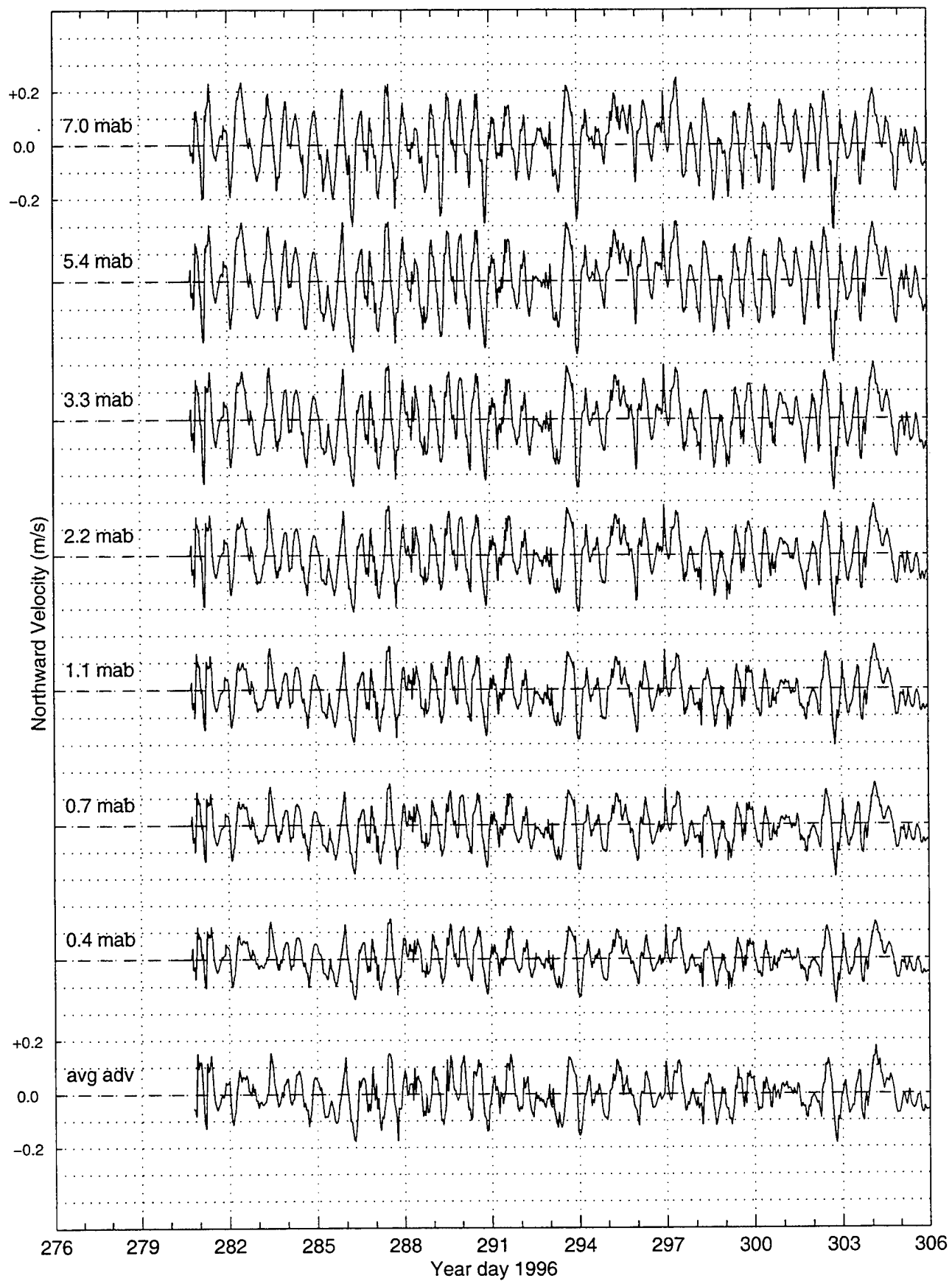


Figure 25

Deployment II (continued on next page)



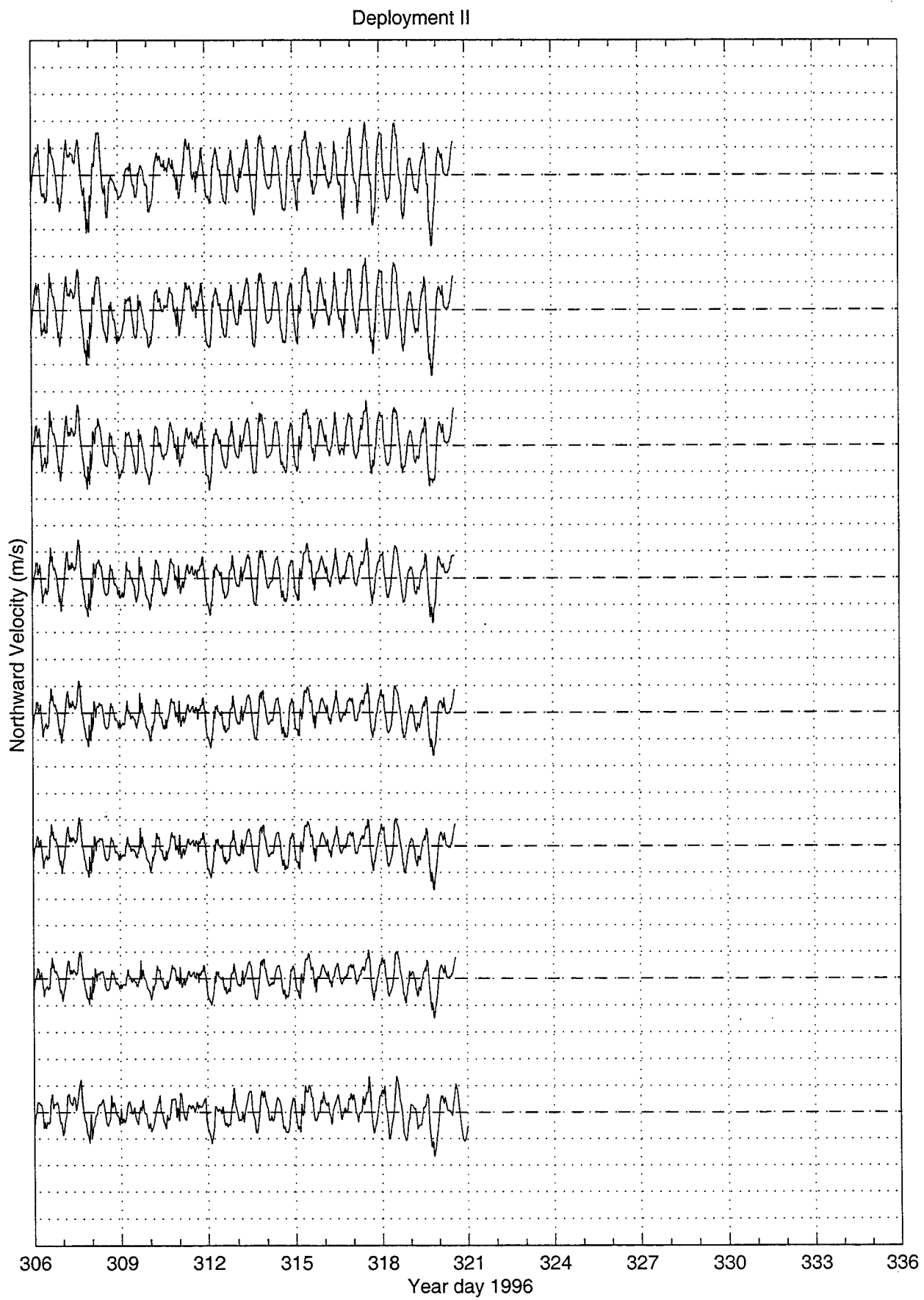
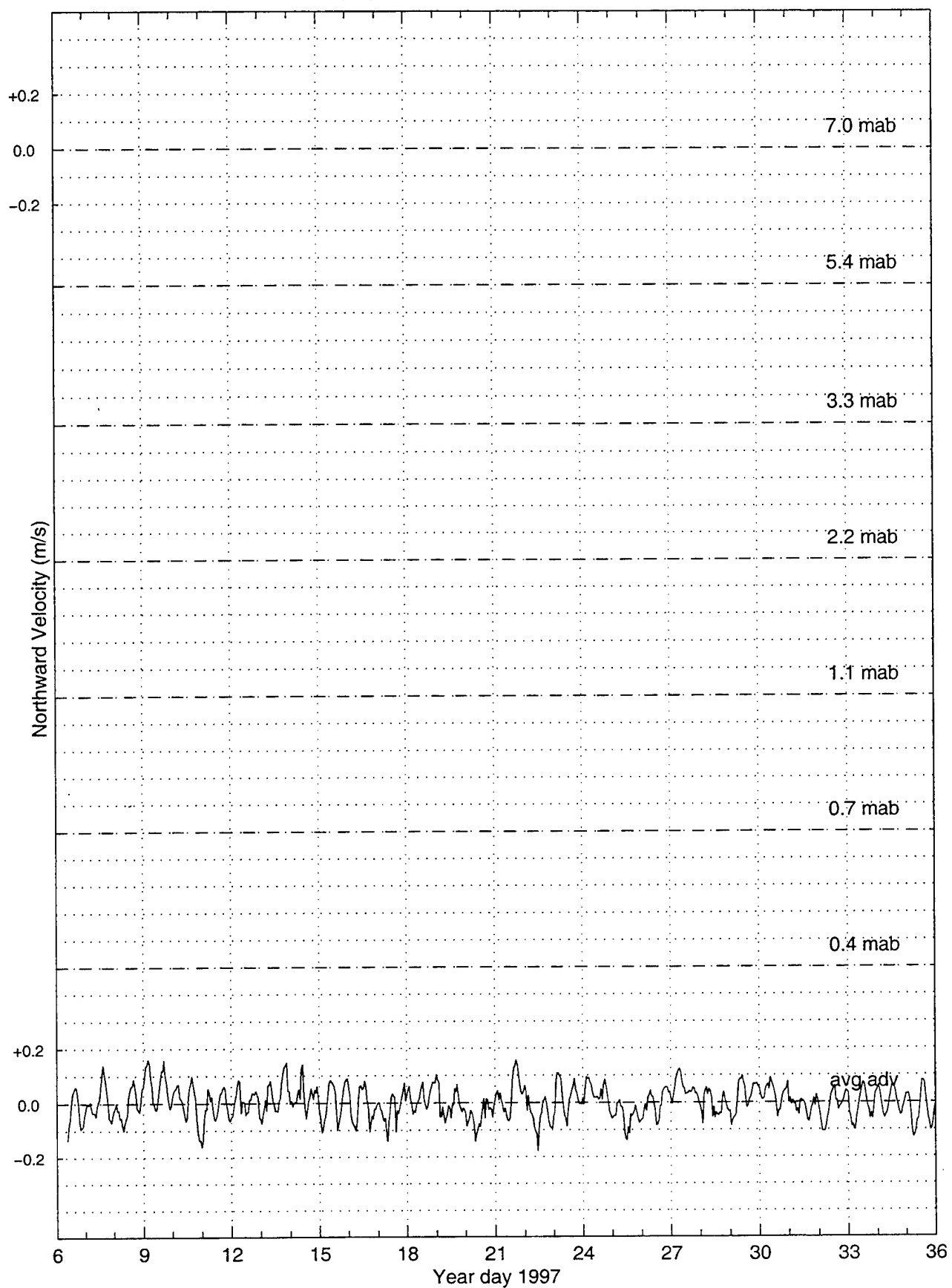


Figure 26

Deployment III (continued on next page)



Deployment III (continued on next page)

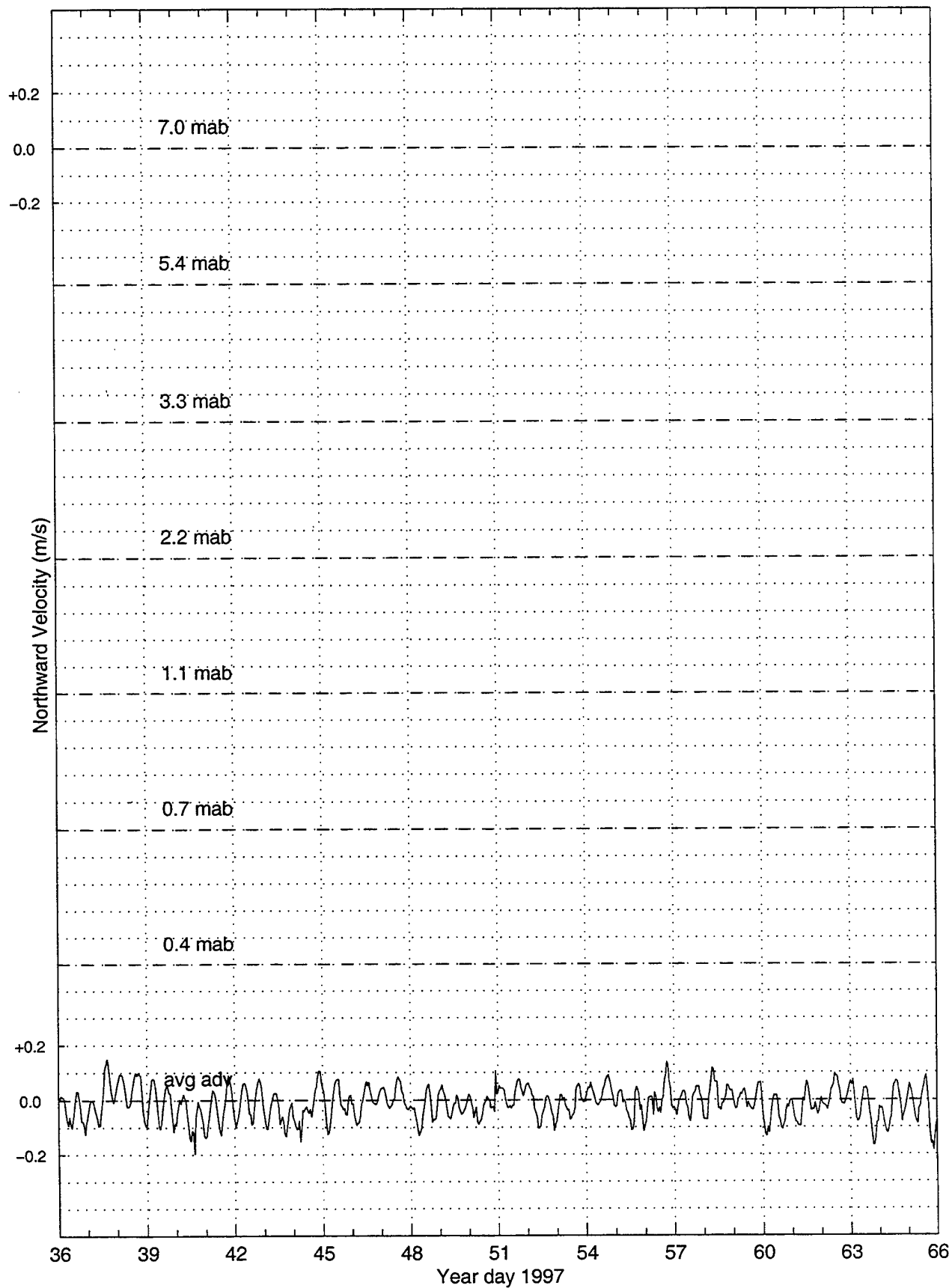


Figure 27

— THIS PAGE INTENTIONALLY LEFT BLANK —

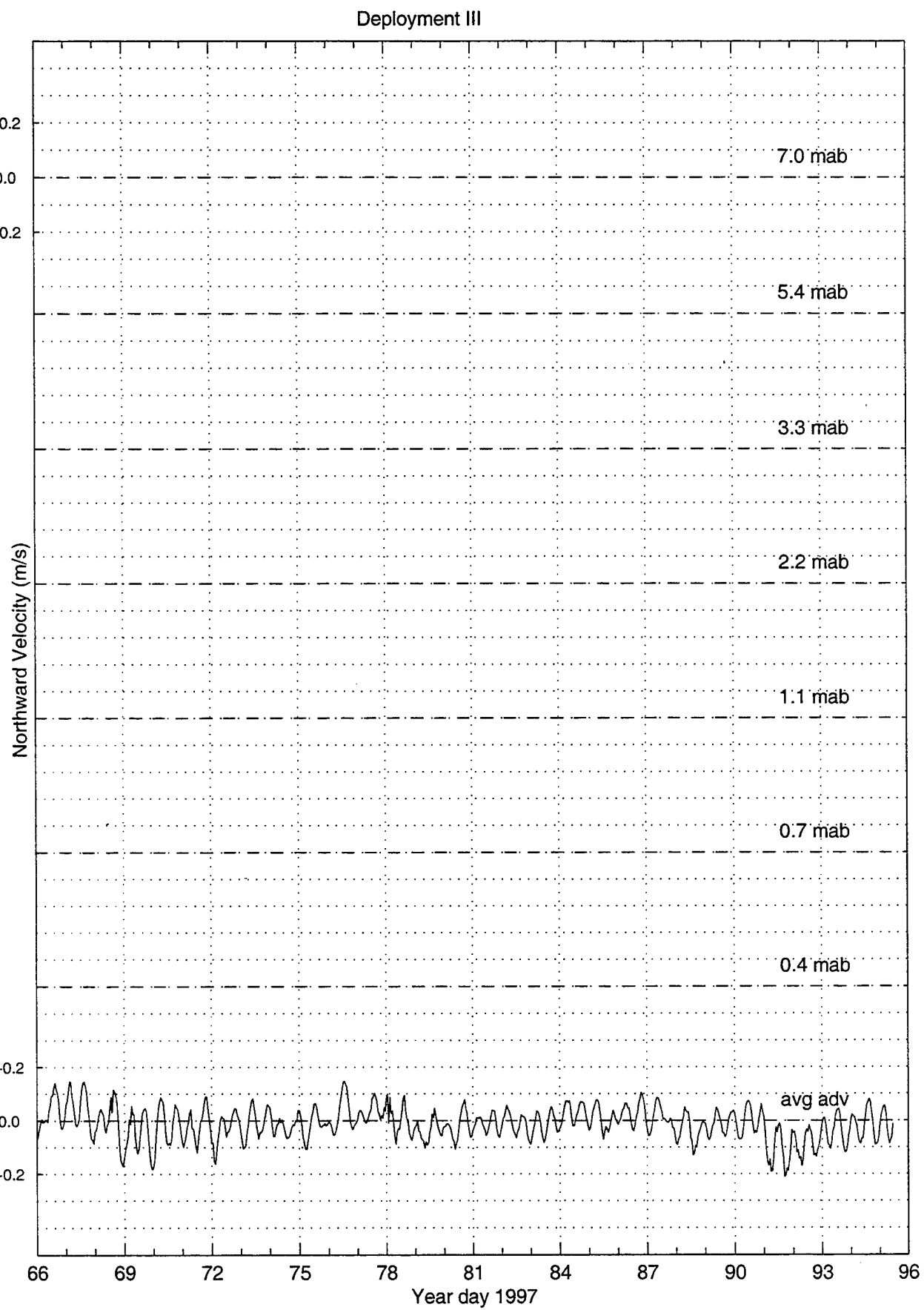
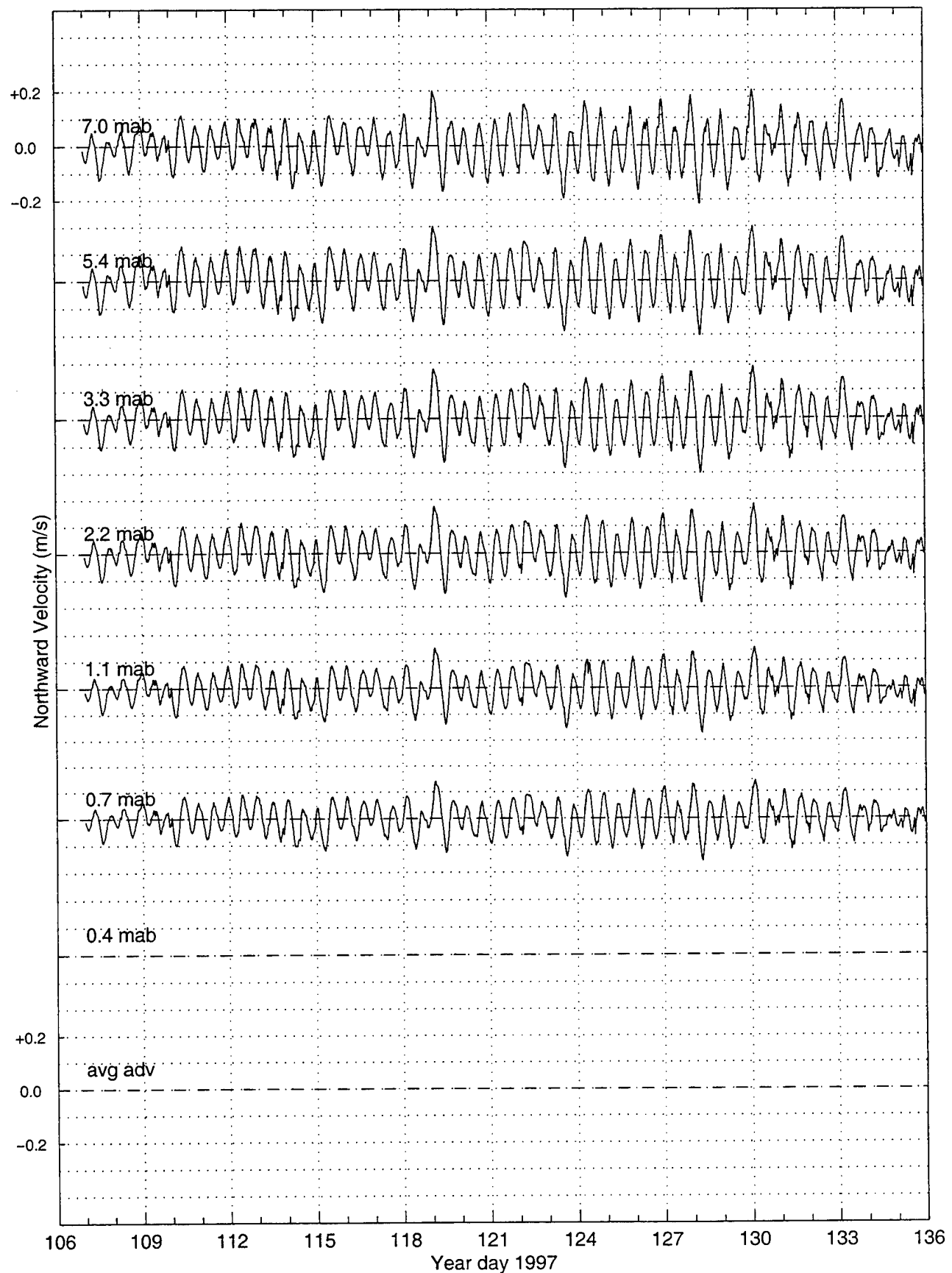


Figure 27 (cont.)

Deployment IV (continued on next page)



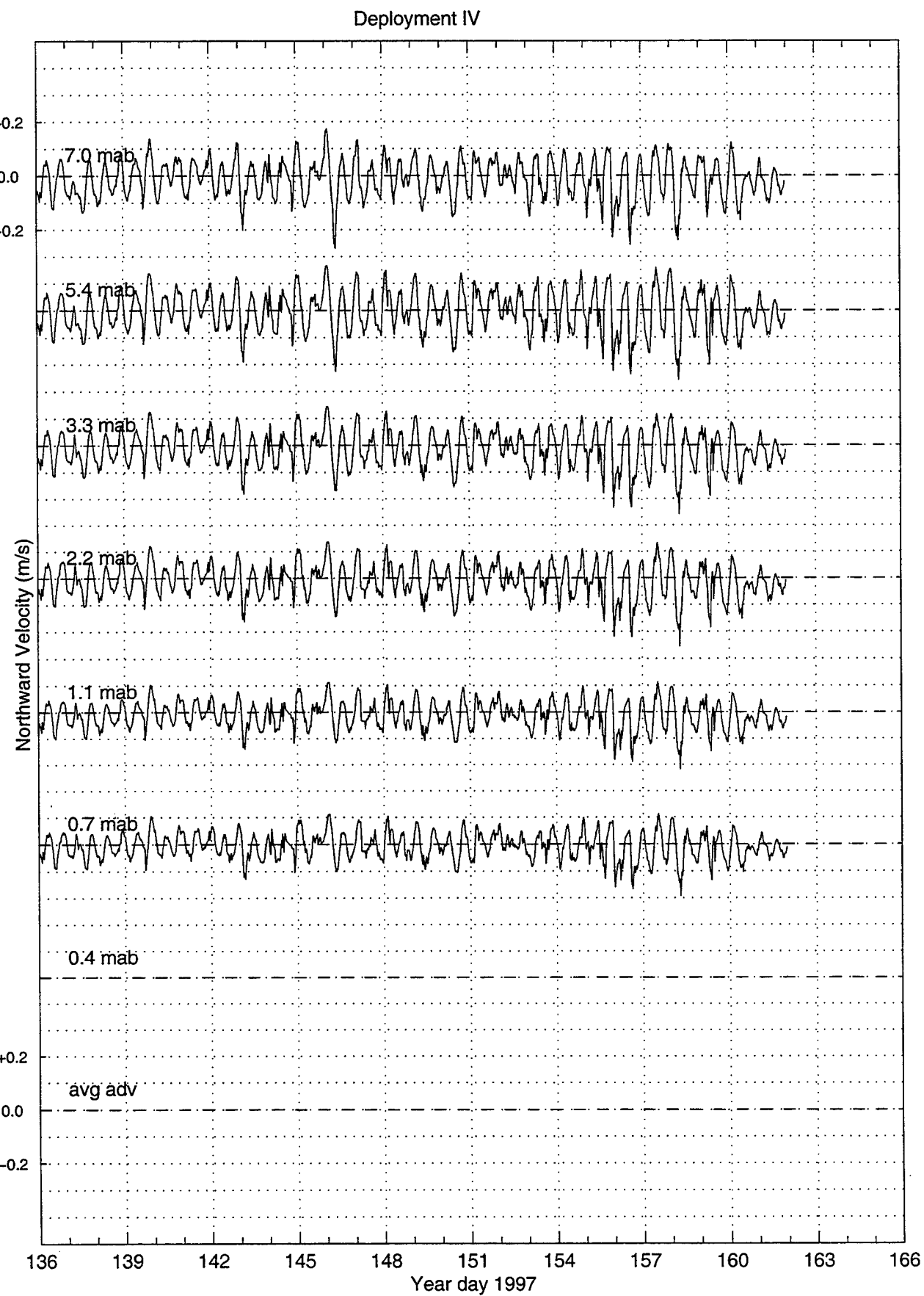


Figure 28

Deployment V (continued on next page)

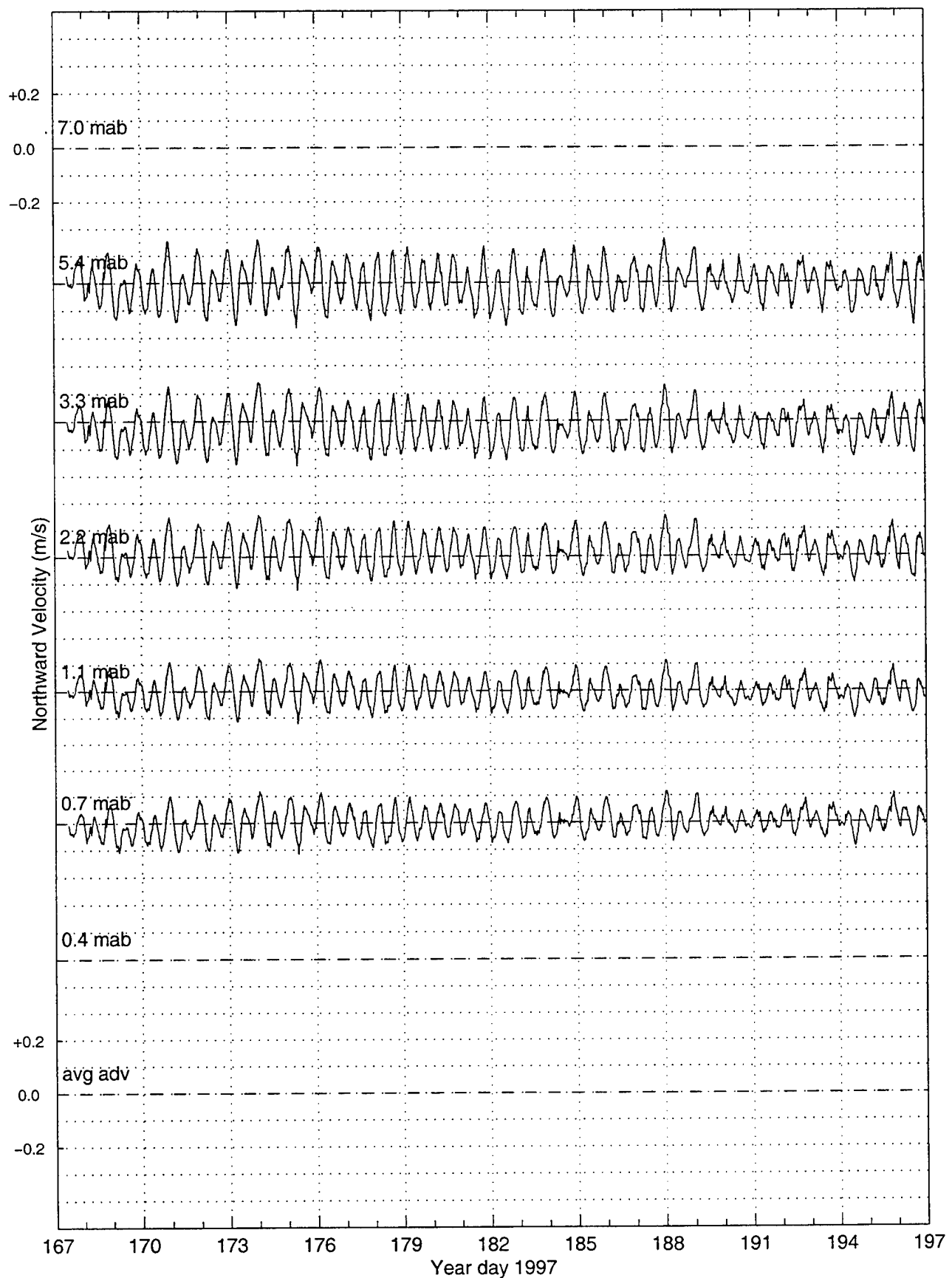
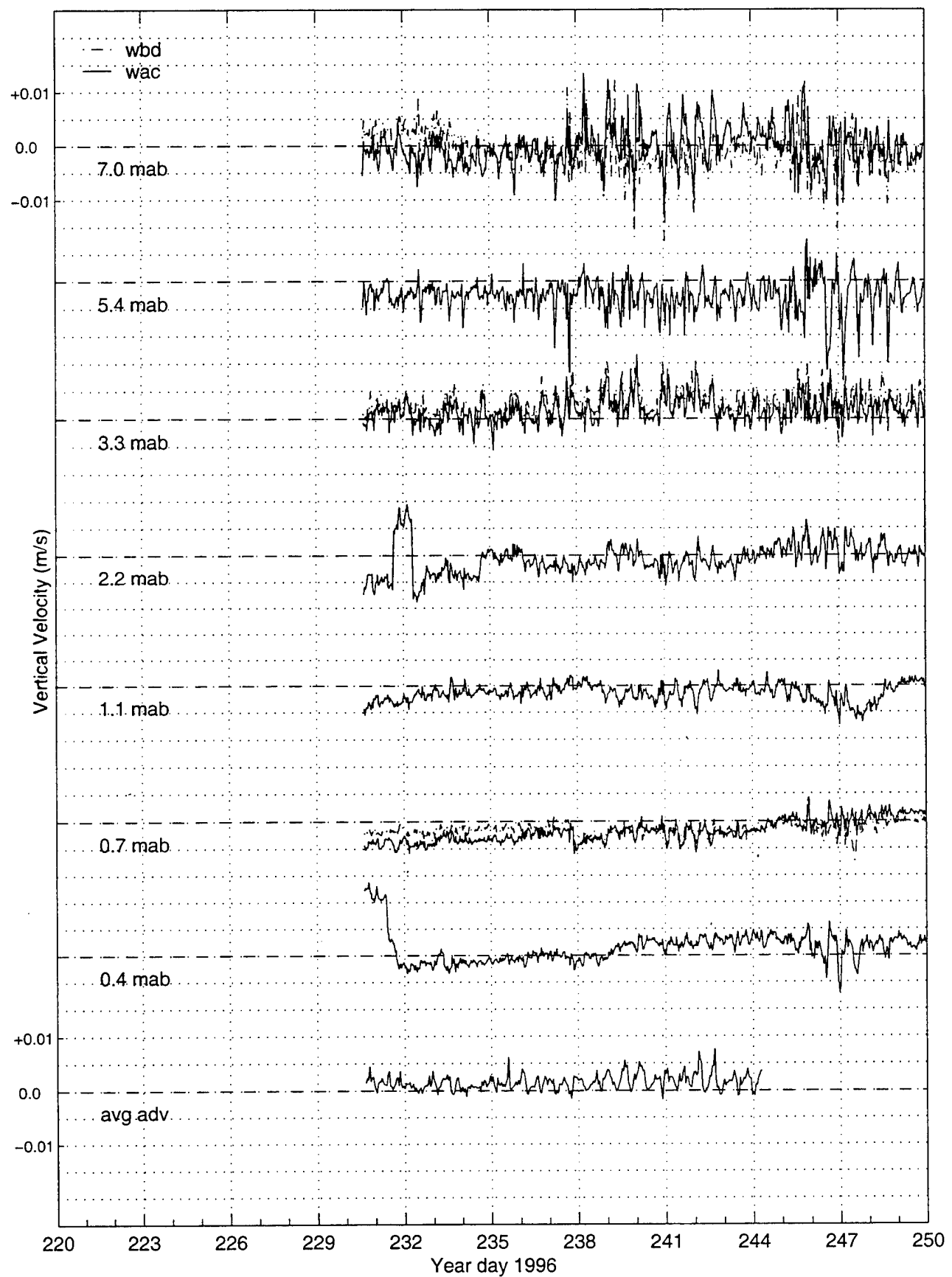




Figure 29

Vertical Velocity

Deployment I (continued on next page)



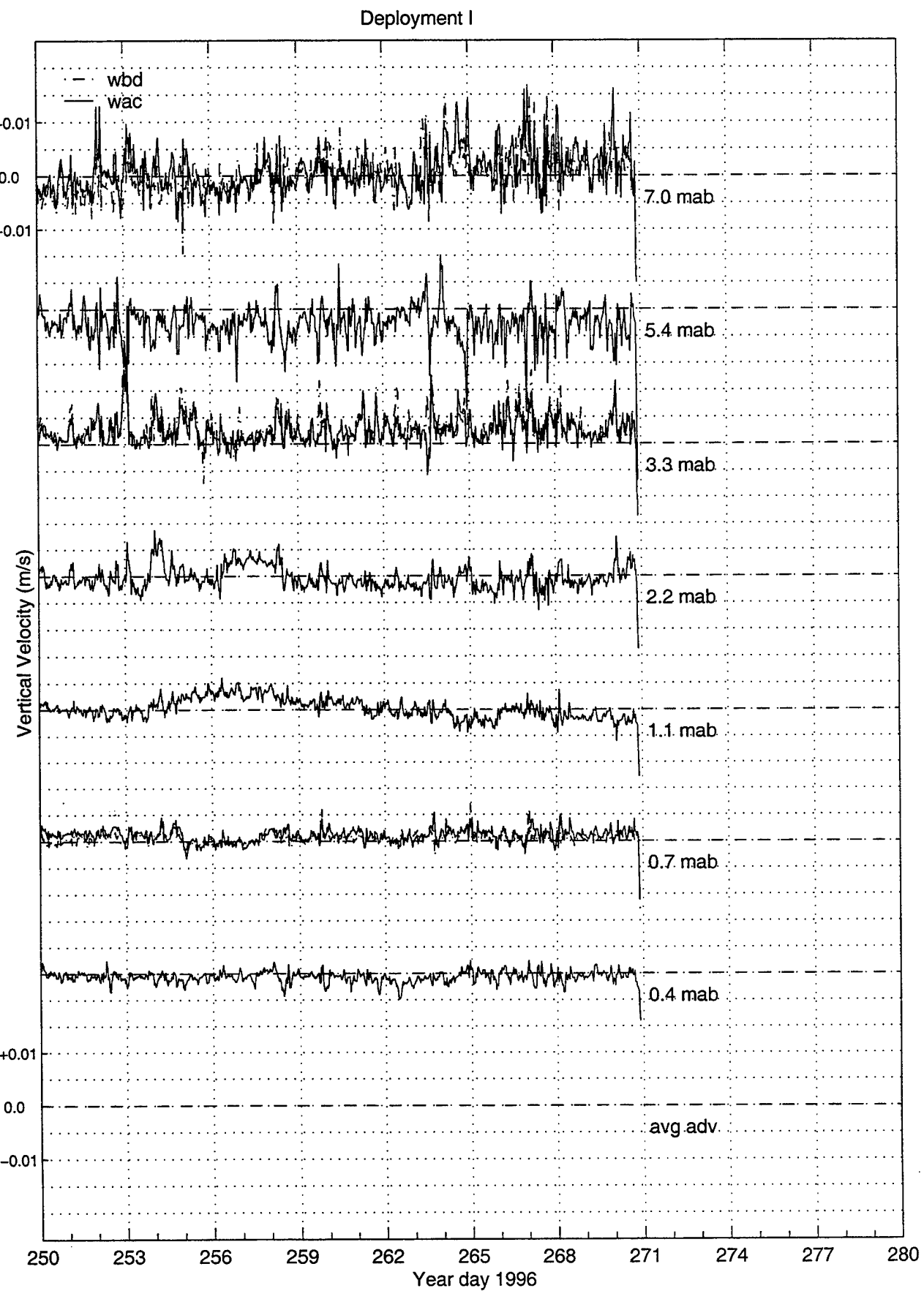
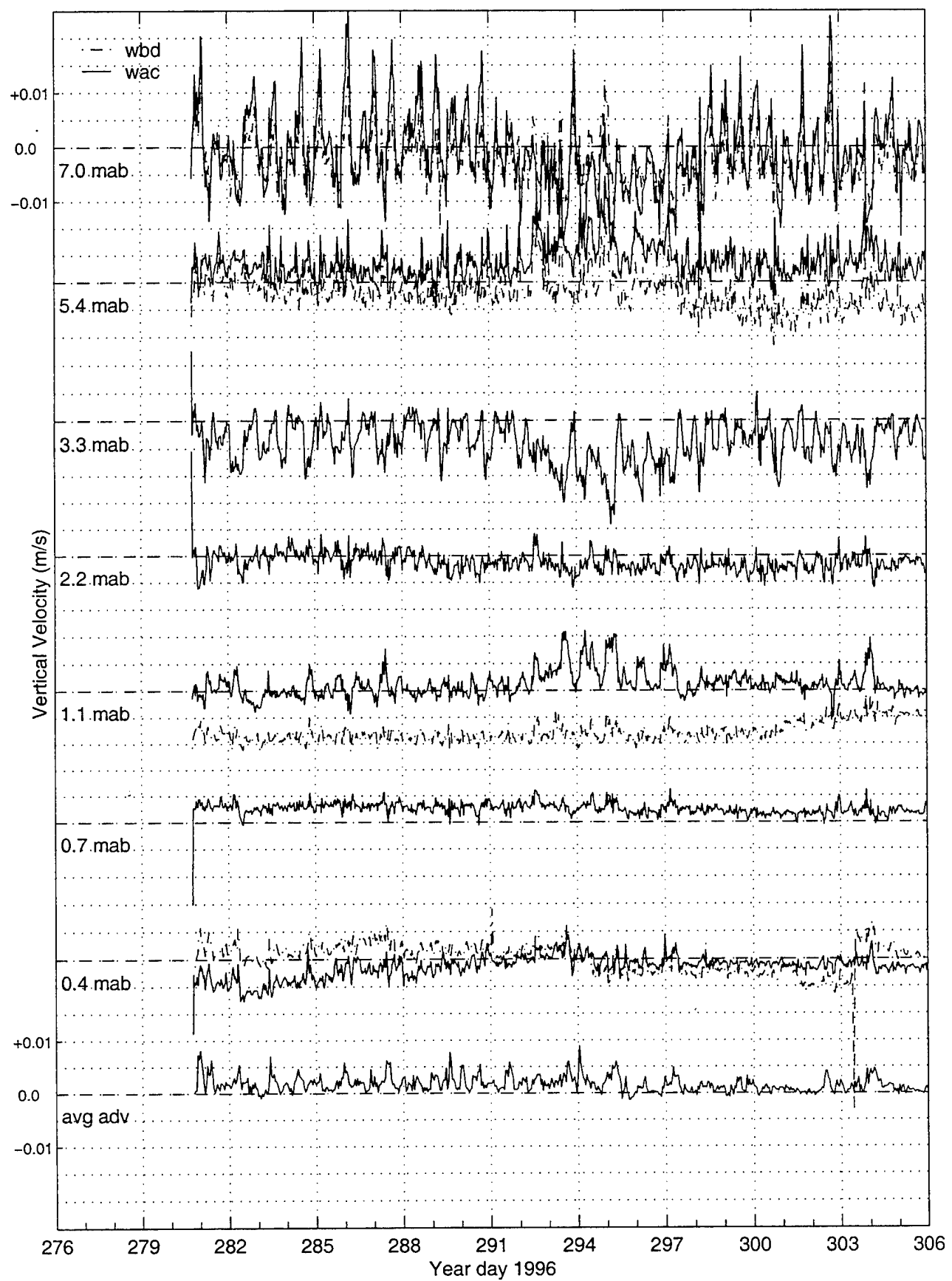


Figure 30

Deployment II (continued on next page)



Deployment II

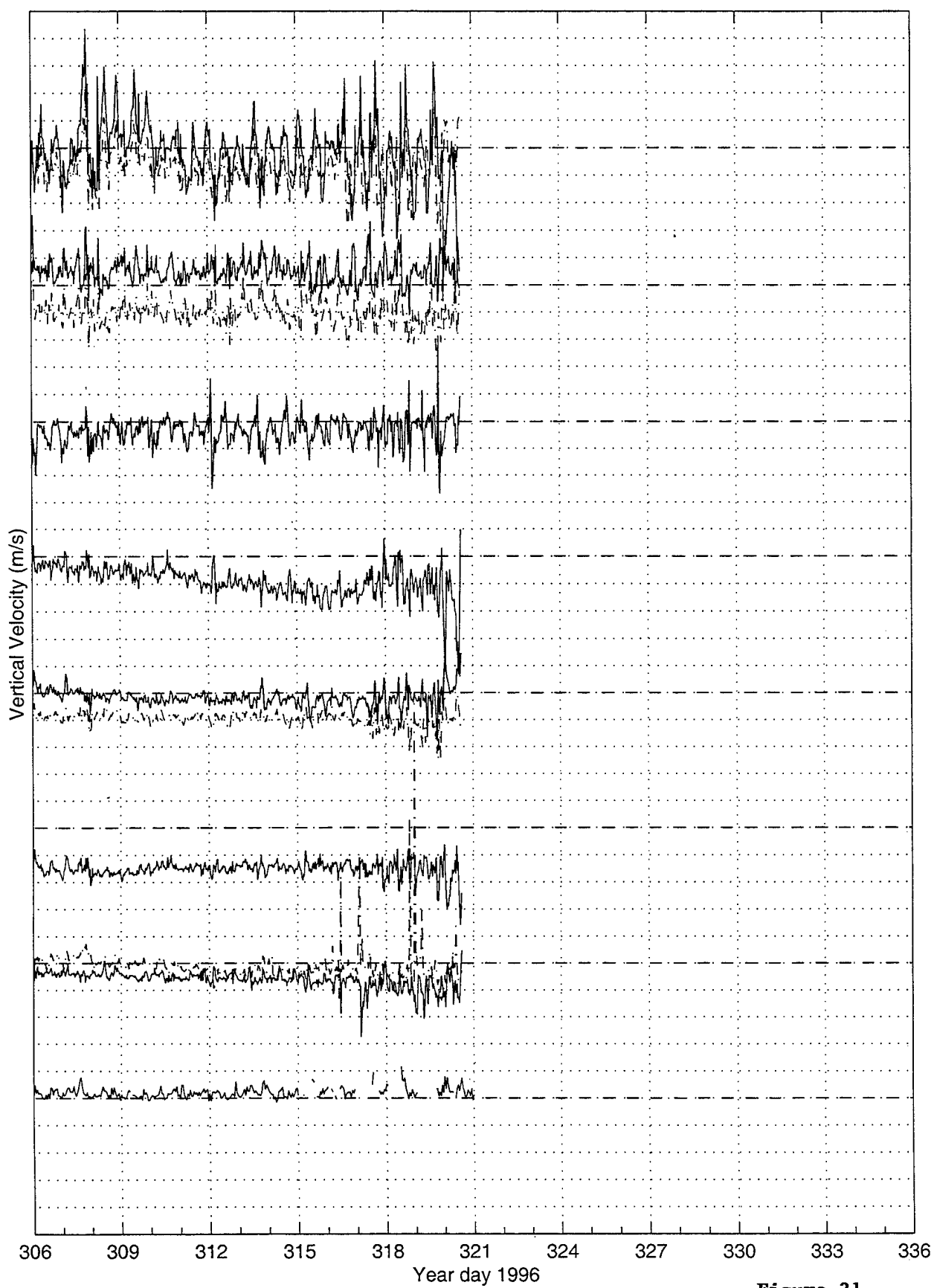
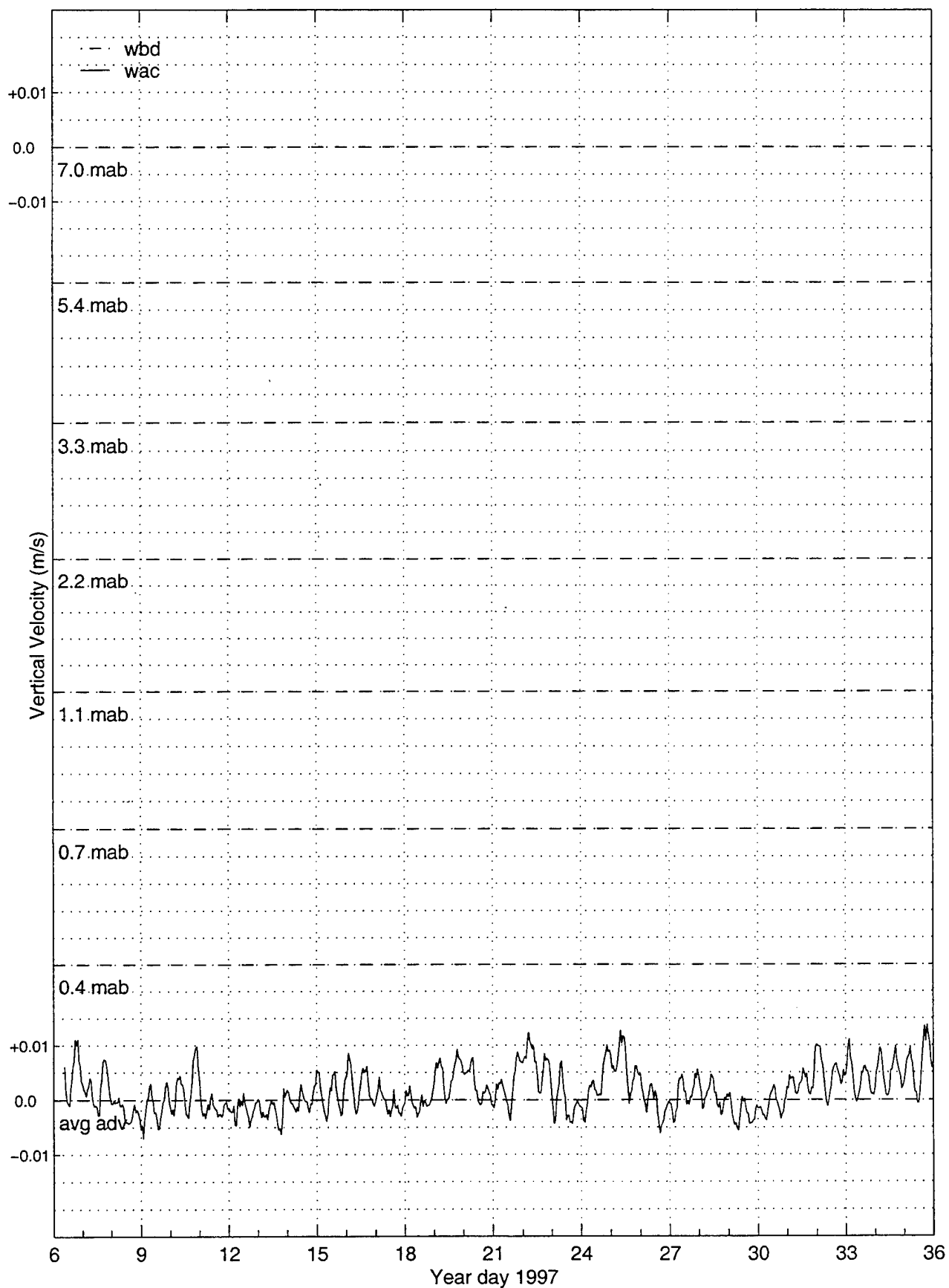


Figure 31

Deployment III (continued on next page)



Deployment III (continued on next page)

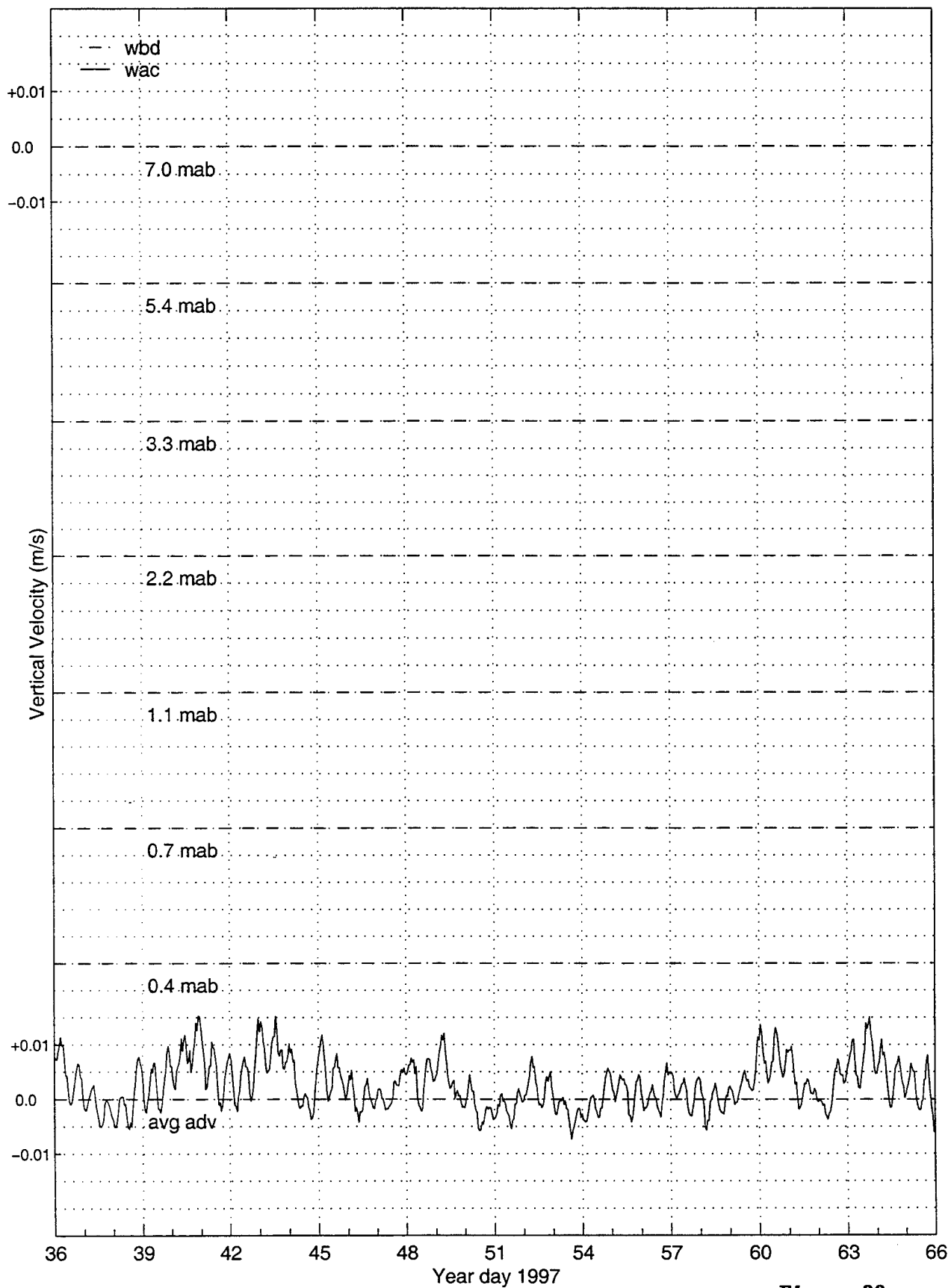


Figure 32

— THIS PAGE INTENTIONALLY LEFT BLANK —

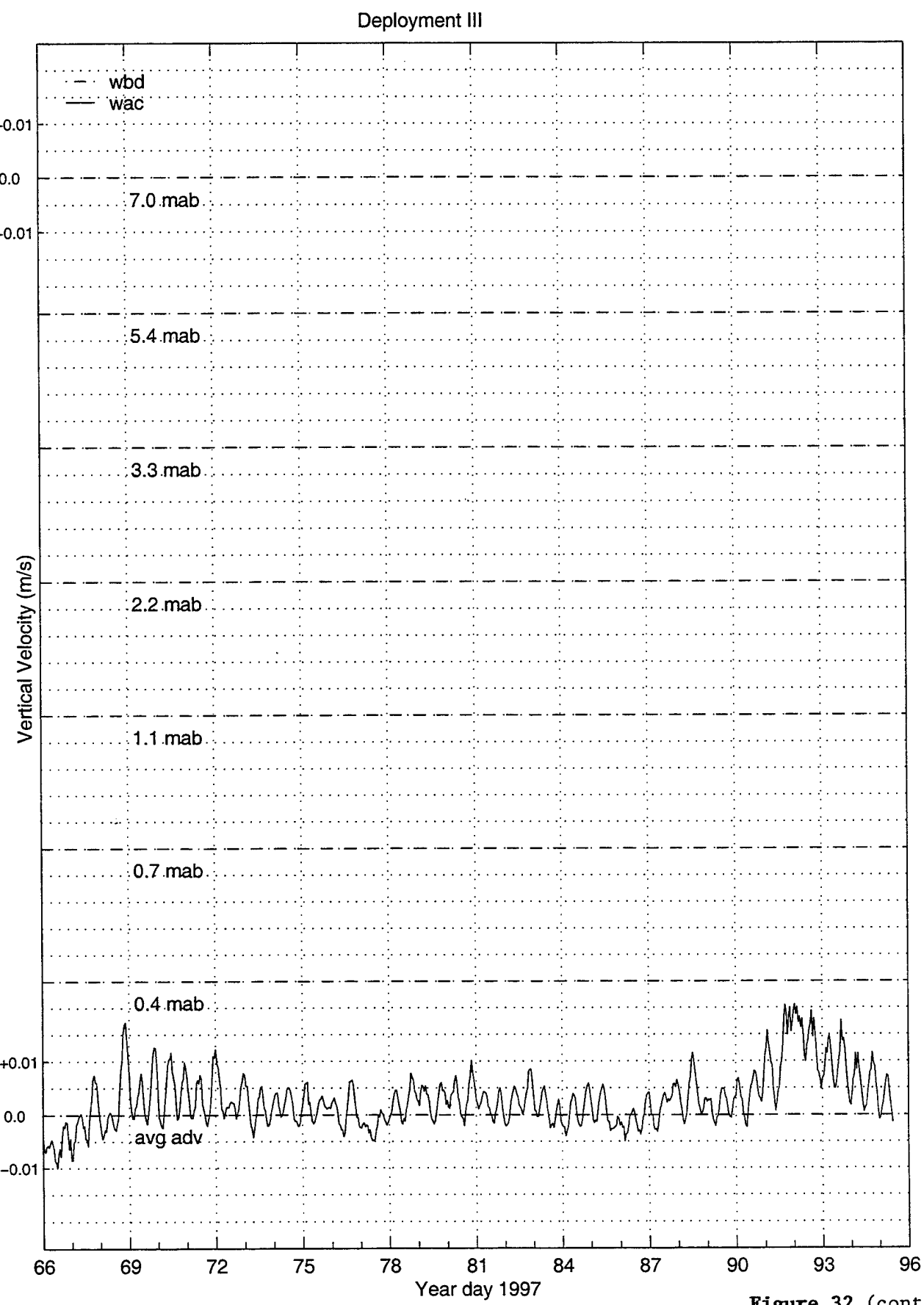
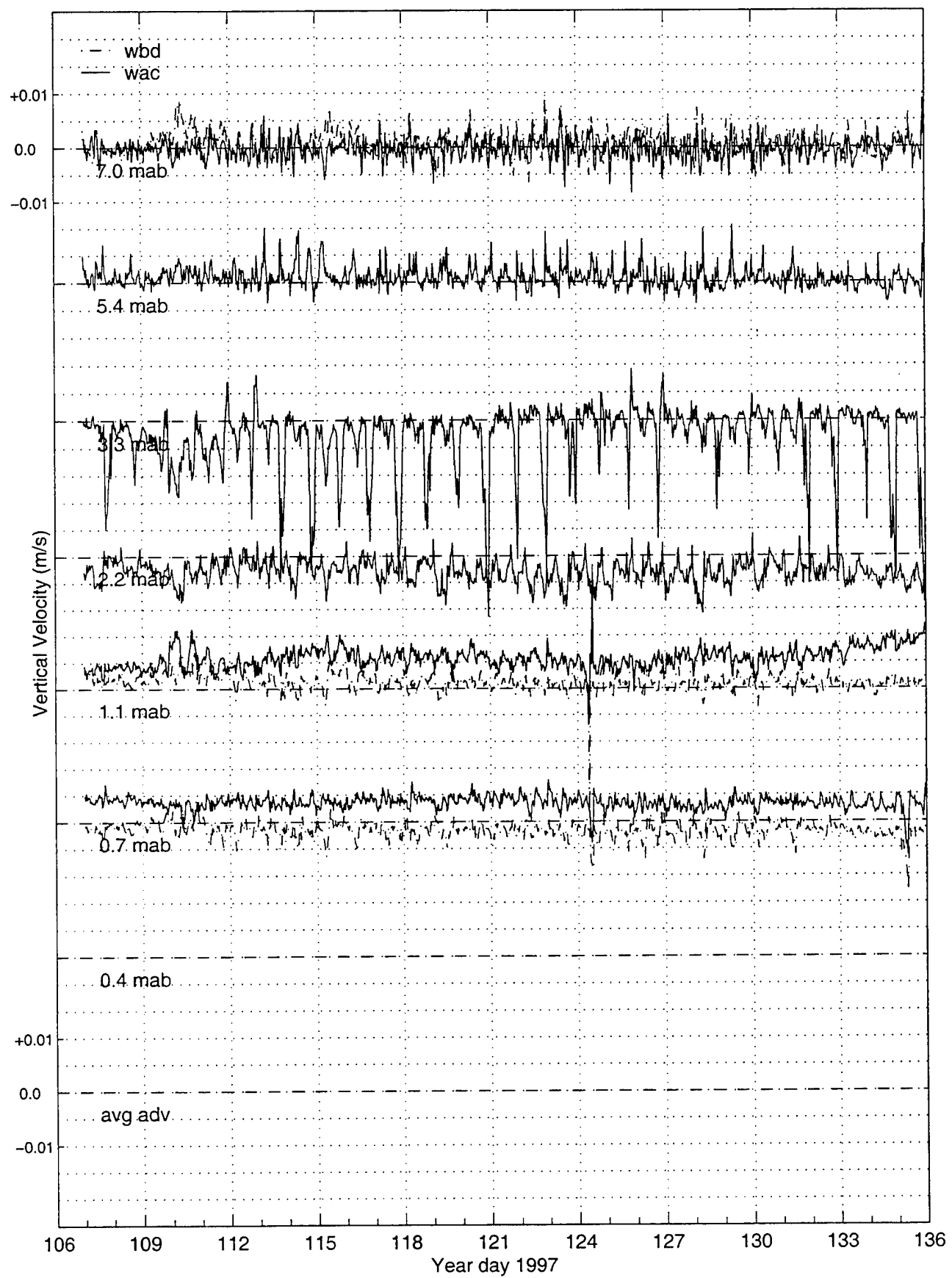


Figure 32 (cont.)

Deployment IV (continued on next page)



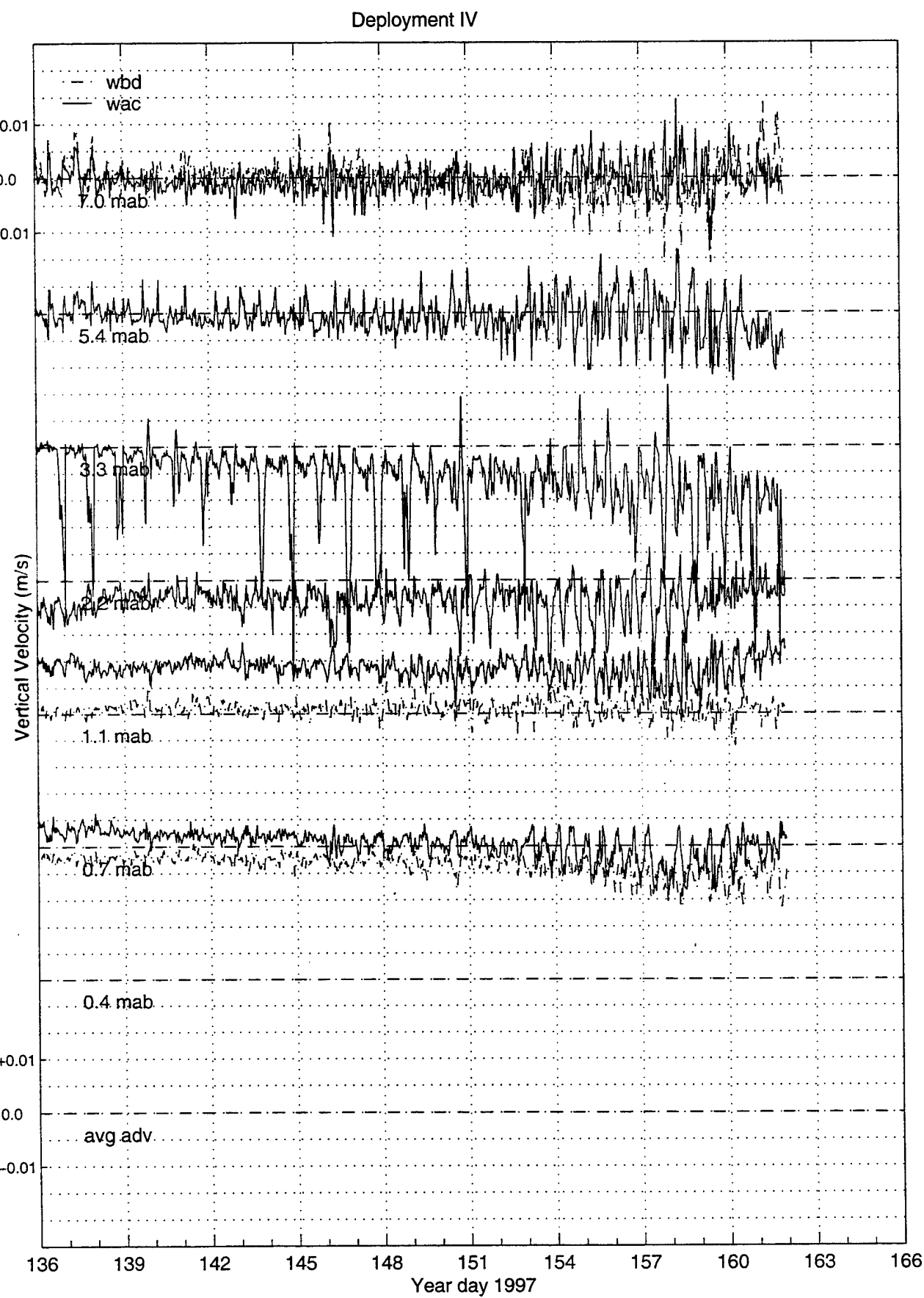
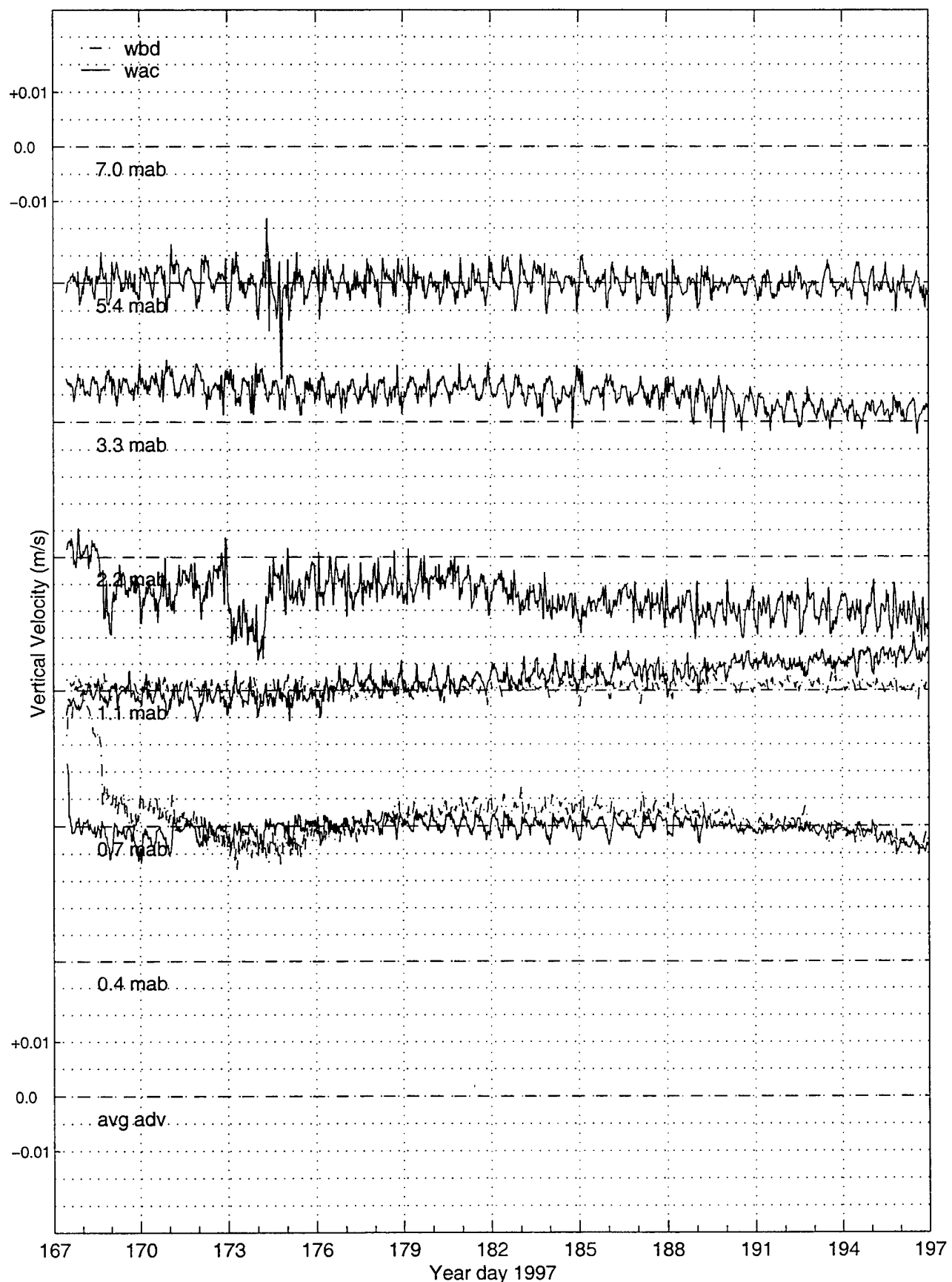


Figure 33

Deployment V (continued on next page)



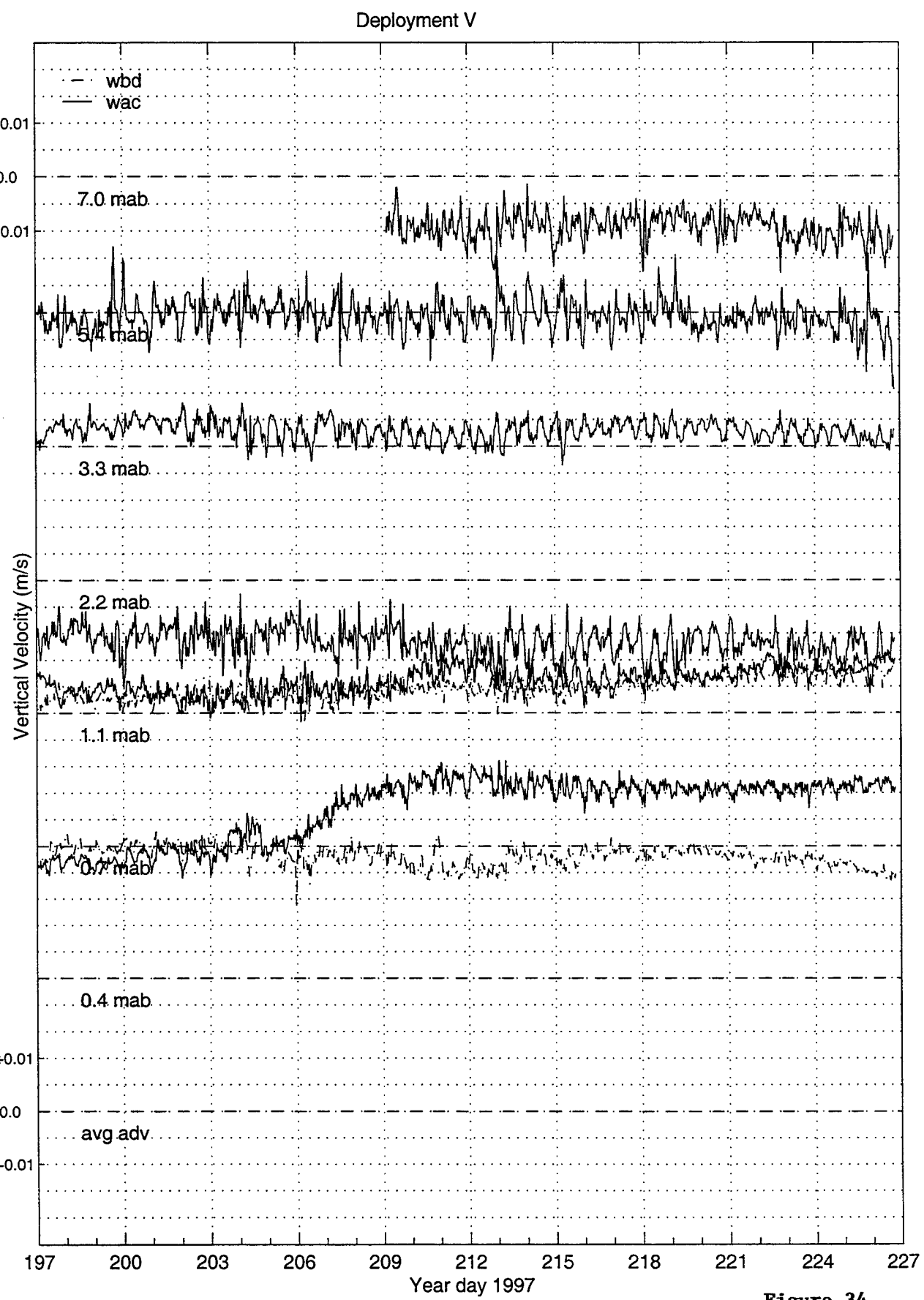
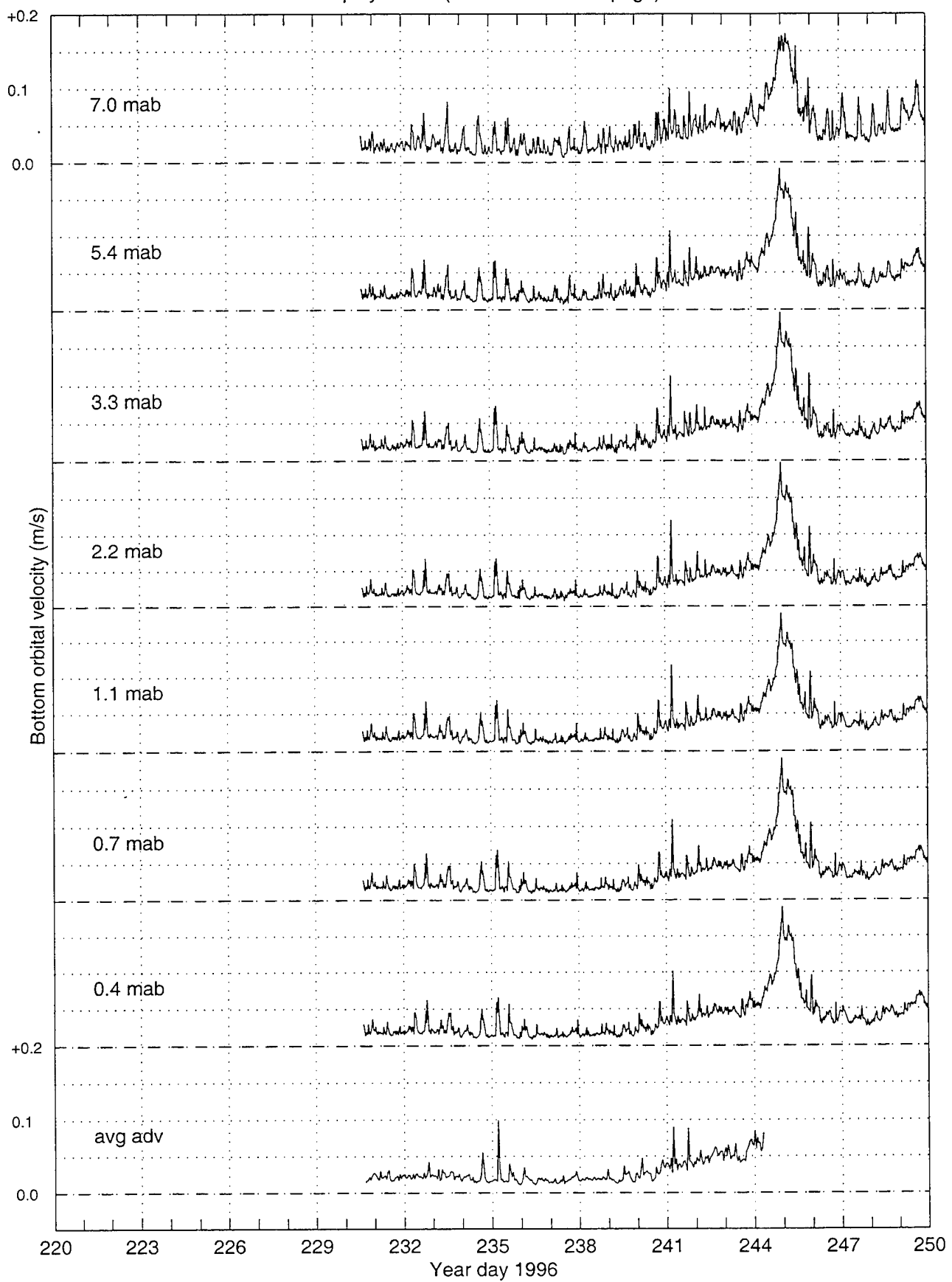


Figure 34

Bottom-orbital Velocity

Deployment I (continued on next page)



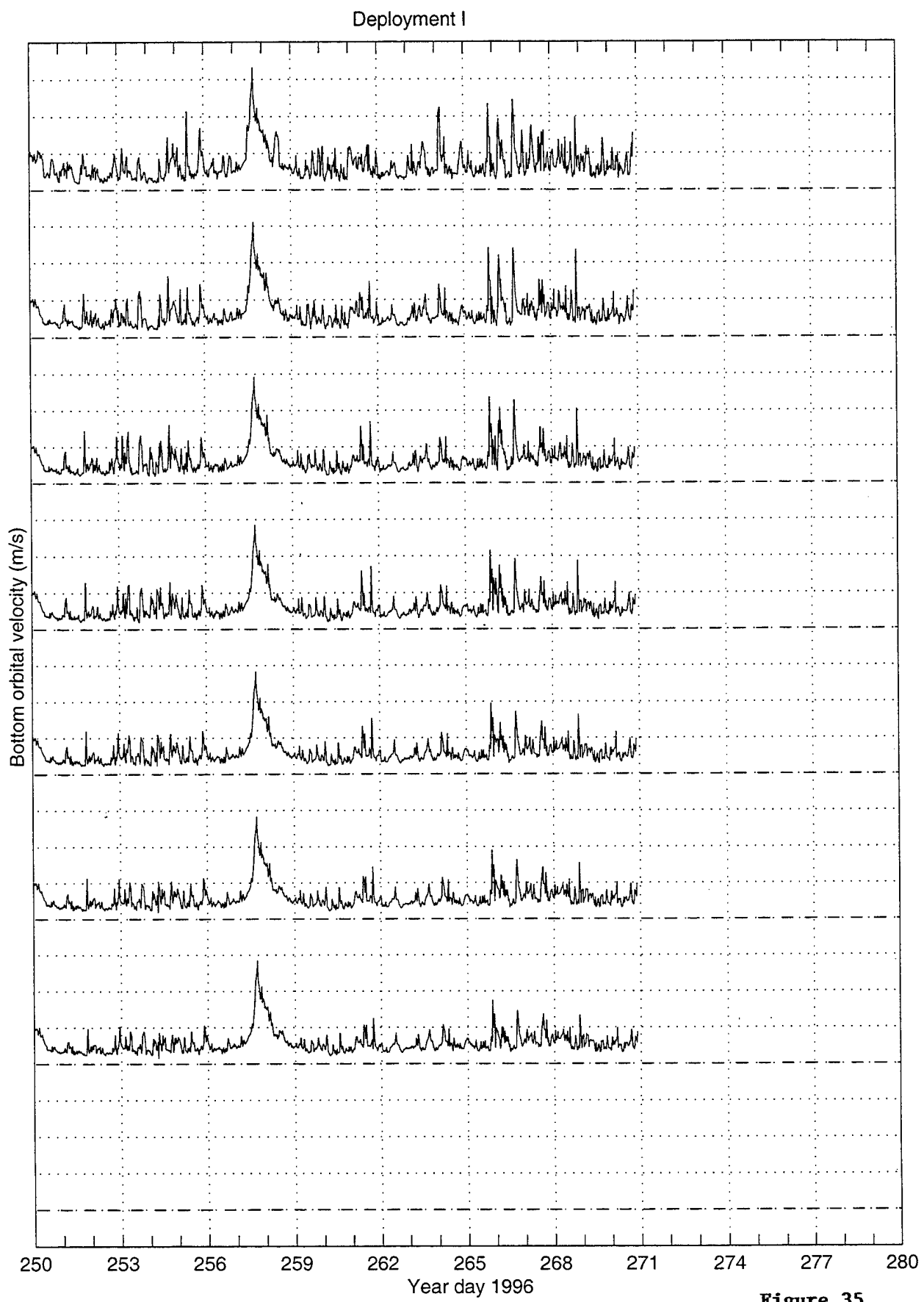
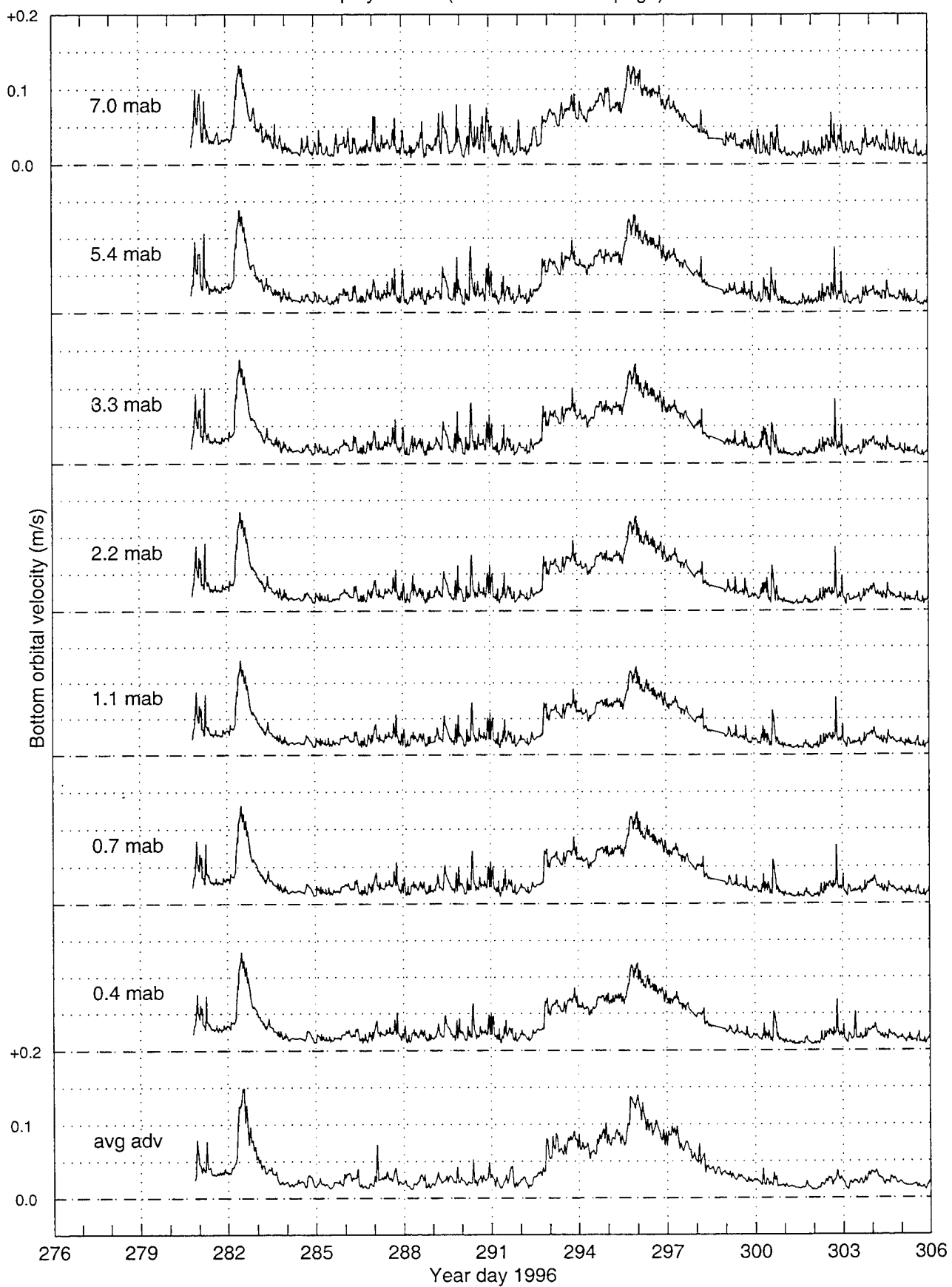


Figure 35

Deployment II (continued on next page)



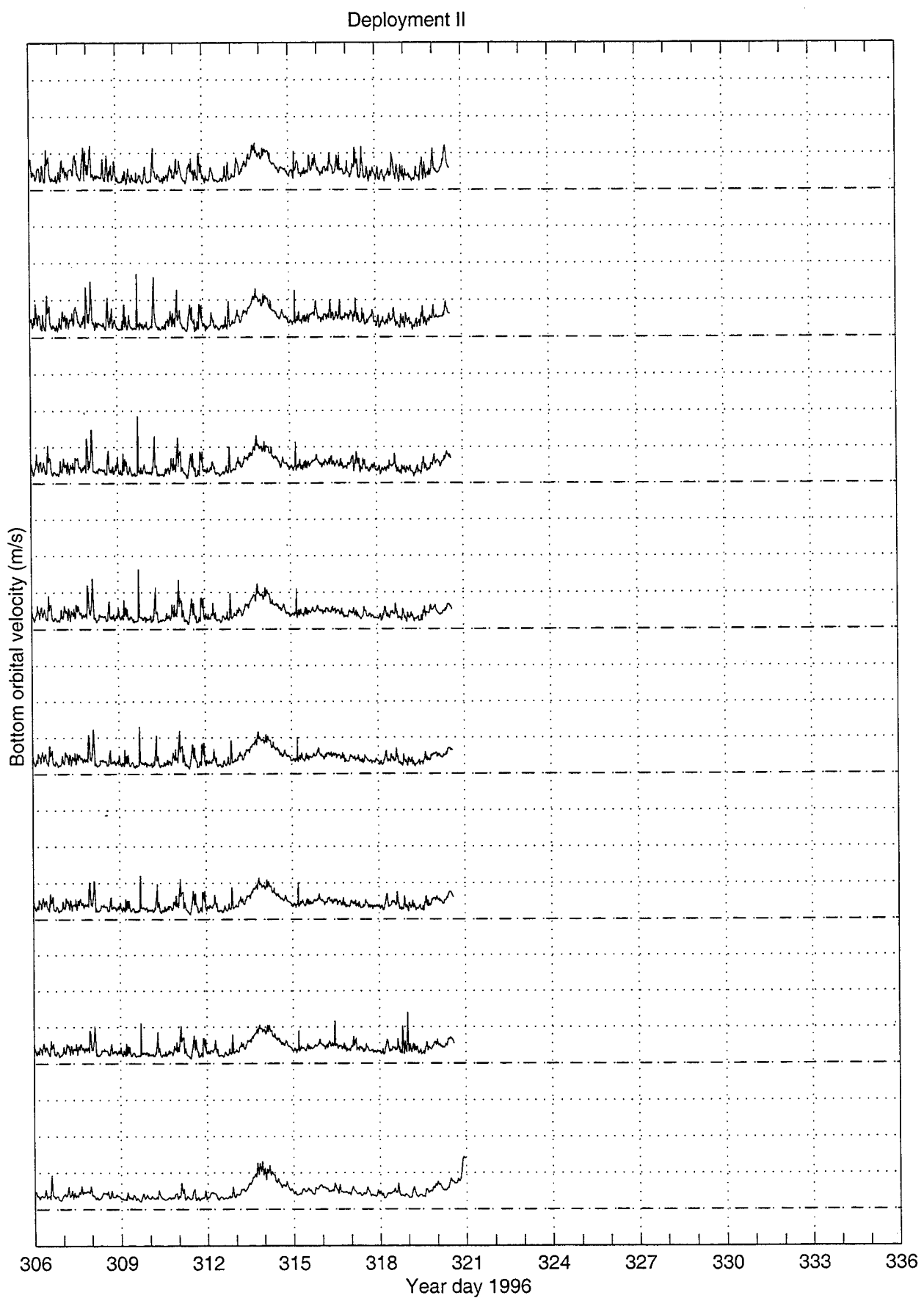
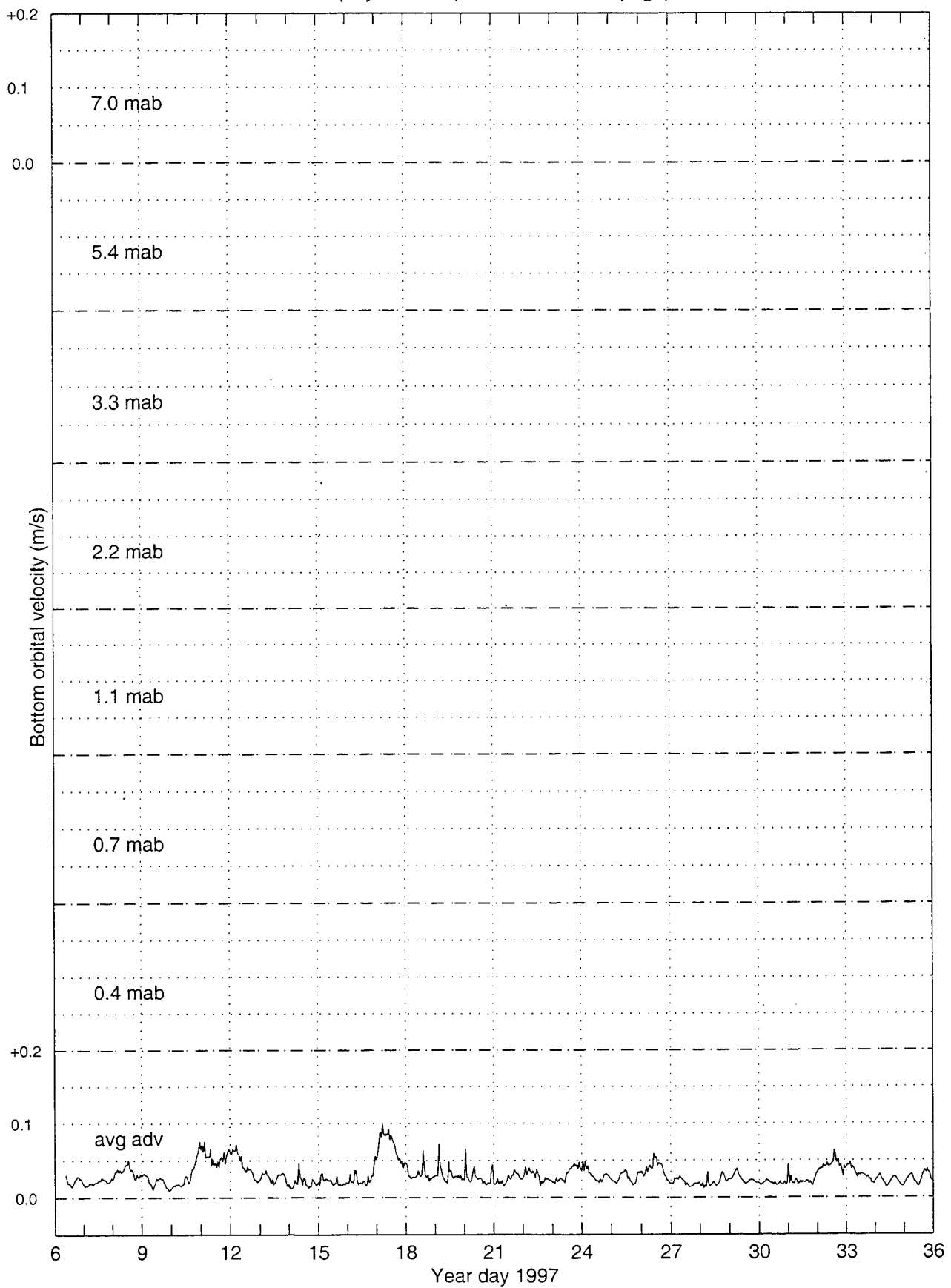


Figure 36

Deployment III (continued on next page)



Deployment III (continued on next page)

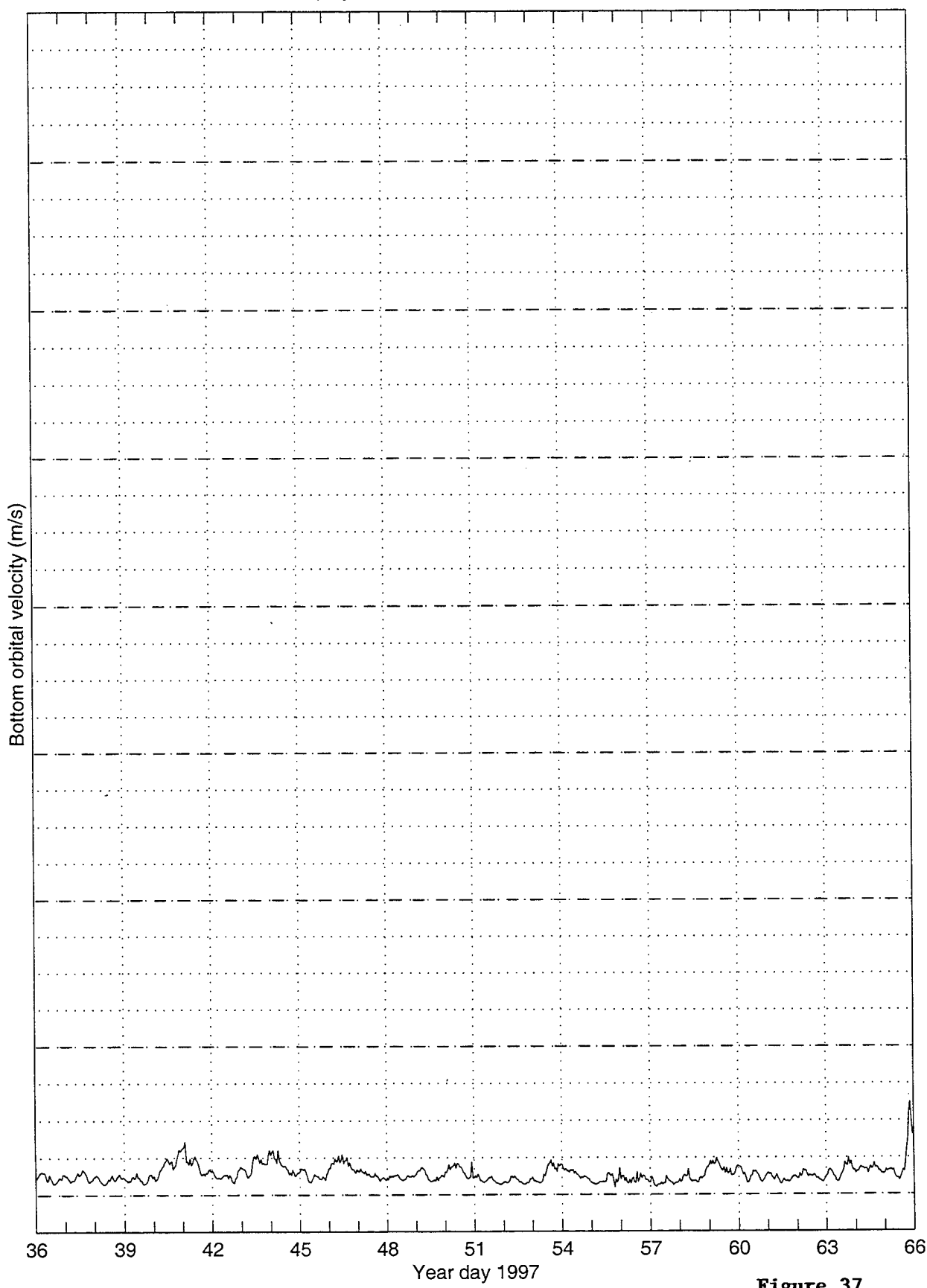


Figure 37

— THIS PAGE INTENTIONALLY LEFT BLANK —

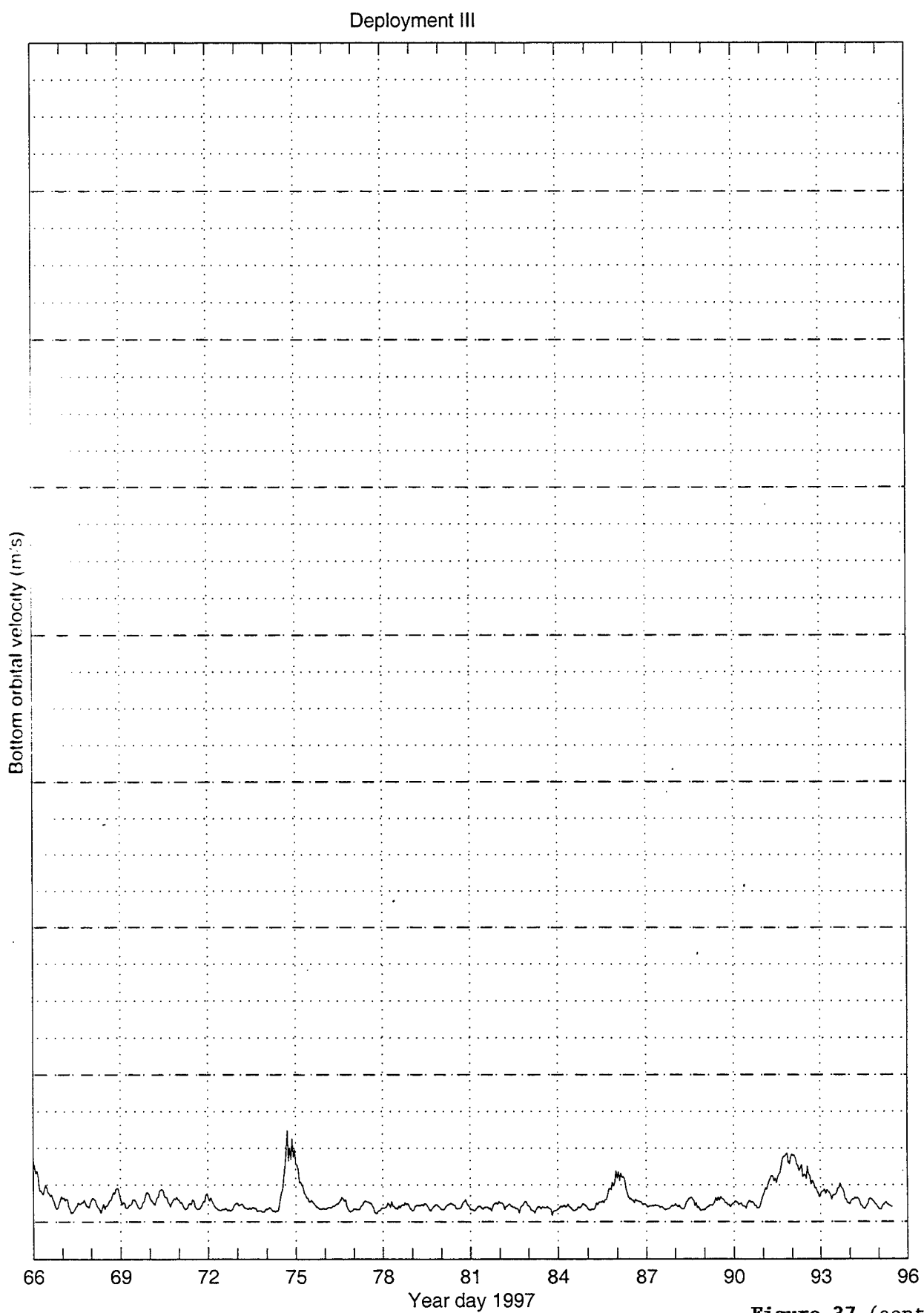
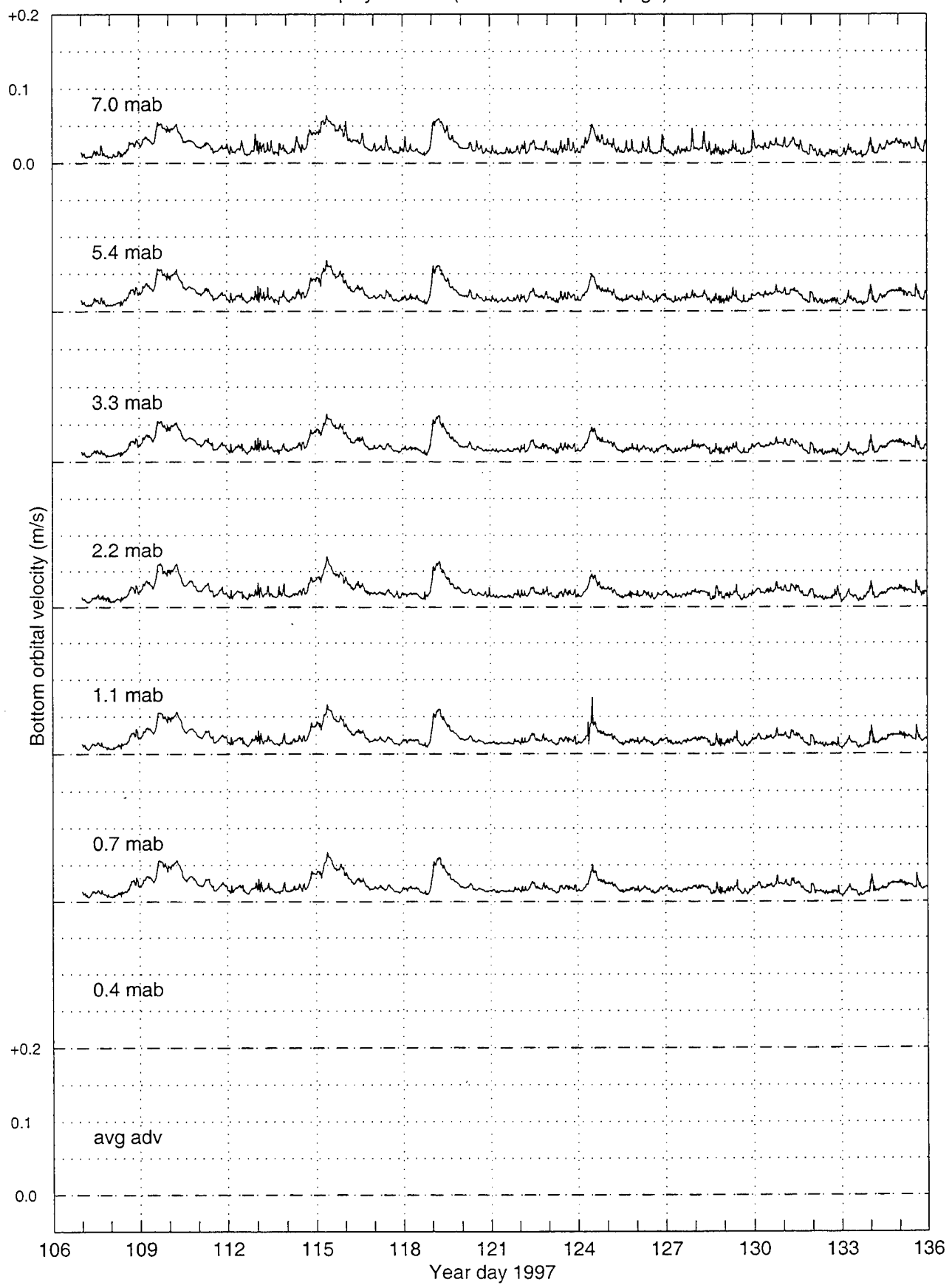


Figure 37 (cont.)

Deployment IV (continued on next page)



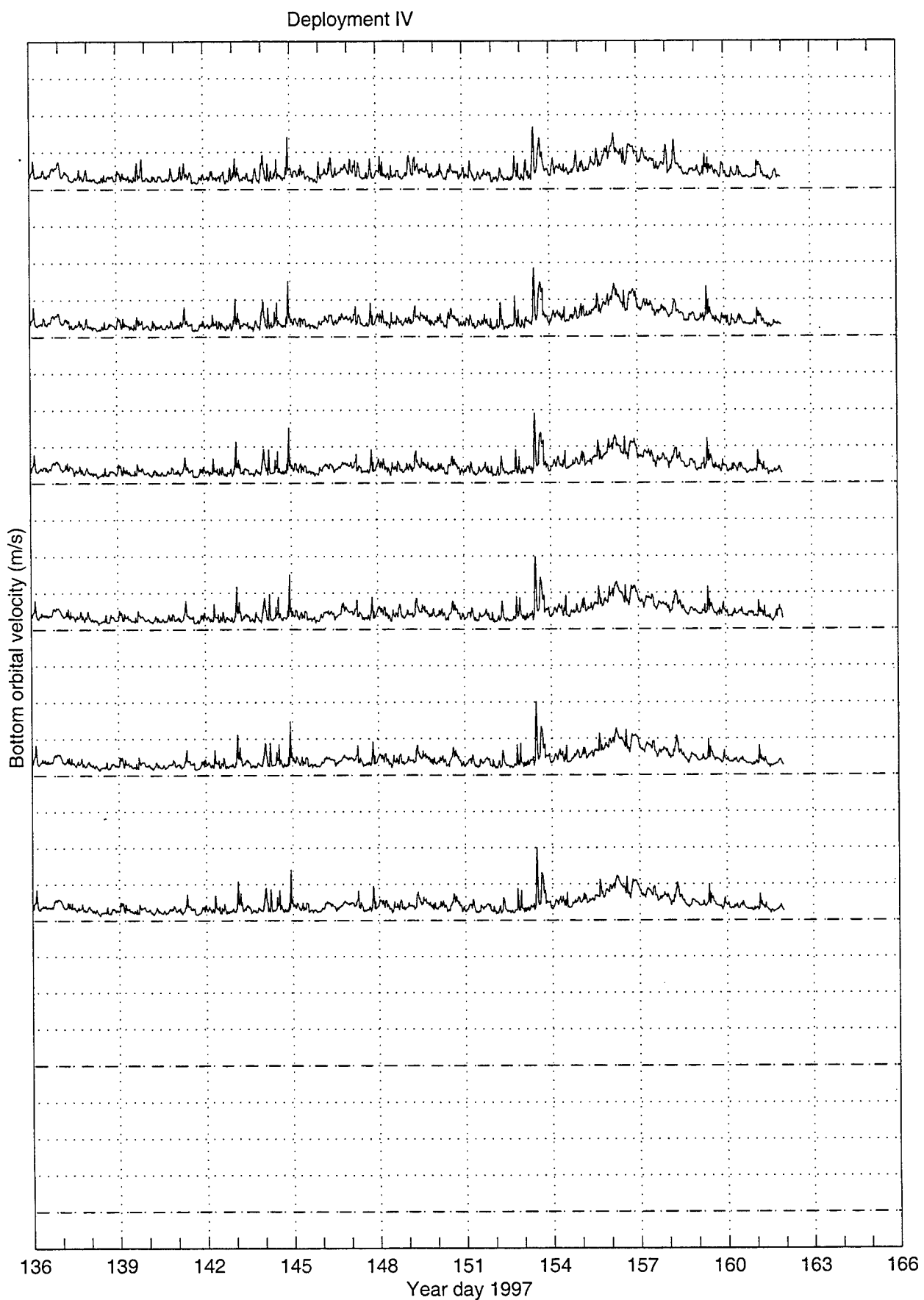
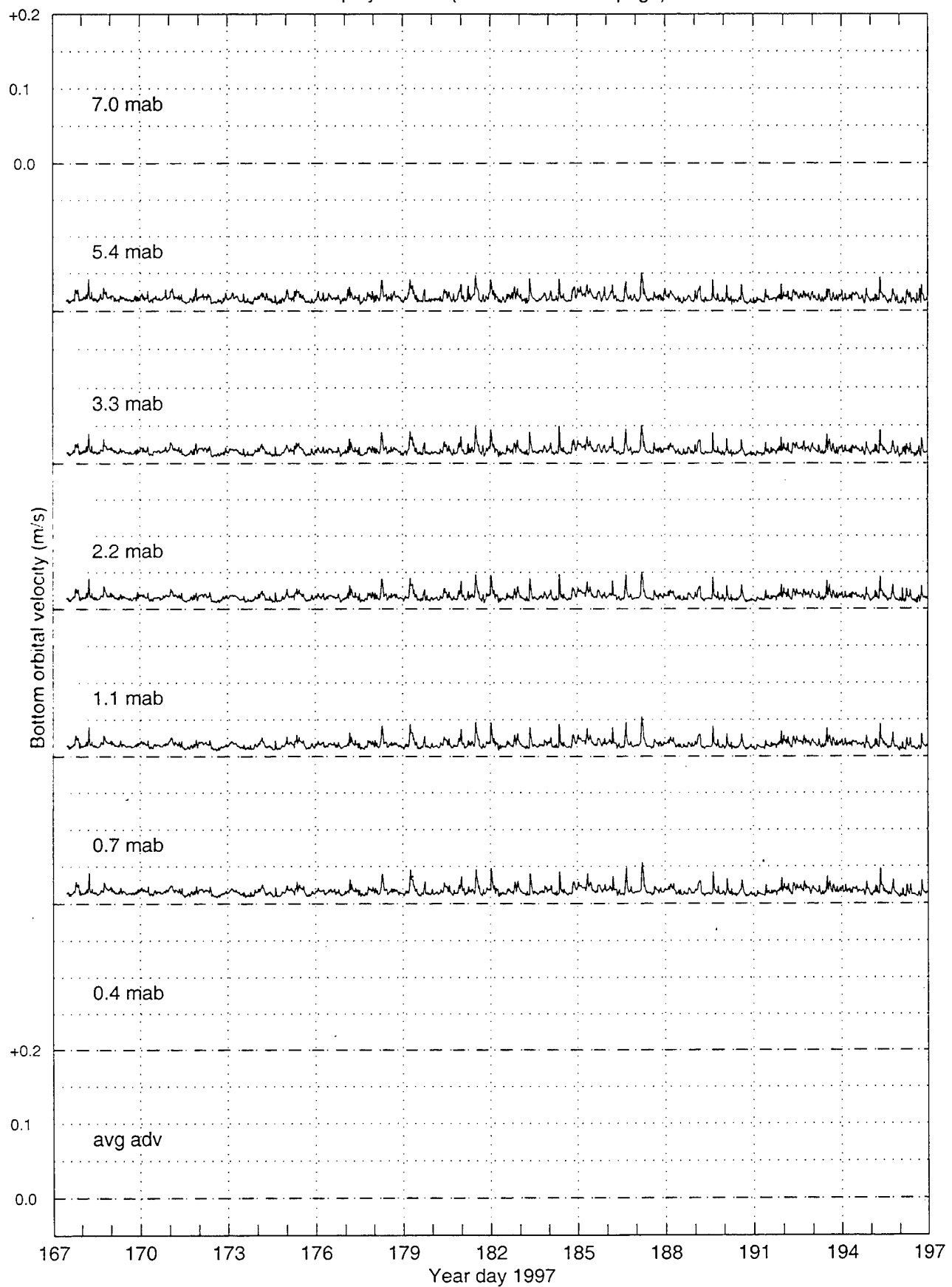


Figure 38

Deployment V (continued on next page)



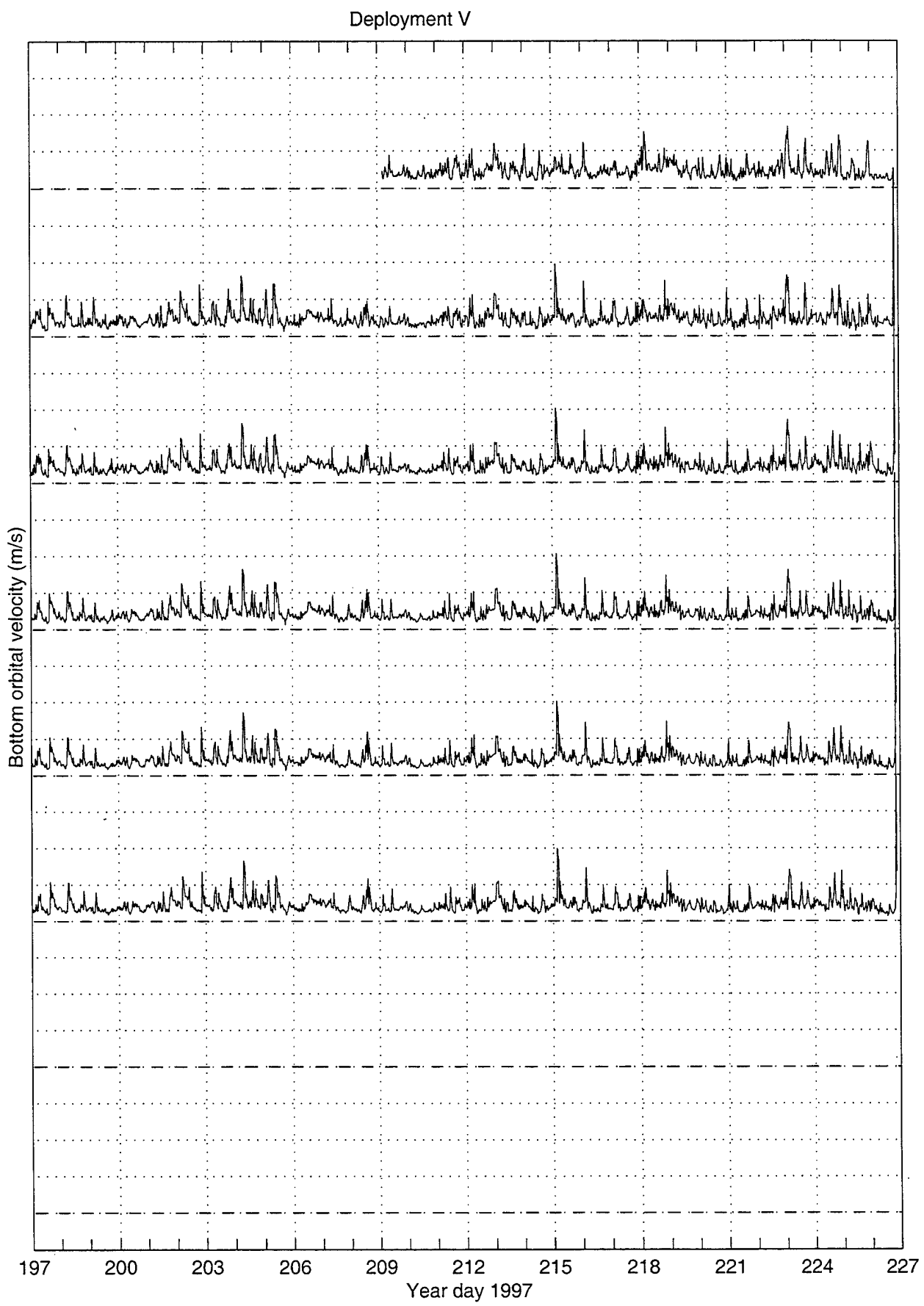


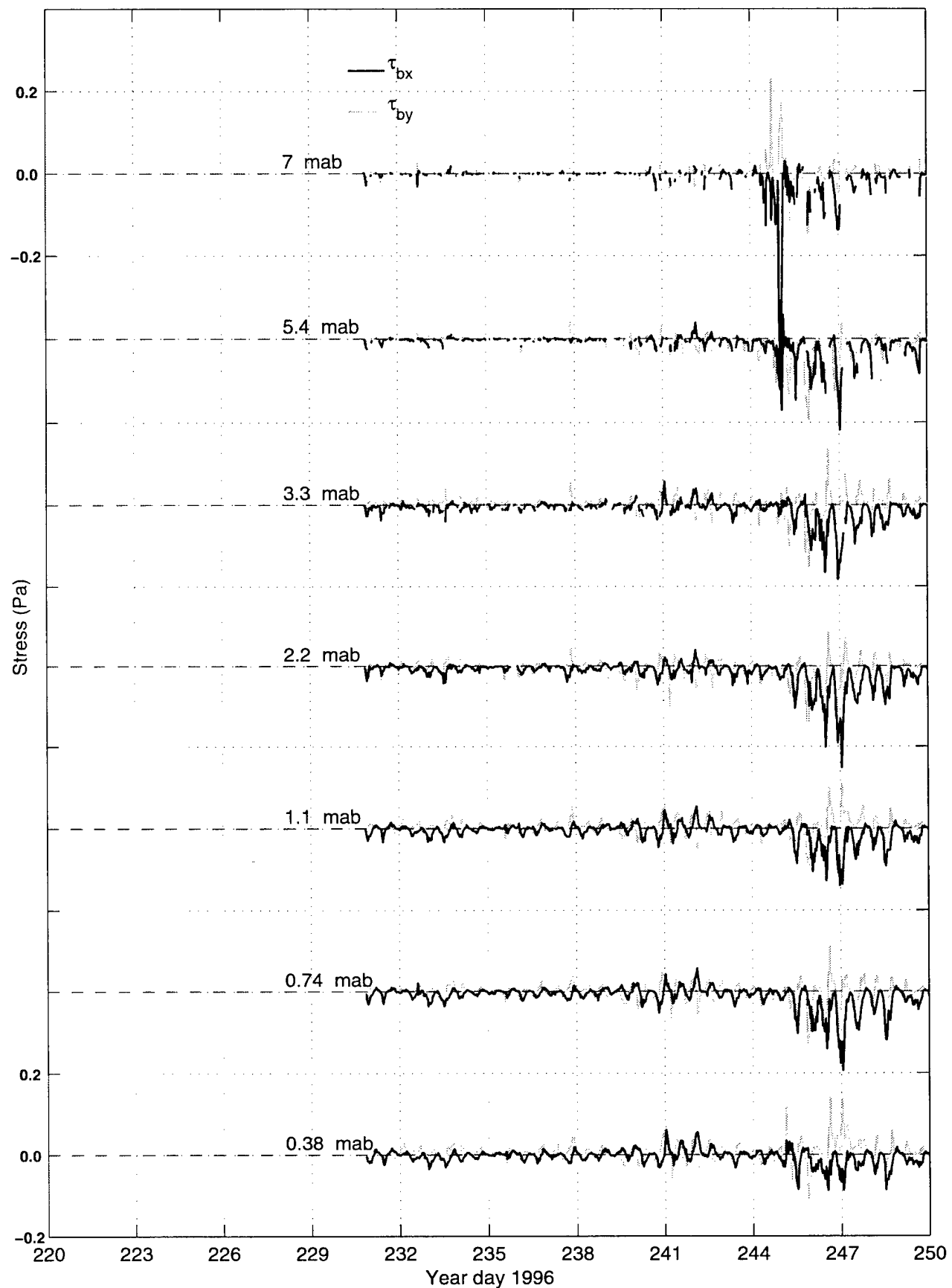
Figure 39

Reynolds Stress

τ_{bx} - East-West component

τ_{by} - North-South component

Deployment I (continued)



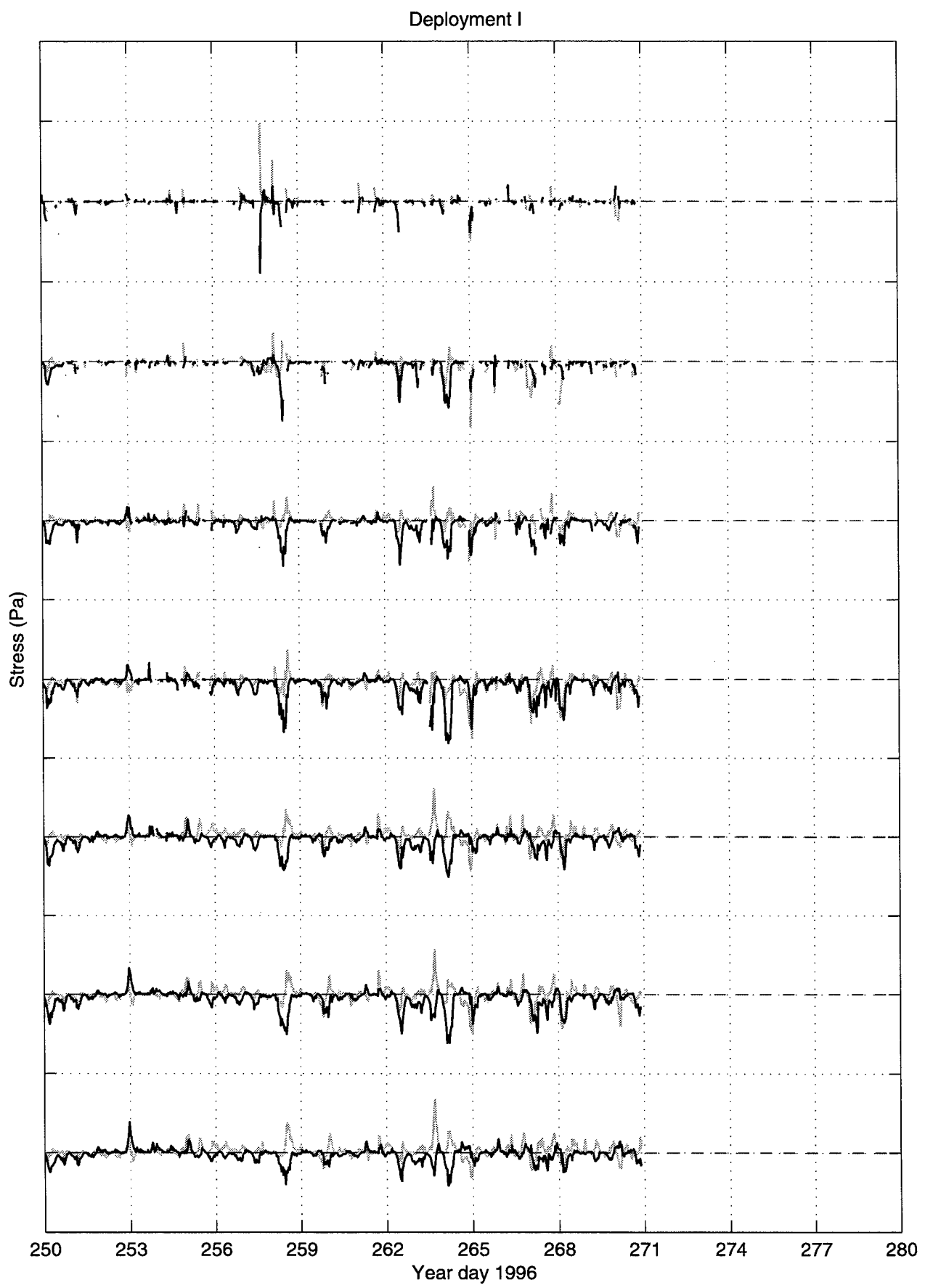
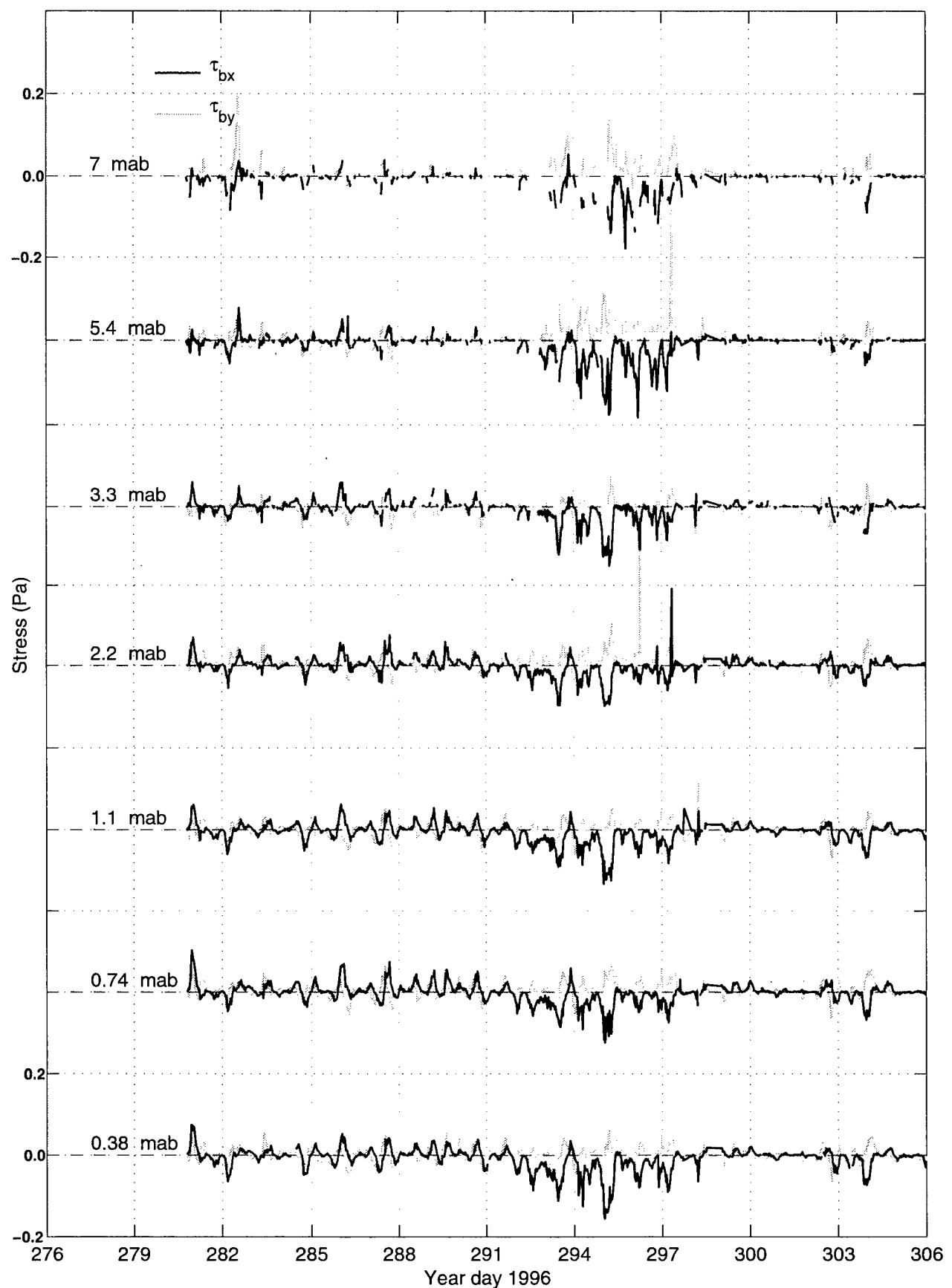


Figure 40

Deployment II (continued)



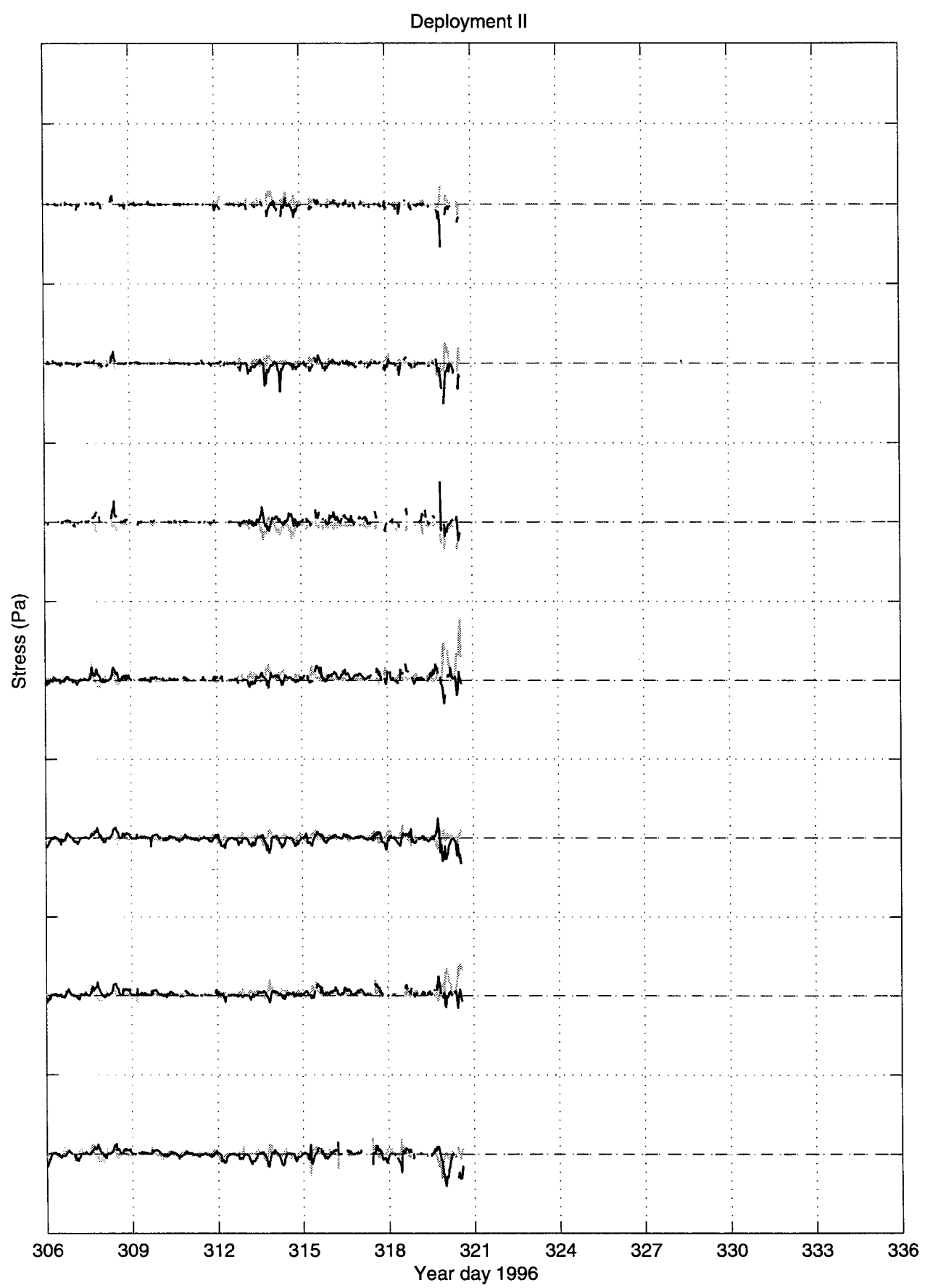
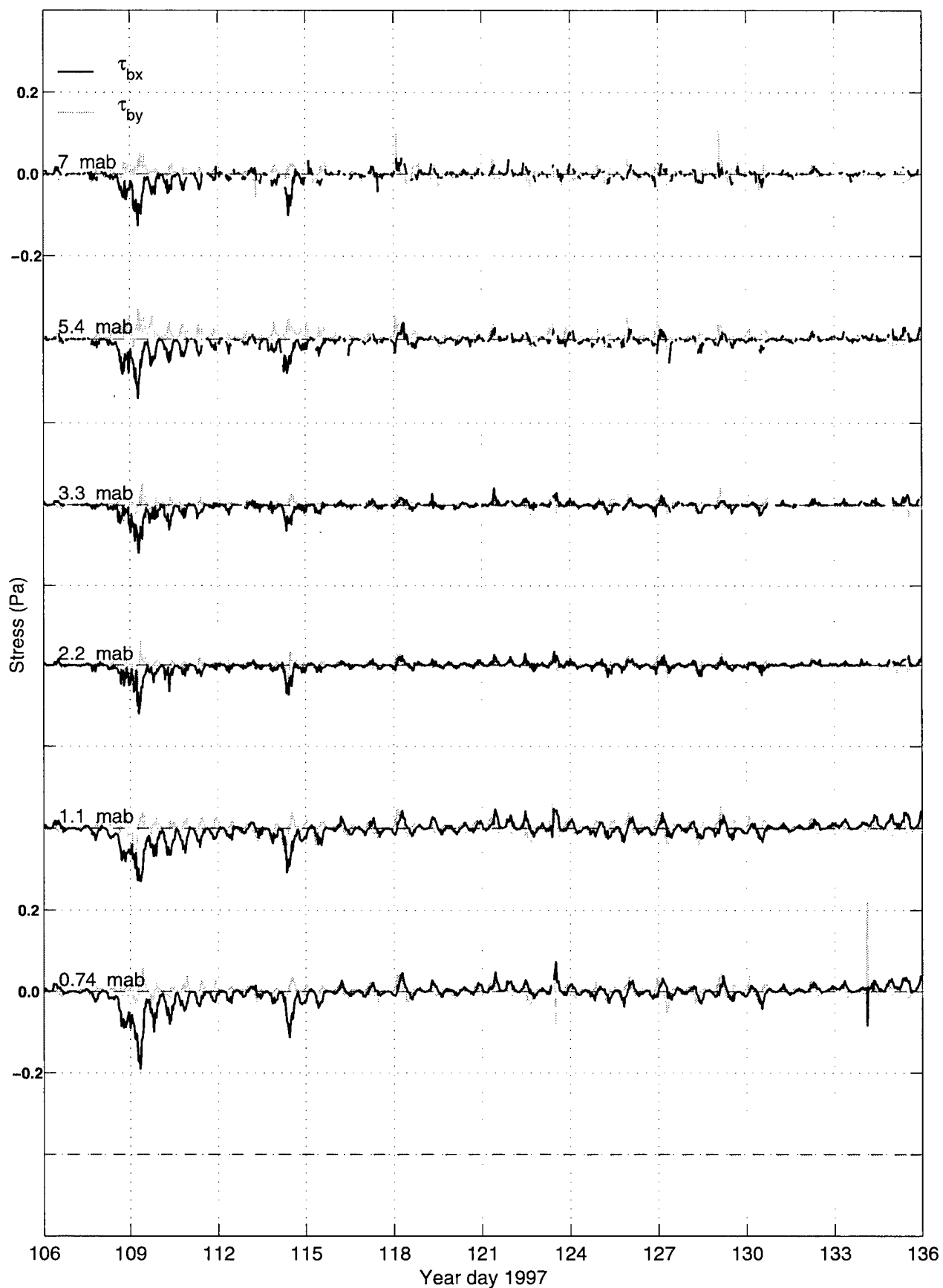


Figure 41

Deployment IV (continued)



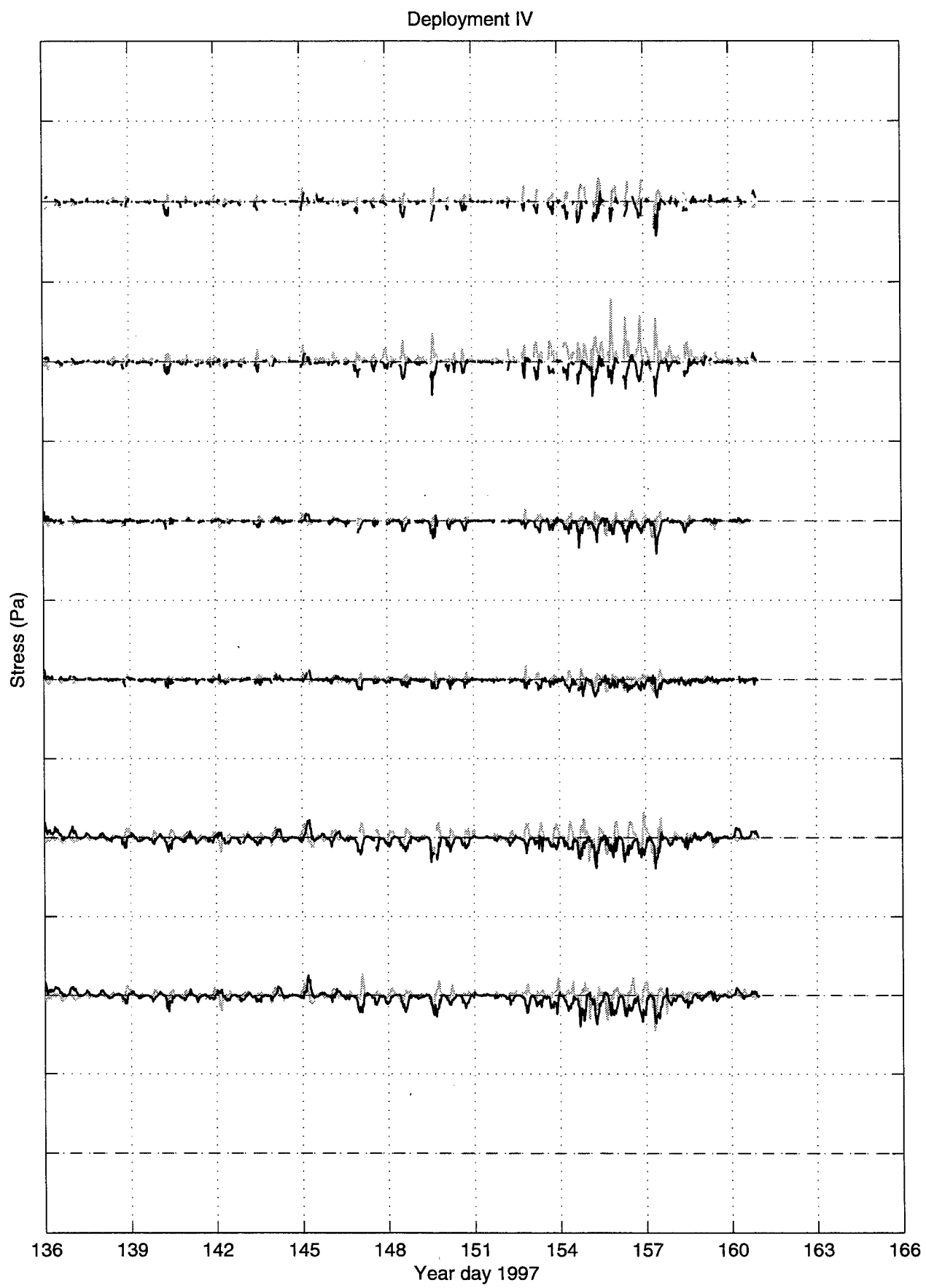
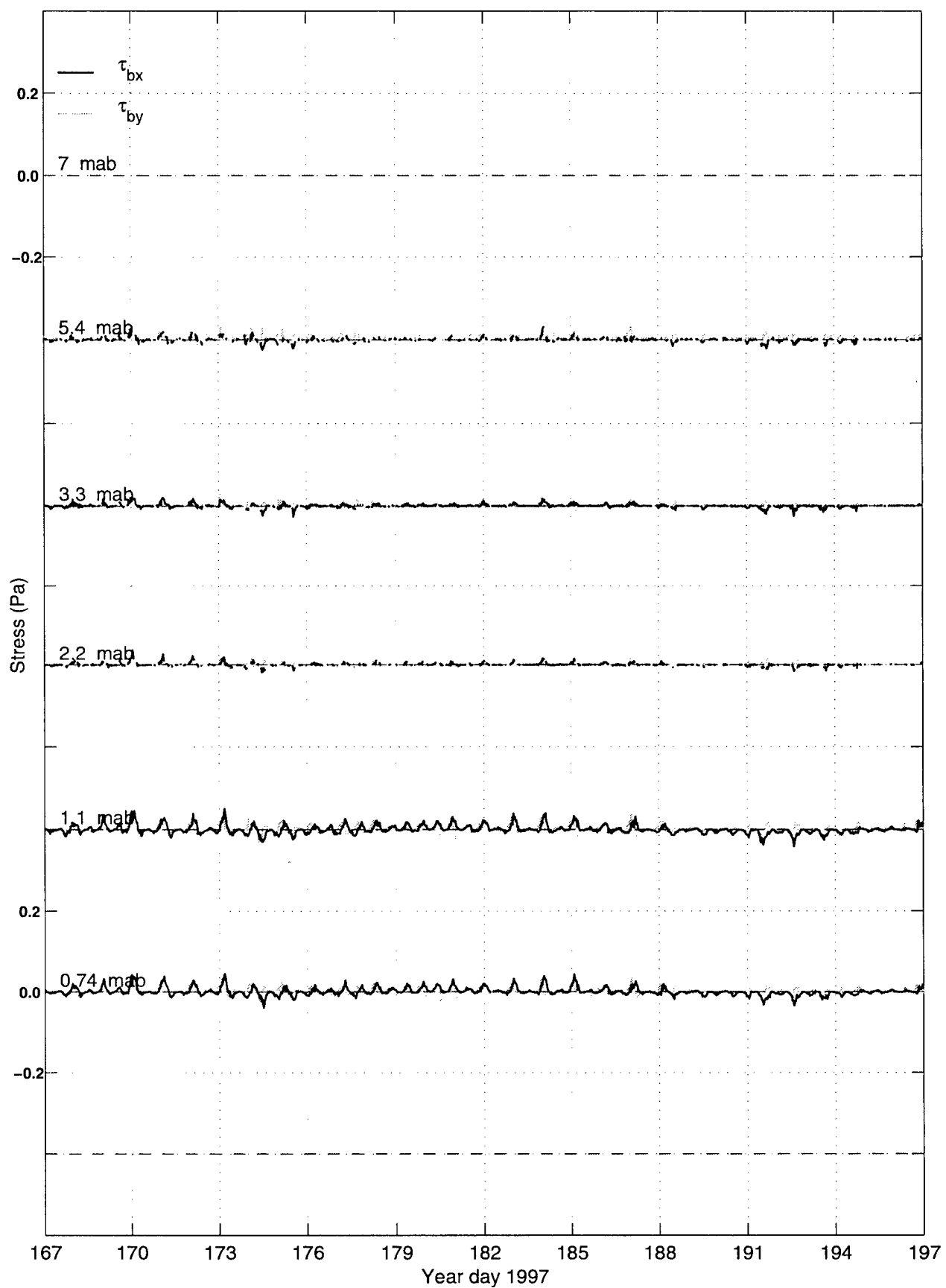


Figure 42

Deployment V (continued)



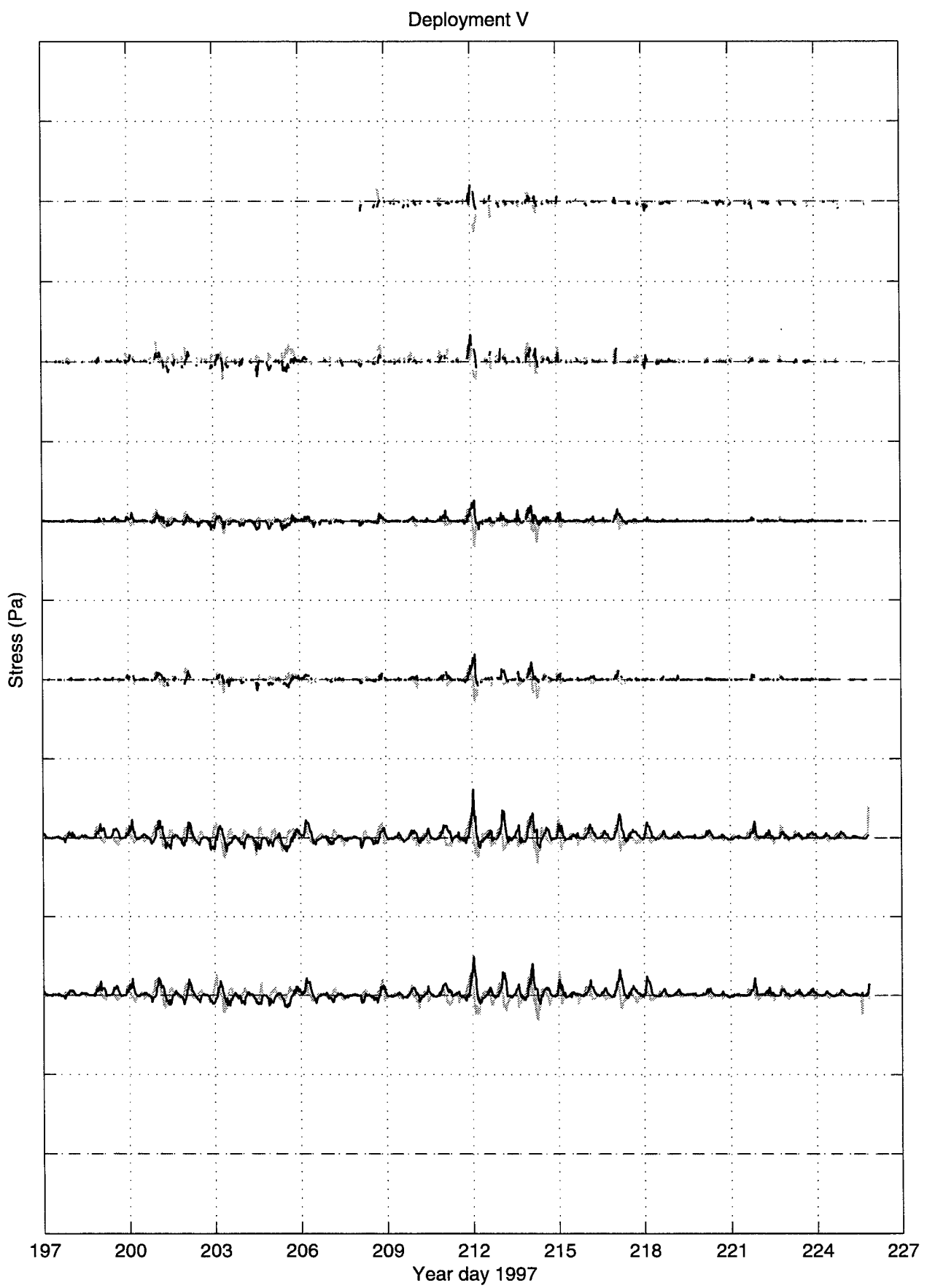
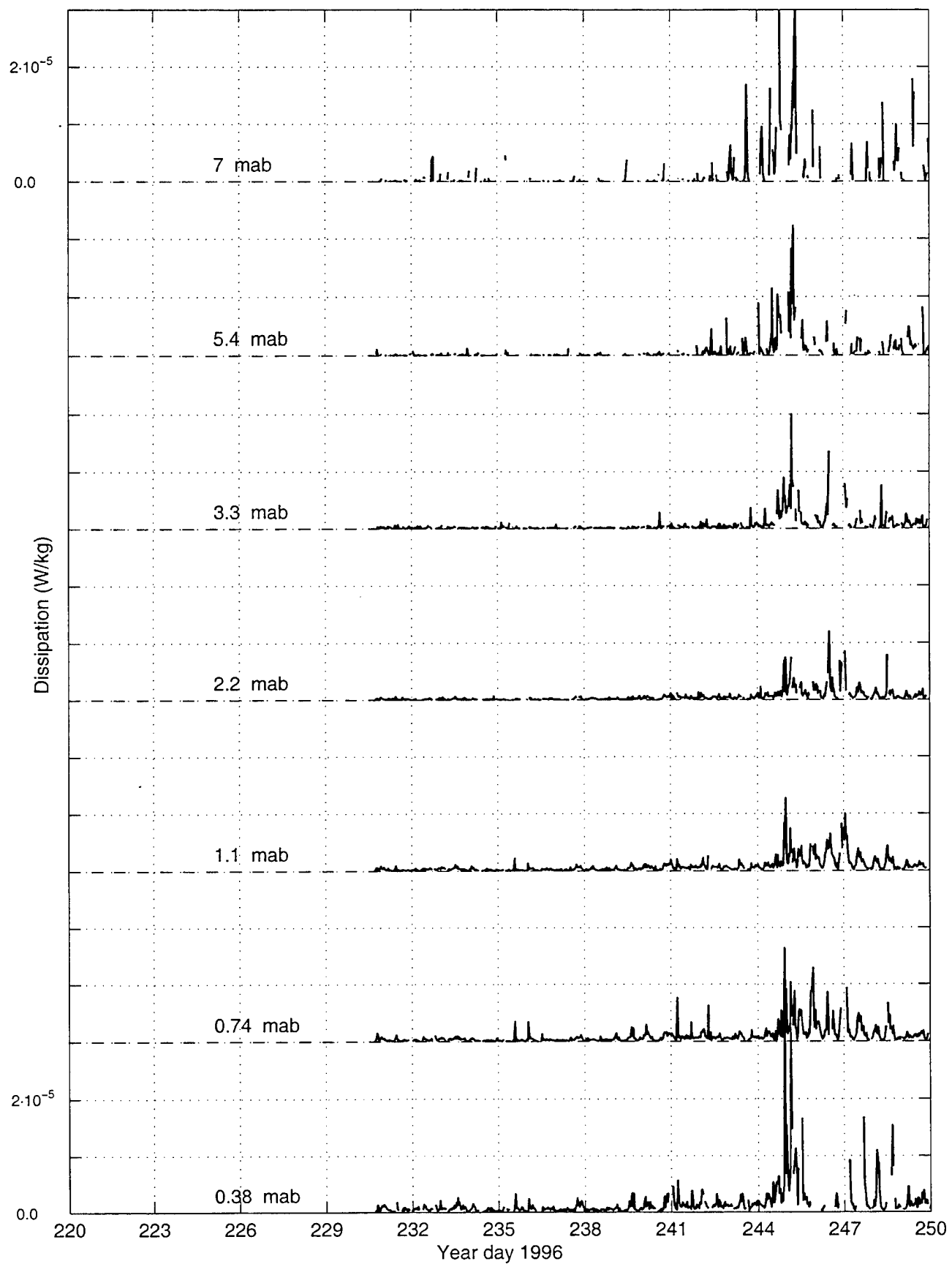


Figure 43

Dissipation of Turbulent Kinetic Energy (ε)

Deployment I (continued)



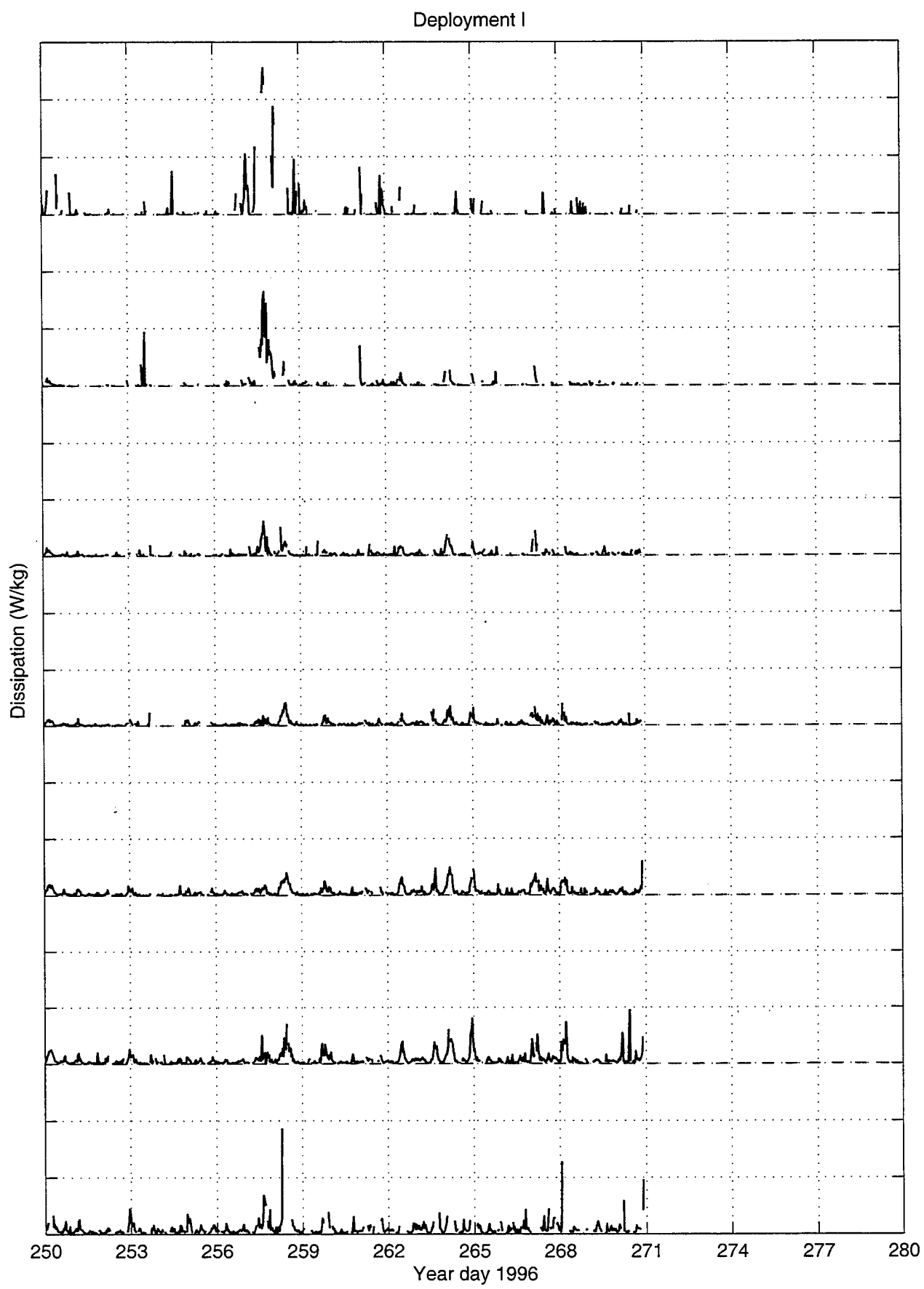
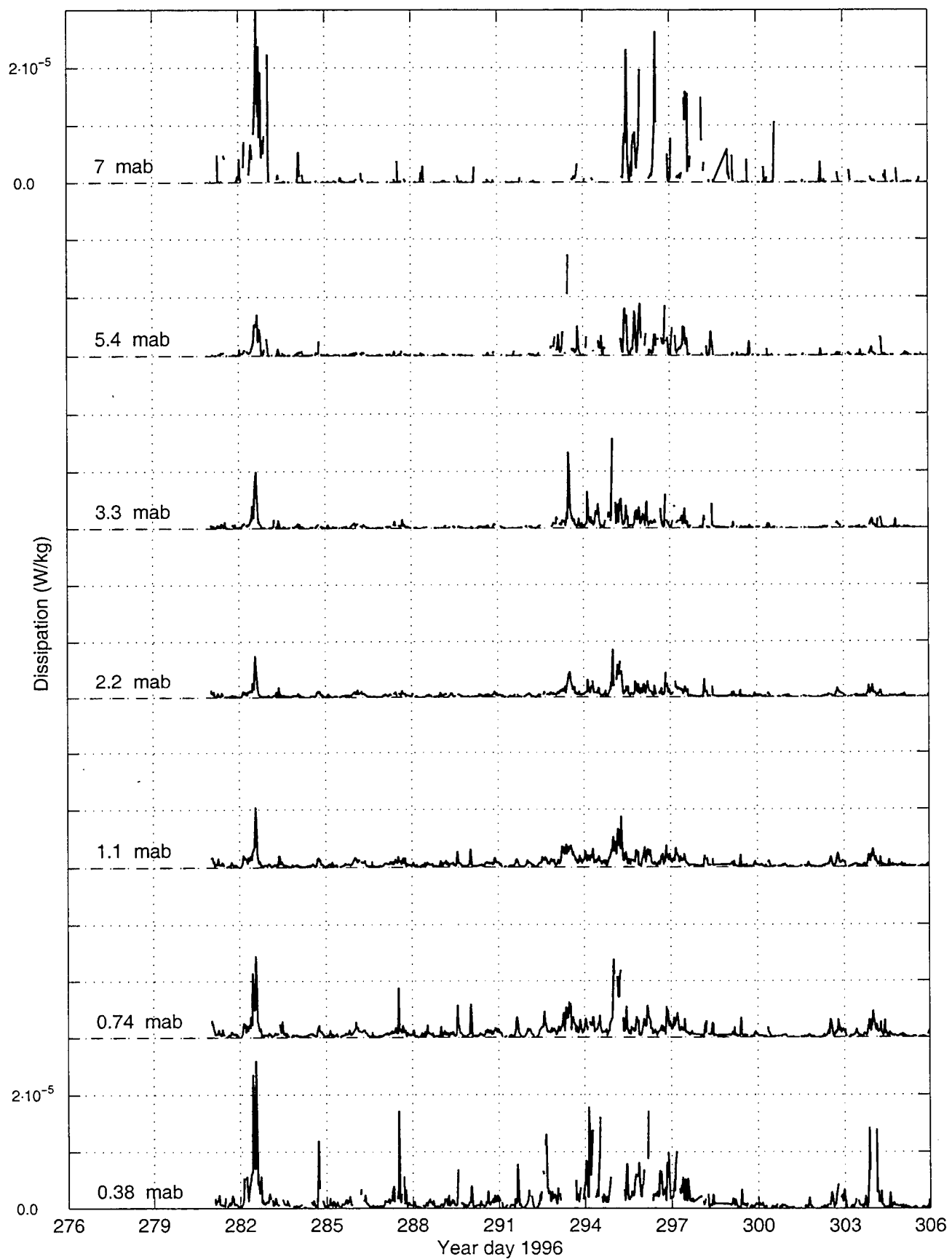


Figure 44

Deployment II (continued)



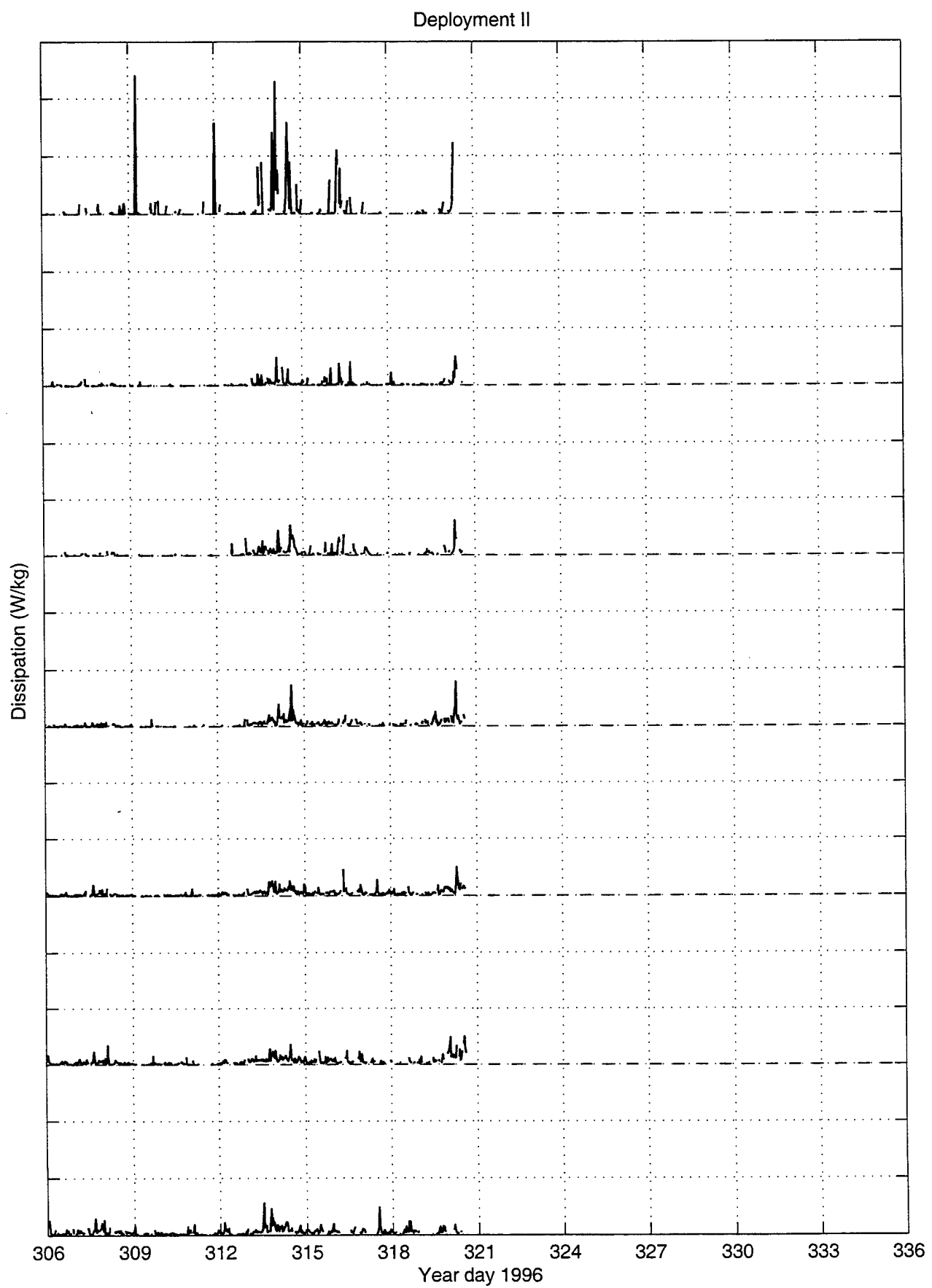
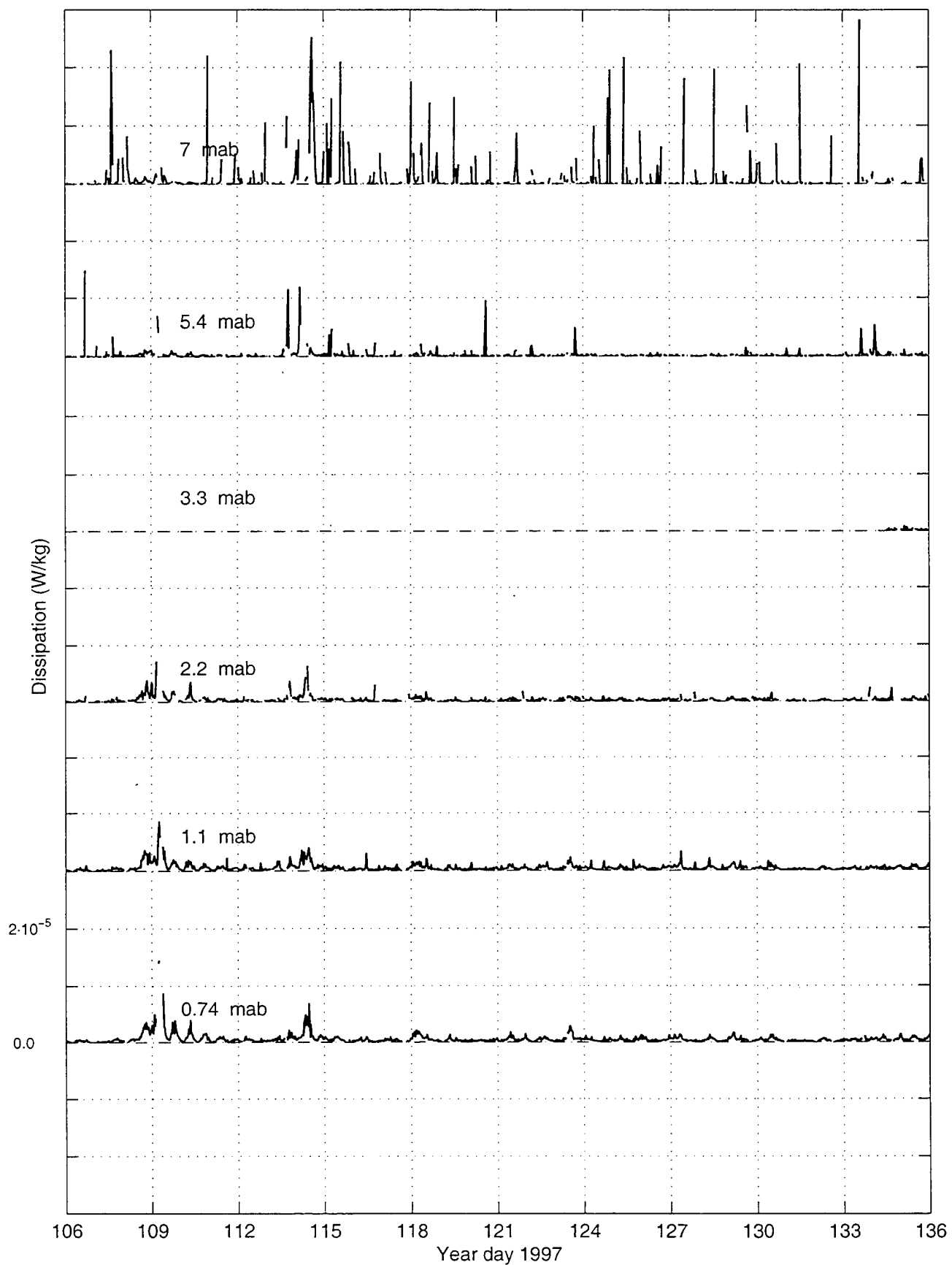


Figure 45

Deployment IV (continued)



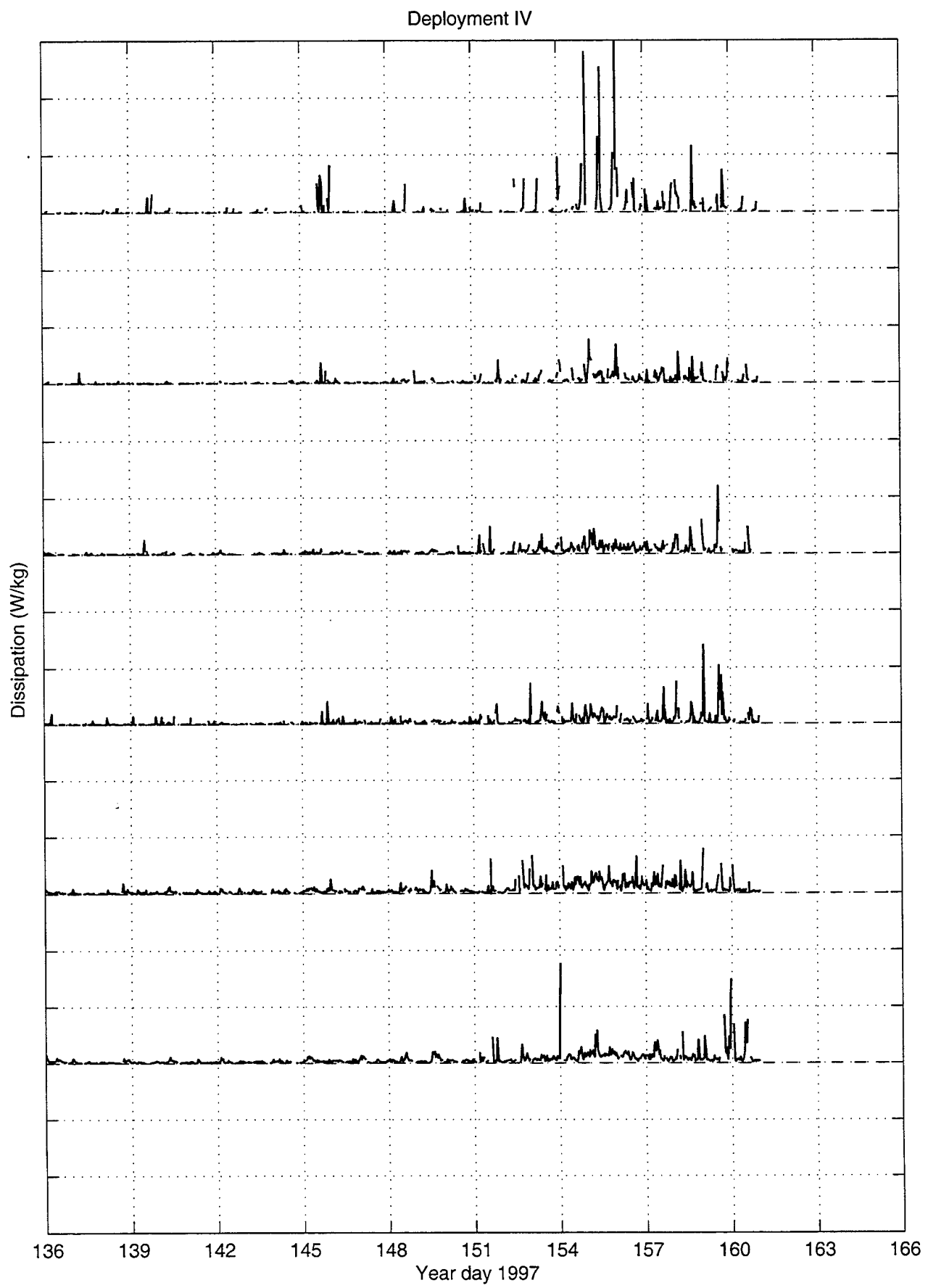
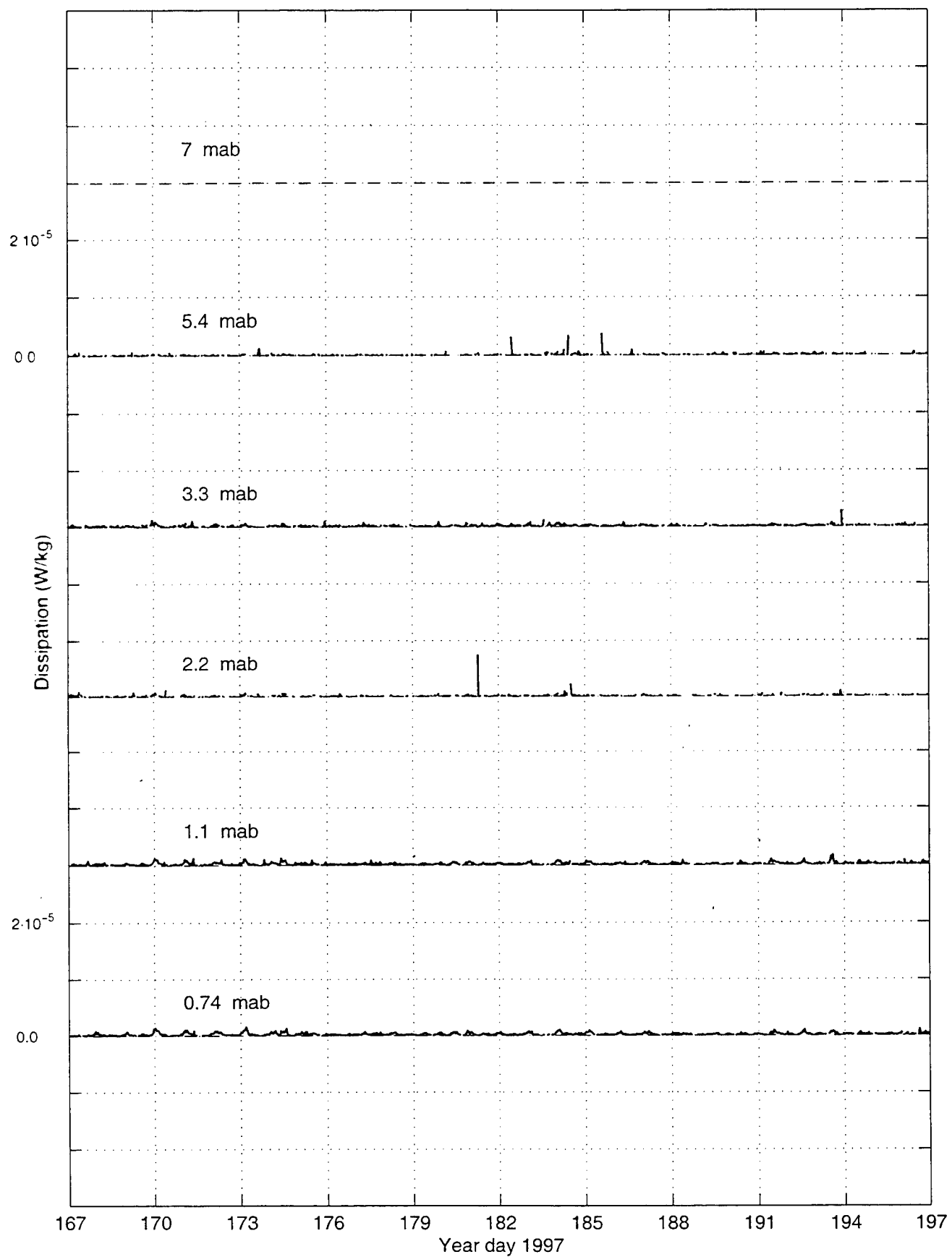


Figure 46

Deployment V (continued)



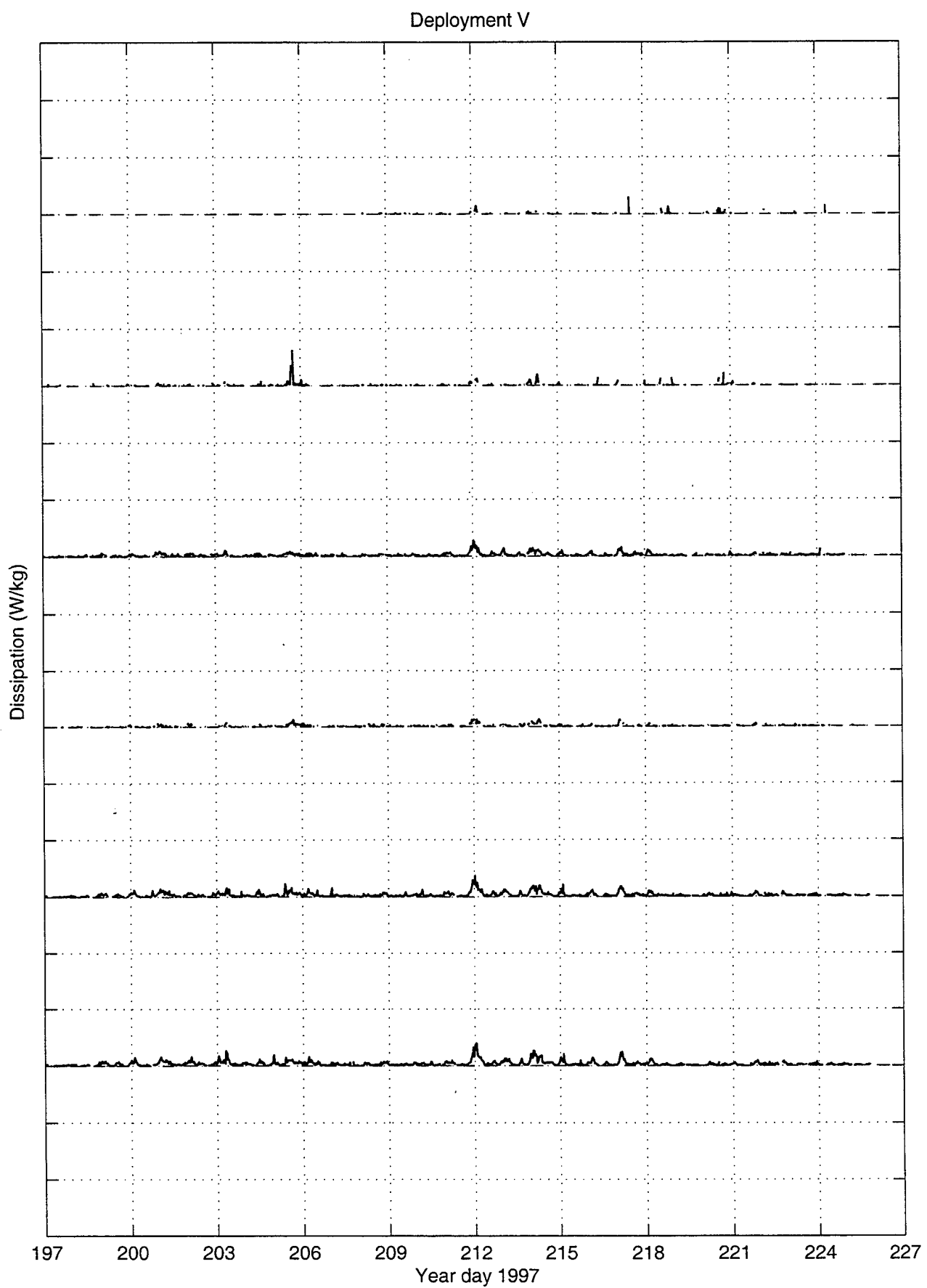
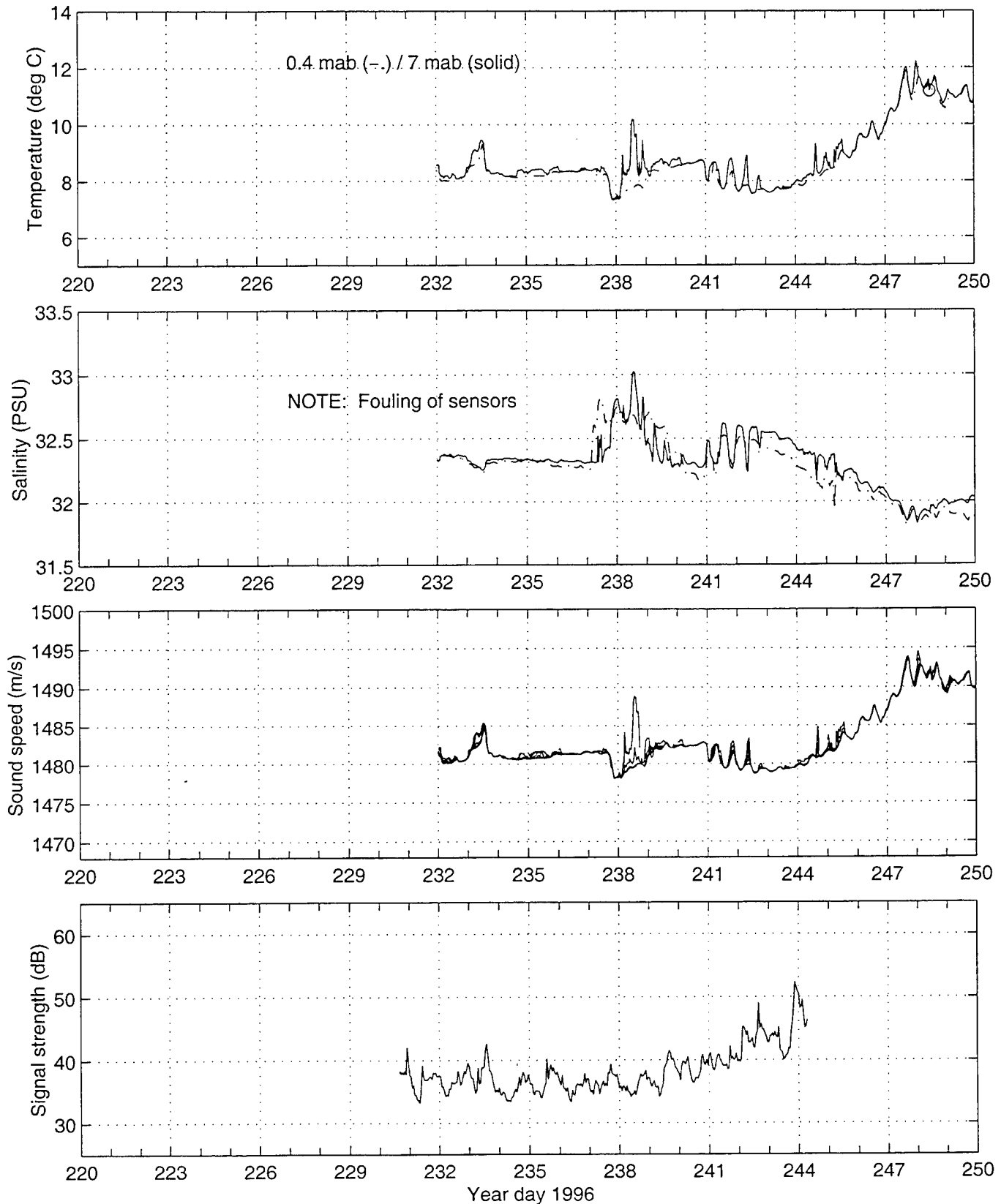


Figure 47

**Salinity, Temperature,
Sound Speed &
ADV Signal Strength**

Deployment I (continued on next page)



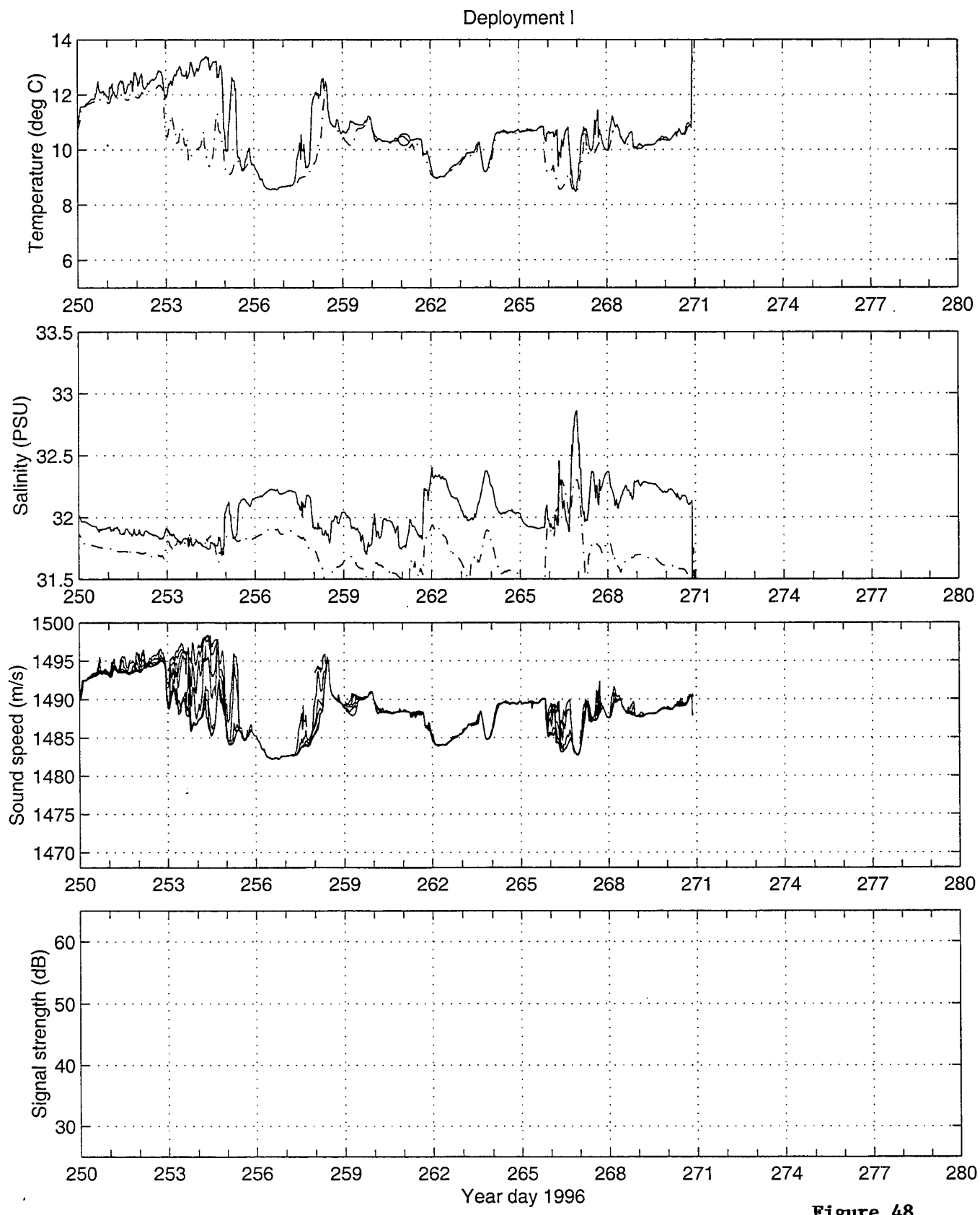
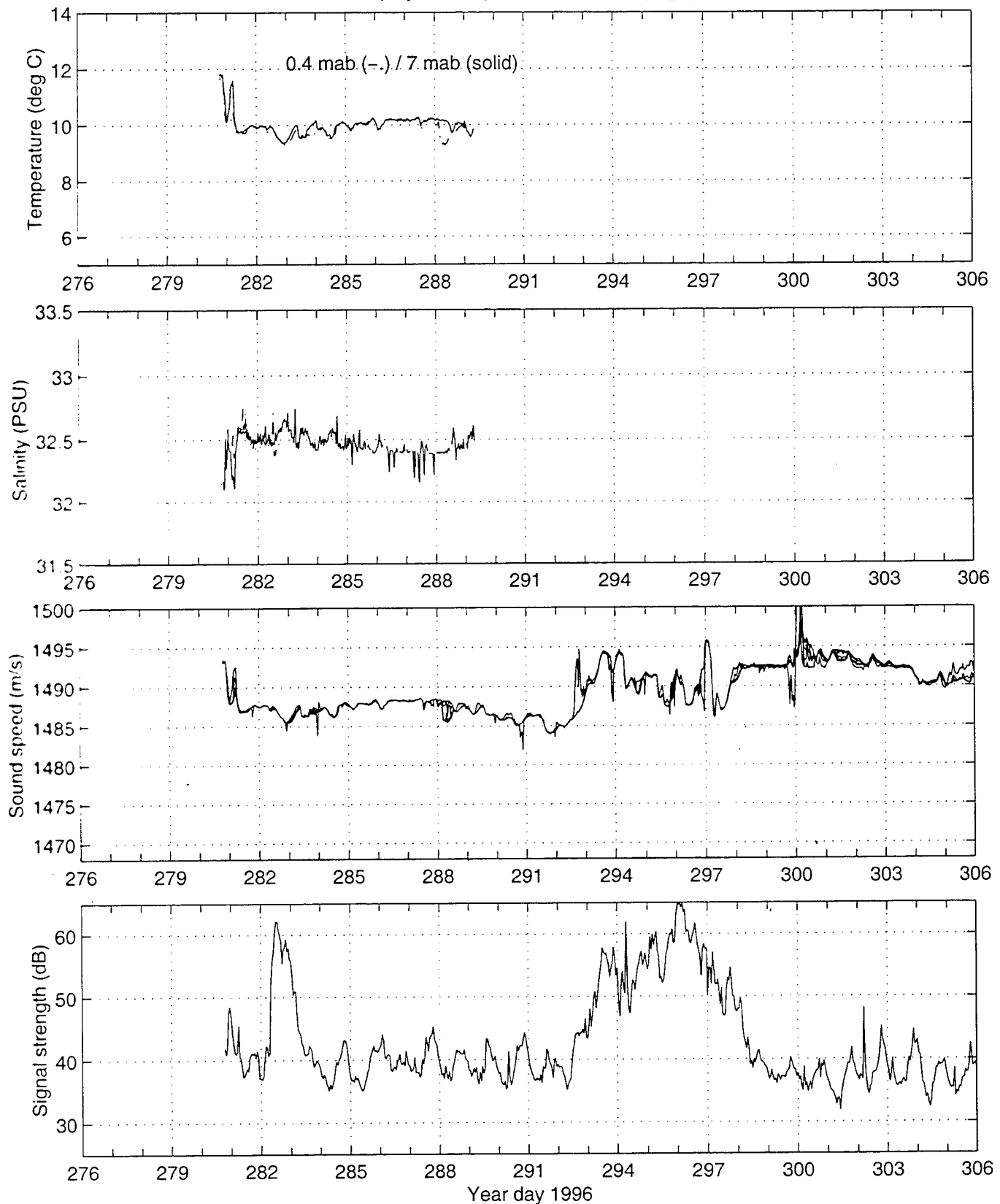


Figure 48

Deployment II (continued on next page)



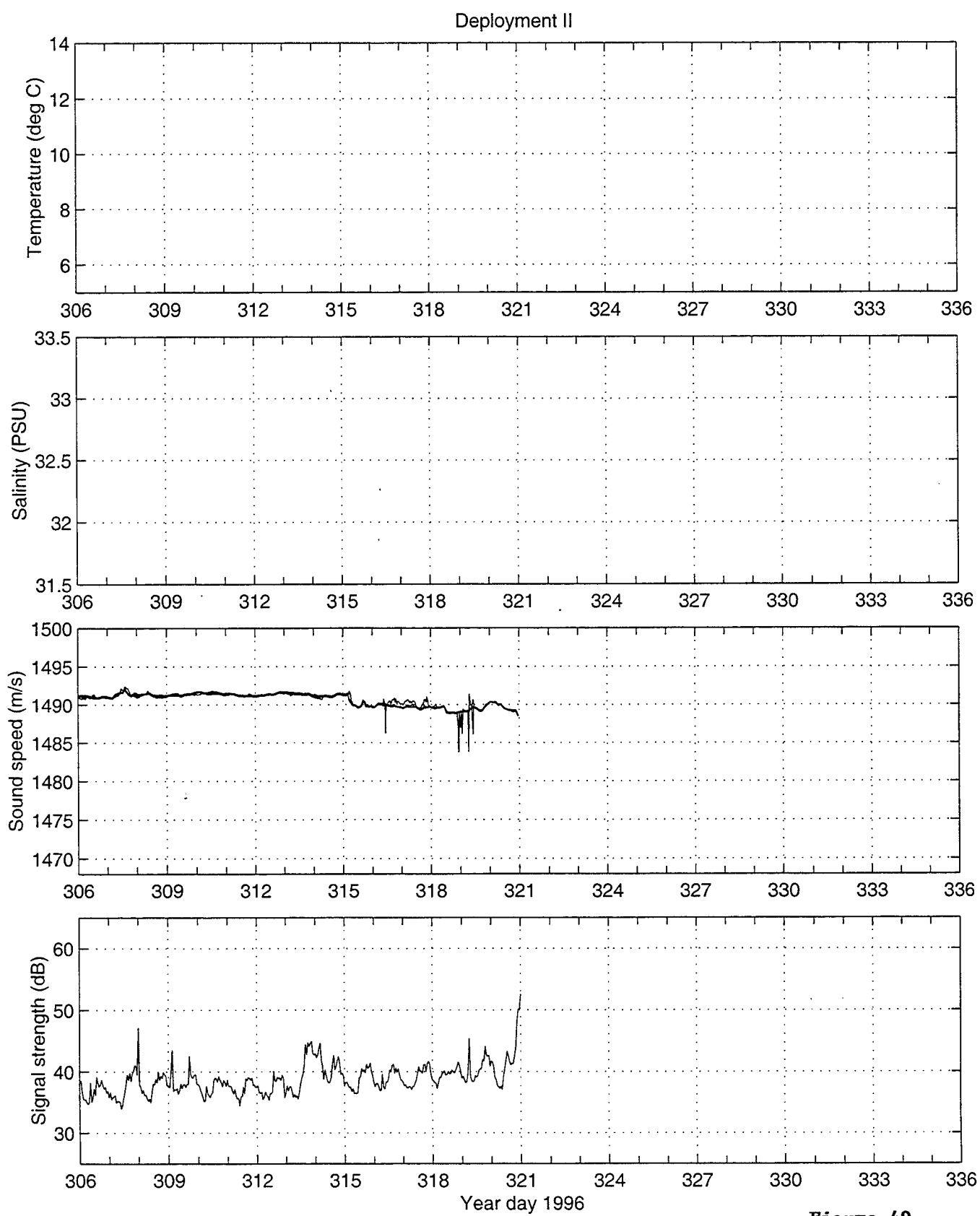
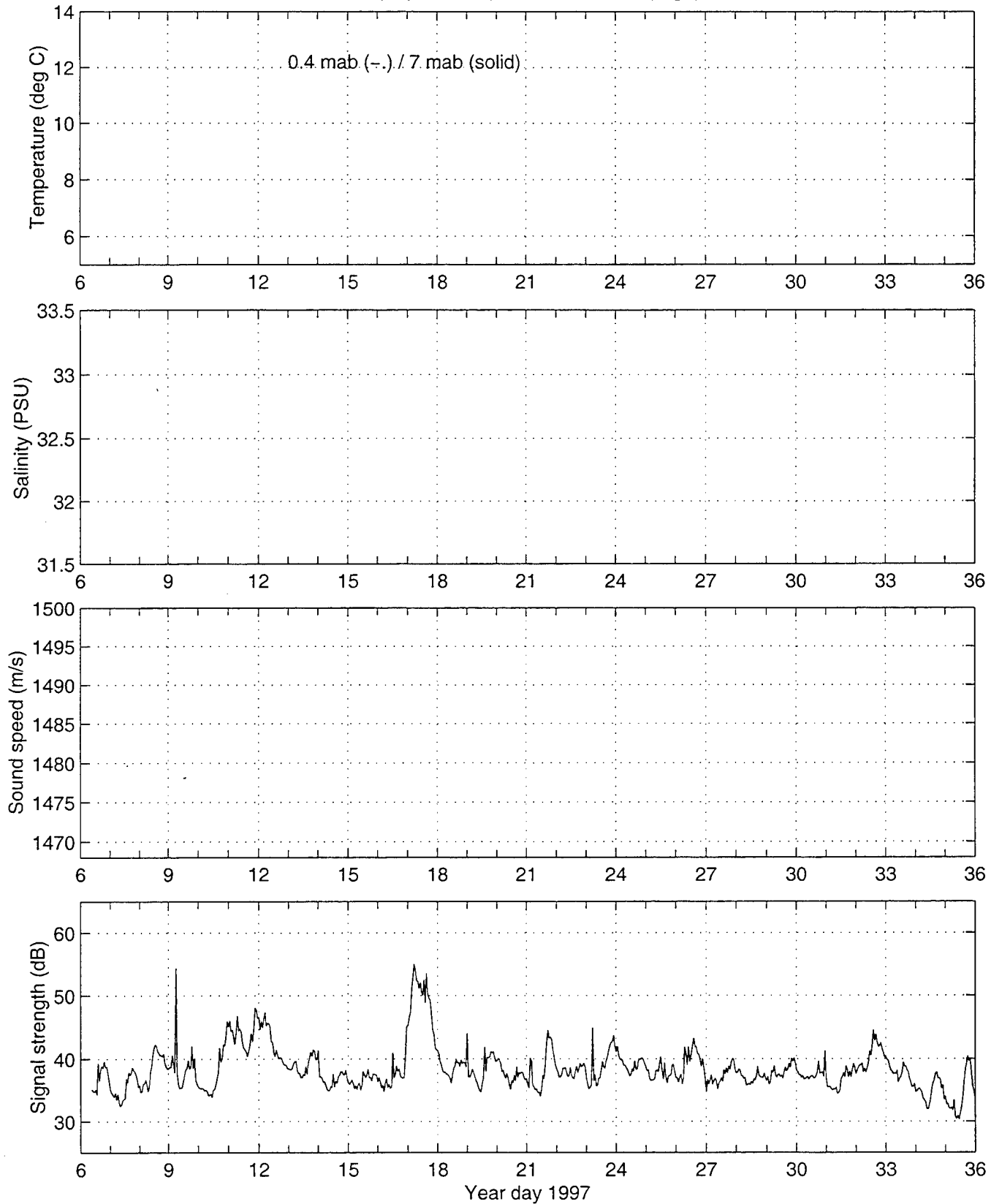


Figure 49

Deployment III (continued on next page)



Deployment III (continued on next page)

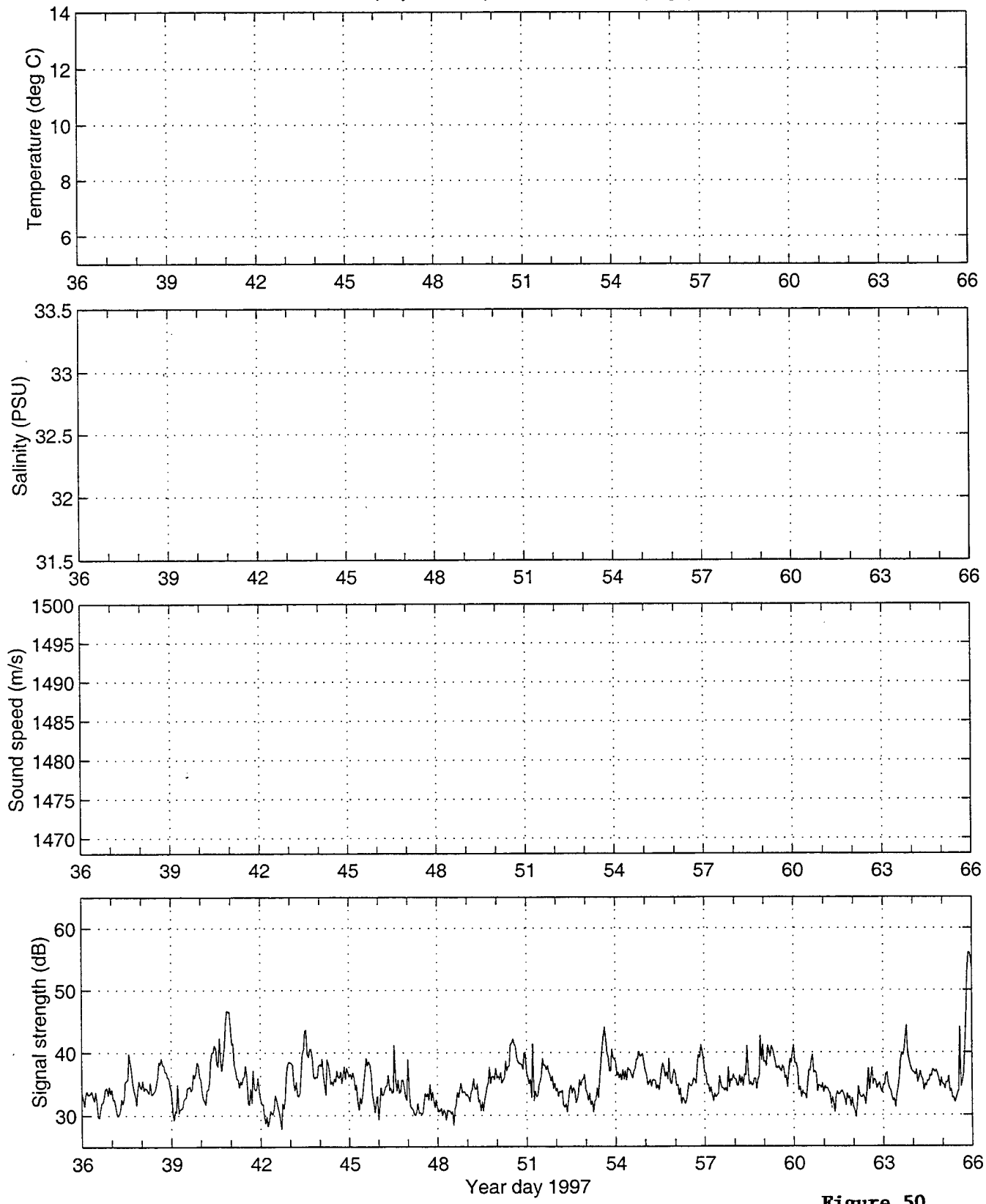


Figure 50

— THIS PAGE INTENTIONALLY LEFT BLANK —

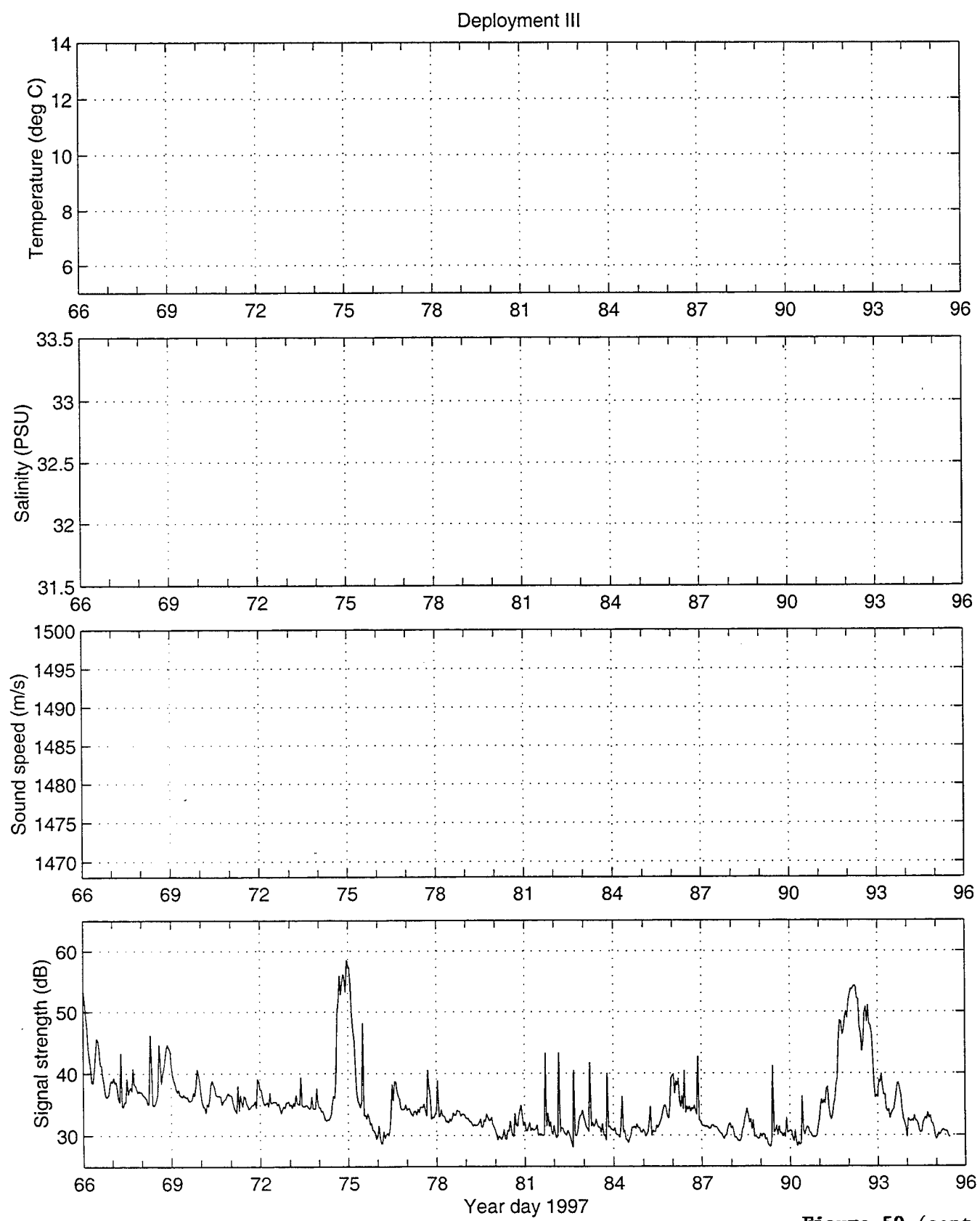
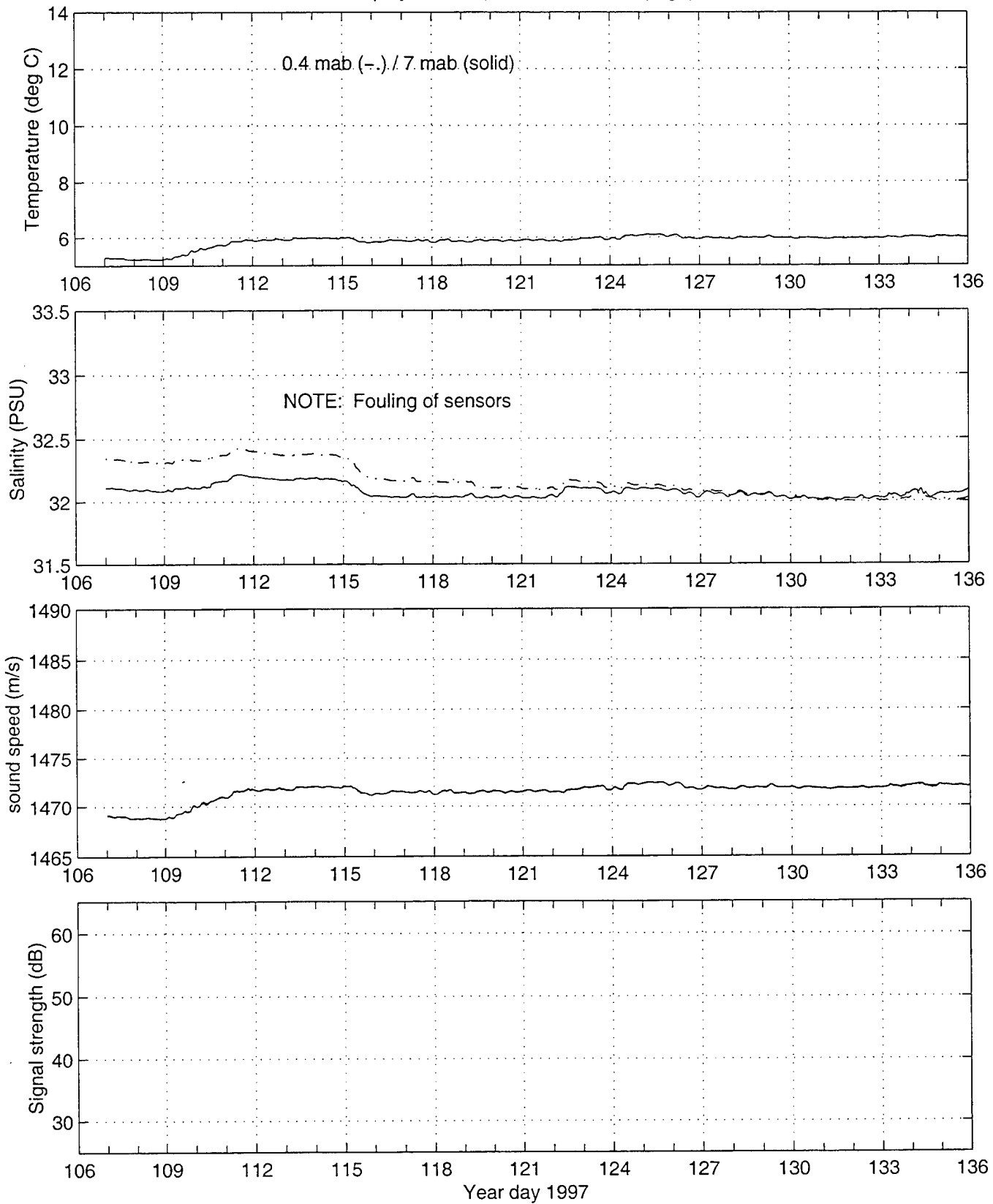


Figure 50 (cont.)

Deployment IV (continued on next page)



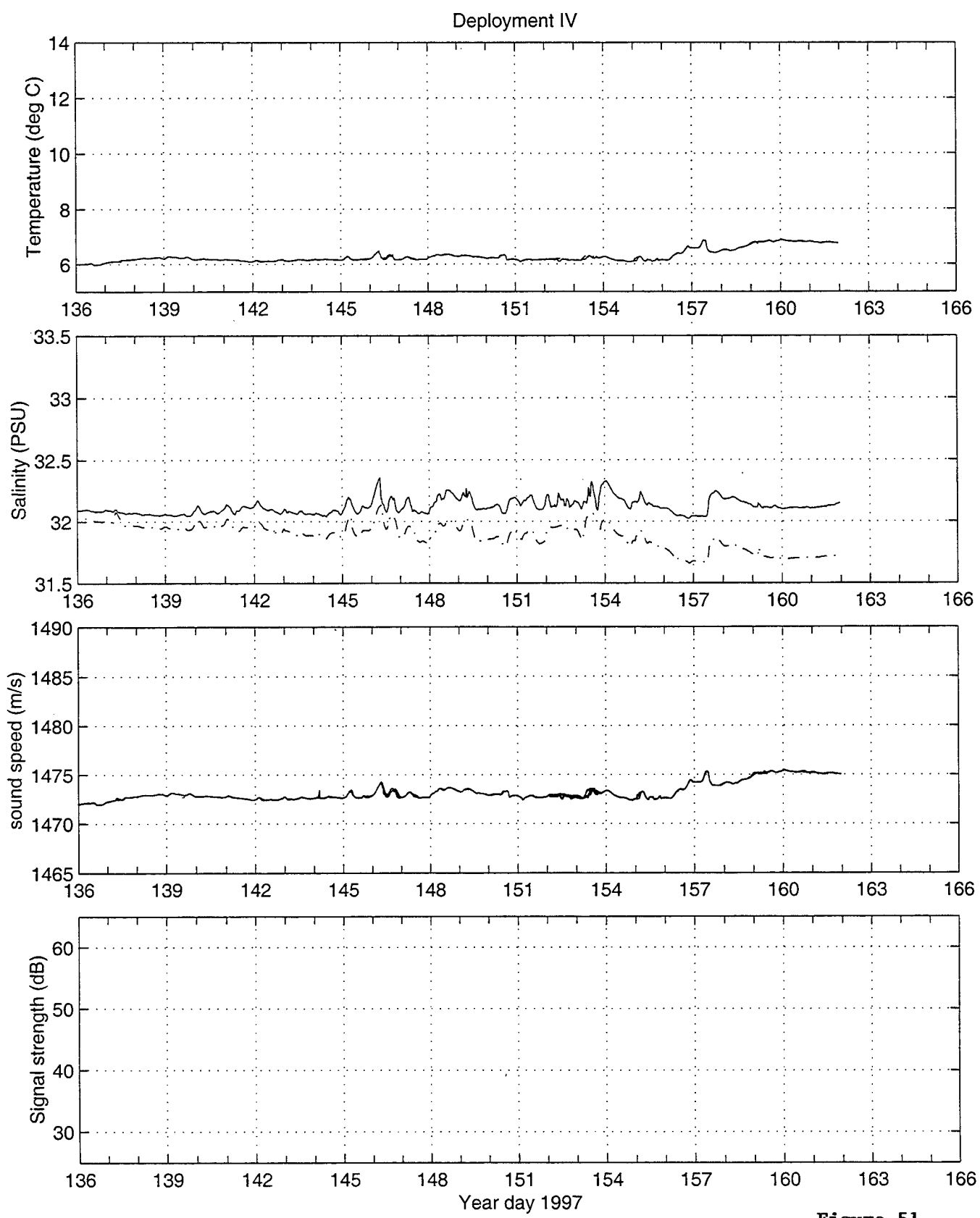
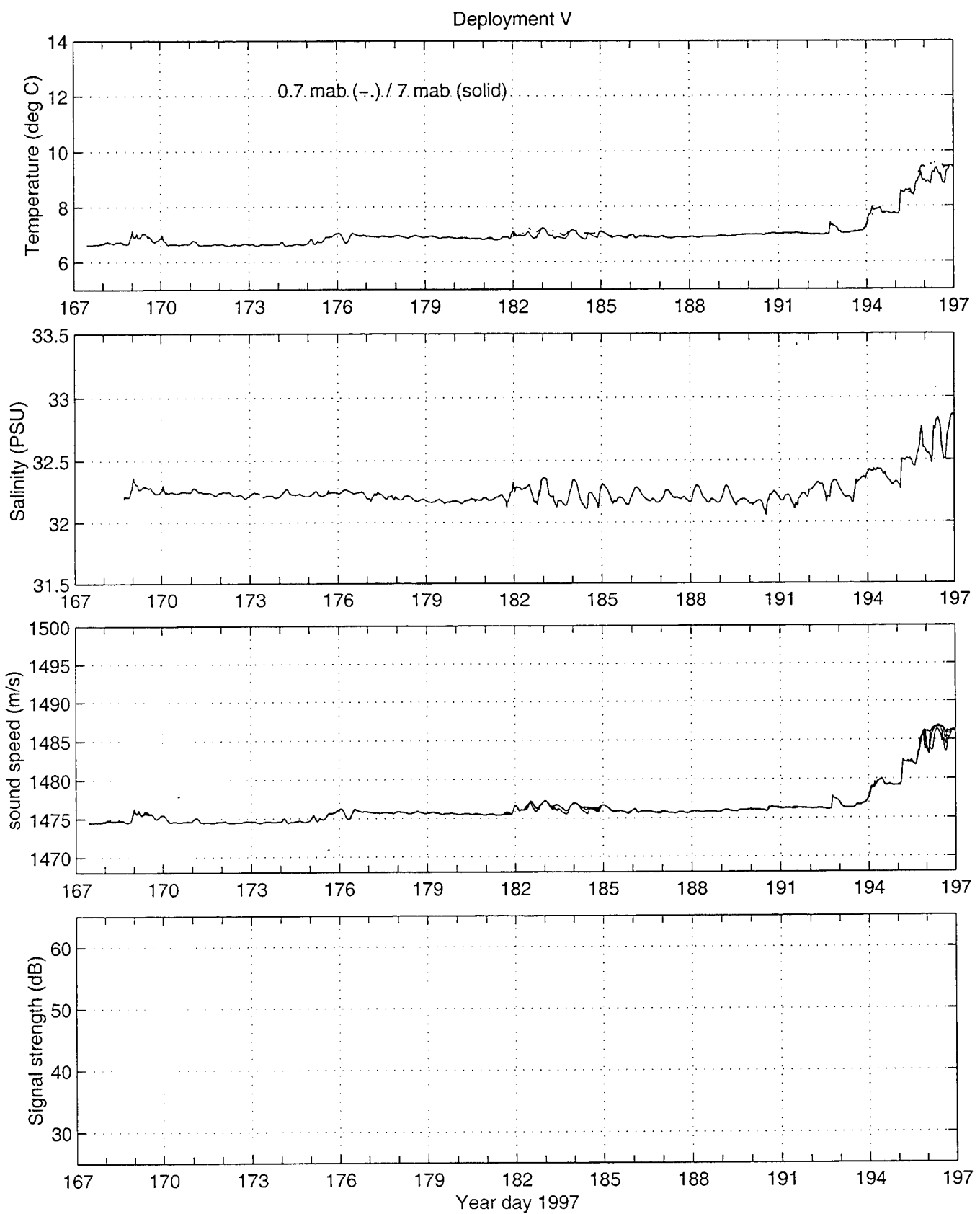


Figure 51



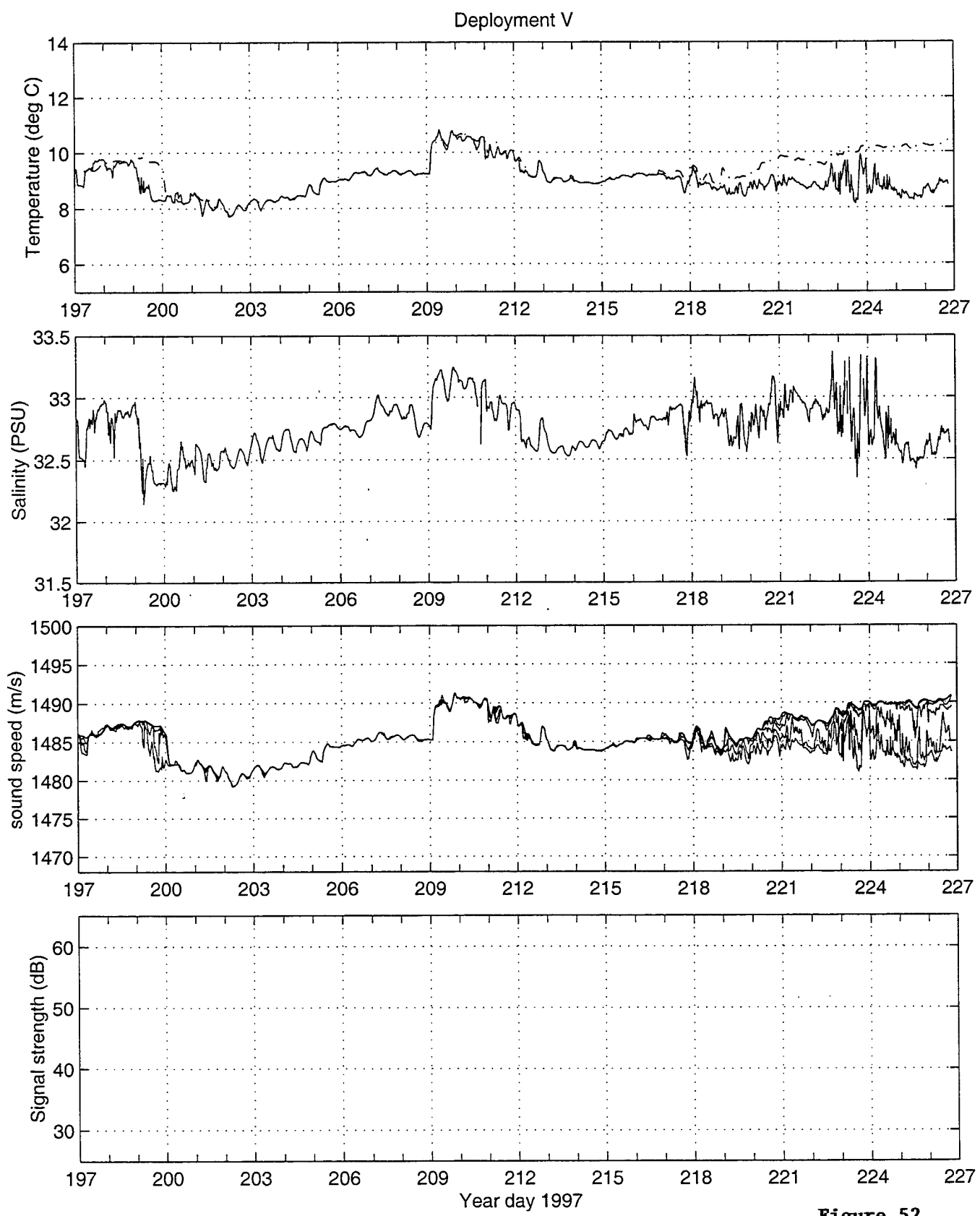
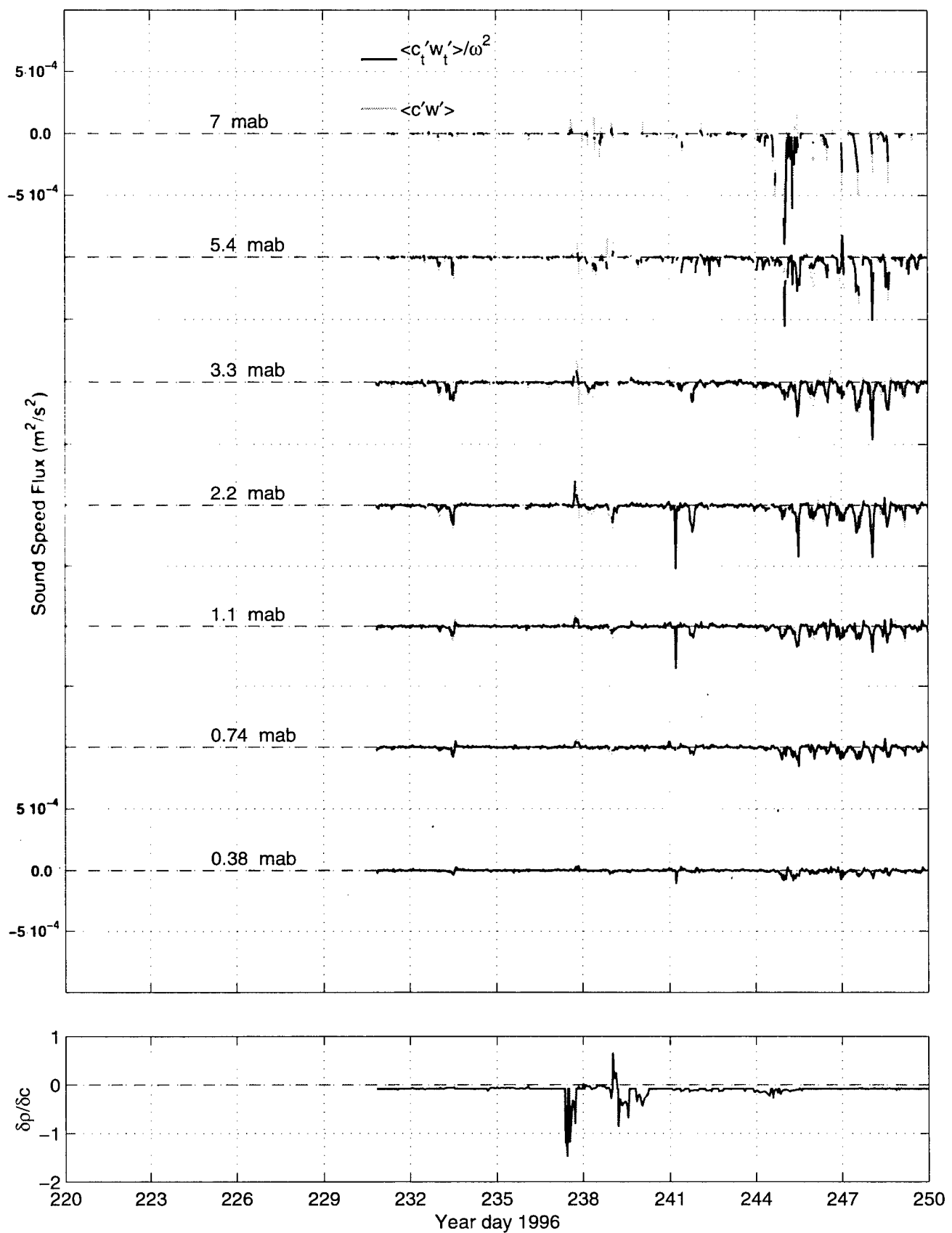


Figure 52

**Sound Speed Flux and the
Gradient of Density with
Sound Speed ($\partial\rho/\partial c$)**

Deployment I (continued)



Deployment I

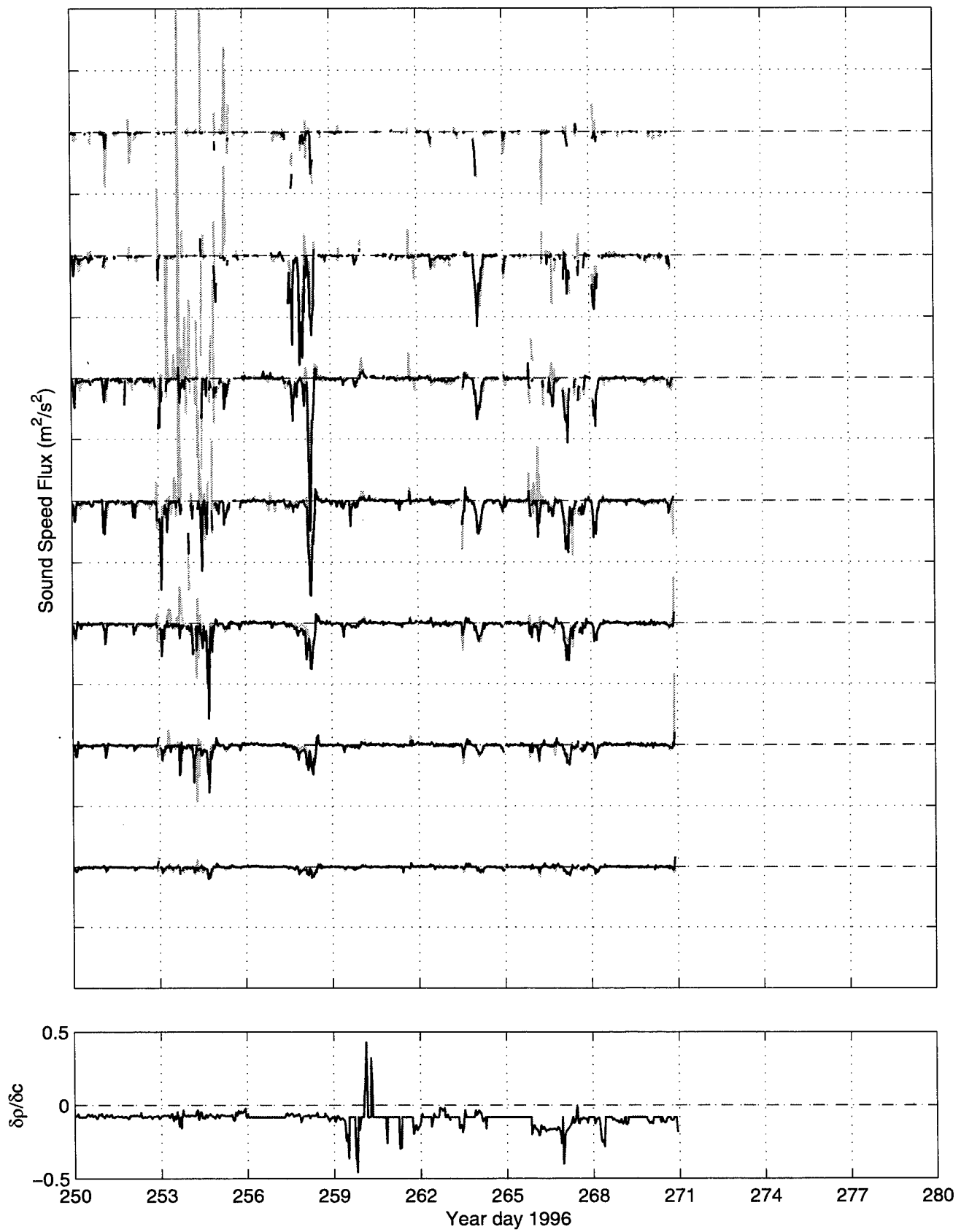
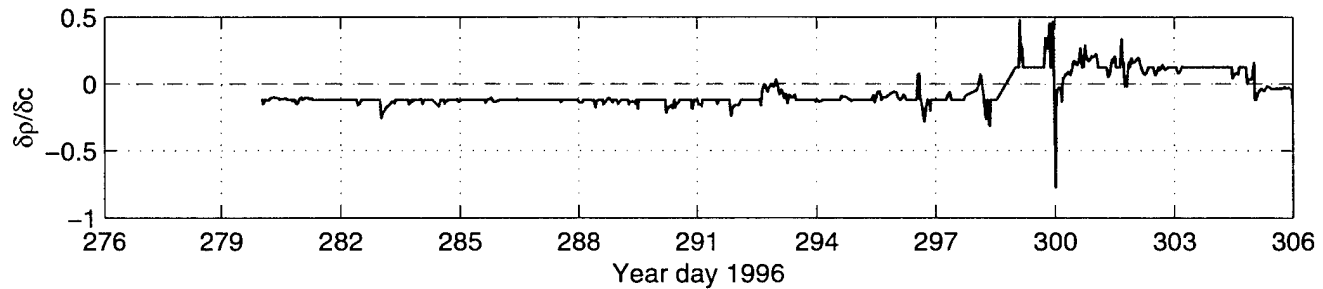
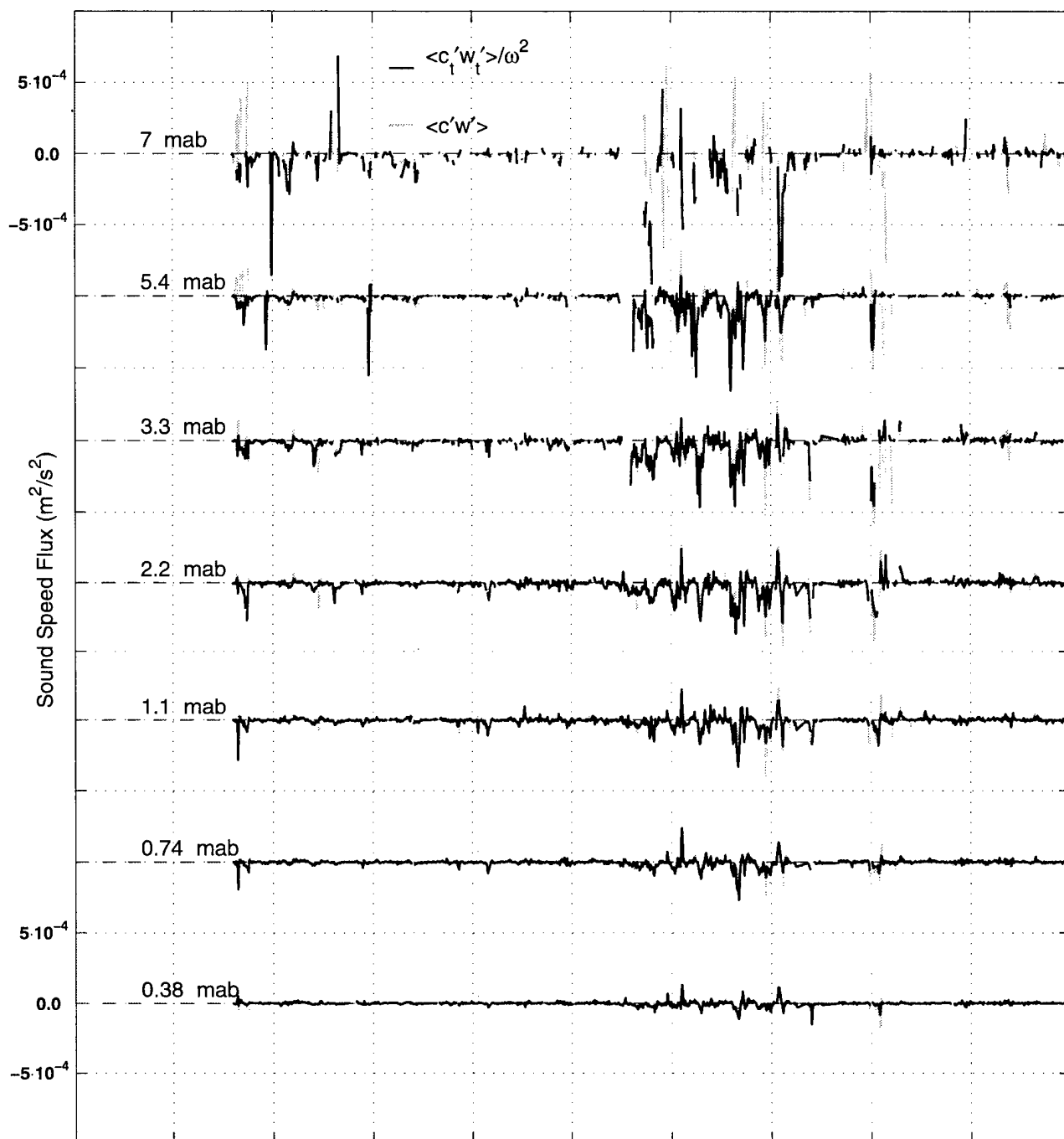
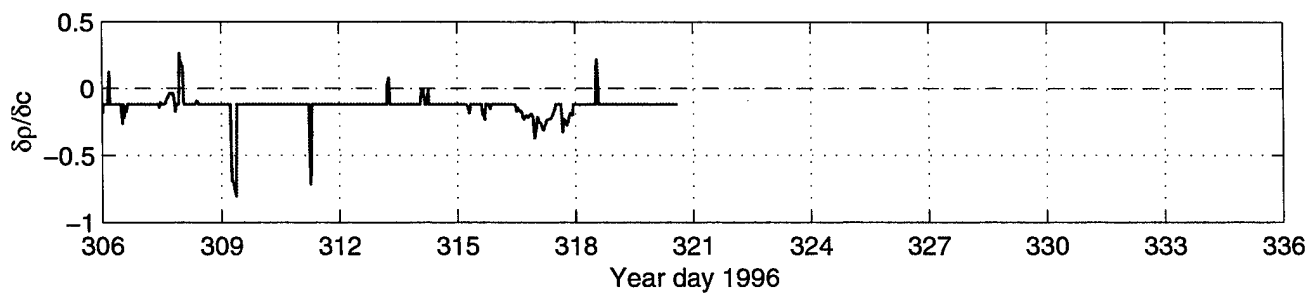
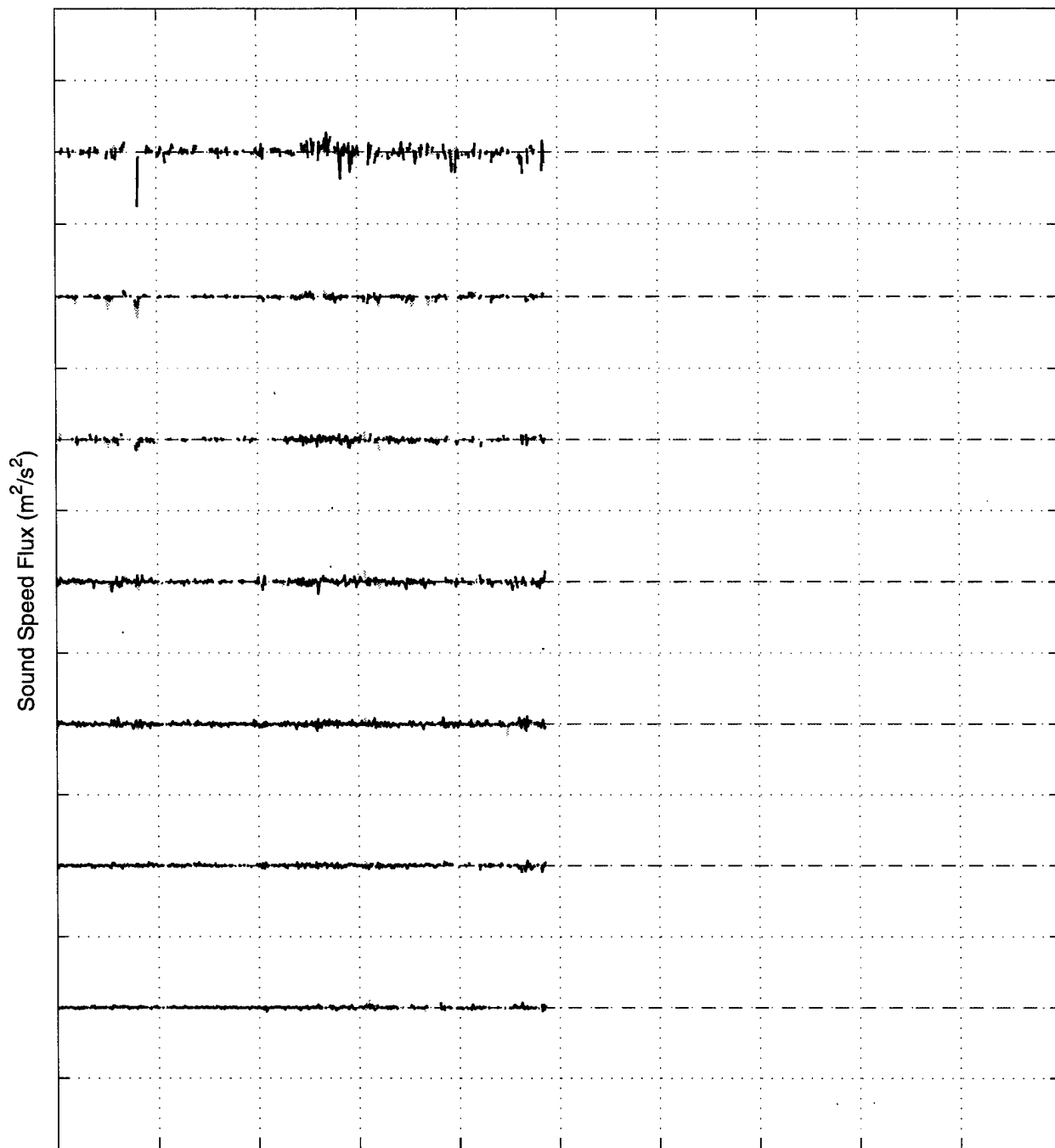


Figure 53

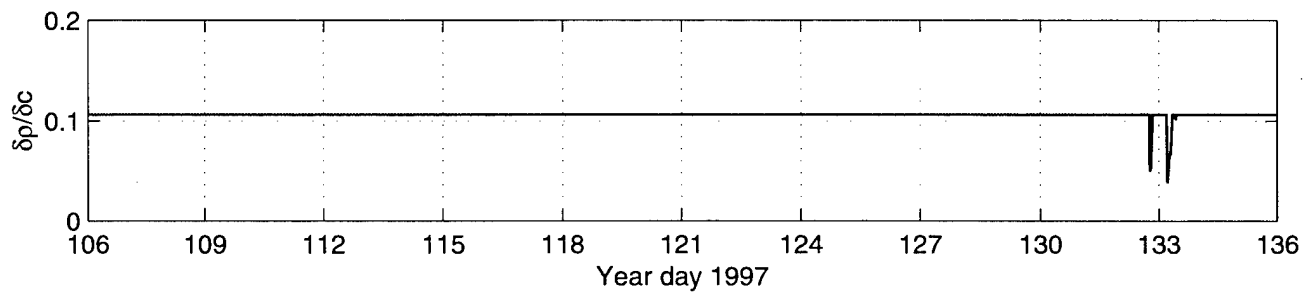
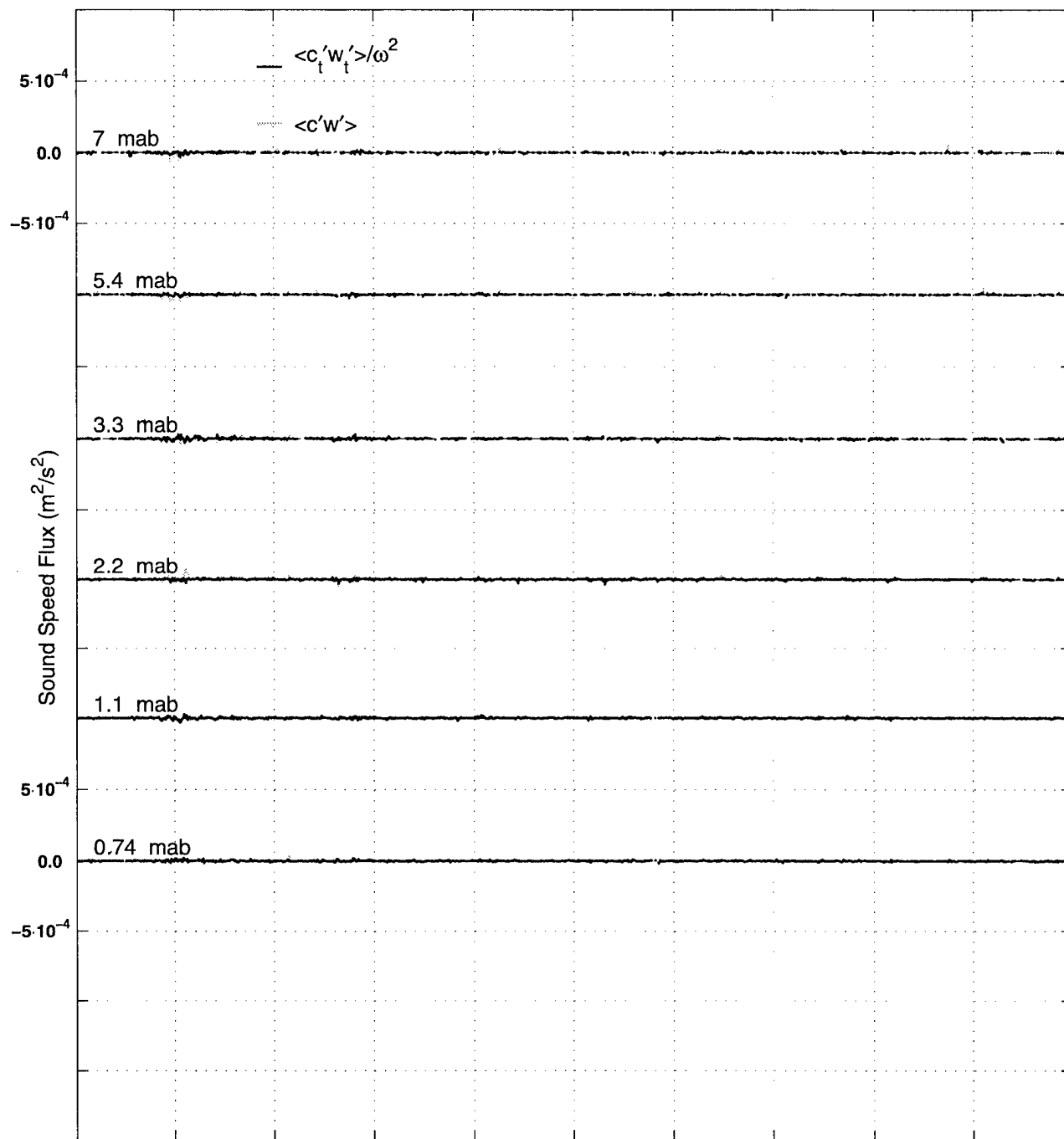
Deployment II (continued)



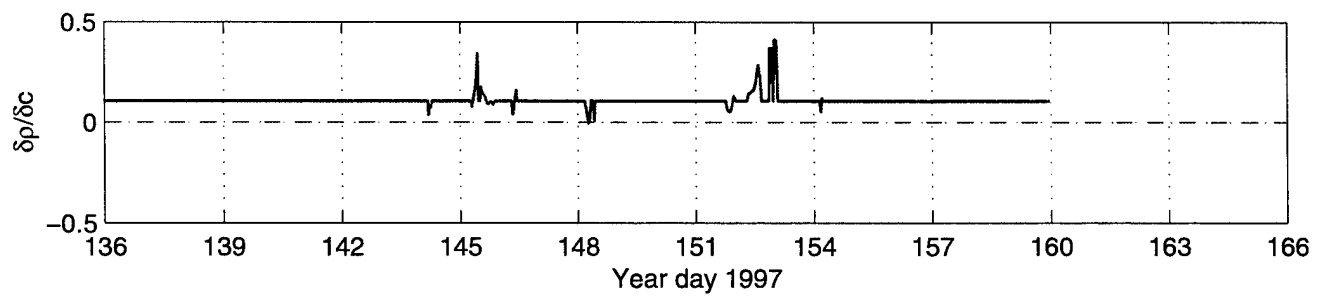
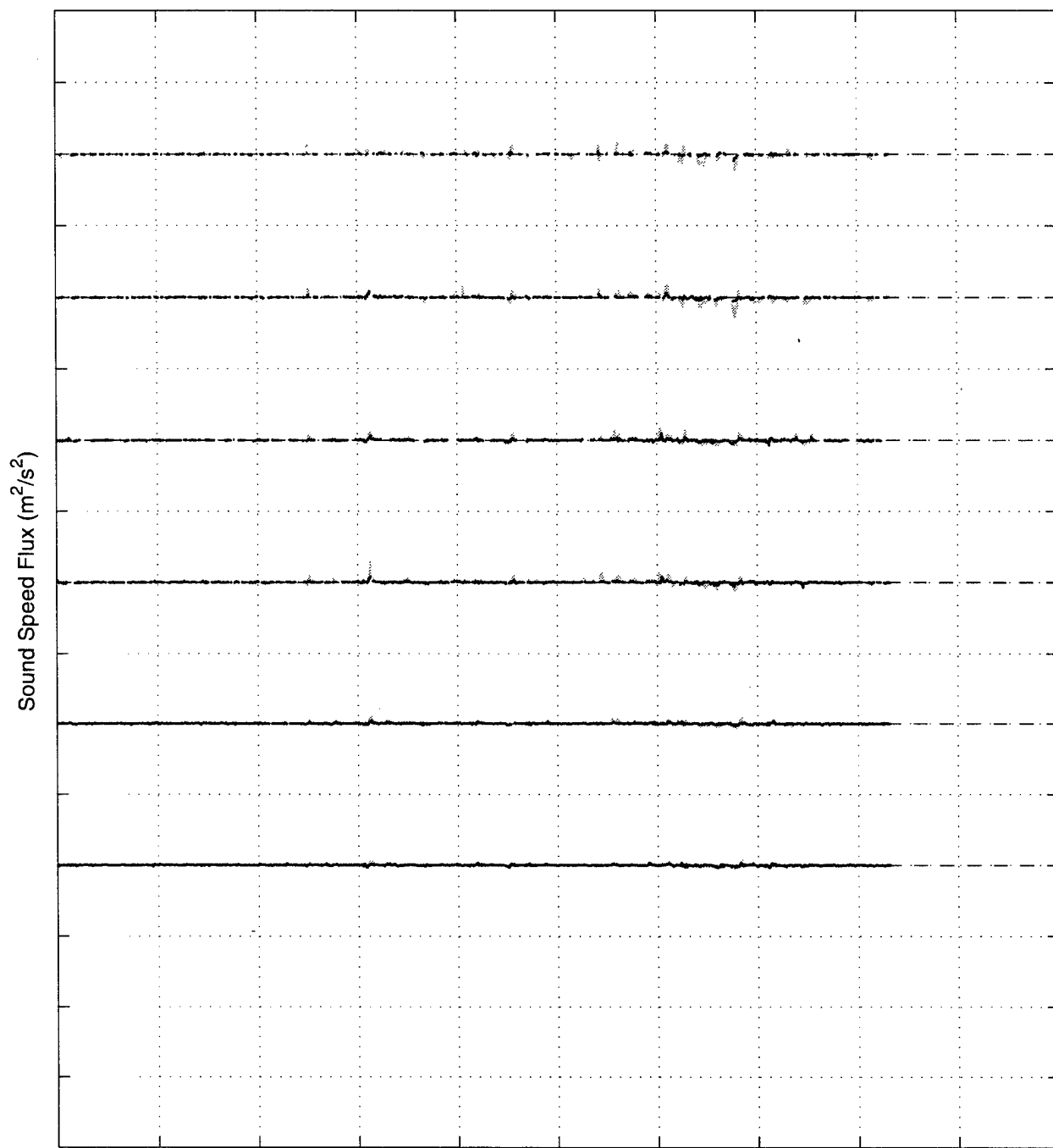
Deployment II



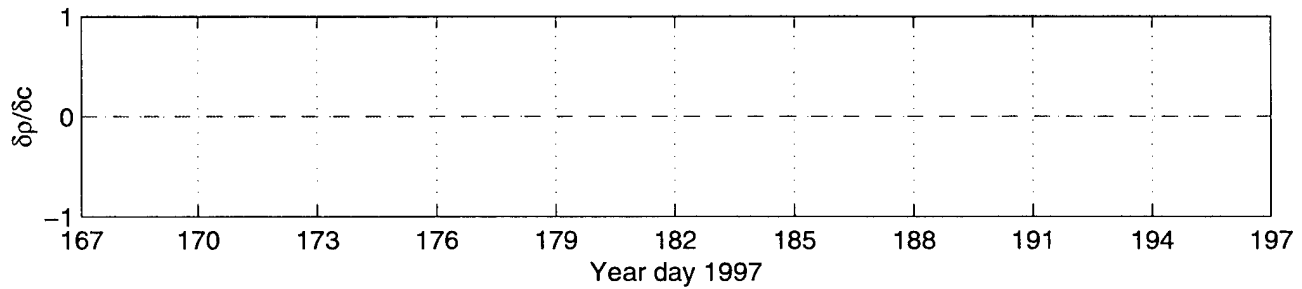
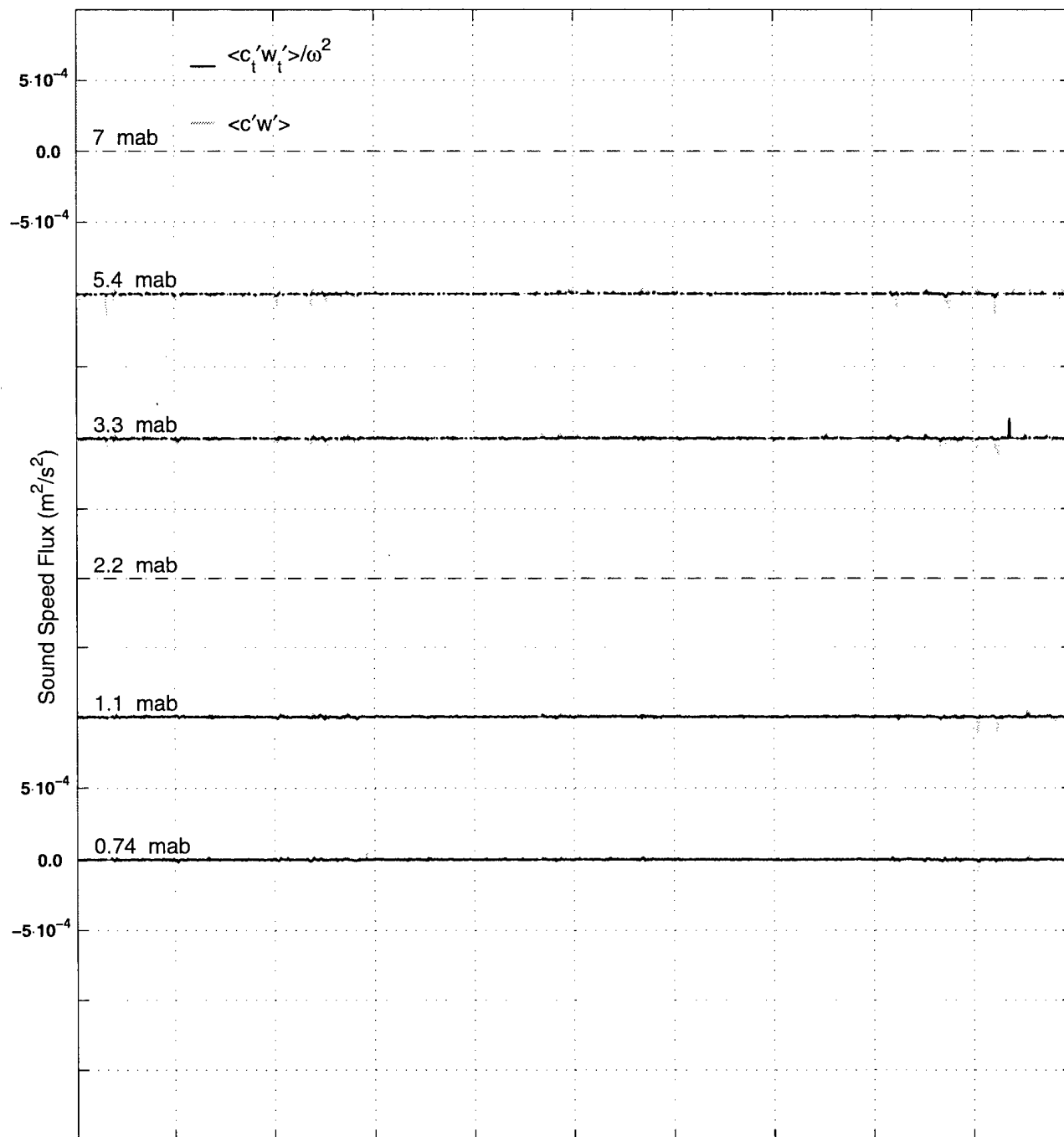
Deployment IV (continued)



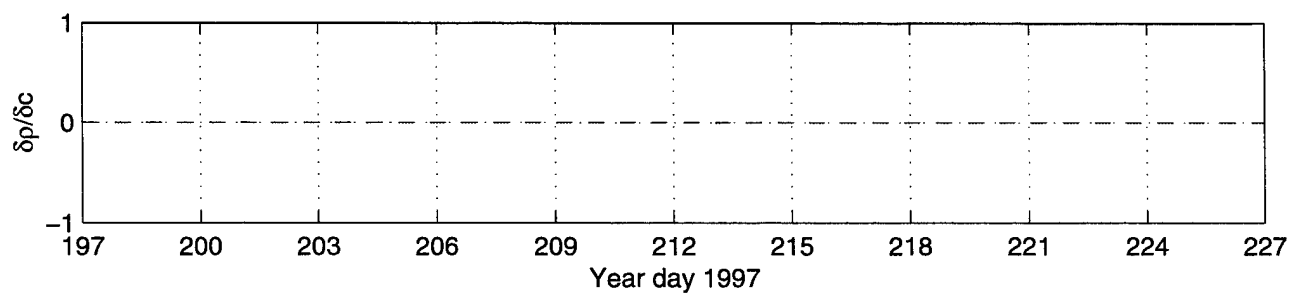
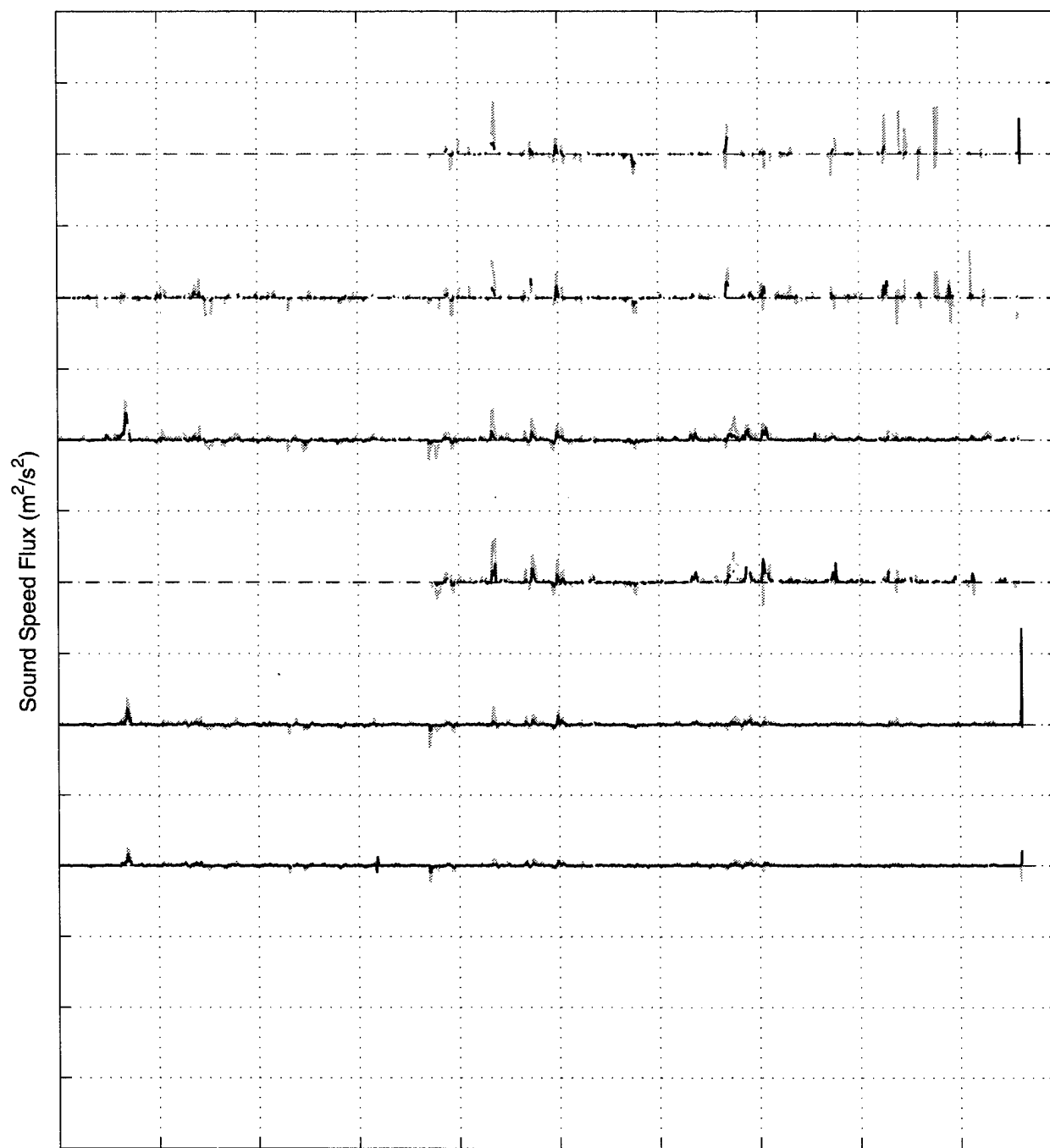
Deployment IV



Deployment V (continued)

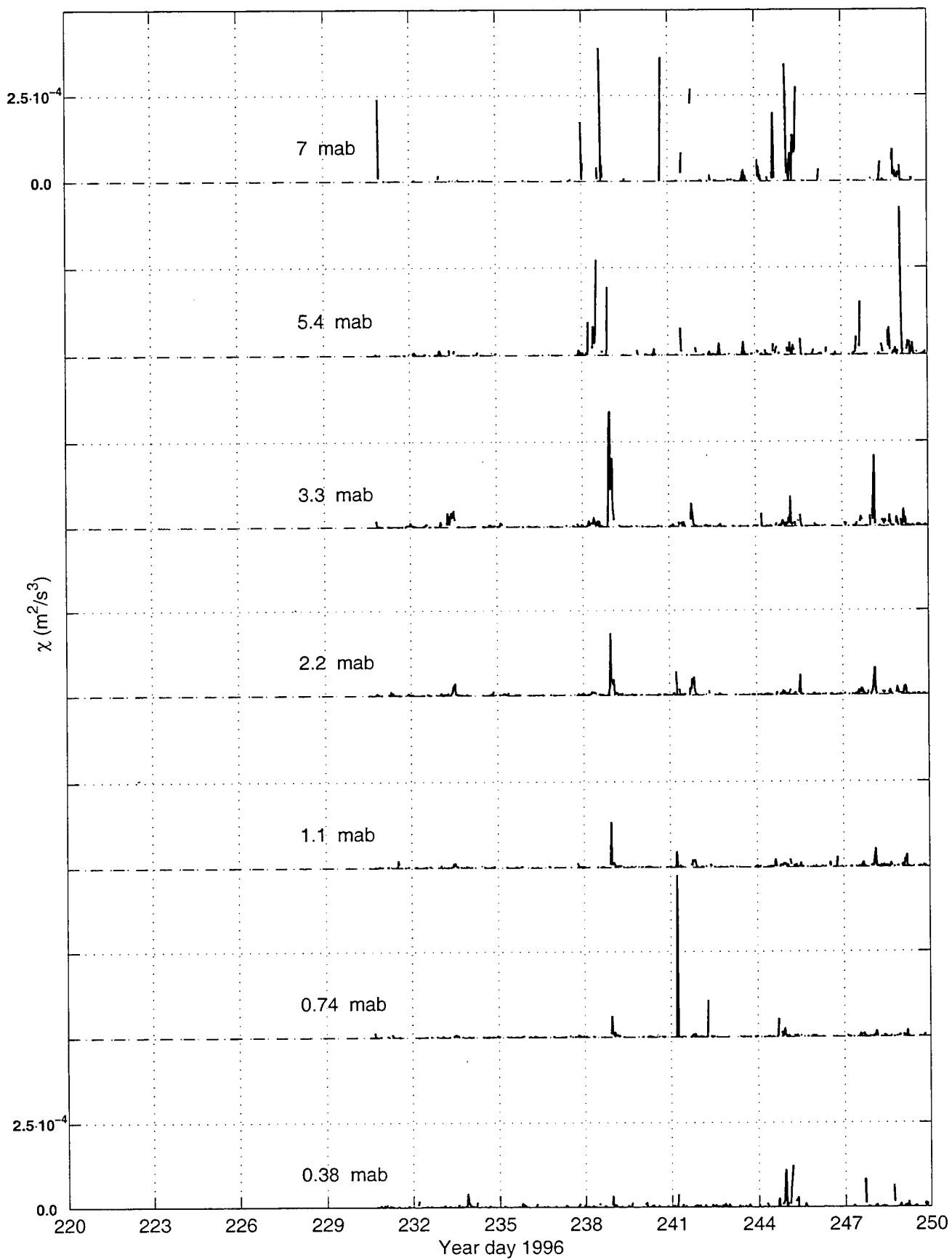


Deployment V



Dissipation of Turbulent Temperature Variance (χ)

Deployment I (continued)



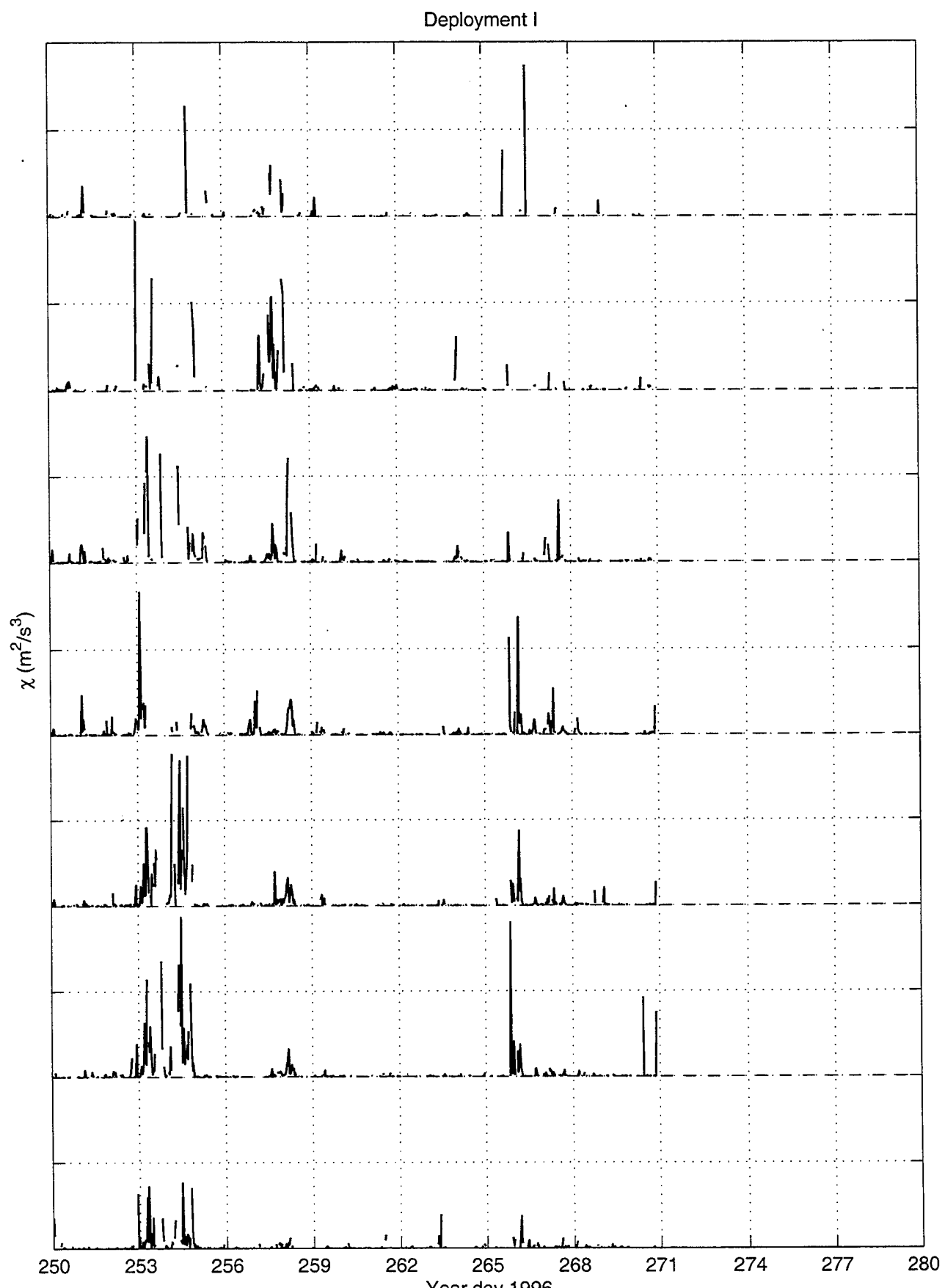
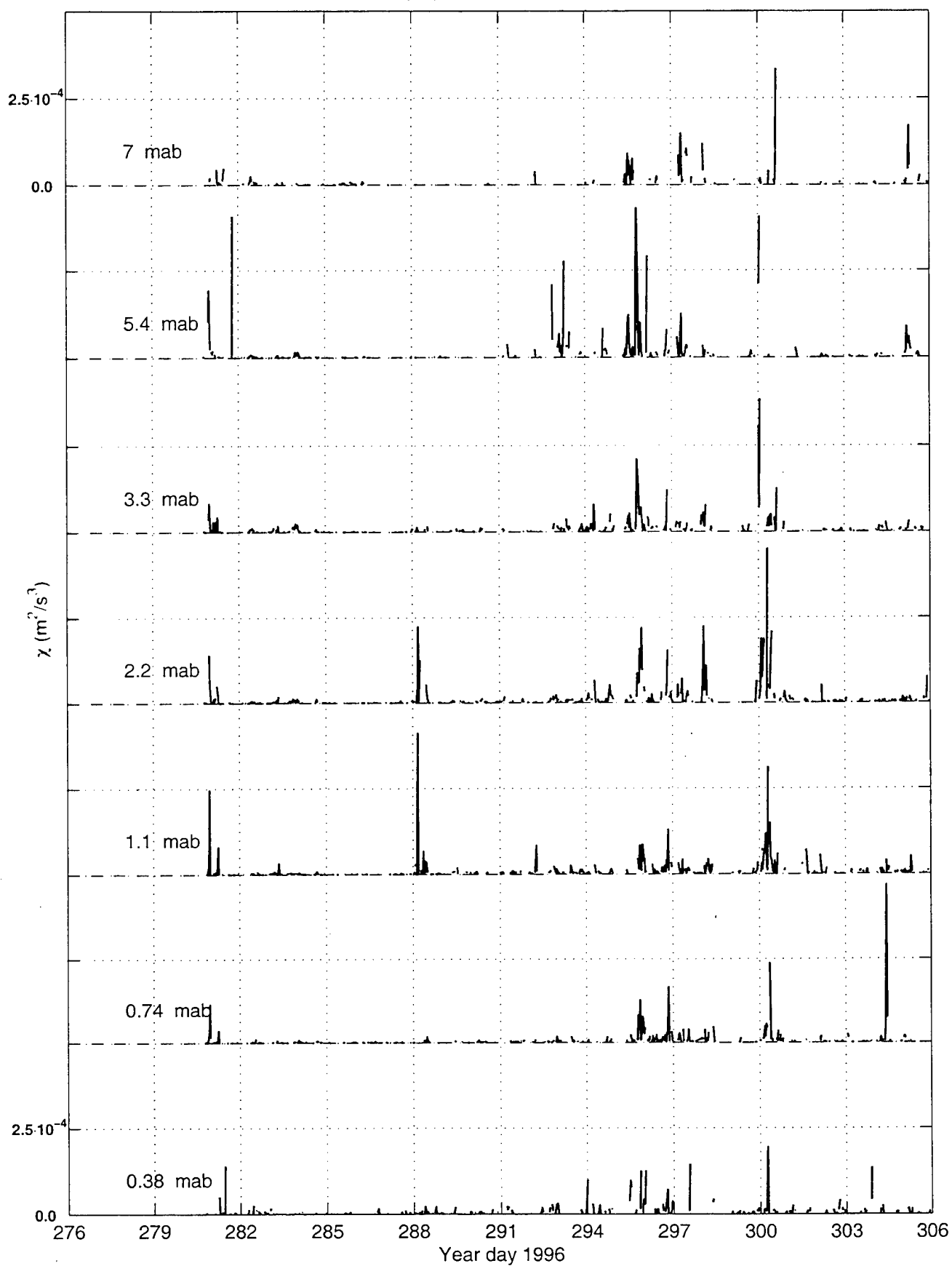


Figure 57

Deployment II (continued)



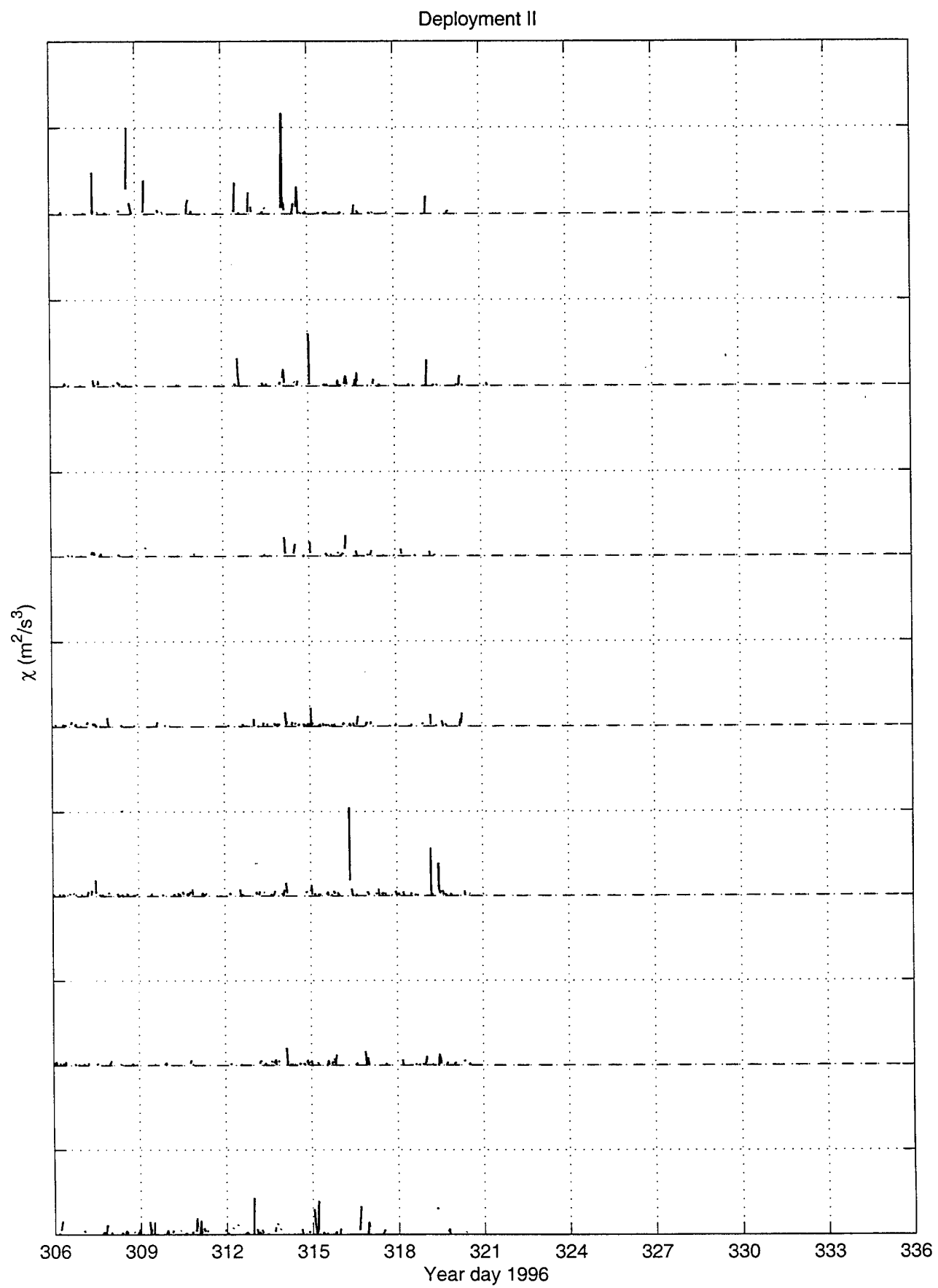
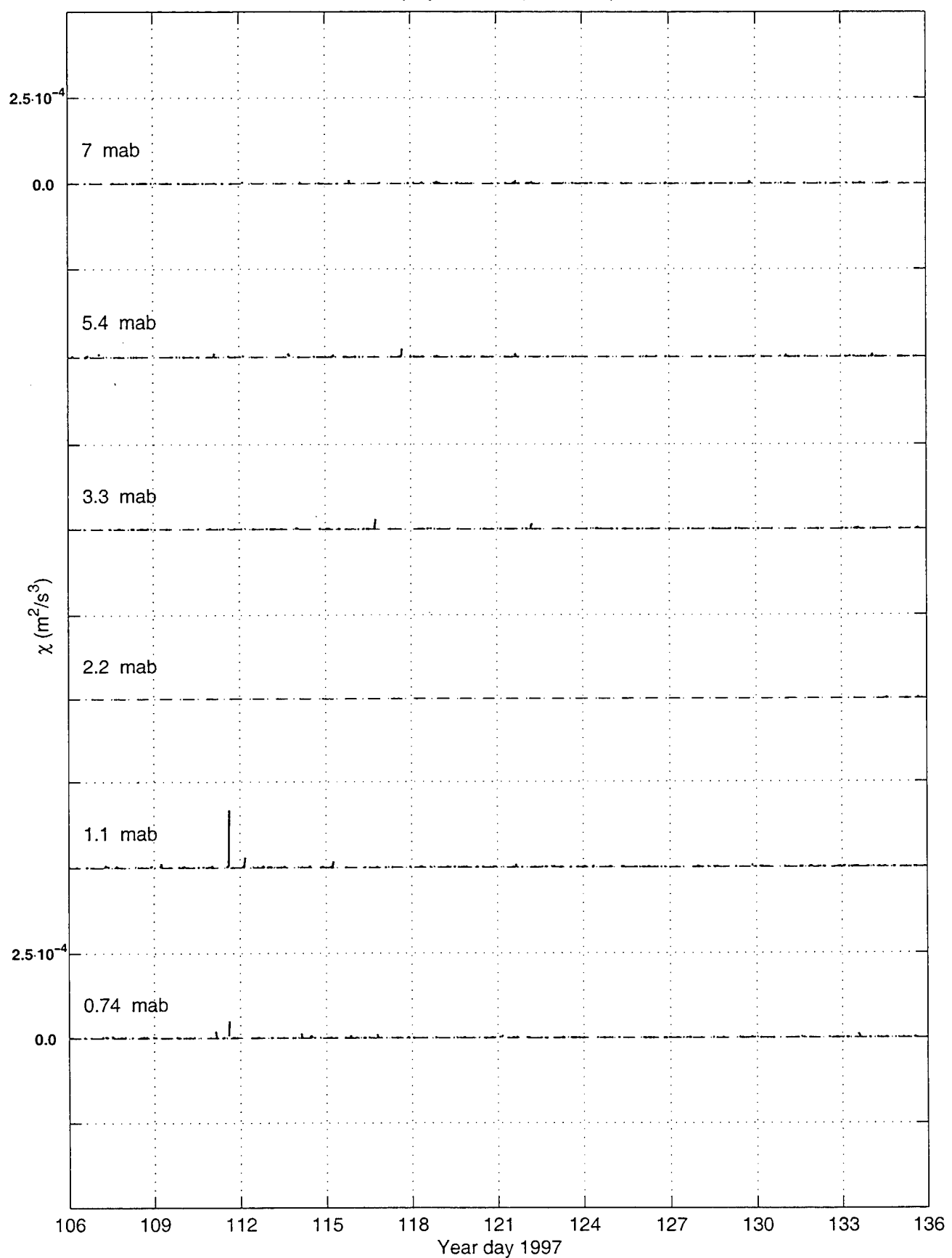


Figure 58

Deployment IV (continued)



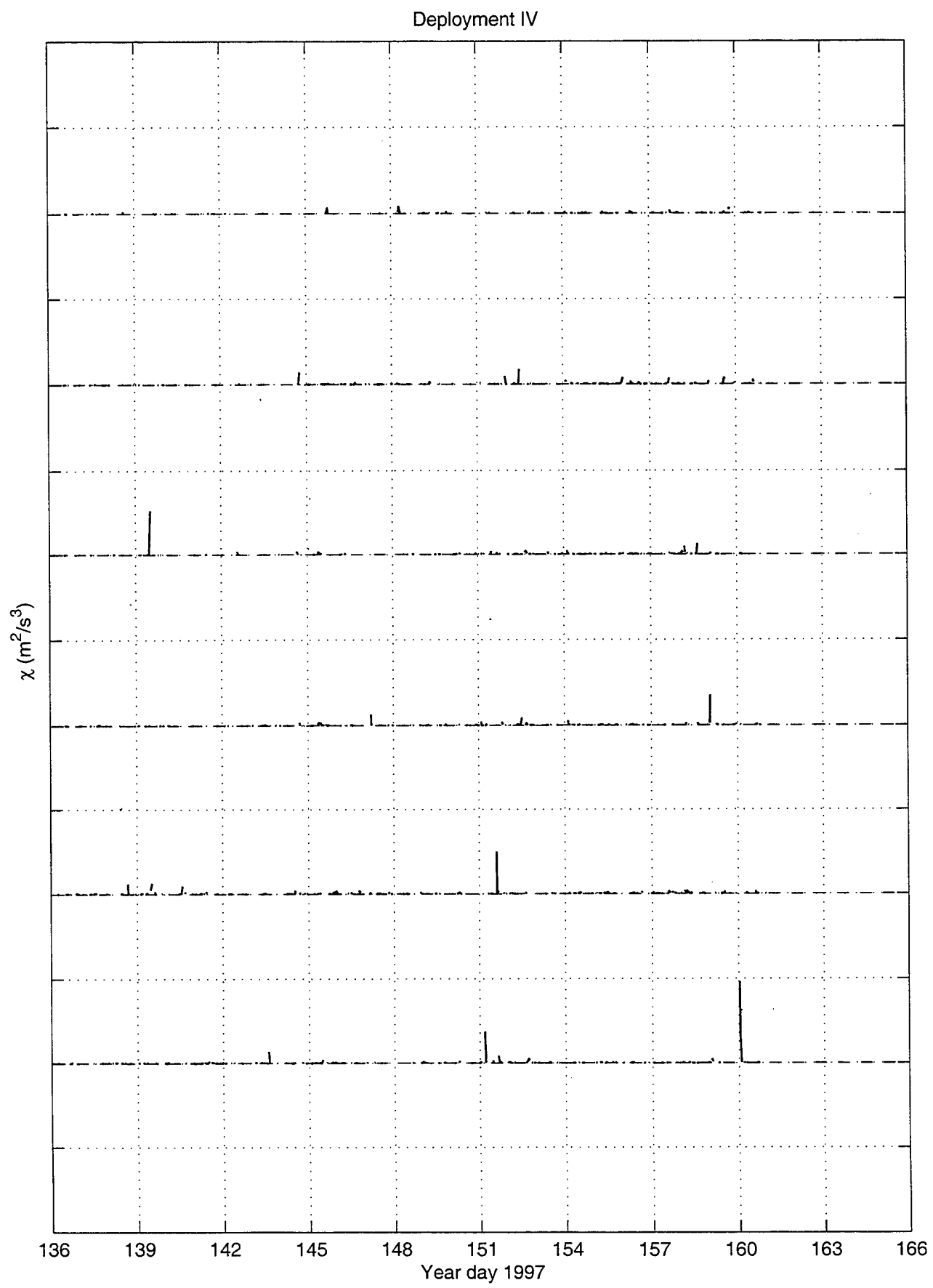
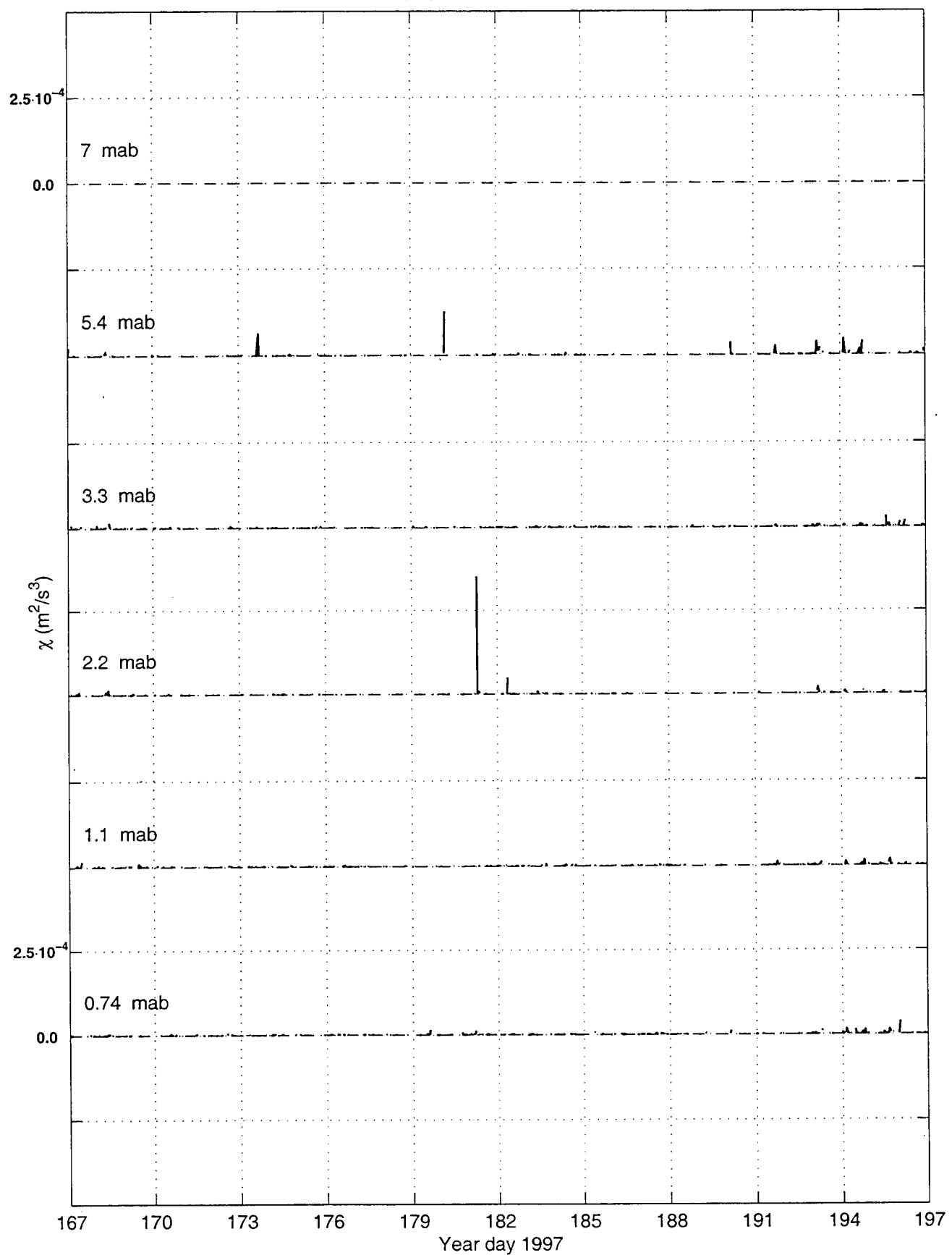


Figure 59

Deployment V (continued)



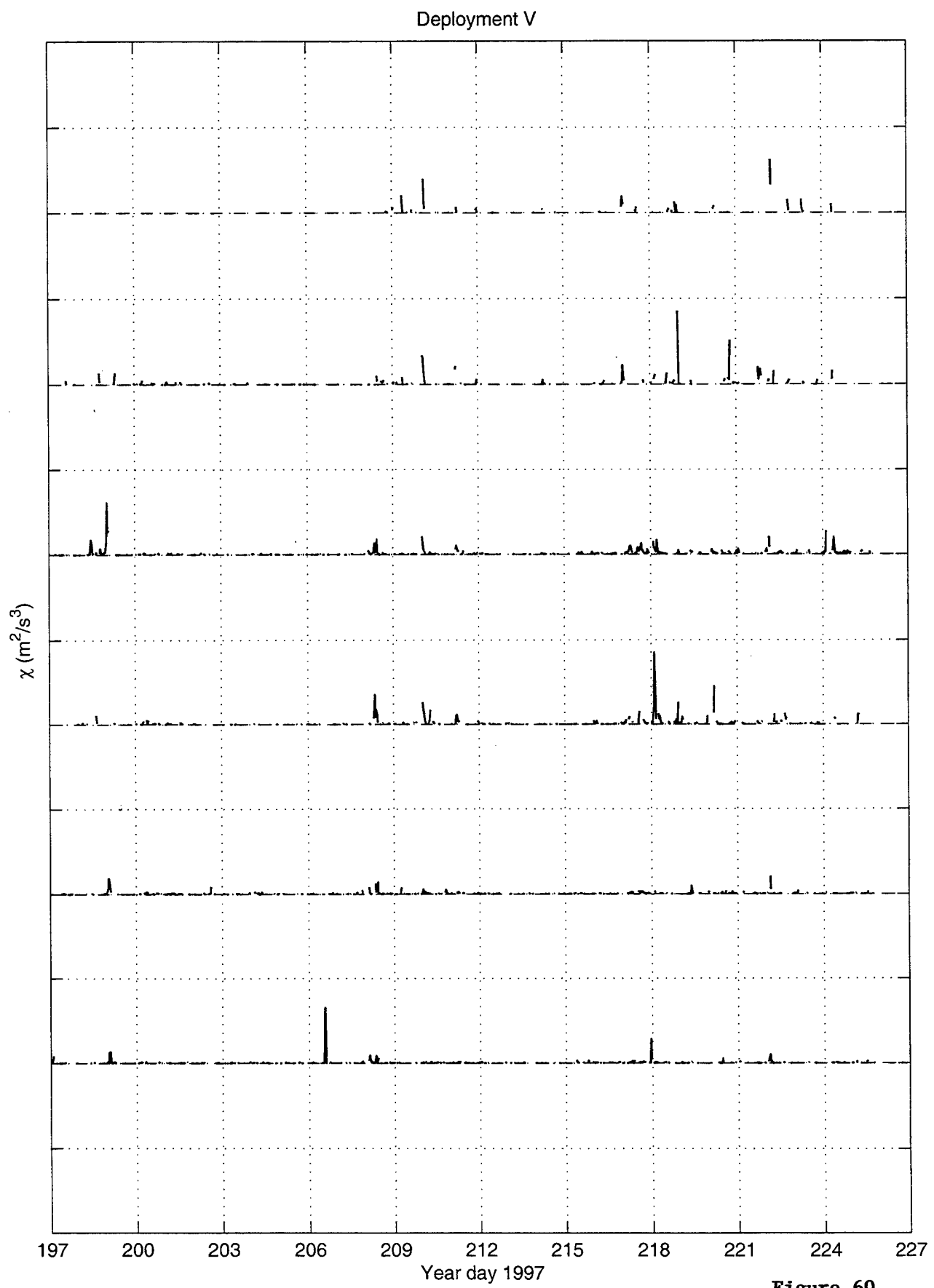


Figure 60

— THIS PAGE INTENTIONALLY LEFT BLANK —

SECTION V: DATA COMPARISONS

Evaluation of ADV and BASS velocity data

When each ADV is compared with the mean of the other two ADVs (Figures 61 - 63), flow reduction is evident when flow is along the channel in either direction. ADV_B was tipped during Deployment III, as seen in Figures 64a-d. Figures 65a-d show that the BASS sensor, at the same height as the ADVs, logged lower mean velocities than were observed by the ADV sensors.

Comparisons of velocity from the central mooring and the SuperBASS tripod

Vertical profiles of the burst averaged data from the SuperBASS tripod and the bottom 30 meters of the central mooring VMCMs are presented in Figures 66 - 69, along with vertical profiles of the standard deviation of the low-pass filtered (pl64) mean velocities. For these plots, we interpolated over the times when the sensor was in the wake of the leg. Figures 70 - 73 present the empirical orthogonal function (EOF) for these data. A vane on the bottom-most VMCM failed, so we have omitted the data from the central mooring site at 65.5 meters depth. (Personal communication, Steve Lentz, WHOI)

Comparisons of salinity and temperature from the central mooring and the SuperBASS tripod

Data from Seacat 1878, which was mounted on the mooring at 67.5 m depth, are compared with SeaBird derived salinities and temperatures from the SuperBASS tripod in Figures 74a-b and Figures 75a-b. The moored salinity data were corrected for drift (personal communication, N. Galbraith, WHOI), with adjustment up to 0.06 S/m. As seen in the figures, the SeaBird data from the SuperBASS tripod are also fouled from sediment trapping.

Comparisons of temperatures from YSI thermistors and the SeaBirds

Figures 76a-c show the comparison of the bottom-most and top-most YSI temperatures with those from the SeaBird temperatures at the same height.

Figure 61

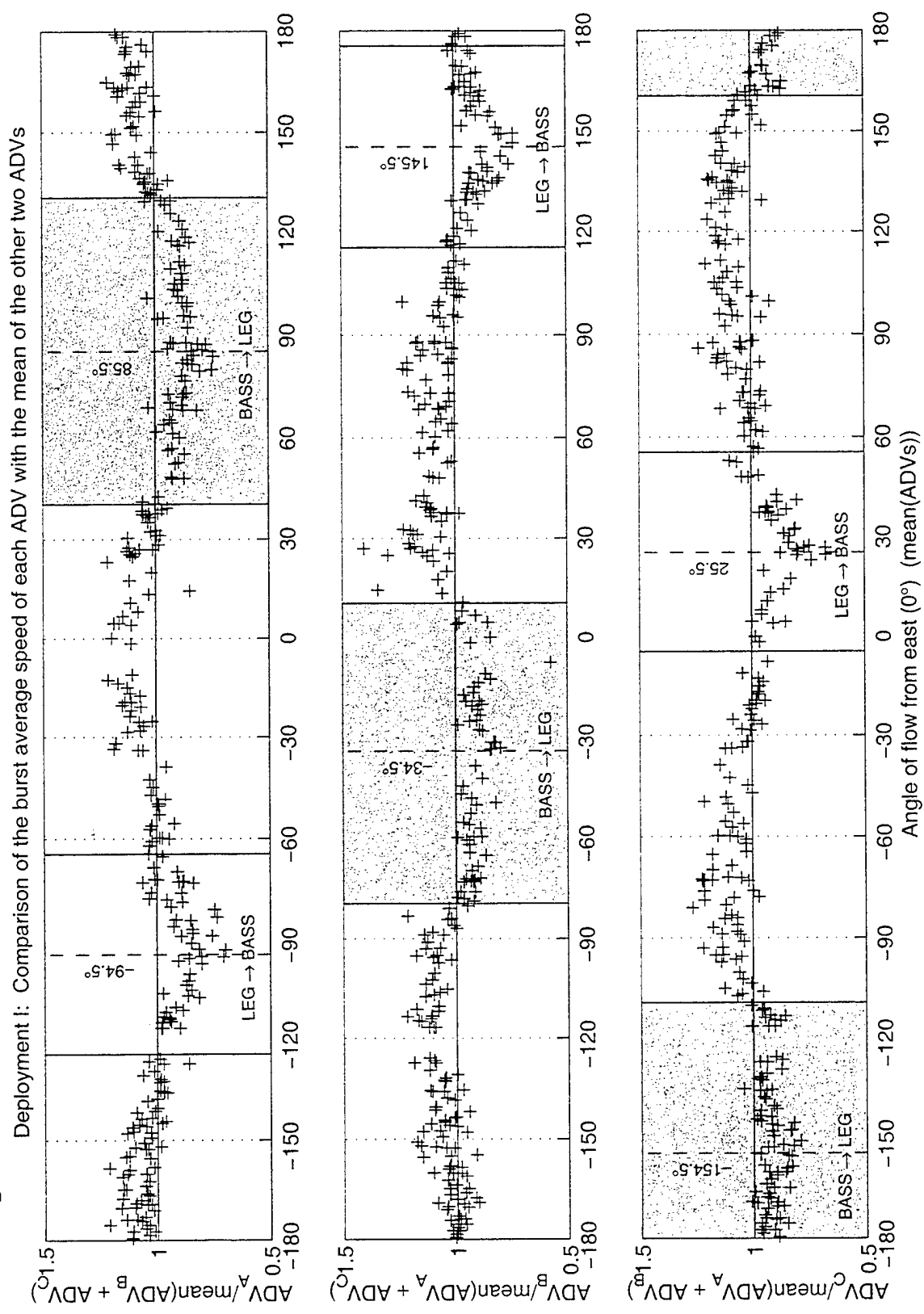


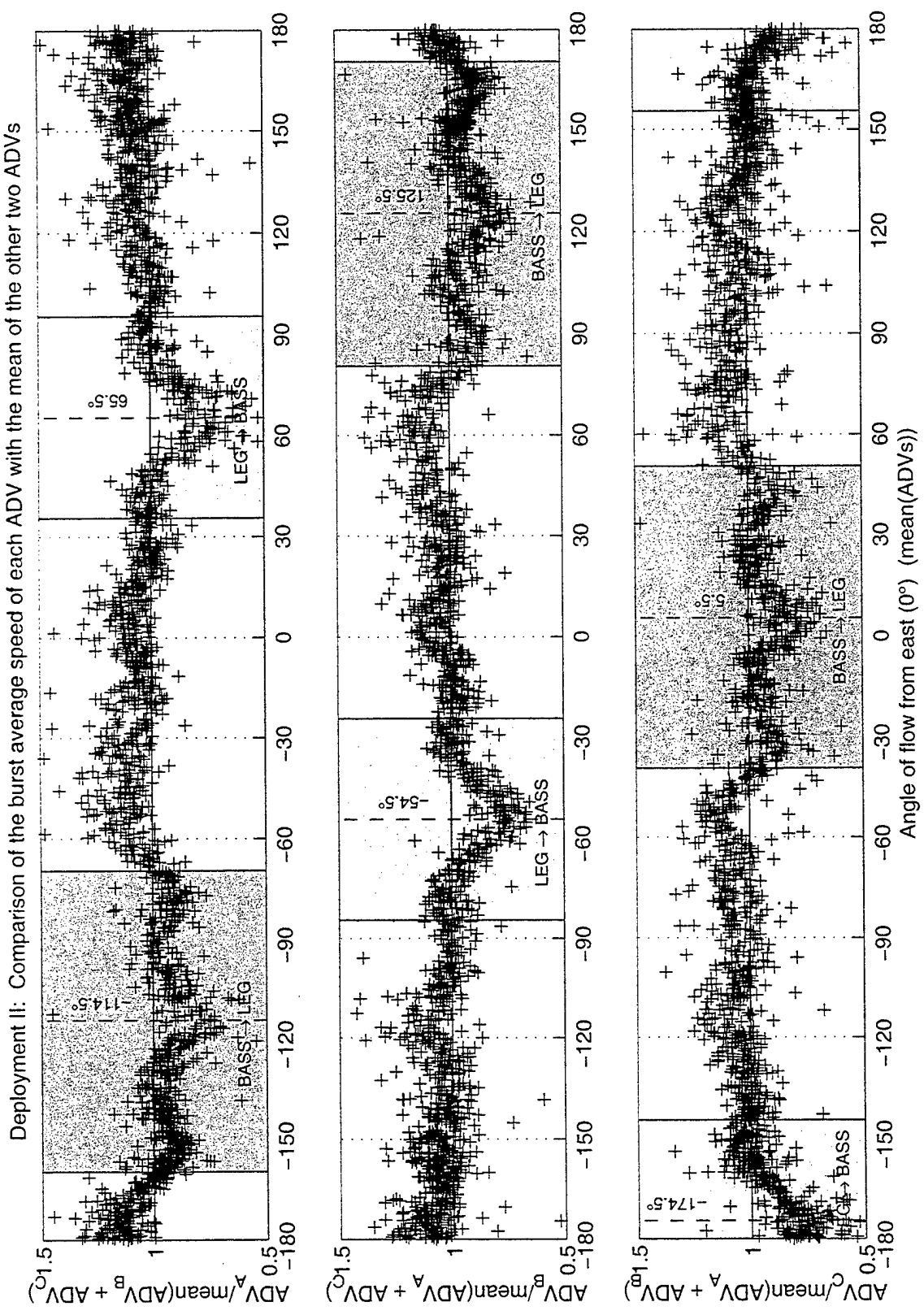
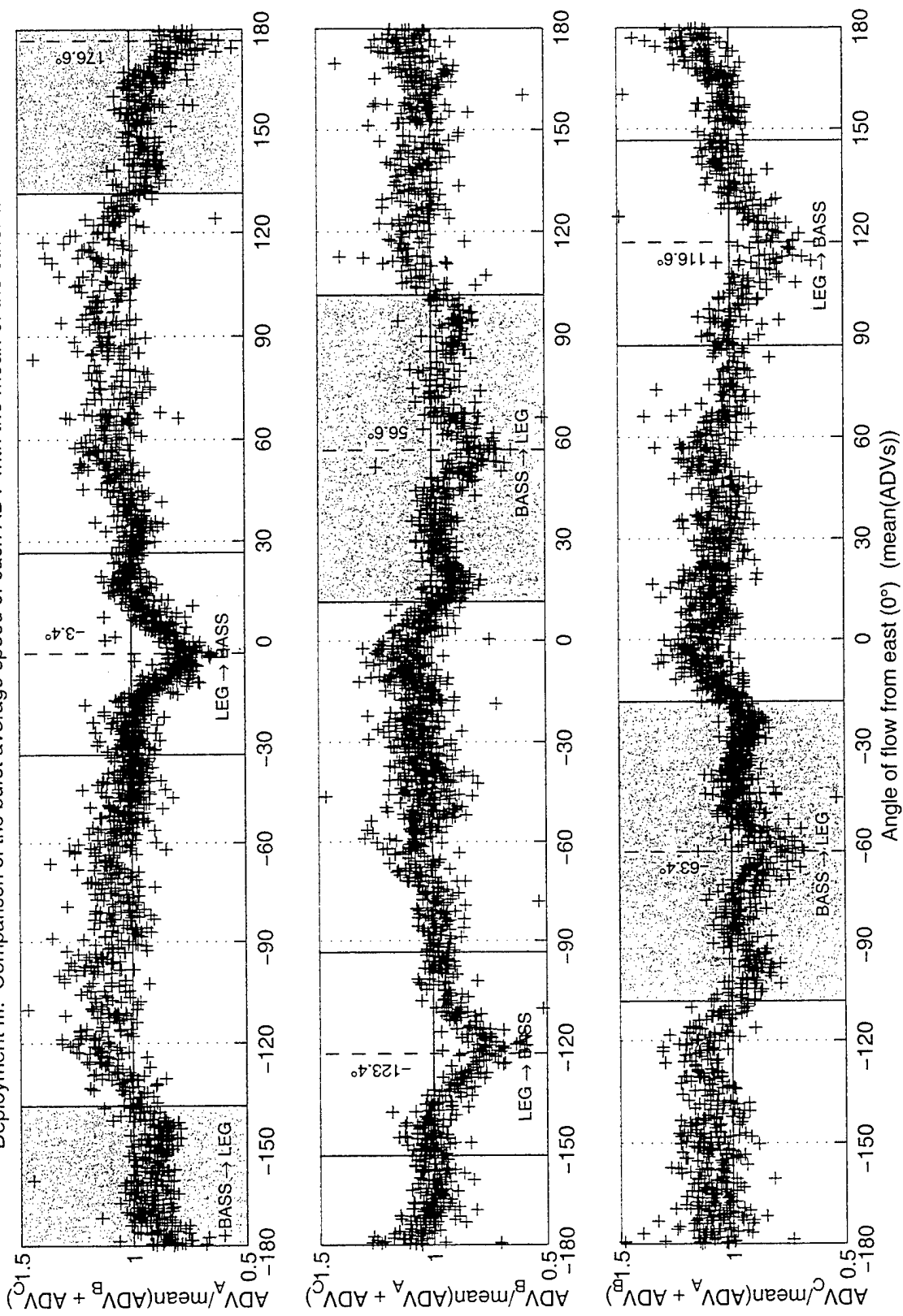
Figure 62

Figure 63

Deployment III: Comparison of the burst average speed of each ADV with the mean of the other two ADVs



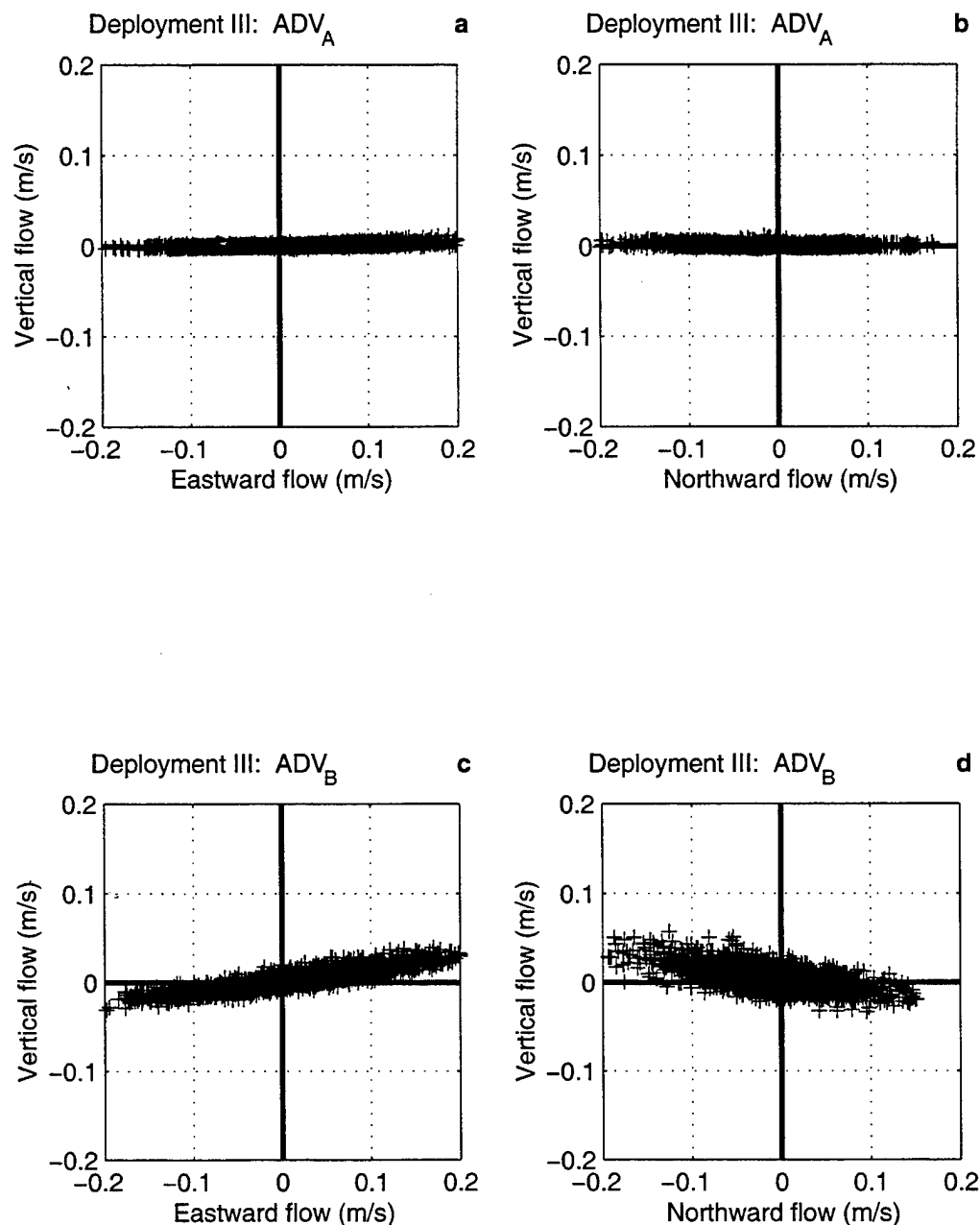


Figure 64. ADV_B was rotated in the vertical plane.

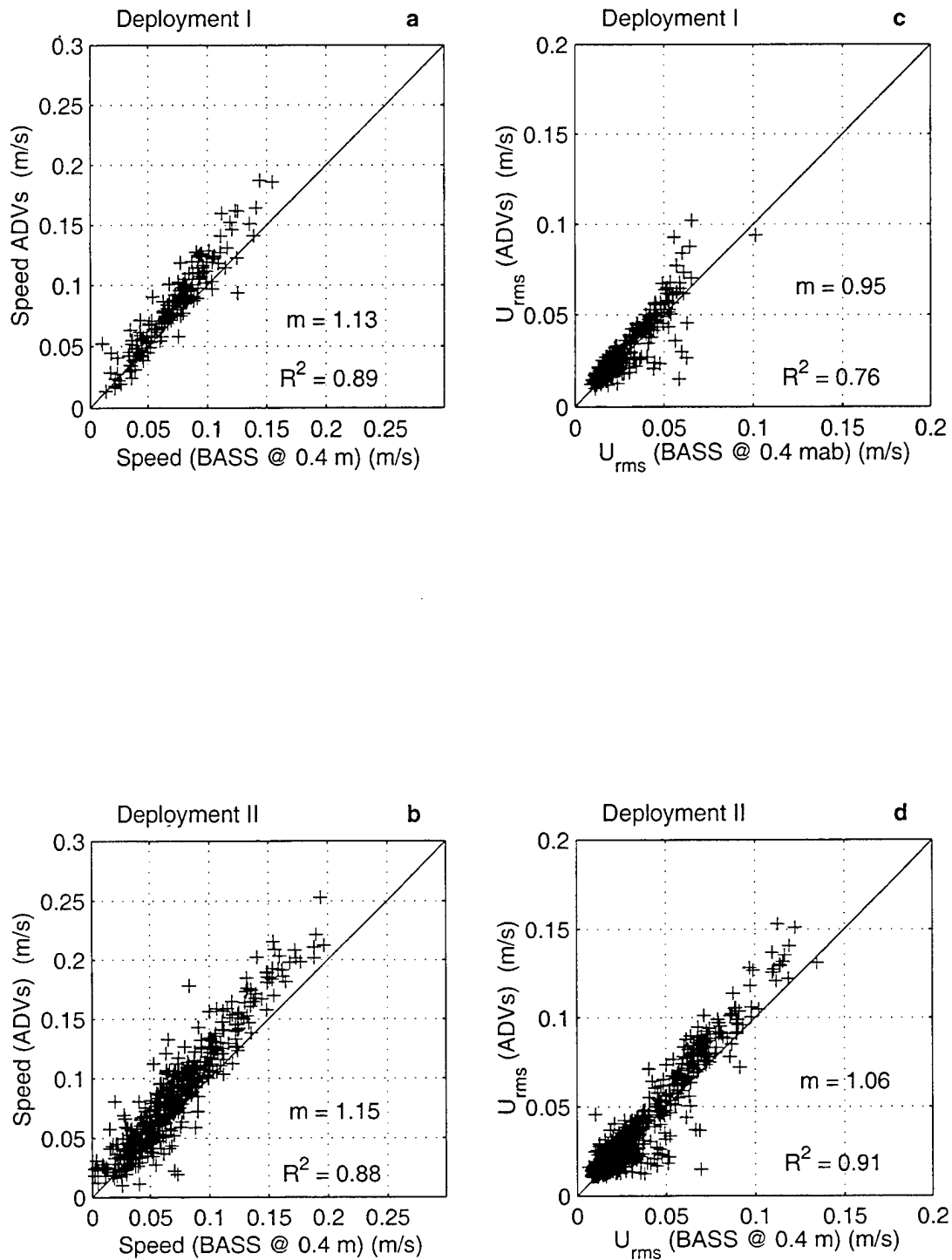
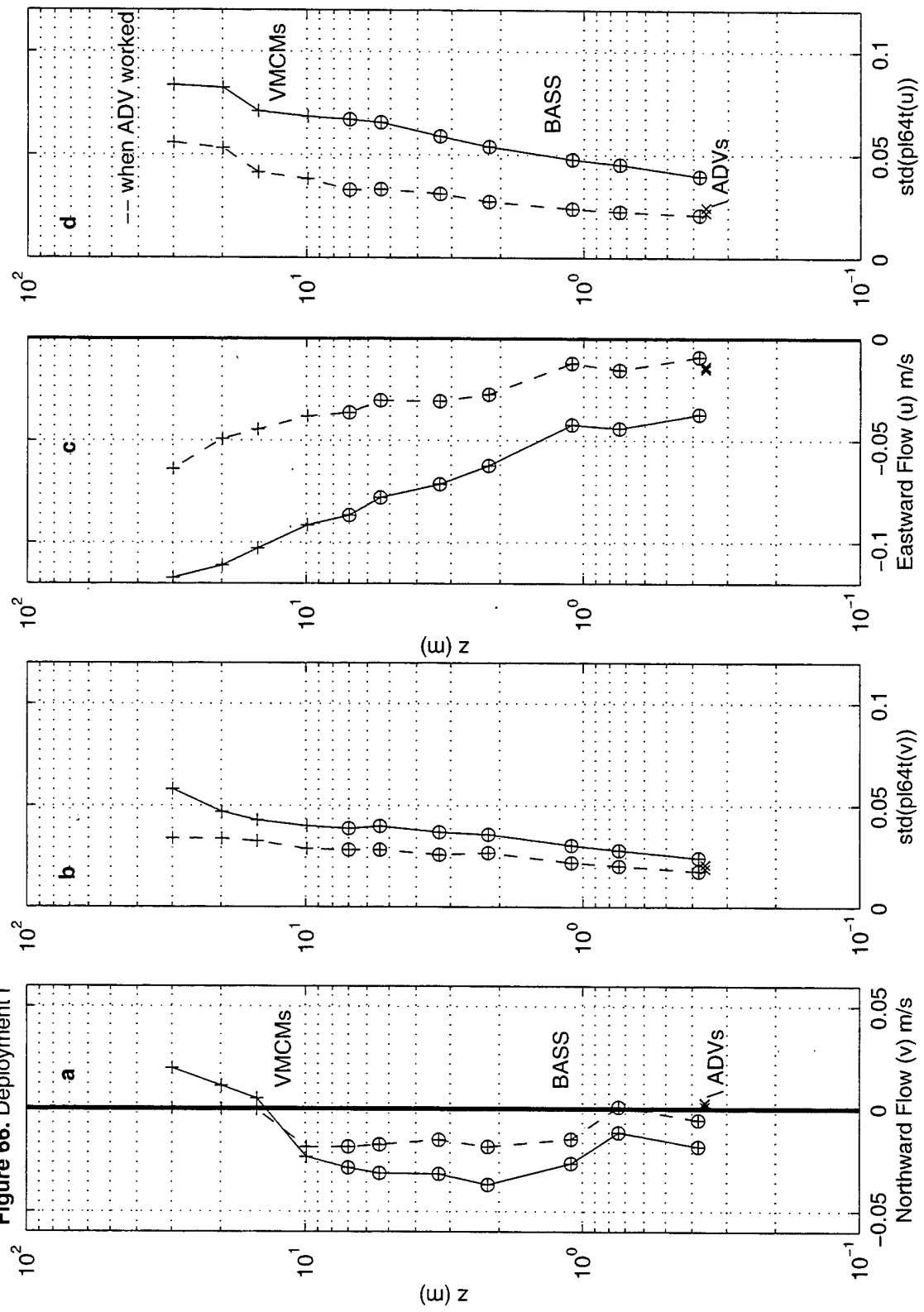


Figure 65

Figure 66. Deployment I



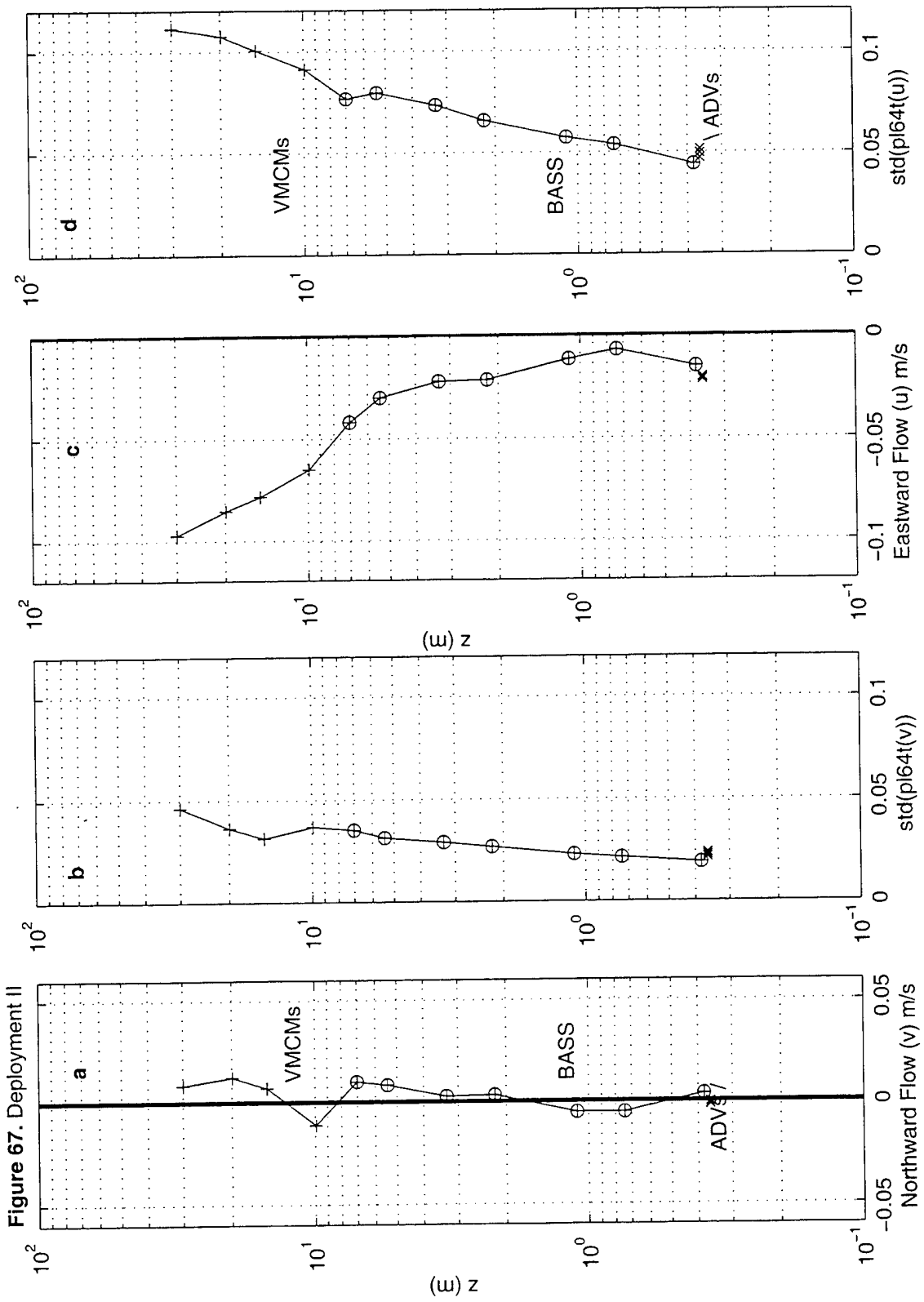


Figure 68. Deployment IV

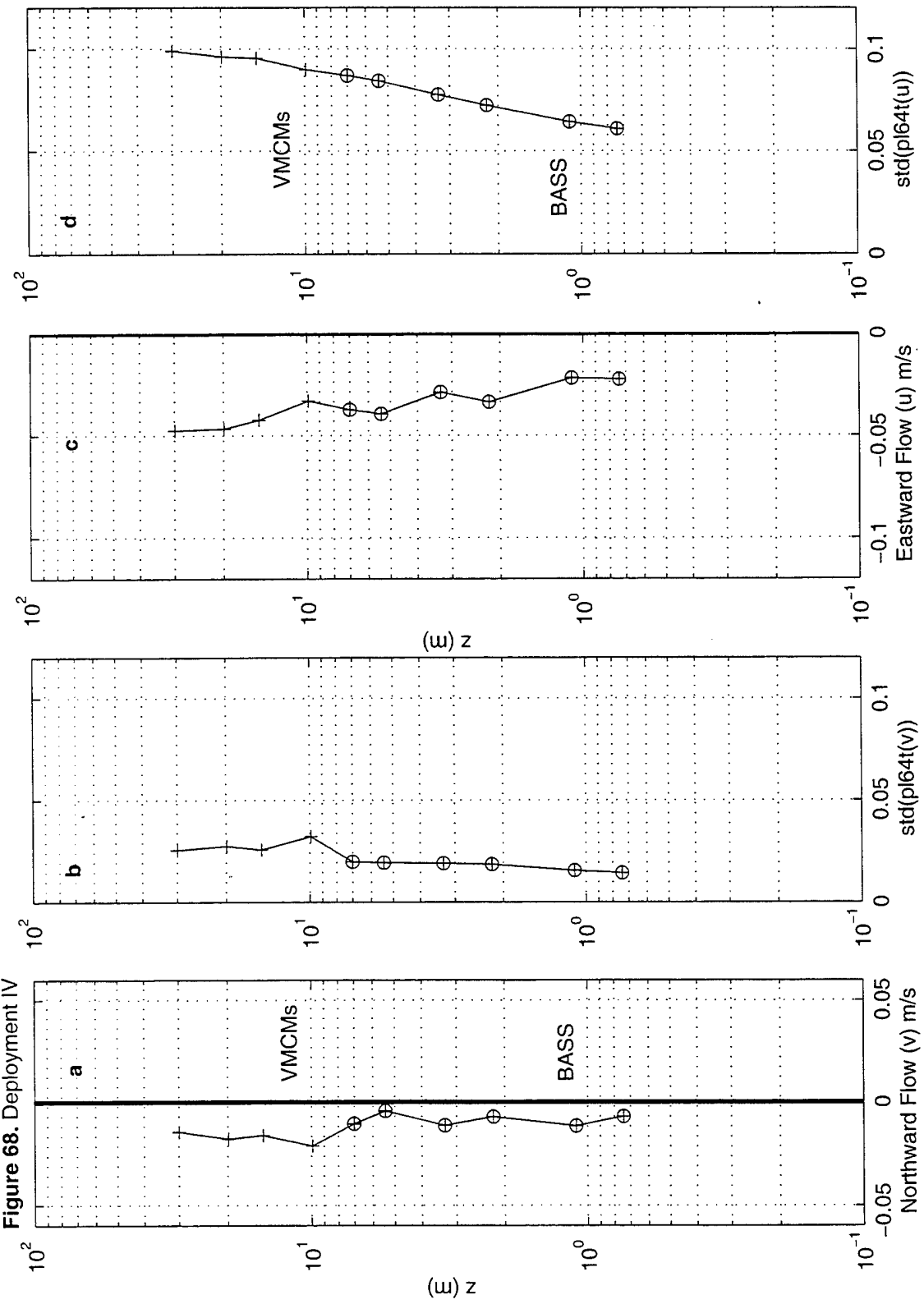
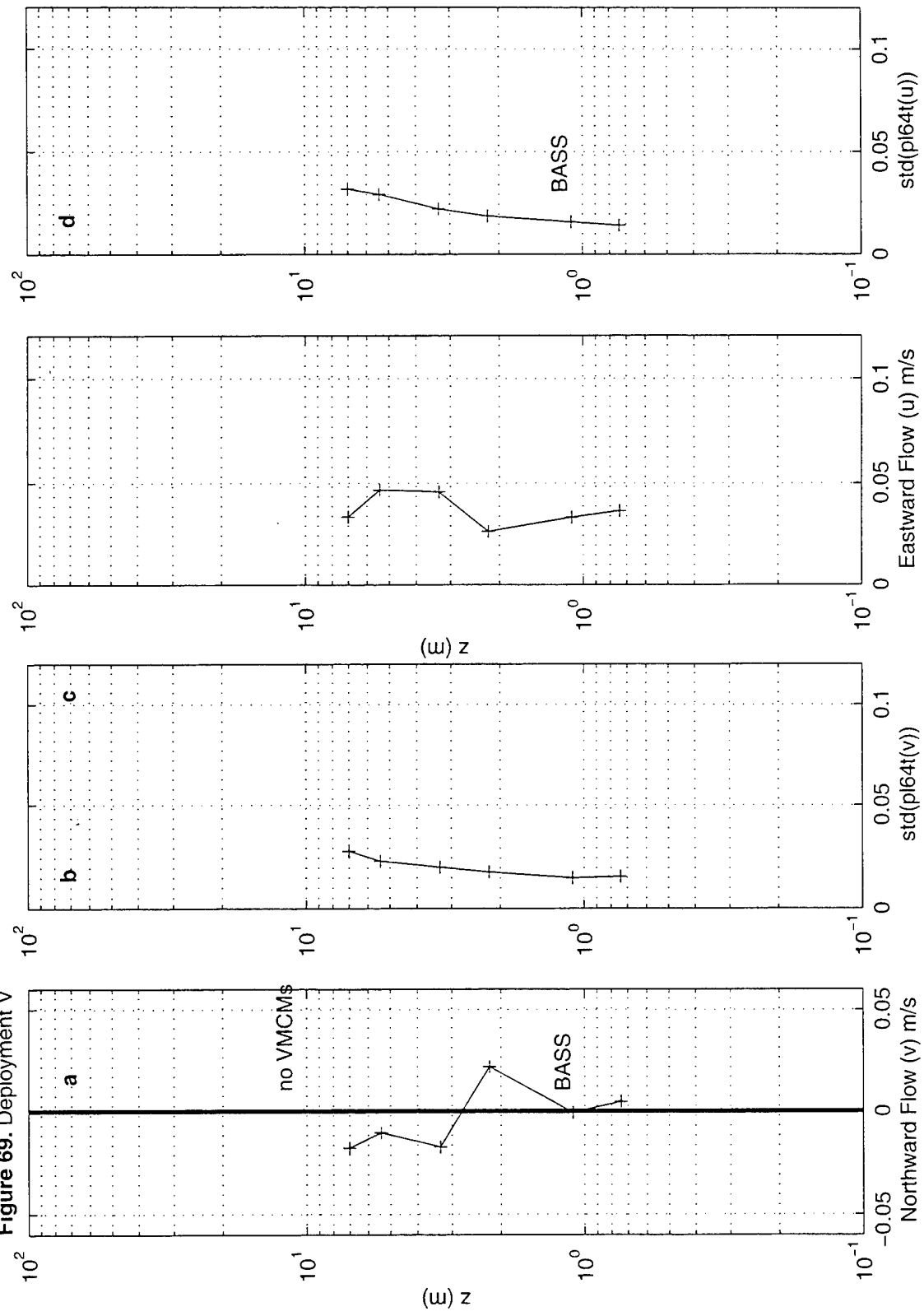


Figure 69. Deployment V



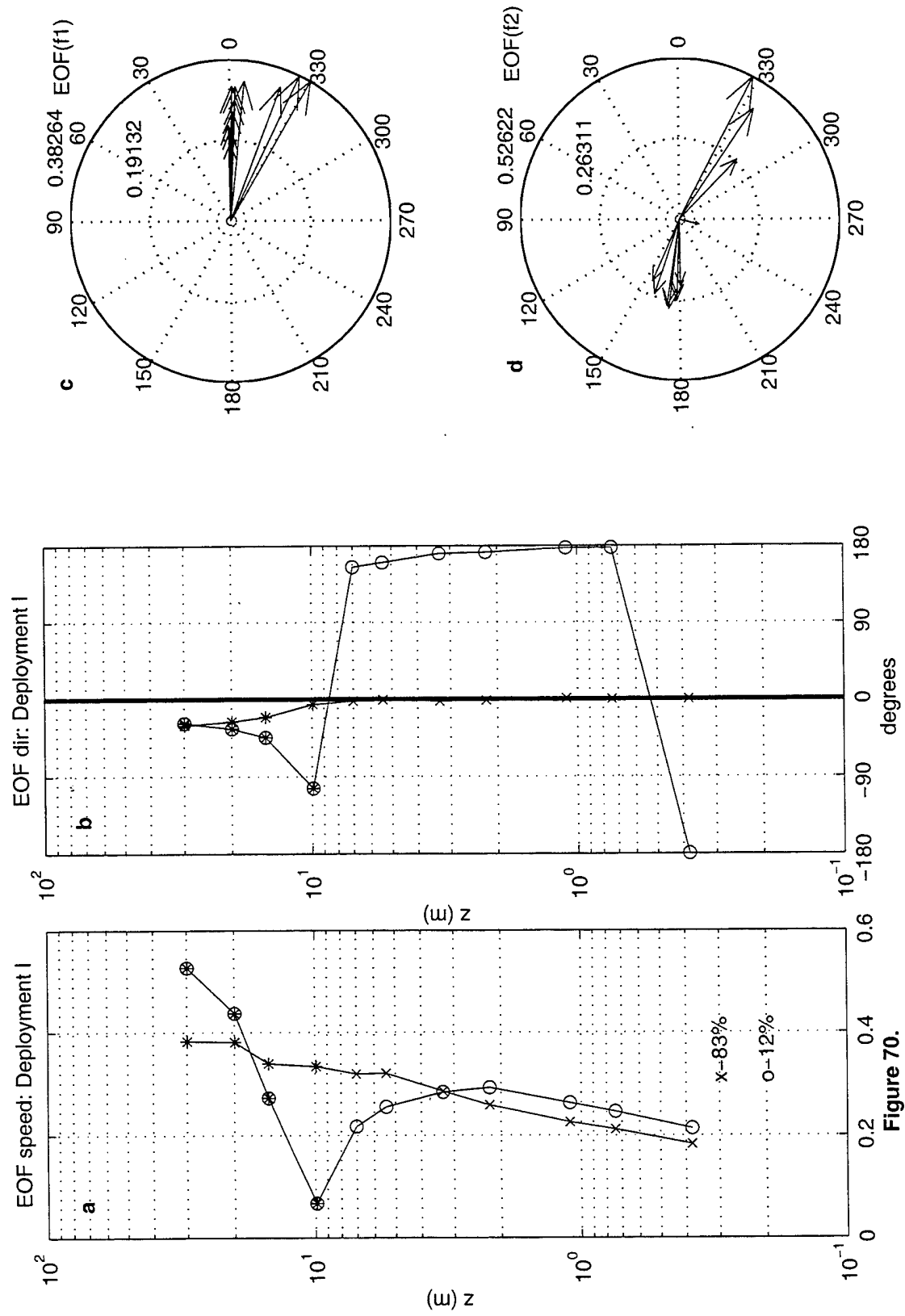
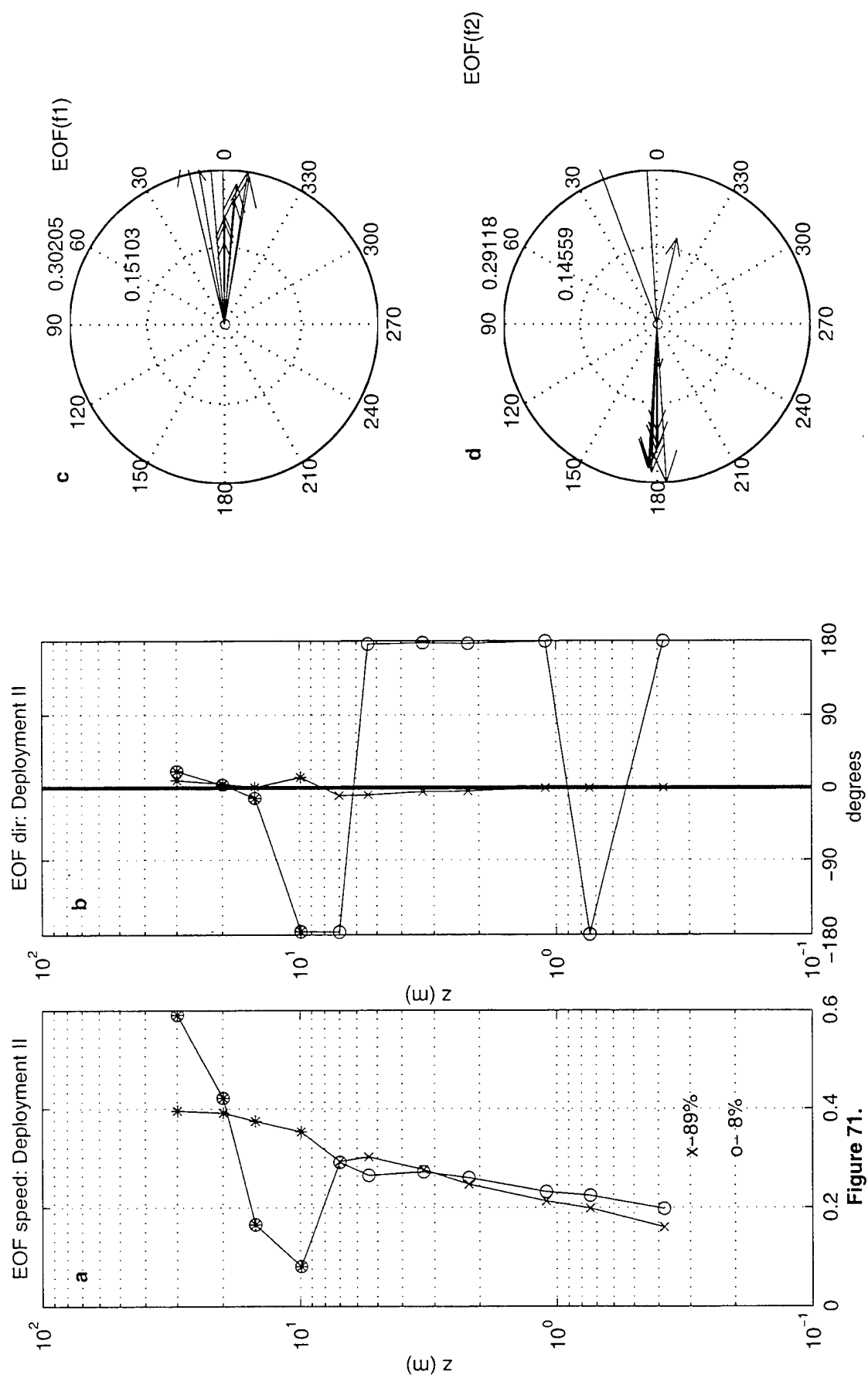


Figure 70.



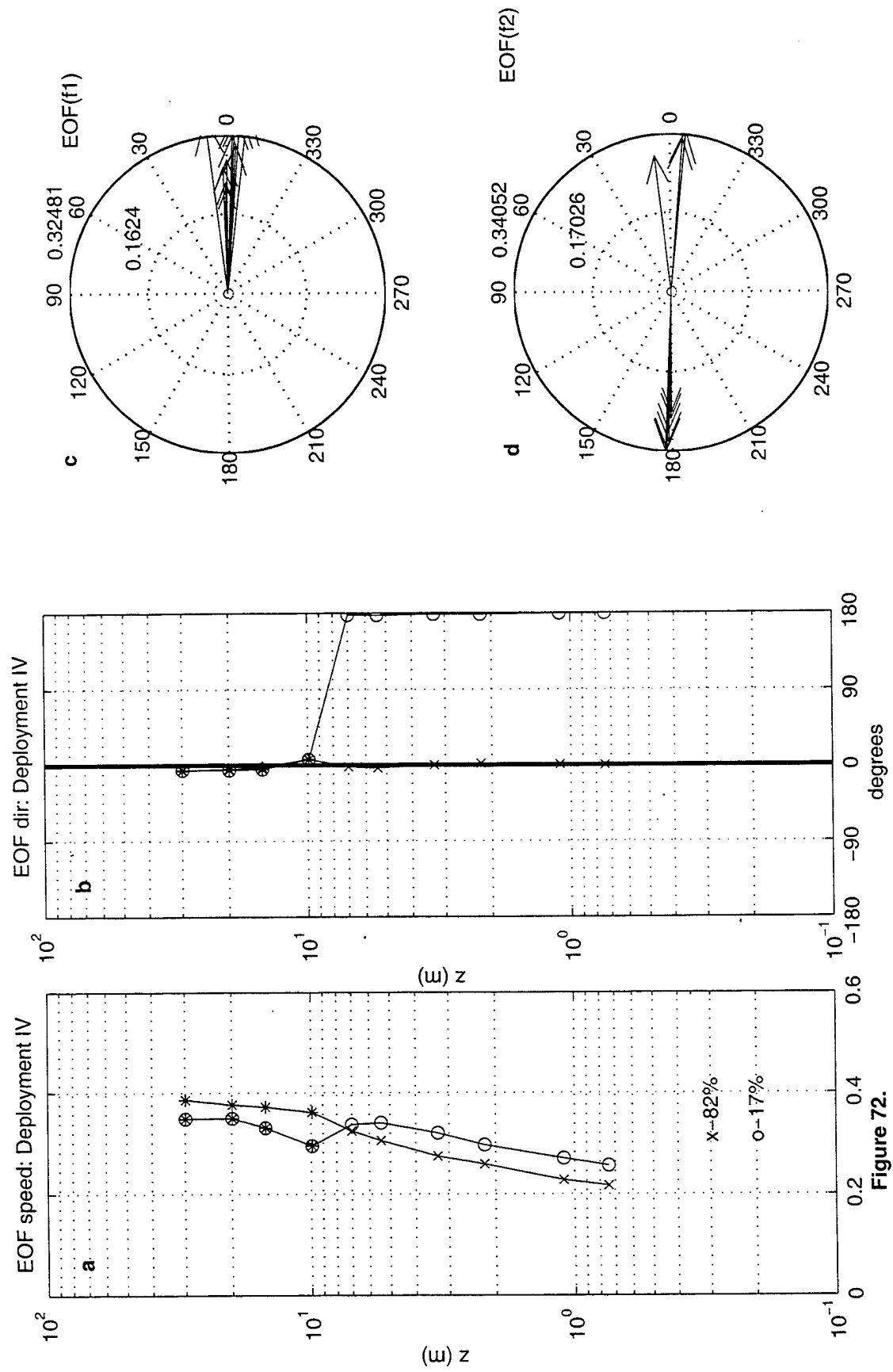


Figure 72.

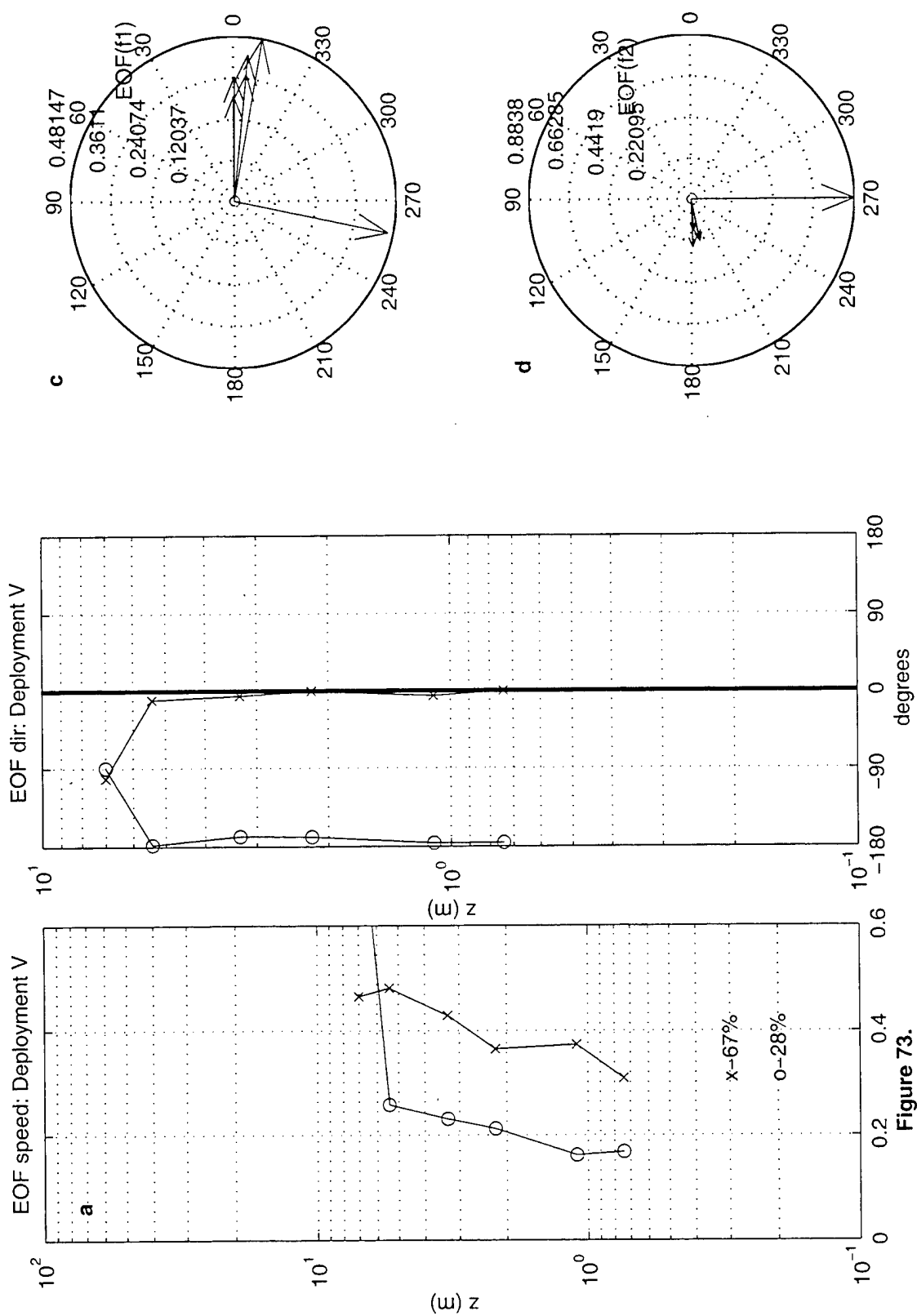
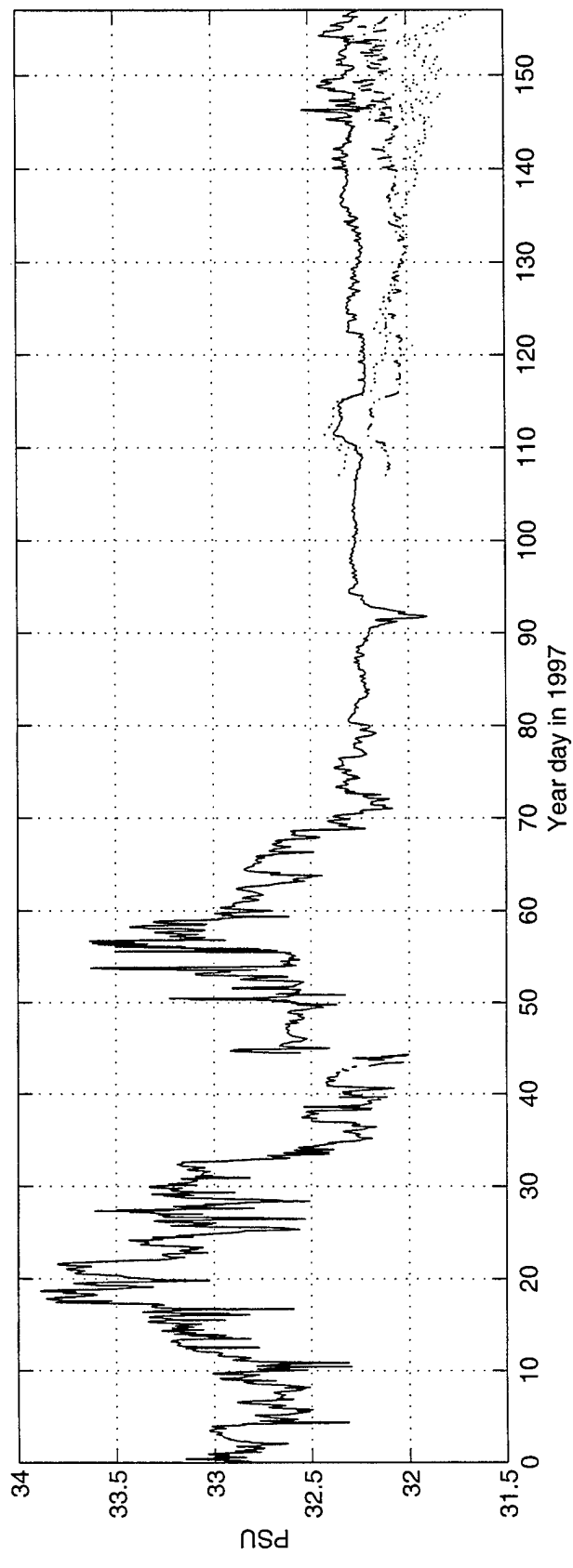
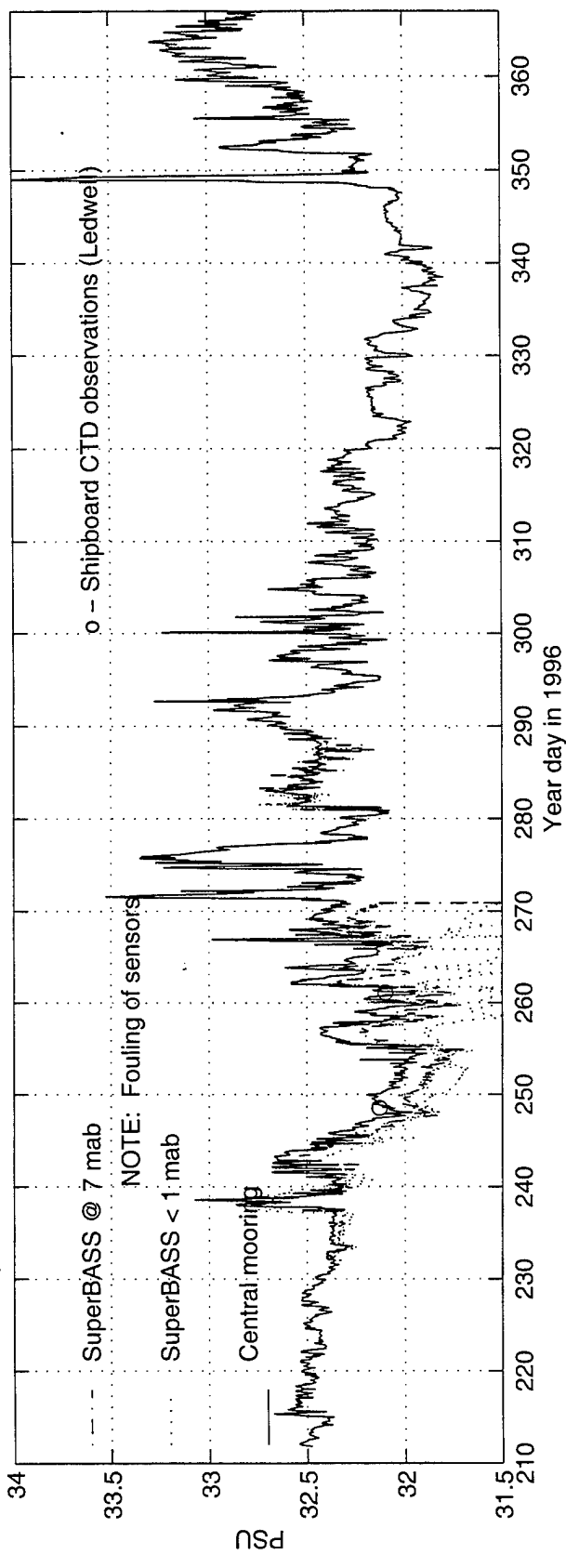
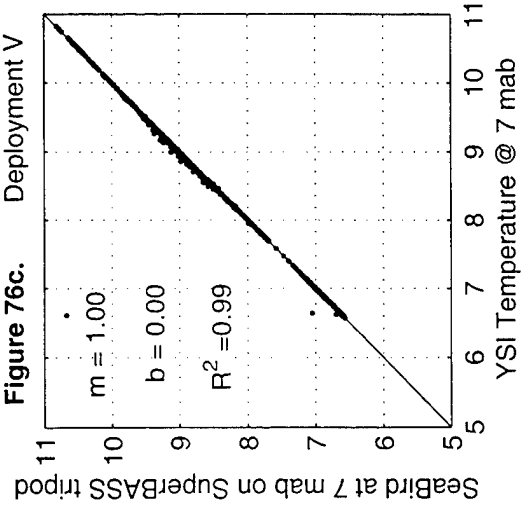
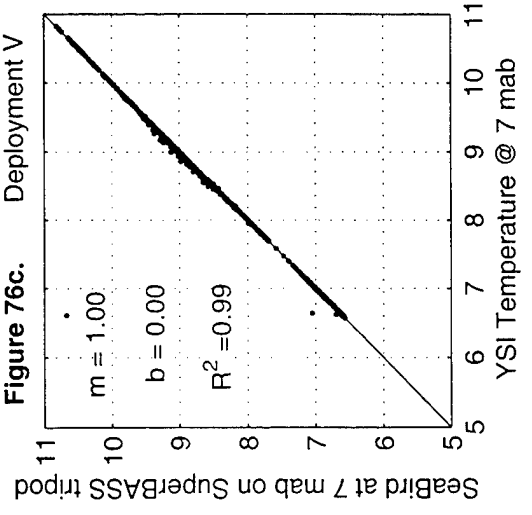
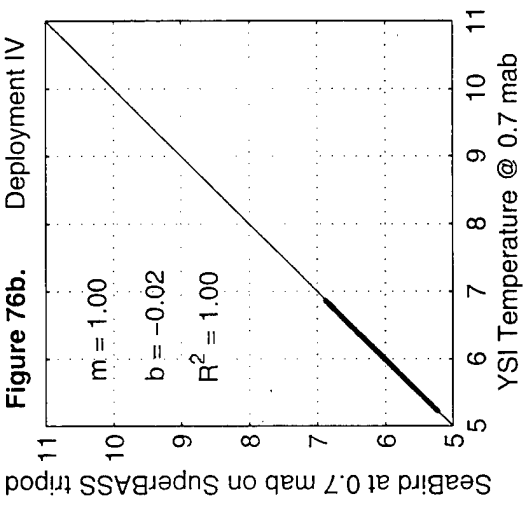
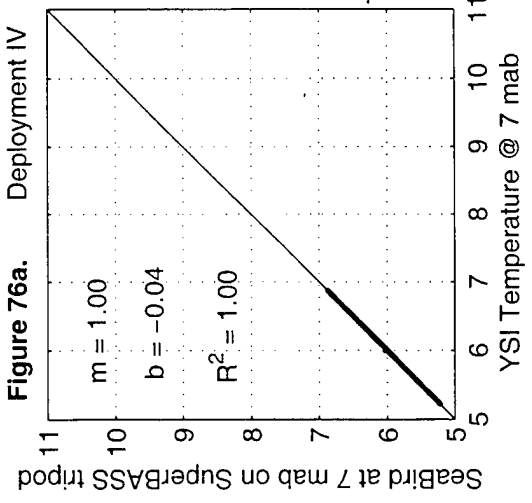
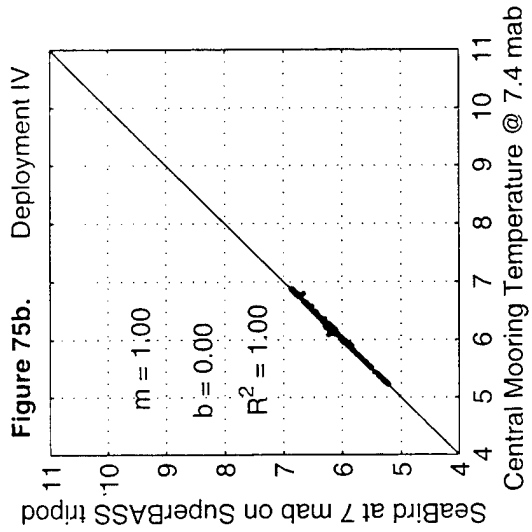
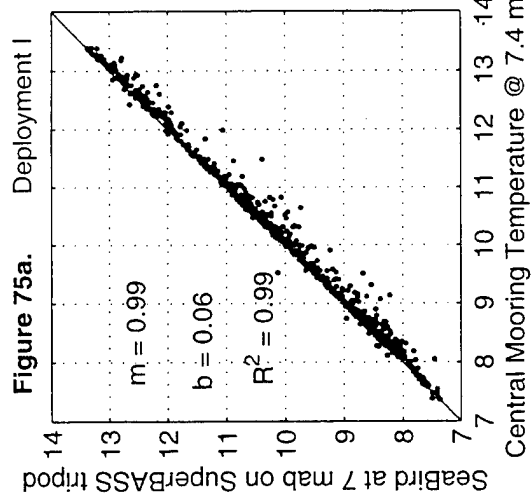


Figure 73.

Comparison of bottom-most salinity at central mooring, SuperBASS and observed shipboard salinity





SECTION VI: DATA FILE DESCRIPTIONS

BASS Binary File Formats

Data were recorded in 229,376 byte blocks. Two formats describe the raw data files of the BASS logger. The first format was used during Deployments I - III, when there were seven ACM sensors and no YSI thermistors, and the sampling interval was 840 ms. The second format was implemented for later deployments, when the bottom-most ACM was dropped and eight YSI thermistors were added, and the sampling interval was 850 ms. All deployments sampled three half-hour bursts every two hours. (See Section II.)

Deployment I-III				Deployment IV-V			
Variable	# variables	bytes/variable	bytes	Variable	# variables	bytes/variable	bytes
Key word(ABC1)	1	2	2	Key word(ABC2)	1	2	2
Time word	5	1	5	Time word	5	1	5
Travel Time	14	2	28	Travel Time	12	2	24
pitch	1	2	2	YSI Temps	8	2	16
roll	1	2	2	pitch	1	2	2
ACM	28	2	56	roll	1	2	2
compass	1	2	2	ACM	24	2	48
pressure	1	4	4	compass	1	2	2
SeaBirds	4	2	8	pressure	1	4	4
PresTemp	1	2	2	SeaBirds	4	2	8
Total bytes/record:			111				115

Processed BASS Data

Processed data were archived as Matlab®¹ files, creating a set of the following files (on CDs) for each deployment:

Half-day files (see loadnew.m, Appendix B.)

v_ne_NNn.mat north & east velocity

v_w_NNn.mat vertical velocity in m/s

v_doy_NNn.mat - time file (day of month, GMT)

Daily files:

v_vel_NN.mat along-path velocity (see loadpaths.m, Appendix B.)

v_doy_NN.mat - time file (day of month, GMT)

v_therm_NN.mat - acoustic travel time data (counts) (See loadss.m., Appendix B.)

v_ysi_NN.mat - YSI thermistor data (°C) (for deployments IV & V)

where NN is an arbitrary file number and can be related to day of month using file **fnlist.doc**, and n represents 'a' or 'b' denoting whether it is the first or second part of the day.

¹Mathworks, Inc., Natick, MA 01760

Burst Averaged BASS Data

Burst averaged data were stored in the files below:

BASSmeans_MMYY.mat, where MMYY indicates the month and year in which the deployment began..

Variables include:

```
tdoy - year day (0.5 = 1/1/96 noon GMT)
       (representing the burst average time)
real(wne) - eastward flow (m/s)
imag(wne) - northward flow (m/s)
wstd - standard deviation of detrended velocity
       (east +i*north, as above)
dmean - height of water above platform (4.2 m)
urms - bottom orbital velocity (m/s)
z - height above bottom of soundsd & BASS sensors (m)
wacmean - burst average of vertical vel from C+A (m/s)
wbdmean - burst average of vertical vel from D+B
wPPstd - standard deviation of detrended vertical velocities, as
       above
lrec - number of records in burst
dispn - dissipation (mean of all four paths) (W/kg)
smean - salinity (PSU) at z(1) & z(7)
tmean - temperature (deg C) at z(1) & z(7)
soundsd - sound speed (m/s) at z mab
Tu, Tv - Reynolds stress, east-west(u) & north-south(v) (PA)
mask - ones=nowake NaN=in wake of tripod
cw - sound speed (c) flux (m2/s2)
 cwd - sound speed flux
       (normalized time derivative technique)
drhodc - ∂ρ/∂c (density from central mooring)
Chi - dissipation of sound speed flux (m2/s3)
```

For Deployments IV & V:

```
tempmean - mean YSI temperatures (Deg C)
tempstd - burst standard deviation of detrended YSI temperatures
tz - height of YSI thermistors
```

mask.mat contains the mask that identifies wake contaminated points in the burst averaged files. The mask is an array of ones and NaNs, which provides a means to identify the bad points by taking the product of a burst statistic with the mask . Eg., by multiplying $\text{abs}(\text{wne}) * \text{mask}$, the flow speed will contain NaNs when the sensor is in the wake of the leg.

ADV Binary File Formats

All three loggers placed a time stamp at the beginning of each 529288 byte block. Each block contained two records, one collected at the hour specified at the beginning of the block and one collected one hour later. Data were logged continuously for 9.6 minutes at 25 Hz and formatted as described below.

Deployment I-III				
Each block began with a date stamp: MMDDHHMN (month,day,hour,minute) and was followed by two sets of about 14400 records as follows:				
Variable	# variables	bytes/variable	bytes	units
Keyword(8112)	1	2	2	
Sample Id	1	2	2	1 - number of samples in burst
Velocity	3	2	6	(0.1 mm/sec)
Signal Strength	3	1	3	(counts, where 0.43 dB/count)
Correlation Coefficient	3	1	3	(0 to 100, where > 70 is considered ok)
Checksum	1	2	2	sum of bytes plus base (0xa596)
Total bytes/record:			18	

Processed ADV Data

Using the time stamp, data were unpacked, processed and stored on a set of three CDs, one for each deployment. Data files are named according to the date and instrument: **xMMDDHH.mat**, where x represents the ADV sensor (a, b or c) and MMDDHH represents month, day, and hour (GMT) when sampling began. The data are stored as follows:

Ix - quality index (mean(correlation coefficient)/10), where > 7
is recommended as being acceptable.
Ux - northerly flow (0.10 mm/sec)
Vx - easterly flow (0.10 mm/sec)
Wx - vertical flow (upwards) (0.10 mm/sec)

where x is a, b or c, which specifies the ADV sensor.

A second set of CDs was created containing signal strength and vertical velocity:

xz - vertical velocity in 0..1 mm/sec for sensor x (a, b or c)
xamp - signal strength of three paths (dB * 100)
xnz - indices into xz where outliers had been detected

Burst Averaged ADV Data

For each deployment, a file exists as **ADVmeans_MMYY.mat**, where MMYY is the month and year of the beginning of the deployment (0896, 1096, 0197). Each file includes the following variables:

```
mmon, mday, mhr - month, day and year of beginning of burst (tdoy  
is the day of year (GMT), 0.5 is noon on 1/1)  
Ex - average Easterly flow (1/10 mm/sec)  
Nx - average Northerly flow (1/10 mm/sec)  
Vtx - average upward flow (1/10 mm/sec)  
Lx - number of 'good' samples in each burst (maximum = 144000) and  
'good' is defined as  $I_x > 7$   
Nx_std, Ex_std, Vtx_std - standard deviation of detrended velocities  
urms - bottom orbital velocity (urms) in  $m^2/s^2$   
ngood_x - number of valid points used in burst statistics
```

where x is a, b or c, which specifies the ADV sensor.

A secondary burst averaged file exists containing signal strength statistics (ampmeans_MMYY.mat):

```
xampmean - average signal strength (dB) at ADV_x  
xampstd - standard deviation of signal strength (dB) at ADV_x
```

SECTION VIII: REFERENCES

Galbraith, N., W. Ostrom, B. Way, S. Lentz, S. Anderson, M. Baumgartner, A. Plueddemann and J. Edson, "Coastal Mixing and Optics Experiment: Mooring Deployment Cruise Report, ...", Woods Hole Oceanographic Institution Technical Report, WHOI-97-13, 81 pp.

Mackenzie, K.V. "Nine-term Equation for Sound Speed in the Oceans", *J. Acoust. Soc. Am.* 70 (1981), pp. 807-812.

Morrison, A. T., III, Williams, A. J., 3rd, Martini, M., "Calibration of the BASS Acoustic Current Meter with Carrageenan Agar", *Proceedings OCEANS '93, IEEE/OES*, October 1993, Vol. III, pp. 143-148.

Limeburner, R., 1985, Woods Hole Oceanographic Institution, Technical Report, WHOI-85-35.

Shaw, W. J., A.J.Williams 3rd, and J.H.Trowbridge, "Measurement of Turbulent Sound Speed Fluctuations with an Acoustic Travel-Time Meter", *Proceedings OCEANS'96 MTS/IEEE*, pp. 105 - 110.

Shaw, W. J. and J. H.Trowbridge, "Measurement of Near-bottom Turbulent Fluxes in the Presence of Energetic Wave Motions". *J. Atm. and Ocean. Tech.*, in press.

Shaw, W. J., J. H. Trowbridge A. J. Williams 3rd, "Budgets of Turbulent Kinetic Energy and Scalar Variance in the Continental Shelf Bottom Boundary Layer", *Journal of Geophysical Research*, Vol. 106, No. C5, pp. 9551-9564, 2001.

Trivett, D. A., "Diffuse Flow from Hydrothermal Vents", Sc.D. thesis, Woods Hole Oceanographic Institution and Massachusetts Institute of Technology, Woods Hole and Cambridge, Massachusetts, 1991.

Trowbridge, J. H. "On a Technique for Measurement of Turbulent Shear Stress in the Presence of Surface Waves", *J. Atm. and Ocean. Tech.*, 15:290-298, 1998.

Voulgaris, G., J. H. Trowbridge, W. J. Shaw and A. J. Williams 3rd, "High Resolution Measurements of Turbulent Fluxes and Dissipation Rates in the Benthic Boundary Layer", *Coastal Dynamics '97, ASCE*: 177-186.

Williams, A.J. 3rd, J. S. Tochko, R. L. Koehler, W. D. Grant, T. F. Gross and C. V. R. Dunn, "Measurement of Turbulence in the Oceanic Bottom Boundary Layer with an Acoustic Current Meter Array", *Journal of Atmospheric and Oceanic Technology*, 4, pp. 312-327, 1987.

Williams, A. J., 3rd, and Fraenkel, N. R., "Simultaneous Measurement of Pressure, Temperature, and Conductivity with Counters", *Proceedings OCEANS '95, IEEE/MTS*, 1995, pp. 626-630.

Williams, A. J., 3rd, D. B. Peters, A. G. Gordon, and J. H. Trowbridge, "SuperBASS Tripod for Benthic Turbulence Measurement", *Proceedings Oceans '97, IEEE/MTS*, 1995, pp. 524-527.

APPENDIX A

SEA-BIRD ELECTRONICS, INC.

1808 136th Place N.E., Bellevue, Washington 98005 USA
 Phone: (206) 643 - 9866 Fax: (206) 643 - 9954 Internet: seabird@seabird.com

SENSOR SERIAL NUMBER = 1425
 CALIBRATION DATE: 11-Dec-96s

CONDUCTIVITY CALIBRATION DATA
 PSS 1978: C(35,15,0) = 4.2914 Siemens/meter

GHIJ COEFFICIENTS

g = -4.07796026e+00
 h = 4.99401015e-01
 i = -2.08399078e-04
 j = 3.55267889e-05
 CPcor = -9.57e-08 (nominal)
 CTcor = 3.25e-06 (nominal)

ABCDM COEFFICIENTS

a = 8.21880894e-06
 b = 4.98774171e-01
 c = -4.07617241e+00
 d = -8.54995759e-05
 m = 4.4
 CPCor = -9.57e-08 (nominal)

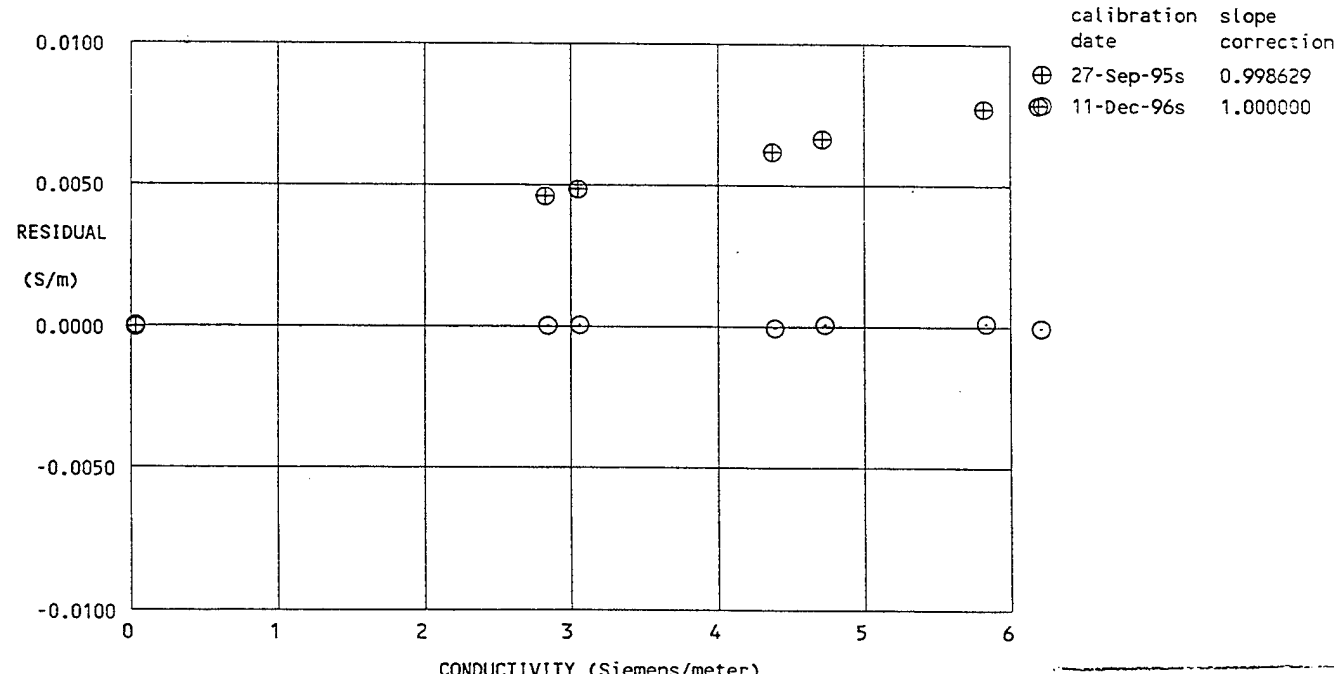
BATH TEMP (IPTS-68 °C)	BATH SAL (PSU)	BATH COND (Siemens/m)	INST FREQ (kHz)	INST COND (Siemens/m)	RESIDUAL (Siemens/m)
0.0000	0.0000	0.00000	2.85844	-0.00000	-0.00000
-1.3370	35.4115	2.81910	8.03338	2.81910	0.00000
1.0973	35.4121	3.03052	8.29162	3.03054	0.00002
15.2151	35.4095	4.35762	9.75543	4.35753	-0.00009
18.6526	35.4030	4.70277	10.10099	4.70281	0.00004
29.1955	35.3877	5.80552	11.13155	5.80560	0.00008
32.6352	35.3839	6.17754	11.45768	6.17748	-0.00006

$$\text{Conductivity} = (g + hf^2 + if^3 + jf^4) / [10(1 + \delta t + \epsilon p)] \text{ Siemens/meter}$$

$$\text{Conductivity} = (af^m + bf^2 + c + dt) / [10(1 + \epsilon p)] \text{ Siemens/meter}$$

t = temperaure [deg C]; p = pressure [decibars]; δ = CTcor; ϵ = CPCor;

Residual = (instrument conductivity - bath conductivity) using g, h, i, j coefficients



SEA-BIRD ELECTRONICS, INC.

1808 136th Place N.E., Bellevue, Washington 98005 USA
 Phone: (206) 643 - 9866 Fax: (206) 643 - 9954 Internet: seabird@seabird.com

SENSOR SERIAL NUMBER = 1425
 CALIBRATION DATE: 20-Dec-96s

CONDUCTIVITY CALIBRATION DATA
 PSS 1978: C(35,15,0) = 4.2914 Siemens/meter

GHIJ COEFFICIENTS

g = -4.07046884e+00
 h = 4.98356171e-01
 i = -1.39076038e-04
 j = 3.21297599e-05
 CPcor = -9.57e-08 (nominal)
 CTcor = 3.25e-06 (nominal)

ABCDM COEFFICIENTS

a = 1.08019880e-05
 b = 4.98002927e-01
 c = -4.06984378e+00
 d = -9.02124366e-05
 m = 4.3
 CPcor = -9.57e-08 (nominal)

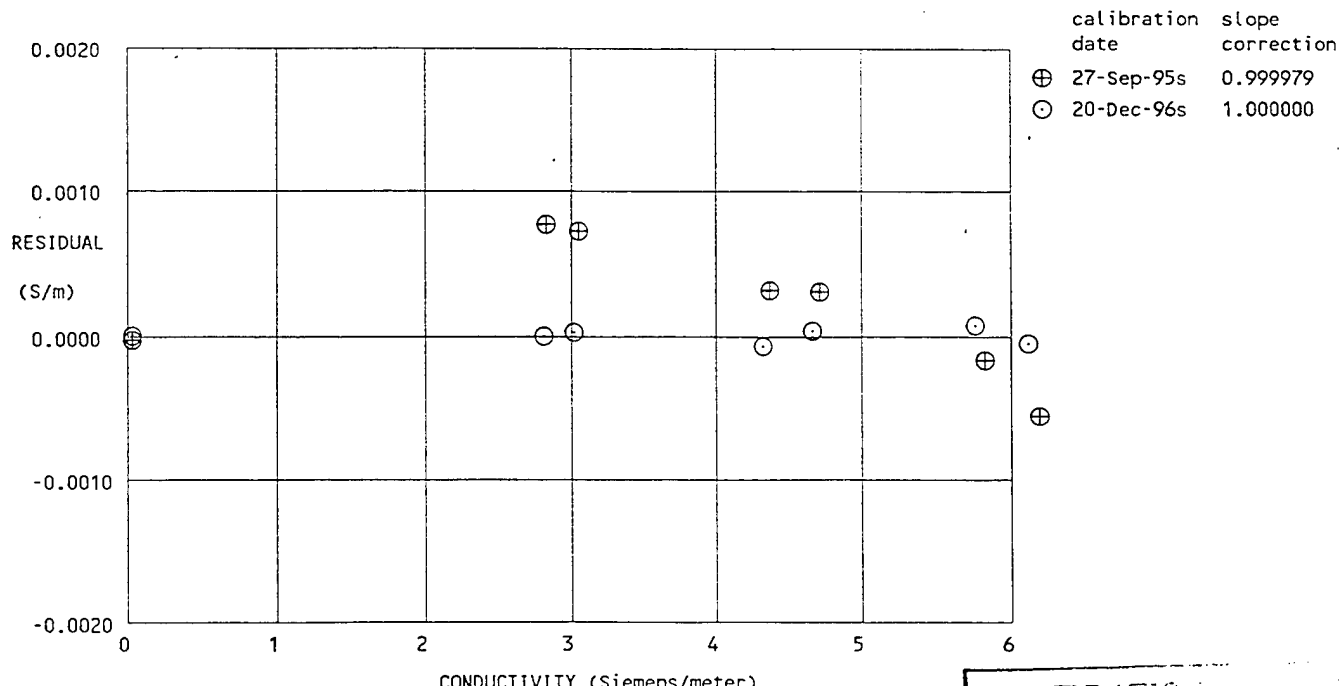
BATH TEMP (IPTS-68 °C)	BATH SAL (PSU)	BATH COND (Siemens/m)	INST FREQ (kHz)	INST COND (Siemens/m)	RESIDUAL (Siemens/m)
0.0000	0.0000	0.00000	2.85832	-0.00000	-0.00000
-1.2766	34.8611	2.78444	7.99495	2.78444	-0.00000
1.0967	34.8625	2.98790	8.24512	2.98792	0.00002
15.2138	34.8591	4.29692	9.69930	4.29685	-0.00007
18.6511	34.8519	4.63729	10.04255	4.63732	0.00003
29.1943	34.8332	5.72464	11.06625	5.72471	0.00007
32.6340	34.8137	6.08915	11.38825	6.08910	-0.00005

$$\text{Conductivity} = (g + hf^2 + if^3 + jf^4) / [10(1 + \delta t + \epsilon p)] \text{ Siemens/meter}$$

$$\text{Conductivity} = (af^m + bf^2 + c + dt) / [10(1 + \epsilon p)] \text{ Siemens/meter}$$

t = temperaure [deg C]; p = pressure [decibars]; δ = CTcor; ϵ = CPcor;

Residual = (instrument conductivity - bath conductivity) using g, h, i, j coefficients



CALIBRATIC
 CLEANING
 REPLATINIZING

SEA-BIRD ELECTRONICS, INC.

1808 136th Place N.E., Bellevue, Washington 98005 USA
 Phone: (206) 643 - 9866 Fax: (206) 643 - 9954 Internet: seabird@seabird.com

SENSOR SERIAL NUMBER = 1481
 CALIBRATION DATE: 27-Sep-95s

CONDUCTIVITY CALIBRATION DATA
 PSS 1978: C(35,15,0) = 4.2914 Siemens/meter

GHIJ COEFFICIENTS

g = -4.17961125e+00
 h = 5.08438178e-01
 i = -1.06971045e-04
 j = 3.33368219e-05
 CPcor = -9.57e-08 (nominal)
 CTcor = 3.25e-06 (nominal)

ABCDM COEFFICIENTS

a = 1.58091542e-05
 b = 5.08178116e-01
 c = -4.17920075e+00
 d = -8.89644797e-05
 m = 4.2
 CPcor = -9.57e-08 (nominal)

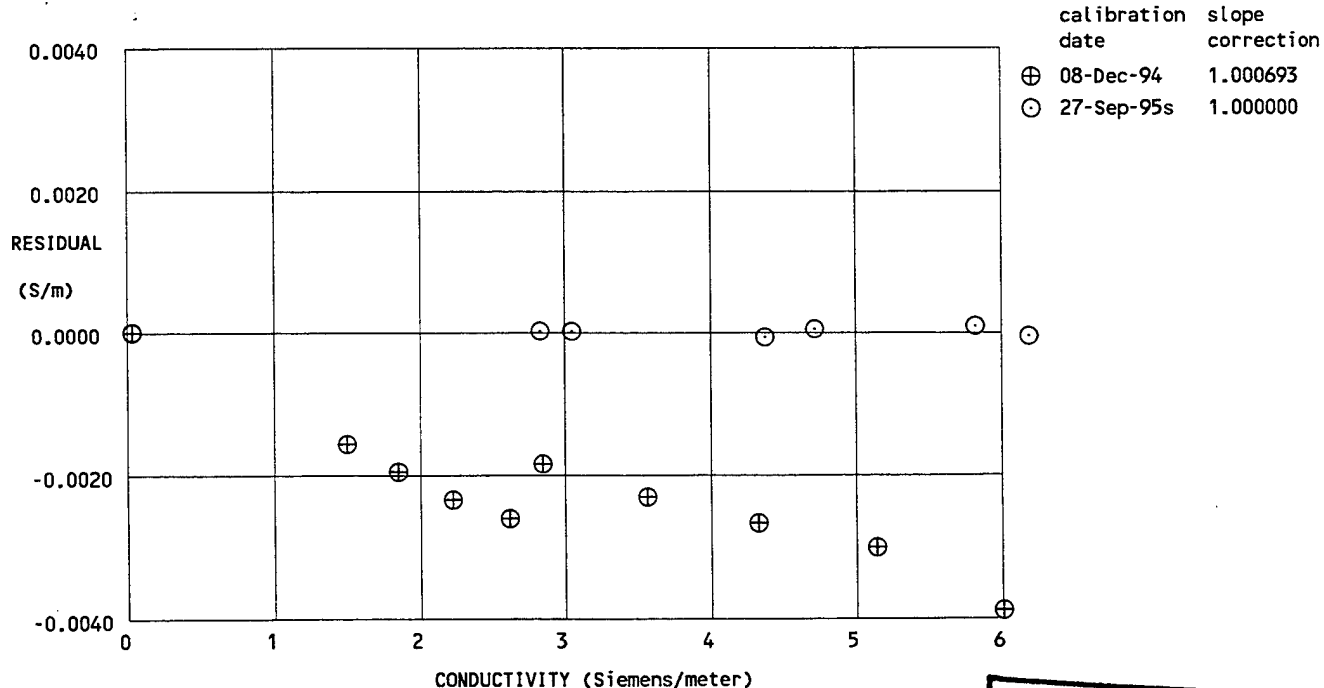
BATH TEMP [deg C]	BATH SAL [PSU]	BATH COND [Siemens/m]	INST FREQ [kHz]	INST COND [Siemens/m]	RESIDUAL [Siemens/m]
0.0000	0.0000	0.00000	2.86723	-0.00000	-0.00000
-1.4600	35.3013	2.80065	7.94657	2.80066	0.00001
1.0791	35.3023	3.02042	8.21249	3.02043	0.00001
15.1962	35.3037	4.34411	9.65828	4.34403	-0.00008
18.6329	35.3031	4.68894	10.00019	4.68898	0.00004
29.1740	35.3017	5.79070	11.01996	5.79079	0.00009
32.6121	35.2988	6.16186	11.34222	6.16180	-0.00006

Conductivity = $(g + hf^2 + if^3 + jf^4) / [10(1 + \delta t + \epsilon p)]$ Siemens/meter

Conductivity = $(af^m + bf^2 + c + dt) / [10(1 + \epsilon p)]$ Siemens/meter

t = temperaure [deg C]; p = pressure [decibars]; δ = CTcor; ϵ = CPcor;

Residual = (instrument conductivity - bath conductivity) using g, h, i, j coefficients



CALIBRATION AFTER
 CLEANING AND
 REPLATINIZING CELL

SEA-BIRD ELECTRONICS, INC.

1808 136th Place N.E., Bellevue, Washington 98005 USA
 Phone: (206) 643 - 9866 Fax: (206) 643 - 9954 Internet: seabird@seabird.com

SENSOR SERIAL NUMBER = 1482
 CALIBRATION DATE: 20-Sep-95s

GHIJ COEFFICIENTS

g = -4.07016387e+00
 h = 4.96980326e-01
 i = -1.89232187e-04
 j = 3.54699078e-05
 CPCor = -9.57e-08 (nominal)
 CTCor = 3.25e-06 (nominal)

CONDUCTIVITY CALIBRATION DATA
 PSS 1978: C(35,15,0) = 4.2914 Siemens/meter

ABCDM COEFFICIENTS

a = 8.51722533e-06
 b = 4.96469411e-01
 c = -4.06903954e+00
 d = -9.11186222e-05
 m = 4.4
 CPCor = -9.57e-08 (nominal)

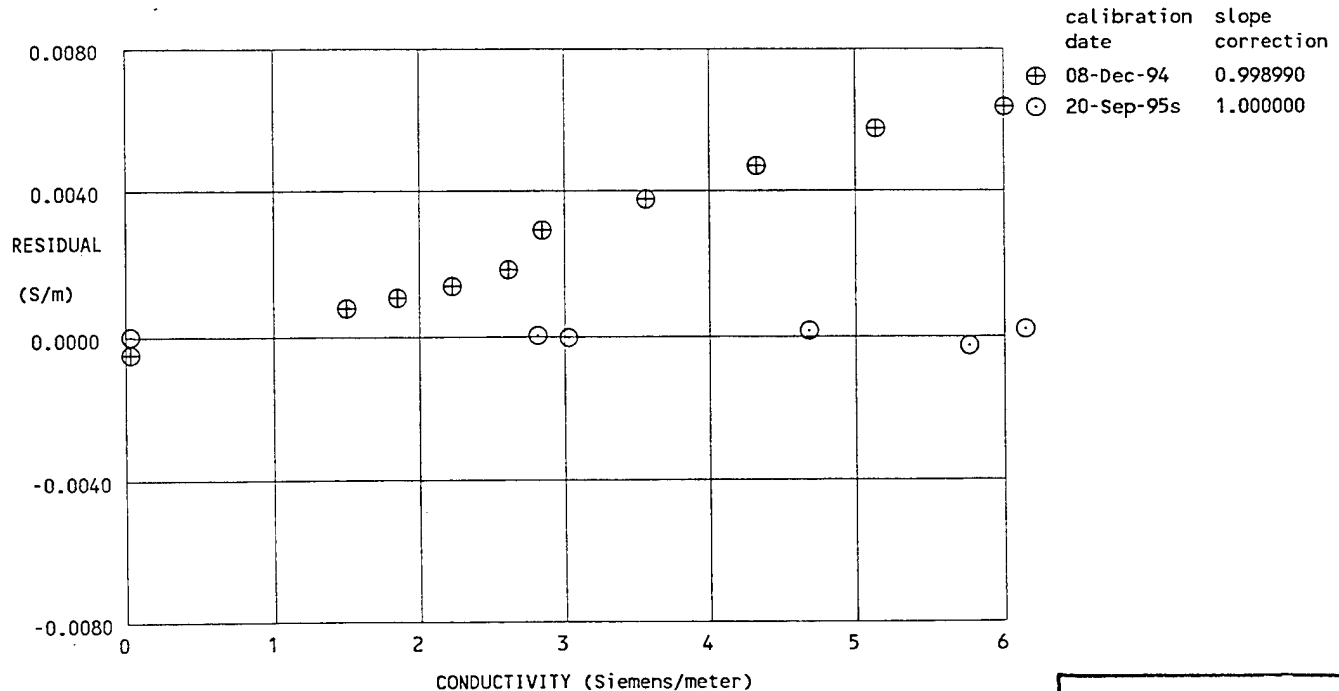
BATH TEMP [deg C]	BATH SAL [PSU]	BATH COND [Siemens/m]	INST FREQ [kHz]	INST COND [Siemens/m]	RESIDUAL [Siemens/m]
0.0000	0.0000	0.00000	2.86251	0.00000	0.00000
-1.4025	35.0106	2.78460	8.00763	2.78461	0.00001
1.0538	35.0122	2.99577	8.26742	2.99572	-0.00005
18.6474	34.9990	4.65437	10.07498	4.65451	0.00014
29.0346	34.9957	5.73132	11.08864	5.73104	-0.00028
32.5848	34.9884	6.11091	11.42450	6.11109	0.00018

$$\text{Conductivity} = (g + hf^2 + if^3 + jf^4) / [10(1 + \delta t + \epsilon p)] \text{ Siemens/meter}$$

$$\text{Conductivity} = (af^m + bf^2 + c + dt) / [10(1 + \epsilon p)] \text{ Siemens/meter}$$

t = temperature [deg C]; p = pressure [decibars]; δ = CTCor; ϵ = CPCor;

Residual = (instrument conductivity - bath conductivity) using g, h, i, j coefficients



POST CRUISE
 CALIBRATION

SEA-BIRD ELECTRONICS, INC.

1808 136th Place N.E., Bellevue, Washington 98005 USA
 Phone: (206) 643 - 9866 Fax: (206) 643 - 9954 Internet: seabird@seabird.com

SENSOR SERIAL NUMBER = 1482
 CALIBRATION DATE: 29-Sep-95s

CONDUCTIVITY CALIBRATION DATA
 PSS 1978: C(35,15,0) = 4.2914 Siemens/meter

GHIJ COEFFICIENTS

g = -4.06218749e+00
 h = 4.96813670e-01
 i = -2.77286831e-04
 j = 4.01122591e-05
 CPcor = -9.57e-08 (nominal)
 CTcor = 3.25e-06 (nominal)

ABCDM COEFFICIENTS

a = 6.57167965e-06
 b = 4.95933803e-01
 c = -4.05945334e+00
 d = -8.37269288e-05
 m = 4.5
 CPcor = -9.57e-08 (nominal)

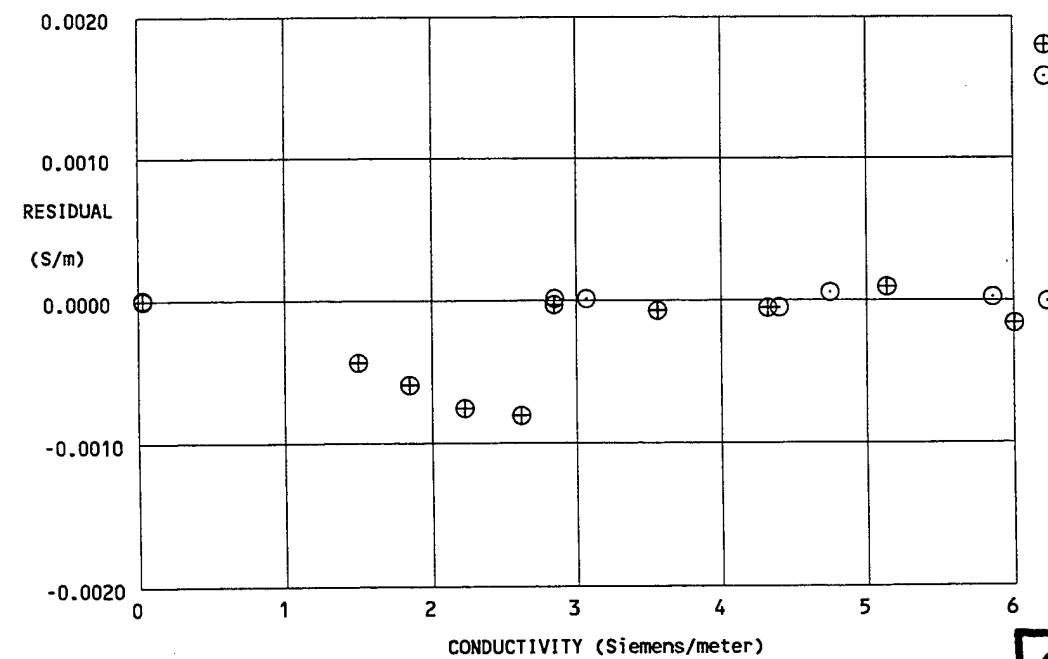
BATH TEMP [deg C]	BATH SAL [PSU]	BATH COND [Siemens/m]	INST FREQ [kHz]	INST COND [Siemens/m]	RESIDUAL [Siemens/m]
0.0000	0.0000	0.00000	2.86079	-0.00000	-0.00000
-1.4604	35.5667	2.81970	8.05505	2.81971	0.00001
1.0800	35.5677	3.04103	8.32596	3.04103	0.00000
15.1941	35.5687	4.37301	9.79703	4.37295	-0.00006
18.6308	35.5679	4.72006	10.14482	4.72011	0.00005
29.1726	35.5667	5.82908	11.18192	5.82910	0.00002
32.6114	35.5626	6.20254	11.50956	6.20252	-0.00002

$$\text{Conductivity} = (g + hf^2 + if^3 + jf^4) / [10(1 + \delta t + \epsilon p)] \text{ Siemens/meter}$$

$$\text{Conductivity} = (af^m + bf^2 + c + dt) / [10(1 + \epsilon p)] \text{ Siemens/meter}$$

t = temperaure [deg C]; p = pressure [decibars]; δ = CTcor; ϵ = CPcor;

Residual = (instrument conductivity - bath conductivity) using g, h, i, j coefficients



calibration date	slope correction
⊕ 08-Dec-94	1.000057
○ 29-Sep-95s	1.000000

CALIBRATION AFTER
 CLEANING AND
 REPLATINIZING CELL

SEA-BIRD ELECTRONICS, INC.

1808 136th Place N.E., Bellevue, Washington 98005 USA
 Phone: (206) 643 - 9866 Fax: (206) 643 - 9954 Internet: seabird@seabird.com

SENSOR SERIAL NUMBER = 2100
 CALIBRATION DATE: 23-Feb-96s

TEMPERATURE CALIBRATION DATA ITS-90 TEMPERATURE SCALE

ITS-90 COEFFICIENTS

g = 4.14627034e-03
 h = 6.27125153e-04
 i = 2.10467819e-05
 j = 2.27215955e-06
 f₀ = 1000.000

IPTS-68 COEFFICIENTS

a = 3.68027895e-03
 b = 5.99187907e-04
 c = 1.58873738e-05
 d = 2.27369108e-06
 f₀ = 2140.205

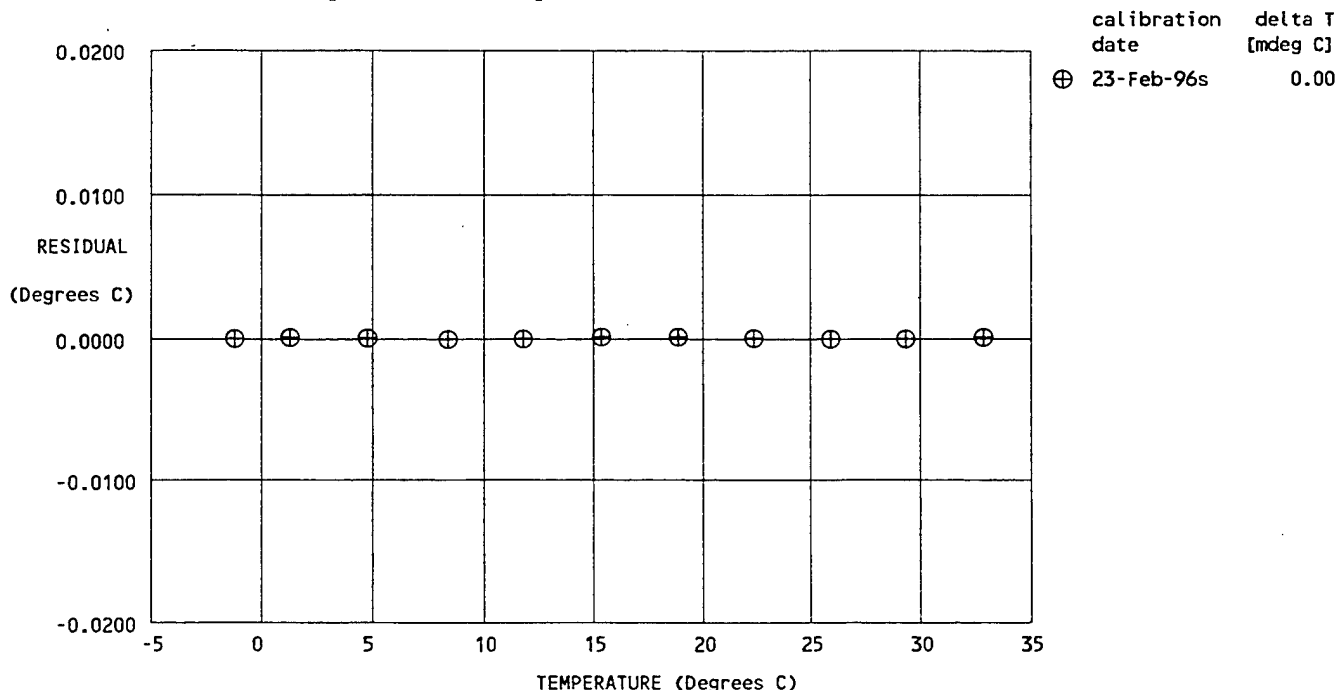
BATH TEMP (ITS-90 °C)	INSTRUMENT FREQ (Hz)	INST TEMP (ITS-90 °C)	RESIDUAL (ITS-90 °C)
-1.4311	2140.205	-1.4311	-0.00002
1.0794	2264.220	1.0795	0.00005
4.5701	2445.179	4.5701	0.00001
8.1689	2642.410	8.1688	-0.00007
11.6014	2840.890	11.6013	-0.00005
15.1589	3057.563	15.1590	0.00006
18.6629	3282.127	18.6630	0.00009
22.1618	3517.653	22.1618	-0.00001
25.7212	3769.100	25.7212	-0.00005
29.1362	4021.790	29.1361	-0.00007
32.6701	4295.316	32.6702	0.00006

$$\text{Temperature ITS-90} = 1/\{g + h[\ln(f_0/f)] + i[\ln^2(f_0/f)] + j[\ln^3(f_0/f)]\} - 273.15 \text{ (°C)}$$

$$\text{Temperature IPTS-68} = 1/\{a + b[\ln(f_0/f)] + c[\ln^2(f_0/f)] + d[\ln^3(f_0/f)]\} - 273.15 \text{ (°C)}$$

Following the recommendation of JPOTS: T₆₈ is assumed to be 1.00024 * T₉₀ (-2 to 35 °C).

Residual = instrument temperature - bath temperature



SEA-BIRD ELECTRONICS, INC.

1808 136th Place N.E., Bellevue, Washington 98005 USA
 Phone: (206) 643 - 9866 Fax: (206) 643 - 9954 Internet: seabird@seabird.com

SENSOR SERIAL NUMBER = 2101
 CALIBRATION DATE: 23-Feb-96s

TEMPERATURE CALIBRATION DATA ITS-90 TEMPERATURE SCALE

ITS-90 COEFFICIENTS

$g = 4.11663341e-03$
 $h = 6.28308761e-04$
 $i = 2.09641616e-05$
 $j = 2.20772351e-06$
 $f_0 = 1000.000$

IPTS-68 COEFFICIENTS

$a = 3.68027891e-03$
 $b = 6.02022306e-04$
 $c = 1.62888792e-05$
 $d = 2.20928243e-06$
 $f_0 = 2034.119$

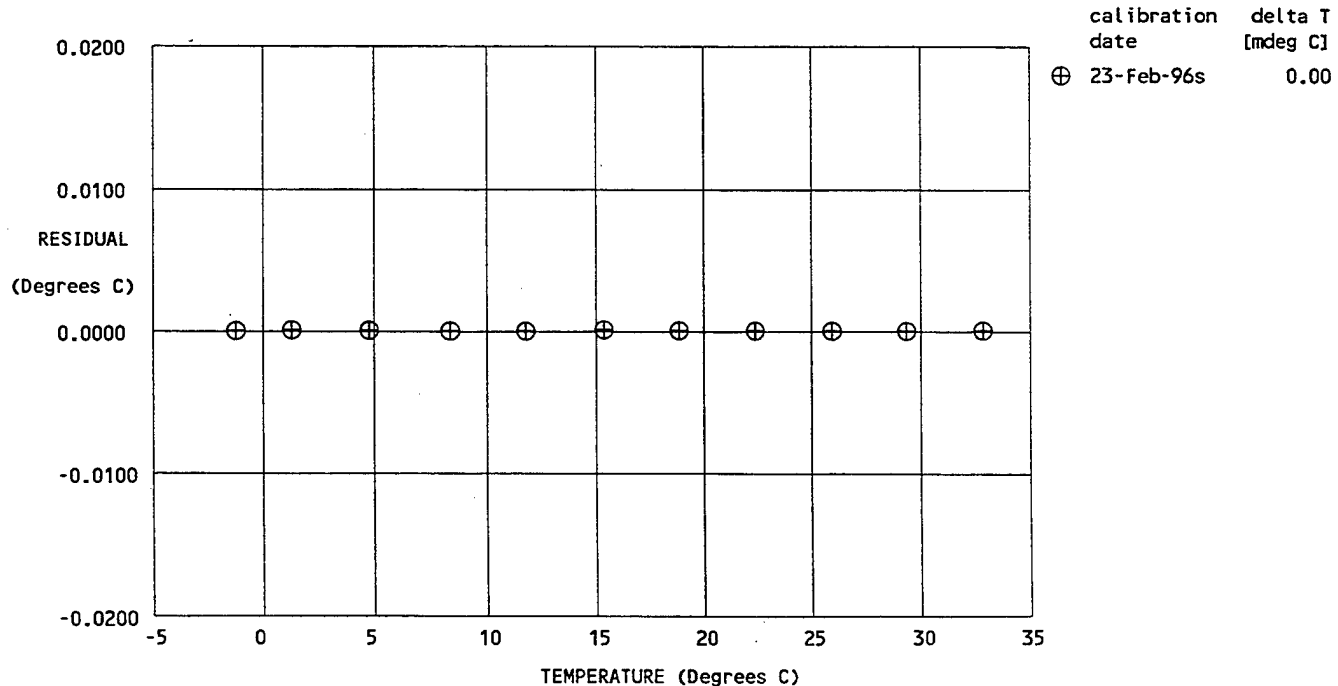
BATH TEMP (ITS-90 °C)	INSTRUMENT FREQ (Hz)	INST TEMP (ITS-90 °C)	RESIDUAL (ITS-90 °C)
-1.4311	2034.119	-1.4311	-0.00002
1.0794	2151.418	1.0795	0.00003
4.5701	2322.537	4.5701	0.00002
8.1689	2508.991	8.1689	-0.00005
11.6014	2696.576	11.6013	-0.00003
15.1589	2901.304	15.1590	0.00005
18.6629	3113.439	18.6630	0.00002
22.1618	3335.892	22.1618	-0.00000
25.7212	3573.334	25.7212	-0.00001
29.1362	3811.906	29.1362	-0.00002
32.6701	4070.102	32.6701	0.00002

$$\text{Temperature ITS-90} = 1/\{g + h[\ln(f_0/f)] + i[\ln^2(f_0/f)] + j[\ln^3(f_0/f)]\} - 273.15 \text{ (°C)}$$

$$\text{Temperature IPTS-68} = 1/\{a + b[\ln(f_0/f)] + c[\ln^2(f_0/f)] + d[\ln^3(f_0/f)]\} - 273.15 \text{ (°C)}$$

Following the recommendation of JPOTS: T_{68} is assumed to be $1.00024 * T_{90}$ (-2 to 35 °C).

Residual = instrument temperature - bath temperature



CALIBRATION COEFFICIENTS
PRESSURE TRANSDUCER

SERIAL NO: 59118

DATE: 01-31-1997

MODEL:	PRESSURE RANGE:	TEMP. RANGE:	PORT:
8DP0700-2	0 to 700 meters	-2 to 40 deg C	oil filled

PRESSURE COEFFICIENTS

U = temperature
 (deg C)

$$C = C_1 + C_2U + C_3U^2$$

$$D = D_1 + D_2U$$

$$T_0 = T_1 + T_2U + T_3U^2 + T_4U^3 + T_5U^4$$

T = pressure period
 (μsec)

Pressure: (psia)

$$P = C \left(1 - \frac{T_0^2}{T^2}\right) \left(1 - D \left(1 - \frac{T_0^2}{T^2}\right)\right)$$

C ₁	-4053.351	psia
C ₂	-3.68873E-02	psia/deg C
C ₃	7.68770E-04	psia/deg C ²

D ₁	0.062747
D ₂	0

T ₁	28.42048	μsec
T ₂	-3.24660E-04	μsec/deg C
T ₃	2.65656E-06	μsec/deg C ²
T ₄	6.52367E-10	μsec/deg C ³
T ₅	0	

(01-31-1997)

PAROScientIFIC, INC.
 4500 148th AVENUE N.E.
 REDMOND, WA. 98052

CUSTOMER: WOODS HOLE OCEANOGRAPHIC INST.

SALES ORDER: 59118 PREPARED BY: T.C.

APPENDIX B

loadnew.m

```
% loadiuv - to load v_iuv and v_doy & convert to m/s
eval(['load /mnt/cdrome/v_doy_','afn'])
eval(['load /mnt/cdrome/v_ne_','afn'])
eval(['load /mnt/cdrome/v_w_','afn'])

wAC=iwac./1000;
wBD=iwbd./1000;

nbad=find(iu(:) > 2000);
%disp(['percent bad: ',num2str(length(nbad)./length(iu(:)).*100)])
if (length(nbad))
iu(nbad)=NaN*ones(length(nbad),1);
wBD(nbad)=NaN*ones(length(nbad),1);
end

nbad=find(iv(:) > 2000);
%disp(['percent bad: ',num2str(length(nbad)./length(iv(:)).*100)])
if (length(nbad))
iv(nbad)=NaN*ones(length(nbad),1);
wAC(nbad)=NaN*ones(length(nbad),1);
end

u=iu./1000;
v=iv./1000;

clear iu iv iwac iwbd
```

loadss.m

```
% fix soundspeed
eval(['load /mnt/cdrom/oct/thrm_','num2str(fn)])
eval(['load /mnt/cdrom/oct/doy_','num2str(fn)])
nc=1:2:14;nc2=2:2:14;

% below are slopes & intercepts specific to Deployment II
% See Table 3 for other deployments

slope=[0.7872 0.7778 0.7773 0.7571 0.7651 0.7469 0.7326]*-1e-9;
b=[0.7239 0.7232 0.7244 0.7258 0.7251 0.7241 0.7260]*1e-3;

tt=reshape(therm,14,length(doy))';
tt=tt(:,nc)+tt(:,nc2);
ss=1./((slope(ones(length(doy),1),:).*tt + b(ones(length(doy),1),:)));
ss=rmoutliers(ss,4,0);
```

loadpaths.m

```
ida='a';
nt=nt1;
for ihalf=1:2
eval(['load /mnt/cdrom/velsabcd/v_doy_',num2str(fn),ida])
eval(['load /mnt/cdrom/velsabcd/v_vels_',num2str(fn),ida])
disp(['fn: ',num2str(fn),' mind: ',num2str(min(doy)), ' maxd: ',num2str(max(doy)), ' meand: ',num2str(mean(doy))])

nbad=find(ia(:) > 2000);
ia(nbad)=NaN*ones(size(nbad));
nbad=find(ib(:) > 2000);
ib(nbad)=NaN*ones(size(nbad));
nbad=find(ic(:) > 2000);
ic(nbad)=NaN*ones(size(nbad));
nbad=find(id(:) > 2000);
id(nbad)=NaN*ones(size(nbad));

ia=ia./1000-iaz(ones(length(doy),1),:);
ib=ib./1000-ibz(ones(length(doy),1),:);
ic=ic./1000-icz(ones(length(doy),1),:);
id=id./1000-idz(ones(length(doy),1),:);

% below is specific to Deployment II
%     check Table 1 for other deployments
%id(:,1)=ic(:,1)+ia(:,1)-ib(:,1);
%ib(:,2)=ic(:,2)+ia(:,2)-id(:,2);
%ic(:,5)=id(:,5)+ib(:,5)-ia(:,5);
% ib(:,4) was already substituted in vels data
ia=rmoutliers(ia,4,0);
ib=rmoutliers(ib,4,0);
ic=rmoutliers(ic,4,0);
id=rmoutliers(id,4,0);

u=(id-ib)./sqrt(2);
v=(ic-ia)./sqrt(2);
wAC=(ic+ia)./sqrt(2);
wBD=(id+ib)./sqrt(2);

..... processing body ......

ida='b';
nt=nt2;
end % each half day
```

DOCUMENT LIBRARY

Distribution List for Technical Report Exchange - July 1998

University of California, San Diego
SIO Library 0175C
9500 Gilman Drive
La Jolla, CA 92093-0175

Hancock Library of Biology & Oceanography
Alan Hancock Laboratory
University of Southern California
University Park
Los Angeles, CA 90089-0371

Gifts & Exchanges
Library
Bedford Institute of Oceanography
P.O. Box 1006
Dartmouth, NS, B2Y 4A2, CANADA

NOAA/EDIS Miami Library Center
4301 Rickenbacker Causeway
Miami, FL 33149

Research Library
U.S. Army Corps of Engineers
Waterways Experiment Station
3909 Halls Ferry Road
Vicksburg, MS 39180-6199

Marine Resources Information Center
Building E38-320
MIT
Cambridge, MA 02139

Library
Lamont-Doherty Geological Observatory
Columbia University
Palisades, NY 10964

Library
Serials Department
Oregon State University
Corvallis, OR 97331

Pell Marine Science Library
University of Rhode Island
Narragansett Bay Campus
Narragansett, RI 02882

Working Collection
Texas A&M University
Dept. of Oceanography
College Station, TX 77843

Fisheries-Oceanography Library
151 Oceanography Teaching Bldg.
University of Washington
Seattle, WA 98195

Library
R.S.M.A.S.
University of Miami
4600 Rickenbacker Causeway
Miami, FL 33149

Maury Oceanographic Library
Naval Oceanographic Office
Building 1003 South
1002 Balch Blvd.
Stennis Space Center, MS, 39522-5001

Library
Institute of Ocean Sciences
P.O. Box 6000
Sidney, B.C. V8L 4B2
CANADA

National Oceanographic Library
Southampton Oceanography Centre
European Way
Southampton SO14 3ZH
UK

The Librarian
CSIRO Marine Laboratories
G.P.O. Box 1538
Hobart, Tasmania
AUSTRALIA 7001

Library
Proudman Oceanographic Laboratory
Bidston Observatory
Birkenhead
Merseyside L43 7 RA
UNITED KINGDOM

IFREMER
Centre de Brest
Service Documentation - Publications
BP 70 29280 PLOUZANE
FRANCE

REPORT DOCUMENTATION PAGE	1. REPORT NO. WHOI-2001-08	2.	3. Recipient's Accession No.
4. Title and Subtitle Fluid Mechanical Measurements within the Bottom Boundary Layer During Coastal Mixing and Optics			5. Report Date August 2001
			6.
7. Author(s) J.J. Fredericks, John H. Trowbridge, A.J. Williams III, George Voulgaris, William Shaw			8. Performing Organization Rept. No. WHOI-2001-08
9. Performing Organization Name and Address Woods Hole Oceanographic Institution Woods Hole, Massachusetts 02543			10. Project/Task/Work Unit No.
			11. Contract(C) or Grant(G) No. (C) 13025500 (G)
12. Sponsoring Organization Name and Address Office of Naval Research			13. Type of Report & Period Covered Technical Report
			14.
15. Supplementary Notes This report should be cited as: Woods Hole Oceanog. Inst. Tech. Rept., WHOI-2001-08.			
16. Abstract (Limit: 200 words) To quantify and understand the role of vertical mixing processes in determining mid-shelf vertical structure of hydrographic and optical properties and particulate matter, the Office of Naval Research (ONR) funded a program called Coastal Mixing and Optics (CMO), which was conducted at a mid-shelf location in the Mid-Atlantic Bight, south of Martha's Vineyard, Massachusetts. As part of the CMO program, a tall tripod, called 'SuperBASS,' was equipped to collect a year-long, near-bottom time-series of velocity, temperature, salinity and pressure. The BASS sensors were modified to measure absolute as well as differential acoustic travel time, to provide sound speed (a surrogate for temperature) and velocity in a single sample volume. Seven BASS velocity and travel time sensors were placed between 0.4 and 7 meters above bottom (mab). Three acoustic Doppler velocity (ADV) meters were mounted near the bottom-most BASS sensor at 0.3 meters above bottom. The sensors were used to obtain high-quality time-series measurements of velocity and temperature throughout a large fraction of the bottom boundary layer on the New England shelf. The measurements provide vertical structure of the Reynolds-averaged velocity and temperature fields, direct covariance estimates of turbulent Reynolds stress and turbulent heat flux, and indirect inertial range estimates of dissipation rate for turbulent kinetic energy and temperature variance. The purpose of this report is to describe the SuperBASS instrumentation and deployments, to provide summaries of the data collected, and to document the processing, preliminary analysis and archival of the data collected for this component of the program.			
17. Document Analysis a. Descriptors Bottom boundary layer Stress Dissipation			
b. Identifiers/Open-Ended Terms			
c. COSATI Field/Group			
18. Availability Statement Approved for public release; distribution unlimited.		19. Security Class (This Report) UNCLASSIFIED	21. No. of Pages 194
		20. Security Class (This Page)	22. Price